γδ T CELLS IN CANCER

EDITED BY: Ilan Bank, Bruno Silva-Santos, Jurgen Kuball, Dieter Kabelitz, Seth Coffelt and Willi Born

PUBLISHED IN: Frontiers in Immunology

IUIS

frontiers Research Topics

frontiers

ISSN 1664-8714
ISBN 978-2-88966-362-0
DOI 10.3389/978-2-88966-362-0

About Frontiers

Frontiers is more than just an open-access publisher of scholarly articles: it is a pioneering approach to the world of academia, radically improving the way scholarly research is managed. The grand vision of Frontiers is a world where all people have an equal opportunity to seek, share and generate knowledge. Frontiers provides immediate and permanent online open access to all its publications, but this alone is not enough to realize our grand goals.

Frontiers Journal Series

The Frontiers Journal Series is a multi-tier and interdisciplinary set of open-access, online journals, promising a paradigm shift from the current review, selection and dissemination processes in academic publishing. All Frontiers journals are driven by researchers for researchers; therefore, they constitute a service to the scholarly community. At the same time, the Frontiers Journal Series operates on a revolutionary invention, the tiered publishing system, initially addressing specific communities of scholars, and gradually climbing up to broader public understanding, thus serving the interests of the lay society, too.

Dedication to Quality

Each Frontiers article is a landmark of the highest quality, thanks to genuinely collaborative interactions between authors and review editors, who include some of the world's best academicians. Research must be certified by peers before entering a stream of knowledge that may eventually reach the public - and shape society; therefore, Frontiers only applies the most rigorous and unbiased reviews.
Frontiers revolutionizes research publishing by freely delivering the most outstanding research, evaluated with no bias from both the academic and social point of view. By applying the most advanced information technologies, Frontiers is catapulting scholarly publishing into a new generation.

What are Frontiers Research Topics?

Frontiers Research Topics are very popular trademarks of the Frontiers Journals Series: they are collections of at least ten articles, all centered on a particular subject. With their unique mix of varied contributions from Original Research to Review Articles, Frontiers Research Topics unify the most influential researchers, the latest key findings and historical advances in a hot research area! Find out more on how to host your own Frontiers Research Topic or contribute to one as an author by contacting the Frontiers Editorial Office: frontiersin.org/about/contact

γδ T CELLS IN CANCER

Topic Editors:
Ilan Bank, Sheba Medical Center, Israel
Bruno Silva-Santos, University of Lisbon, Portugal
Jurgen Kuball, Utrecht University, Netherlands
Dieter Kabelitz, University of Kiel, Germany
Seth Coffelt, University of Glasgow, United Kingdom
Willi Born, National Jewish Health (United States), United States

We acknowledge the initiation and support of this Research Topic by the International Union of Immunological Societies (IUIS). Dr. Dieter Kabelitz currently serves as the chairman for the IUIS Education Committee.

Topic Editor Prof. Ilan Bank is Chief Scientific Officer of GammaCell Bio-Technologies Ltd. Topic Editor Prof. Jurgen Kuball is co-founder and scientific advisor of GADETA. Topic Editor Prof. Bruno Silva-Santos is co-founder of Lymphact S.A., a company now owned by GammaDelta Therapeutics. All other Topic Editors declare no competing interests with regards to the Research Topic subject.

Citation: Bank, I., Silva-Santos, B., Kuball, J., Kabelitz, D., Coffelt, S., Born, W., eds. (2021). γδ T cells in Cancer. Lausanne: Frontiers Media SA.
doi: 10.3389/978-2-88966-362-0

Table of Contents

frontiers in Immunology

EDITORIAL
published: 20 November 2020
doi: 10.3389/fimmu.2020.602411

Editorial: γδ T Cells in Cancer

Seth B. Coffelt[1,2], Dieter Kabelitz[3*], Bruno Silva-Santos[4*], Jurgen Kuball[5*], Willi Born[6*] and Ilan Bank[7*]*

[1] Institute of Cancer Sciences, University of Glasgow, Glasgow, United Kingdom, [2] Cancer Research UK Beatson Institute, Glasgow, United Kingdom, [3] Institute of Immunology, University of Kiel, Kiel, Germany, [4] Faculdade de Medicina, Instituto de Medicina Molecular, Universidade de Lisboa, Lisbon, Portugal, [5] Department of Hematology and Center for Translational Immunology, Utrecht Medical Center (UMC), Utrecht, Netherlands, [6] Department of Immunology and Genomic Medicine, National Jewish Health, Denver, CO, United States, [7] Rheumatology Unit, Division of Medicine, Sheba Medical Center, Tel Hashomer, Israel

Keywords: γδ T cells, cancer, butyrophilin, immunotherapy, bisphoshonates

Editorial on the Research Topic

γδ T Cells in Cancer

Since the discovery of γδ T cells, this rare and unique component of the immune system has been recognized for its potential in cancer immunology and immunotherapy. In the mid-1980s, it became clear that a major component of adaptive immune responses is the ability of T cell receptors (TCR) to undergo somatic recombination in order to recognize multiple antigens. TCRs consisting of either αβ and γδ chains were discovered in rapid succession (1–6). An important observation was made in these initial studies: γδ T cells stimulated through their TCR are able to kill cancer cells (2). Over these past decades, researchers have learned that γδ T cells share many similarities with αβ T cells, as well as major differences. However, discoveries in γδ T cell biology have failed to keep the same pace as αβ T cell biology. The molecular targets of γδTCRs and functions of these cells have largely eluded researchers, partly because γδ T cell recognition of cancer cells and their response kinetics are very different to αβ T cells (7, 8). Recent years have seen major advances in γδ T cell biology and established the non-redundancy of this lymphocyte subset, particularly in the context of cancer (9–11). γδ T cells are being used as cellular vehicles to target tumors and prognostic indicators of cancer progression. The aim of the articles collected in this Research Topic is to describe new developments and approaches to enhance the anti-tumor functions of γδ T cells, and to discuss how expression of their ligands can assist with prognosis of cancer patients.

Given the robust ability of γδ T cells to kill cancer cells, various strategies to enhance their cytotoxic behavior are being pursued in the laboratory. The Vγ9Vδ2 cell subset in humans recognizes transformed cells with dysfunctional metabolism, primarily through the up-regulation of phosphoantigens stemming from abnormalities in the mevalonate pathway. One of the best studied phosphoantigens is isopentenyl pyrophosphate (IPP), which activates a receptor complex in cancer cells consisting of butyrophilin (BTN)-3A1 and BTN2A1 (12, 13). However, very little information exists on how this receptor complex is presented on the cell surface and its other interacting partners. Laplagne et al. report on the importance of the GTPase, RhoB, in regulating BTN3A1 presentation on the cell membrane. They observed that the differential susceptibility of lung tumor cell lines to Vγ9Vδ2 T-cell killing correlated with differential subcellular and plasma membrane distribution of RhoB. There are a few methods to increase Vγ9Vδ2 cell recognition of cancer cells, primarily *via* boosting the IPP-activated BTN3A1/BTN2A1 complex. Bisphosphonate drugs increase accumulation of IPP making cancer cells more susceptible to Vγ9Vδ2 cell killing, but these drugs also induce proliferation of Vγ9Vδ2 cells in culture. Okuno et al. report on a newly synthesized bisphosphonate drug, pivaloyloxymethyl 2-(thiazole-2-ylamino)ethylidene-1,1-

OPEN ACCESS

Edited by:
Alexandre M. Carmo, University of Porto, Portugal

Reviewed by:
David L. Wiest, Fox Chase Cancer Center, United States

***Correspondence:**
Seth B. Coffelt
seth.coffelt@glasgow.ac.uk
Dieter Kabelitz
dietrich.kabelitz@uksh.de
Bruno Silva-Santos
bssantos@medicina.ulisboa.pt
Jurgen Kuball
J.H.E.Kuball@umcutrecht.nl
Willi Born
bornw@njhealth.org
Ilan Bank
ibank@tauex.tau.ac.il

Specialty section:
This article was submitted to T Cell Biology, a section of the journal Frontiers in Immunology

Received: *03 September 2020*
Accepted: *28 October 2020*
Published: *20 November 2020*

Citation:
Coffelt SB, Kabelitz D, Silva-Santos B, Kuball J, Born W and Bank I (2020) Editorial: γδ T Cells in Cancer. Front. Immunol. 11:602411. doi: 10.3389/fimmu.2020.602411

bisphosphonate (PTA), that both expands Vγ9Vδ2 cells and increases their ability to recognize cancer cells.

γδ T cells are also being equipped with chimeric antigen receptors (CAR) for hematological and epithelial-derived malignancies. Most likely, γδ CAR T cells will associate with a lower risk of cytokine release syndrome as reported for NK CAR cells. Whether γδ CAR T cells will overcome the scarce infiltration of tumors by classical αβ CAR T cells remains to tested and might depend on the type of γδ T cells (i.e. Vδ1 cells versus Vδ2 cells), which have naturally different homing tissues. Rozenbaum et al. describe a new expansion protocol that generates high numbers of pure (> 99%) γδ T cells which could be efficiently transduced with CAR constructs. CD19-directed γδ CAR T cells efficiently killed CD19+ leukemic cells *in vitro* and *in vivo*. To test these various strategies whose goal is augment γδ T cell cytotoxic function, a variety of pre-clinical models are used that evaluate killing efficacy, but these models come with their own challenges. Joalland and Scotet summarize the advantages and disadvantages of the most commonly used pre-clinical models in γδ T cell immunotherapy. In addition to the use of immunodeficient mice transplanted with human tumor cells and γδ T cells, they also discuss the urgent need for improved animal-free *in vitro* models such as spheroids and organoids.

Another outstanding question in the field is how γδ T cell function may be suppressed by tumors. Siegers et al. show that an embryonic-associated molecule, called NODAL, expressed by breast cancer cells, impacts γδ T cell function. In human breast tumors, γδ T cells are found in close proximity to NODAL+ cancer cells. Through gain-of-function and loss-of-function experiments, the authors report that NODAL expression on breast cancer cell lines reduces γδ T-cell cytotoxicity. Gonnermann et al. describe a novel immunosuppression pathway in pancreatic cancer, where Galectin-3 secreted by cancer cells inhibits γδ T cell proliferation *via* α3β1 integrin. Interestingly, the cytotoxic activity of γδ T cells was not impaired by Galectin-3.

This Research Topic includes two clinical trials. One trial investigated the ability of β-adrenergic receptor activation to mobilize γδ T cells into the peripheral blood of test subjects. Baker et al. found that drugs antagonizing the β-adrenergic receptor pathway not only prevent γδ T cell accumulation in blood, but that this pathway is also important for γδ T cell expansion *ex vivo*. These data suggest that β-adrenergic receptor agonists may improve expansion protocols or γδ T cell cytotoxic function. The second clinical trial included 46 children with acute leukemia that received hematopoietic stem cell transplantation of αβTCR/CD19-depleted haploidentical grafts. Merli et al. tested the ability of the bisphosphonate drug, zoledronic acid, to counteract graft-versus-host-disease in these patients, and they show that zoledronic acid is well tolerated. Moreover, the children that received more doses of zoledronic acid had a better outcome than the children receiving fewer doses.

Finally, two articles in this collection discuss the importance of γδ T cell ligands in cancer immunotherapy. Bartish et al. summarize the role of immunosuppressive molecules that contain sugar residues as well as the relationship between these glyco-molecules and γδ T cells, highlighting opportunities for intervention. Wang et al. wrote a meta-analysis on publications pertaining to the BTN family. In this review, the authors also provide prognostic data for several BTN family members in lung adenocarcinoma and lung squamous cell carcinoma.

Together, this Research Topic features new developments in γδ T cell cancer immunotherapy, providing insight into mechanisms that both increase and suppress their effector functions. Finding the right patient population in which to manipulate these pathways and exploit this new information may be key to counteracting cancer.

AUTHOR CONTRIBUTIONS

SC, DK, BS-S, JK, WB, and IB wrote the editorial and invited authors to participate in the collection. All authors contributed to the article and approved the submitted version.

FUNDING

The authors acknowledge funding from the Cancer Research UK Glasgow Centre (A25142 to SBC), the Wellcome Trust (208990/Z/17/Z to SBC), the Medical Research Council (MR/R502327/1 to SBC), Breast Cancer Now (2018JulPR1101 and 2019DecPhD1349 to SBC), Tenovus Scotland (S17-17 to SBC), the Deutsche Forschungsgemeinschaft (Ka 502/19-2 to DK), the Wilhelm Sander Foundation (2018.045.1 to DK), "la Caixa" Banking Foundation (HR18-00069 to BS-S), the Dutch Research Council (NWO ZonMW 43400003 to JK), the Dutch Cancer Society (KWF UU 2014-6790, UU 2015-7601, UU 2018-11393, UU 2018-11979, UU 2019-12586, UU 2020-13043 to JK).

REFERENCES

1. Saito H, Kranz DM, Takagaki Y, Hayday AC, Eisen HN, Tonegawa S. Complete primary structure of a heterodimeric T-cell receptor deduced from cDNA sequences. *Nature* (1984) 309(5971):757–62. doi: 10.1038/309757a0
2. Bank I, DePinho RA, Brenner MB, Cassimeris J, Alt FW, Chess L. A functional T3 molecule associated with a novel heterodimer on the surface of immature human thymocytes. *Nature* (1986) 322(6075):179–81. doi: 10.1038/322179a0
3. Brenner MB, McLean J, Dialynas DP, Strominger JL, Smith JA, Owen FL, et al. Identification of a putative second T-cell receptor. *Nature* (1986) 322(6075):145–9. doi: 10.1038/322145a0
4. Borst J, van de Griend RJ, van Oostveen JW, Ang SL, Melief CJ, Seidman JG, et al. A T-cell receptor gamma/CD3 complex found on cloned functional lymphocytes. *Nature* (1987) 325(6106):683–8. doi: 10.1038/325683a0
5. Born W, Miles C, White J, O'Brien R, Freed JH, Marrack P, et al. Peptide sequences of T-cell receptor delta and gamma chains are identical to predicted X and gamma proteins. *Nature* (1987) 330(6148):572–4. doi: 10.1038/330572a0

6. Chien YH, Iwashima M, Kaplan KB, Elliott JF, Davis MM. A new T-cell receptor gene located within the alpha locus and expressed early in T-cell differentiation. *Nature* (1987) 327(6124):677–82. doi: 10.1038/327677a0
7. Hayday AC. gammadelta T Cell Update: Adaptate Orchestrators of Immune Surveillance. *J Immunol* (2019) 203(2):311–20. doi: 10.4049/jimmunol.1800934
8. Willcox BE, Willcox CR. gammadelta TCR ligands: the quest to solve a 500-million-year-old mystery. *Nat Immunol* (2019) 20(2):121–8. doi: 10.1038/s41590-018-0304-y
9. Silva-Santos B, Mensurado S, Coffelt SB. gammadelta T cells: pleiotropic immune effectors with therapeutic potential in cancer. *Nat Rev Cancer* (2019) 19(7):392–404. doi: 10.1038/s41568-019-0153-5
10. Sebestyen Z, Prinz I, Dechanet-Merville J, Silva-Santos B, Kuball J. Translating gammadelta (gammadelta) T cells and their receptors into cancer cell therapies. *Nat Rev Drug Discov* (2020) 19(3):169–84. doi: 10.1038/s41573-019-0038-z
11. Kabelitz D, Serrano R, Kouakanou L, Peters C, Kalyan S. Cancer immunotherapy with gammadelta T cells: many paths ahead of us. *Cell Mol Immunol* (2020) 17:925–39. doi: 10.1038/s41423-020-0504-x
12. Harly C, Guillaume Y, Nedellec S, Peigne CM, Monkkonen H, Monkkonen J, et al. Key implication of CD277/butyrophilin-3 (BTN3A) in cellular stress sensing by a major human gammadelta T-cell subset. *Blood* (2012) 120 (11):2269–79. doi: 10.1182/blood-2012-05-430470
13. Karunakaran MM, Willcox CR, Salim M, Paletta D, Fichtner AS, Noll A, et al. Butyrophilin-2A1 Directly Binds Germline-Encoded Regions of the Vgamma9Vdelta2 TCR and Is Essential for Phosphoantigen Sensing. *Immunity* (2020) 52(3):487–98.e6. doi: 10.1016/j.immuni.2020.02.014

Conflict of Interest: BS-S is a founder and share holder of Lymphact S.A., which has been acquired by GammaDelta Therapeutics (London, UK). JK is scientific co-founder and shareholder of Gadeta. JK received financial research support of Gadeta, Miltenyi Biotech and Novartis.

The remaining authors declare that the research was conducted in the absence of any commercial or financial relationships that could be construed as a potential conflict of interest.

frontiers in Immunology

ORIGINAL RESEARCH
published: 24 January 2020
doi: 10.3389/fimmu.2019.03082

Systemic β-Adrenergic Receptor Activation Augments the *ex vivo* Expansion and Anti-Tumor Activity of Vγ9Vδ2 T-Cells

Forrest L. Baker[1,2,3], *Austin B. Bigley*[1], *Nadia H. Agha*[1], *Charles R. Pedlar*[4], *Daniel P. O'Connor*[1], *Richard A. Bond*[5], *Catherine M. Bollard*[6], *Emmanuel Katsanis*[3,7] *and Richard J. Simpson*[1,2,3,7]*

[1] *Laboratory of Integrated Physiology, Department of Health and Human Performance, University of Houston, Houston, TX, United States,* [2] *Department of Nutritional Sciences, University of Arizona, Tucson, AZ, United States,* [3] *Department of Pediatrics, University of Arizona, Tucson, AZ, United States,* [4] *School of Sport, Health and Applied Science, St. Mary's University, London, United Kingdom,* [5] *Department of Pharmacological and Pharmaceutical Sciences, University of Houston, Houston, TX, United States,* [6] *Center for Cancer and Immunology Research, Children's National Health System and the George Washington University, Washington, DC, United States,* [7] *Department of Immunobiology, University of Arizona, Tucson, AZ, United States*

OPEN ACCESS

Edited by:
Dieter Kabelitz, University of Kiel, Germany

Reviewed by:
Karin Schilbach, University of Tübingen, Germany
Serena Meraviglia, University of Palermo, Italy

***Correspondence:**
Richard J. Simpson
rjsimpson@email.arizona.edu

Specialty section:
This article was submitted to T Cell Biology, a section of the journal Frontiers in Immunology

Received: *11 September 2019*
Accepted: *17 December 2019*
Published: *24 January 2020*

Citation:
Baker FL, Bigley AB, Agha NH, Pedlar CR, O'Connor DP, Bond RA, Bollard CM, Katsanis E and Simpson RJ (2020) Systemic β-Adrenergic Receptor Activation Augments the ex vivo Expansion and Anti-Tumor Activity of Vγ9Vδ2 T-Cells. Front. Immunol. 10:3082. doi: 10.3389/fimmu.2019.03082

TCR-gamma delta (γδ) T-cells are considered important players in the graft-vs.-tumor effect following allogeneic hematopoietic cell transplantation (alloHCT) and have emerged as candidates for adoptive transfer immunotherapy in the treatment of both solid and hematological tumors. Systemic β-adrenergic receptor (β-AR) activation has been shown to mobilize TCR-γδ T-cells to the blood, potentially serving as an adjuvant for alloHCT and TCR-γδ T-cell therapy. We investigated if systemic β-AR activation, using acute dynamic exercise as an experimental model, can increase the mobilization, *ex vivo* expansion, and anti-tumor activity of TCR-γδ T-cells isolated from the blood of healthy humans. We also sought to investigate the β-AR subtypes involved, by administering a preferential β_1-AR antagonist (bisoprolol) and a non-preferential $\beta_1 + \beta_2$-AR antagonist (nadolol) prior to exercise as part of a randomized placebo controlled cross-over experiment. We found that exercise mobilized TCR-γδ cells to blood and augmented their *ex vivo* expansion by ∼182% compared to resting blood when stimulated with IL-2 and ZOL for 14-days. Exercise also increased the proportion of CD56+, NKG2D+/CD62L−, CD158a/b/e+ and NKG2A− cells among the expanded TCR-γδ cells, and increased their cytotoxic activity against several tumor target cells (K562, U266, 221.AEH) *in vitro* by 40–60%. Blocking NKG2D on TCR-γδ cells *in vitro* eliminated the augmented cytotoxic effects of exercise against U266 target cells. Furthermore, administering a $\beta_1 + \beta_2$-AR (nadolol), but not a β_1-AR (bisoprolol) antagonist prior to exercise abrogated the exercise-induced enhancement in TCR-γδ T-cell mobilization and *ex vivo* expansion. Furthermore, nadolol completely abrogated while bisoprolol partially inhibited the exercise-induced increase in the cytotoxic activity of the expanded TCR-γδ T-cells. We conclude that acute systemic β-AR activation in healthy donors markedly augments the mobilization, *ex vivo* expansion, and anti-tumor activity of

TCR-γδ T-cells and that some of these effects are due to β_2-AR signaling and phenotypic shifts that promote a dominant activating signal via NKG2D. These findings highlight β-ARs as potential targets to favorably alter the composition of allogeneic peripheral blood stem cell grafts and improve the potency of TCR-γδ T-cell immune cell therapeutics.

Keywords: exercise immunology, beta-blockers, gamma-delta t-cells, exercise, adoptive transfer immunotherapy

INTRODUCTION

TCR-γδ T-cells comprise 1–5% of the total peripheral blood T-cell pool and predominantly recognize non-classical MHC class I molecules and unconventional antigens such as phosphorylated microbial metabolites and lipids (1). They share properties with NK-cells in that they are capable of killing malignant cells in a non-MHC-restricted manner (2, 3) and have emerged as important players in allogeneic hematopoietic cell transplantation (alloHCT) and immune cell therapy. Prospective studies have shown that the magnitude of TCR-γδ T-cell reconstitution after alloHCT is inversely associated with the incidence of infection (4) and graft-vs.-host disease (GvHD) (5), and is positively associated with leukemia-free and event-free survival (6). The identification of TCR-γδ T-cells as non-alloreactive lymphocytes with potent anti-viral and anti-tumor properties has also seen TCR-γδ T-cells emerge as promising candidates for immunotherapy. The adoptive transfer of *ex vivo* expanded TCR-γδ T-cells has been used successfully to evoke graft- vs.-tumor (GvT) effects against liquid cancers (after alloHCT) such as leukemias and multiple myeloma, and against solid tumors such as renal cell carcinoma, melanoma, and lung cancer (7).

The most widely used method for activating and expanding TCR-γδ T-cells *in vivo* and *ex vivo* is through stimulation with IL-2 and aminobisphosphonates, such as Zoledronate, which preferentially expands the Vγ9Vδ2 subtype (8). However, post-HCT ZOL+IL-2 therapy fails to expand TCR-γδ cells *in vivo* to levels associated with increased survival in ∼58% of alloHCT patients (9), while the *ex vivo* expansion of Vγ9Vδ2 with ZOL+IL-2 for adoptive transfer therapy is sometimes unsuccessful due to low numbers of TCR-γδ T-cells in peripheral blood (10). It is important, therefore, to find new ways of mobilizing TCR-γδ T-cells to enrich peripheral blood hematopoietic stem cell grafts prior to transplant, and also to augment TCR-γδ responses to ZOL+IL-2 both *in vivo* and *ex vivo* (9, 11).

One potential target to increase TCR-γδ T-cell mobilization and expansion is the β-adrenergic receptor (β-AR). Indeed, models of systemic β-AR activation in humans such as dynamic exercise, psychosocial stress, and β-agonist (isoproterenol) infusion have been shown to mobilize large numbers of TCR-γδ T-cells to peripheral blood (12–14). While the β-AR could serve as a therapeutic target to increase the proportion of TCR-γδ T-cells in peripheral blood stem cell grafts (e.g., by administering a β-AR agonist to G-CSF mobilized donors), it is not known if systemic β-AR activation will alter the responsiveness of TCR-γδ T-cells to ZOL+IL-2 *ex vivo* or alter the ability of the expanded cells to recognize and kill tumor targets. Moreover, the β-AR subtype (β_1 vs. β_2) responsible for their mobilization to the blood and potential augmented expansion and anti-tumor activity is not known.

The aim of this study was to determine if systemic β-AR activation, using acute dynamic exercise as an experimental model, can increase the mobilization, *ex vivo* expansion, and anti-tumor activity of TCR-γδ T-cells isolated from the blood of healthy humans. We also sought to determine the β-AR subtypes involved, by administering a preferential β_1-AR antagonist (bisoprolol) and a non-preferential $\beta_1 + \beta_2$-AR antagonist (nadolol) prior to exercise in a randomized placebo controlled cross-over experiment. We show for the first time that systemic β-AR activation *in vivo* augments the mobilization, *ex vivo* expansion, and anti-tumor activity of TCR-γδ T-cells, and that some of these effects are largely mediated by β_2-AR signaling and exercise-induced phenotypic shifts that promote a dominant activating signal via NKG2D.

METHODS

Participants

Fourteen (2 females) healthy cyclists (height: 176.44 ± 2.85 cm, body mass: 77.84 ± 6.91 kg; age: 29.9 ± 6.1 years) volunteered for the first part of this study (Part 1). Participants were excluded if they regularly used any immune modulating medications or tobacco products within the last 6-months, had diagnosed asthma or symptoms of undiagnosed asthma, or had elevated blood pressure, fasting glucose, or fasting cholesterol above normal limits. Participants were required to participate in at least 1–3 h of vigorous exercise per week, corresponding to a score of 5–7 on the Jackson et al. Physical-Activity Rating scale (15). All participants were required to abstain from caffeine consumption and vigorous exercise for 24 h prior to each visit and to arrive at the laboratory following an overnight (8–12 h) fast having consumed only water during this time. A sub-group ($n = 6$; 2 females) of the participants (height: 173.79 ± 9.46 cm, body mass: 72.48 ± 7.84 kg; age: 27.2 ± 3.7 years) also volunteered for the second part of the study (Part 2), which involved taking orally administered β-blockers or placebo prior to exercise. The physiological responses to exercise in the Part 1 group and the Part 2 subgroup are shown in **Table 1**. All experimental procedures were performed at the Laboratory of Integrated Physiology at the University of Houston and all exercise tests were performed between 07:00 and 10:00. Each participant provided written informed consent and the Committee for the Protection of Human Participants (CPHS) at the University of Houston approved the study.

TABLE 1 | Exercise performance and physiological measures of the participants in Part 1 ($n = 14$) and Part 2 ($n = 6$).

	Part 1 ($n = 14$)	Part 2 ($n = 6$)			Trial F (p-value)
		Placebo	Bisoprolol	Nadolol	
Cycling power (watts)	170.71 ± 43.54	150 ± 51.67	150 ± 51.67	150 ± 51.67	ND
Heart rate (bpm)	162.8 ± 11.2	164.5 ± 4.72	127.5 ± 10.84*	120.5 ± 8.22*	99.954 ($p < 0.001$)
Systolic blood pressure (mmHg)	ND	166.7 ± 10.88	141.33 ± 5.54*	137.33 ± 8.52*	63.801 ($p < 0.001$)
Diastolic blood pressure (mmHg)	ND	73 ± 7.21	72.33 ± 5.79	73.5 ± 7.48	0.114 ($p = 0.893$)
Lactate (mM)	3.28 ± 1.47	2.27 ± 0.63	2.67 ± 0.88	2.52 ± 0.73	1.534 ($p = 0.255$)
VO_2 (mL/kg/min)	ND	33.14 ± 10.96	34.8 ± 9.87	35.15 ± 9.15	0.807 ($p = 0.469$)
VE (L/min)	ND	64.72 ± 21.6	72.47 ± 21.2	71.27 ± 22.8	3.567 ($p = 0.064$)
RPE (6–20 Borg Scale)	14.5 ± 1.601	13.83 ± 1.6	15 ± 1.67	15.5 ± 1.87*	6.676 ($p = 0.011$)

*Measures of heart rate, oxygen uptake (VO_2), and ventilation (VE) were averaged during the last 5 min of exercise, while rating of perceived exertion (RPE), capillary blood lactate concentration, and blood pressure were recorded immediately prior to exercise cessation. Data are mean ± SD. ND, not determined. Main effects of trial are reported for the Part 2 participants. Statistical differences from placebo are indicated by *$p < 0.05$.*

Experimental Design

The individual blood lactate threshold (BLT) was determined for each participant using a discontinuous graded exercise protocol we have previously described (16). Participants used either their personal road bike mounted to an indoor cycling ergometer (Computrainer, RacerMate Inc., Seattle, W.A.) or a stationary ergometer provided by the laboratory (Velotron, RacerMate Inc.). For the main exercise trial (Part 1), participants completed a 30-min bout of steady state cycling at a power output corresponding to +10 to +15% of their breakpoint BLT (17). Blood was collected before exercise (Pre-Ex), immediately upon exercise cessation (Post-Ex), and 1 h after exercise completion (1 h-Post). Participants who volunteered for the Part 2 component were asked to visit the laboratory on 5 separate occasions at the same time of day with a period of 7-days interspersed between visits. Participants performed a steady state bout of cycling exercise at a power output corresponding to +10% of the individual BLT 3 h after ingesting: (1) 10 mg bisoprolol (preferential β_1-AR antagonist), (2) 80 mg nadolol (non-preferential β_1+/β_2+AR antagonist), or (3) a placebo. Blood samples were collected immediately prior to drug/placebo ingestion (baseline), 3 h later under resting conditions (Pre-Ex), immediately upon cessation of exercise (Post-Ex), and 1 h after exercise completion (1 h Post-Ex). The tablets were administered in a double-blind fashion and the trials were performed using a block randomization design.

Blood Sampling and Exercise Measures

All intravenous blood samples were collected from an antecubital vein using standard phlebotomy (BD Vacutainer Safety-Lok) and vacutainer tubes spray-coated with sodium-heparin or K_2EDTA (BD Vacutainer Safety-Lok). The K_2EDTA tube was used to determine complete blood counts using an automated hematology analyzer (Mindray BC-2800, Nanshan, Shenzen, PR China) and the sodium-heparin tubes for the isolation of peripheral blood mononuclear cells (PBMCs), immunophenotyping, and *ex vivo* expansion of TCR-γδ T-cells. All resting blood samples were collected from the participant following a 10-min period of seated rest. Participants completed a standardized 10-min warm up (<-10% BLT) prior to engaging in the prescribed exercise intensity and were instructed to maintain a consistent pedaling cadence across all exercise trials The Post-Ex blood sample was collected within 3 min of exercise cessation to ensure the mobilized TCR-γδ T-cells were captured (18). Heart rate and respiratory gas exchange were monitored at rest and continuously during exercise by telemetry and indirect calorimetry (Quark CPET, COSMED, Pavona di Albano Laziale, Italy). Ratings of perceived exertion (RPE; Borg Scale) were recorded at rest and every 5-min during exercise. Capillary blood lactate concentration (P-GM7 Micro-Stat Analyzer, Analox instruments Ltd., London, UK) and blood pressure (Part 2 only) were determined at rest and every 10-min during exercise.

Expansion of TCR-γδ T-Cells

The TCR-γδ T-cells expansion protocol was performed as previously described (8). Briefly, PBMCS were isolated from 10 mL of whole blood collected at Pre-Ex, Post-Ex, and 1 h-Post by density gradient centrifugation (Histopaque-1077, Sigma-Aldrich, St. Louis, MO, USA). PBMCs were counted by flow cytometry and seeded at a concentration of 1×10^6 cells/mL in a 24-well plate with culture media consisting of 100 IU/mL IL-2 and 5 μM of ZOL (Sigma-Aldrich,) in RPMI-1640 (Sigma-Aldrich) with 10% FBS (Sigma-Aldrich) and 1% penicillin streptomycin (Sigma-Aldrich). Media was changed every 3–4 days, with fresh culture media containing 100 IU/mL of IL-2 only (without ZOL). Cells were harvested after 14-days to determine number, phenotype, and function by up to 8-color flow cytometry (MACSQuant 10; Miltenyi Biotec Inc. Bergisch Gladbach, Germany). Expanded TCR-γδ T-cells were enumerated and 2×10^5 cells were labeled with appropriate combinations of the following antibodies, all purchased from eBioscience Inc. (San Diego, CA, USA) unless otherwise stated: CD8-FITC, Vδ2-FITC (BioLegend, San Diego, CA, USA), NKG2C Alexa Flour® 488 (R&D Systems, Minneapolis, MN, USA), CD62L-FITC, CD28-FITC, KLRG1-FITC, CD45RA-FITC, CD3-FITC, TCR-γδ-PE, CD4-PE, CD3-PE, NKG2A-PE (Beckman Coulter, Brea, CA, USA), NKG2D-PE (R&D Systems), CD57-PE, CD27-PE, CD158a-PE (Beckman Coulter), CD158b-PE

(Beckman Coulter), CD18e-PE (Beckman Coulter), CD4-PerCP-Cyanine5.5, CD56-PE-Cyanin5.5, CD8-PerCP-Cyanine5.5, PD-1-PerCP-eFluor-710, TCR-γδ-PerCP (BioLegend), CD3-APC, CD56-APC, Vδ1-APC (Miltenyi), NKp30-APC (Biolegend), NKG2A-APC (Beckman Coulter).

TCR-γδ T-Cell Cytotoxicity Assay With and Without NKG2D Blockade

The HLA-deficient leukemia cell line K562 (ATCC: CCL-243), the HLA-expressing (group 1 HLA-C *0304,*0702) multiple myeloma cell line U266 (ATCC:TIB-196), and the 221.AEH (a HLA-E+ transfectant derived from the 721.221 lymphoma cell line) (19) were maintained as previously described and used as target cells for the cytotoxicity assay (16). On the day of the TCR-γδ T-cells cytotoxicity assay, 3×10^6 target cells were removed and labeled with anti-CD71-FITC and co-cultured with the expanded TCR-γδ T-cells at 0:1 (determine spontaneous death), 1:1, 5:1, 10:1, and 20:1 TCR-γδ T-cell: target cell ratios. All assays were conducted in the presence of RPMI-1640 with 10% FBS and 1% penicillin streptomycin and incubated at 37°C for 4 h in a humidified CO_2 incubator. Flow cytometry was used to determine TCR-γδ T-cell cytotoxic activity following similar methods we have described previously for NK-cells (20). TCR-γδ T-cell cytotoxic activity was calculated as specific lysis (% total lysis – % spontaneous death) and lytic index (number of dead target cells per 100,000 TCR-γδ T-cells). To block activation of TCR-γδ T-cells through the NKG2D receptor, TCR-γδ T-cells were incubated with either media alone, an REA isotype control, or an anti-NKG2D monoclonal antibody (REA, clone REA797) for 30 min prior to performing the TCR-γδ T-cell cytotoxicity assay. Finally, NKG2D ligands were measured on K562 and U266 cells lines using monoclonal antibodies against the following targets: MICA/MICB (Miltenyi), ULBP-2/5/6 (R&D Systems), ULBP-1 (R&D Systems), and ULBP-3 (R&D Systems).

Statistical Analysis

All statistical analyses were completed using SPSS (v24.0, IBM, Chicago, IL). Maximum Likelihood, linear mixed models (LMM) were used to analyze the numeric changes in expansions, cytotoxicity, and phenotypes. The LMM allowed for modeling the dependencies within persons from having multiple measures per person. For Part 1, the model included main effects for exercise time (Pre-Ex, Post-Ex, and 1 h-Post). The effect of NKG2D blockade on TCR-γδ T-cell killing against U266 and K562 was determined by two-way repeated measures ANOVA that included main effects of exercise time (pre-ex and post-ex) and condition (media alone, isotype control, and anti-NKG2D). The model for Part 2 included main effects for exercise time and trial (placebo, bisoprolol, and nadolol), as well as an interaction effect for exercise time and trial. Planned contrasts were used *a priori* to determine overall time effects within each trial (placebo, bisoprolol, or nadolol), the location of the significant time effects (Pre-Ex, Post-Ex, and 1 h-Post), and significant differences across the three trials at each specified time point. All data are represented as the mean ± SD unless otherwise stated and significance was set at $p < 0.05$.

RESULTS

Acute Exercise Mobilizes TCR-γδ T-Cells in a β_2-AR Dependent Manner

First, we examined the effect of exercise on the mobilization of TCR-γδ T-cells to the peripheral blood compartment (**Table 2** and **Figure 1A**). The absolute number ($p < 0.001$; **Table 2**) and percentage ($p < 0.001$; **Figure 1A**) of TCR-γδ T-cells was elevated in blood Post-Ex compared to Pre-Ex and 1 h-Post ($p < 0.01$). When examining the effects of bisoprolol and nadolol on the mobilization of TCR-γδ T-cells after exercise relative to placebo, a main effect of exercise time ($p < 0.001$) and an interaction between exercise time and trial was found for both the absolute number and percentage of TCR-γδ T-cells among CD3+ T-cells ($p < 0.01$; **Table 2** and **Figures 2A,B**). Planned contrasts showed that nadolol but not bisoprolol blunted the effects of exercise on TCR-γδ T-cell mobilization to the blood, indicating the mobilization of TCR-γδ T-cells is dependent on β_2-AR signaling. Neither nadolol nor bisoprolol inhibited the exercise-induced mobilization of total lymphocytes, total CD3+ T-cells, or CD4+ T-cells. Significant time × trial interactions were found for the mobilization of CD8+ T-cells, CD3+/CD4–/CD8– T-cells, and NK-cells with the effect sizes for time were lowest in the nadolol trial (**Table 2**).

Acute Exercise Augments the *ex vivo* Expansion of TCR-γδ T-Cells and Is Dependent on β_2-AR Signaling

We examined the effect of exercise on the expansion of TCR-γδ T-cells (**Figure 1**). As expected, a greater number of TCR-γδ T-cells were present in PBMCs isolated Post-EX compared to both Pre-Ex and 1 h Post-Ex PBMCs ($p < 0.001$; **Figure 1B**). Following 14-day's expansion with ZOL+IL-2, significantly more TCR-γδ T-cells were generated from the PBMCs collected Post-Ex compared to PBMCs collected at baseline/Pre-Ex and 1 h-Post ($p < 0.001$; **Figure 1B**). Also, PBMCs collected at 1 h-Post generated significantly more TCR-γδ T-cells than PBMCs collected at baseline/Pre-Ex ($p < 0.05$; **Figure 1B**). The number of TCR-γδ T-cells generated after 14-days from each TCR-γδ T-cell stimulated on Day-0 was highest from PBMCs collected at 1 h-Post compared to Pre-Ex and Post-Ex ($p < 0.01$; **Figure 1C**). The composition of the expanded TCR-γδ T-cells was primarily Vγ9Vδ2 T-cells (>93%) and exercise had no effect on the percentage and differentiation of Vγ9Vδ2 T-cells among the expanded cell products ($p > 0.05$; **Figures 1D,E**). When examining the effects of bisoprolol and nadolol relative to placebo on the expansion of TCR-γδ T-cells after exercise (**Figure 2**), a main effect of exercise time ($p < 0.001$) and an interaction between exercise time and trial was found ($p = 0.018$; **Figures 2C,E**). Planned contrasts showed that nadolol blunted the exercise-induced increase in TCR-γδ T-cell expansion but bisoprolol did not (**Figure 2E**). Neither nadolol nor bisoprolol affected the percentage of CD3+ T-cells, total TCR-γδ T-cells or Vγ9Vδ2 T-cells among the expanded cell products (**Figures 2F,G**).

TABLE 2 | The total number (cells/μL) of lymphocytes, CD3+ T-cells, CD4+ T-cells, CD8+ T-cells, CD4–/CD8– T-cells, Vγ9Vδ2 T-cells, and NK-cells (CD3–CD56+) before, immediately after, and 1 h after exercise for the participants in Part 1 ($n = 14$) and Part 2 ($n = 6$).

		Baseline	Pre-Ex	Post-Ex	1 h-Post	Time effect F (*p*-value)	Main effects		
							Time	Trial	Interaction
LYMPHOCYTES									
Part 1		ND	1617.9 ± 245.4	3135.7 ± 664.9$^{\#\sim}$	1641.7 ± 365.5	F = 80.37 (<0.001)			
Part 2	Placebo	1816.7 ± 625.03	1700 ± 327.1	3025 ± 479.3$^{*\#\sim}$	1810 ± 386.3	F = 16.71 (<0.001)	F = 43.95	F = 0.45	F = 0.76
	Bisoprolol	1791.7 ± 442.1	2016.7 ± 388.2	3183.3 ± 677.3$^{*\#\sim}$	1760 ± 451.9	F = 18.99 (<0.001)	$p < 0.001$	$p = 0.643$	$p = 0.602$
	Nadolol	1675 ± 448.1	1808.3 ± 327.8	2716.7 ± 805.4$^{*\#\sim}$	1790 ± 449.2	F = 9.77 (<0.001)			
Trial effect:		F = 0.16	F = 0.73	F = 1.6	F = 0.03				
		$p = 0.851$	$p = 0.485$	$p = 0.213$	$p = 0.971$				
CD3+ T-CELLS									
Part 1		ND	1066.2 ± 224.2	1785.5 ± 448.6$^{\#\sim}$	1199 ± 263.3*	F = 39.62 (<0.001)			
Part 2	Placebo	1306.9 ± 483.4	1188.5 ± 225.6	1789.5 ± 356.8$^{*\#\sim}$	1322.3 ± 274.3*	F = 11.86 (<0.001)	F = 28.84	F = 0.21	F = 1.21
	Bisoprolol	1313.1 ± 444.9	1461 ± 361.2	1908.5 ± 476.2$^{*\#\sim}$	1349.8 ± 412.8*	F = 13.18 (<0.001)	$p < 0.001$	$p = 0.816$	$p = 0.316$
	Nadolol	1216.8 ± 421.9	1332.3 ± 326.2	1666 ± 442.5$^{*\#\sim}$	1355.9 ± 411.2*	F = 6.23 (0.001)			
Trial effect:		F = 0.14	F = 0.88	F = 0.7	F = 0.02				
		$p = 0.872$	$p = 0.426$	$p = 0.507$	$p = 0.976$				
CD4+ T-CELLS									
Part 1		ND	646.9 ± 169	1026.1 ± 325$^{\#\sim}$	760.2 ± 222.5	F = 25.94 (<0.001)			
Part 2	Placebo	826.5 ± 371.5	722 ± 188.5	989.7 ± 265.2$^{\#}$	847.7 ± 240.7	F = 5.48 (0.002)	F = 11.8	F = 0.04	F = 1.02
	Bisoprolol	832.8 ± 374.2	889.3 ± 237	1001.4 ± 203$^{\sim}$	850.9 ± 285.6	F = 3.17 (0.032)	$p < 0.001$	$p = 0.959$	$p = 0.424$
	Nadolol	767.9 ± 330.1	823.9 ± 247.4	1014.4 ± 359.5$^{*\#}$	841.7 ± 317.7	F = 5.17 (0.003)			
Trial effect:		F = 0.11	F = 0.62	F = 0.01	F = 0.01				
		$p = 0.895$	$p = 0.549$	$p = 0.987$	$p = 0.987$				
CD8+ T-CELLS									
Part 1		ND	338.1 ± 117.7	582.9 ± 186$^{\#\sim}$	358.8 ± 129	F = 36.8 (<0.001)			
Part 2	Placebo	385.6 ± 178.7	367 ± 148.6	588.2 ± 186.4$^{*\#\sim}$	373.7 ± 165	F = 11.42 (<0.001)	F = 31.64	F = 0.24	F = 2.35
	Bisoprolol	385.7 ± 171.8	460.3 ± 257.3	694.8 ± 379.6$^{*\#\sim}$	405.7 ± 228.3	F = 21.19 (<0.001)	$p < 0.001$	$p = 0.783$	$p = 0.045$
	Nadolol	359.2 ± 146.3	402.2 ± 163.4	500.8 ± 153.9$^{*\#\sim}$	410.4 ± 181.6	F = 3.720 (0.017)			
Trial effect:		F = 0.04	F = 0.387	F = 1.644	F = 0.03				
		$p = 0.960$	$p = 0.683$	$p = 0.215$	$p = 0.974$				
CD4–/CD8– T-CELLS									
Part 1		ND	77.4 ± 37.3	166.9 ± 85.6$^{\#\sim}$	75.2 ± 35.6	F = 26.95 (<0.001)			
Part 2	Placebo	91.3 ± 47.2	95.8 ± 43.5	205.1 ± 100.8$^{*\#\sim}$	95.6 ± 36.7	F = 21.85 (<0.001)	F = 43.33	F = 0.17	F = 2.43
	Bisoprolol	90.5 ± 52.9	106.3 ± 60.7	207.2 ± 69.6$^{*\#\sim}$	88.5 ± 41.7	F = 21.93 (<0.001)	$p < 0.001$	$p = 0.845$	$p = 0.038$
	Nadolol	87 ± 55.4	101.8 ± 44.1	145 ± 59.4*	97.8 ± 53.8	F = 4.42 (0.008)			
Trial effect:		F = 0.01	F = 0.06	F = 2.71	F = 0.08				
		$p = 0.989$	$p = 0.942$	$p = 0.083$	$p = 0.920$				
Vγ9Vδ2 T-CELLS									
Part 1		ND	42.8 ± 32.9	115.6 ± 67.6$^{\#\sim}$	37.9 ± 26.1	F = 31.32 (<0.001)			
Part 2	Placebo	57.5 ± 42	56.5 ± 38.4	145.6 ± 80.5$^{*\#\sim\$}$	44.9 ± 24.2	F = 22.36 (<0.001)	F = 36.33	F = 0.43	F = 3.99
	Bisoprolol	58 ± 49.6	70.3 ± 61.3	147 ± 67.3$^{*\#\sim\$}$	47.9 ± 34	F = 20.37 (<0.001)	$p < 0.001$	$p = 0.657$	$p = 0.002$
	Nadolol	52.3 ± 40.4	56.7 ± 33.2	79.4 ± 47	53.3 ± 32.2	F = 1.58 (0.206)			
Trial effect:		F = 0.03	F = 0.19	F = 4.53	F = 0.07				
		$p = 0.97$	$p = 0.829$	$p = 0.02$	$p = 0.935$				
CD3–CD56+									
Part 1		ND	185.5 ± 62.2	746.3 ± 244.9$^{\#\sim}$	121 ± 44.3	F = 71.41 (<0.001)			
Part 2	Placebo	151 ± 66.6	161.6 ± 64.9	657.2 ± 312.1$^{*\#\sim\$}$	94.2 ± 24.5	F = 17.23 (<0.001)	F = 37.66	F = 2.21	F = 2.41
	Bisoprolol	152 ± 53.6	183.4 ± 75.1	732.5 ± 433.2$^{*\#\sim\$}$	94.1 ± 28.2	F = 22.01 (<0.001)	$p < 0.001$	$p = 0.141$	$p = 0.040$
	Nadolol	145.2 ± 51.4	130.3 ± 49.7	343.7 ± 252.9$^{*\#\sim}$	74.7 ± 19.8*	F = 3.24 (0.03)			
Trial effect:		F = 0.003	F = 0.16	F = 9.4	F = 0.02				
		$p = 0.997$	$p = 0.855$	$p < 0.001$	$p = 0.982$				

*Baseline blood samples were collected from the part 2 participants prior to drug/placebo administration then again 3 h later immediately prior to exercise onset (Pre-Ex). For the part 2 participants, main effects of time, trial, and time x trial interaction effects are shown with the planned contrasts for time and trial. Data are mean ± SD. ND, not determined. Differences from baseline, Pre-Ex, and 1 h post are indicated by *, #, ∼, respectively ($p < 0.05$). Differences from the nadolol trial are indicated by $^{\$}$ ($p < 0.05$).*

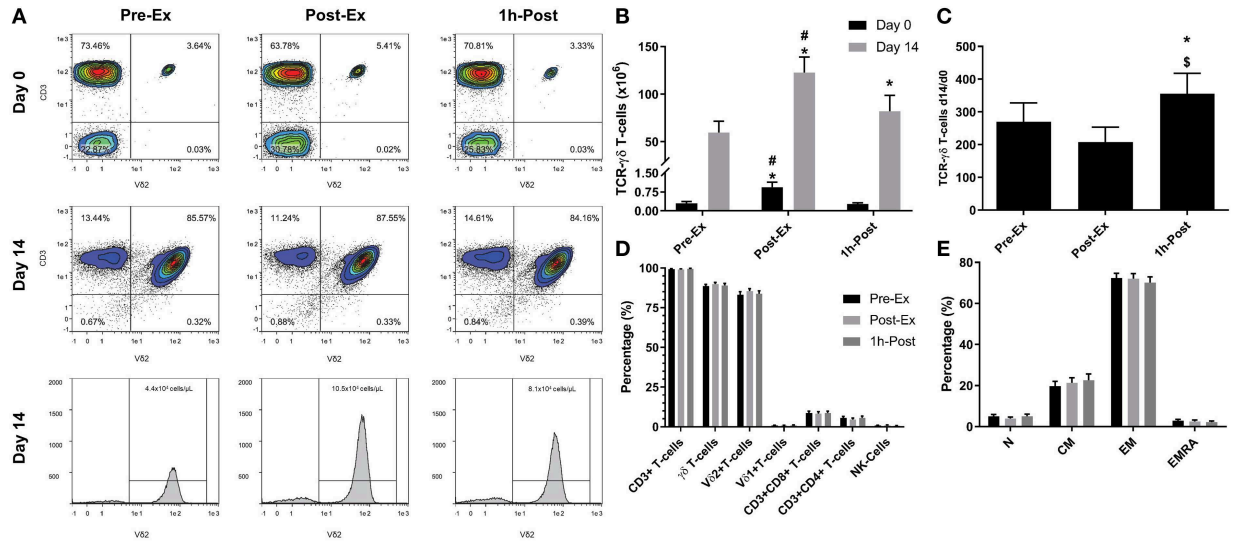

FIGURE 1 | Exercise augments the *ex vivo* expansion of Vγ9δ2 T-cells: **(A)** representative flow cytometry contour plots and histograms showing the effect of exercise on the proportions of Vγ9δ2 T-cells among total PBMCs at Day 0 and after 14-days expansion with ZOL+IL-2. Histogram events are adjusted to reflect the total number of cells isolated per μl of cell culture supernatant. **(B)** The total number of TCR-γδ cells in 1×10^6 PBMCs isolated before (Pre-Ex), immediately after (Post-Ex), and 1 h after exercise (1 h-Post) at Day 0, and the total number of TCR-γδ T-cells generated in the expanded cell products after 14-days stimulation with ZOL+IL-2. Significant differences were only determined within expansion period (Day 0 or 14) and not between. **(C)** The number of TCR-γδ cells generated at Day 14 divided by the number of TCR-γδ cells in the PBMC fractions at Day 0. **(D)** The cellular composition of the expanded TCR-γδ T-cell products at Day 14. **(E)** The proportions of naïve (N), central memory (CM), effector memory (EM), and CD45RA+ effector memory (EMRA) cells among total TCR-γδ T-cells. Values are mean ± SE ($n = 14$). Differences from Pre-Ex, Post-Ex, and 1 h-Post are indicated by *, $, and #, respectively ($p < 0.05$).

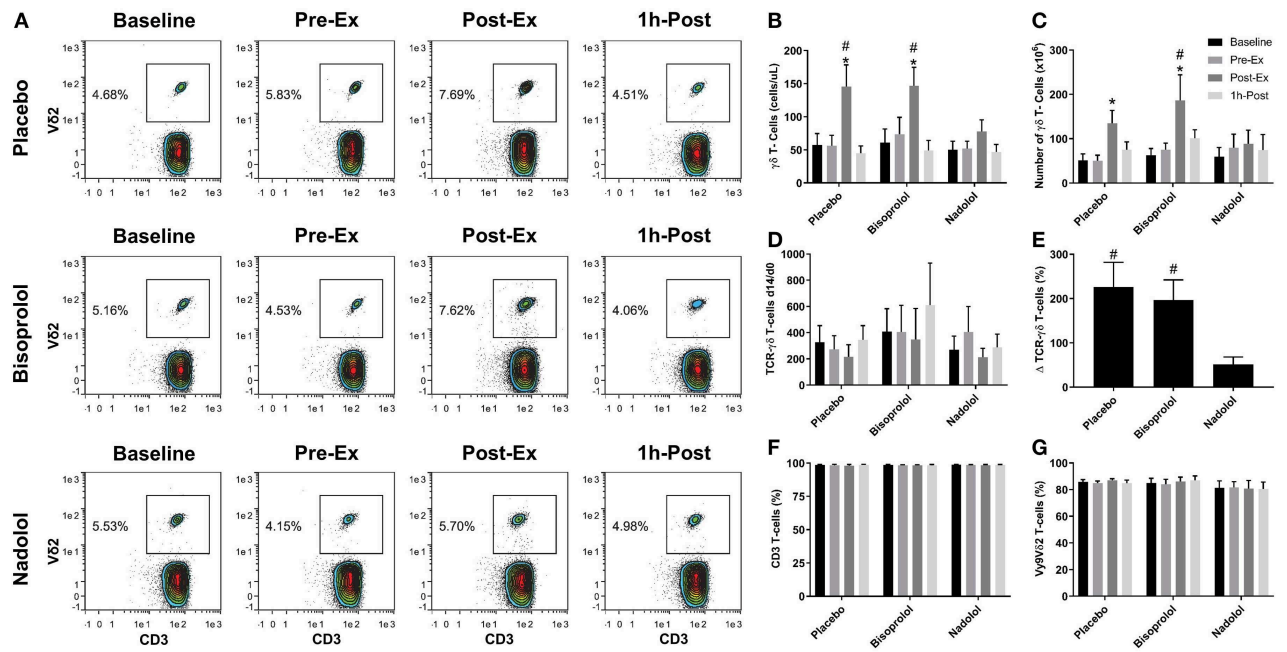

FIGURE 2 | $\beta_1 + \beta_2$-AR but not β_1-AR blockade alone inhibits the mobilization and augmented *ex vivo* expansion of Vγ9δ2 T-cells in response to exercise. **(A)** Representative flow cytometry contour plots showing the effects of a $\beta_1 + \beta_2$-AR antagonist (nadolol) and a β_1-AR antagonist (bisoprolol) on the mobilization of Vγ9δ2 T-cells with exercise. Values shown are the percentage of all CD3+ T-cells. **(B)** The total numbers of TCR-γδ T-cells in blood before and after exercise. After 14 days' expansion with ZOL+IL-2, **(C)** the total number, **(D)** the number of TCR-γδ cells generated at Day 14 divided by the number of TCR -γδ cells in the PBMC fractions at Day 0 and **(E)**, percentage change in number of TCR-γδ T-cells expanded Post-Ex relative to baseline. The percentage of **(F)** CD3+ and **(G)** Vγ9Vδ2+ T-cells among the expanded cell products are shown. Values are mean ± SE ($n = 6$). Significant difference from Baseline/Pre-Ex/1 h-Post and the nadolol trial indicated by * and #, respectively ($p < 0.05$).

Acute Exercise Drives Expanded TCR-γδ T-Cells Toward an Activated Phenotype With Anti-Tumor and Tissue Migration Potential

We performed a detailed phenotypic analysis of the expanded TCR-γδ T-cell products, focusing on the expression of surface markers associated with activation, inhibition, homing, differentiation, and exhaustion (**Figure 3**). We found that Post-Ex expanded TCR-γδ T-cells had higher proportions of CD56+ ($p < 0.01$), NKG2D+/CD62L– ($p < 0.01$), CD158b+ ($p < 0.05$), and CD158e+ ($p < 0.05$) and decreased proportions of NKG2A+ ($p < 0.05$), CD62L+ ($p < 0.001$), NKG2D+/CD62L– ($p < 0.01$) compared to Pre-Ex and 1 h-Post expanded TCR-γδ T-cells (**Figure 3A**). There was no effect of exercise ($p > 0.05$) on the proportions of TCR-γδ T-cells expressing PD-1, indicating that the augmenting effects of exercise did not drive the TCR-γδ T-cell product to exhaustion after 14-days expansion (**Figure 3A**). Administering nadolol but not bisoprolol prior to exercise inhibited the phenotypic shifts seen in the expanded TCR-γδ T-cell products, particularly for CD56+ (**Figure 3B**). Conversely, the proportion of Post-Ex NKG2D+/CD62L– expanded TCR-γδ T-cells was inhibited by administration of bisoprolol or nadolol prior to exercise (**Figure 3B**). These results indicate that exercise drives phenotypic changes within the expanded TCR-γδ T-cell products that are associated with increased cytotoxicity and tissue migration potential in a manner that is also dependent on β_2-AR signaling.

Acute Exercise Augments the *in vitro* Cytotoxicity of the Expanded TCR-γδ T-Cell Products in a Manner That Is Dependent on Both β_1-AR and β_2-AR Signaling

We examined the function of expanded TCR-γδ T-cells by determining their *in vitro* cytotoxicity against three different tumor cells lines, K562, U266, and 221.AEH (**Figure 4**). The TCR-γδ T-cells expanded Post-Ex had increased cytotoxic activity against all tumor targets compared to TCR-γδ T-cells expanded at both Pre-Ex and 1 h-Post ($p < 0.01$; **Figures 4A–C**). This finding held true when data were expressed as specific lysis, lytic index, and total killing capacity (data not shown). The effects of nadolol and bisoprolol on the cytotoxicity of TCR-γδ T-cells expanded after exercise were assessed for the K562 and U266 cell lines only. Due to the small sample size and large intrasubject variability, these data are expressed as a percentage change in killing capacity of the Post-Ex expanded TCR-γδ T-cells compared to those expanded Pre-Ex (**Figures 4D,E**). Compared to placebo, nadolol abrogated the exercise-induced increase in the cytotoxic activity of the expanded TCR-γδ T-cell products against both the K562 and the U266 cell line. Bisoprolol was found to inhibit the exercise effects on the cytotoxic activity of the expanded TCR-γδ T-cells, but not to the same extent as nadolol. These findings indicate that TCR-γδ T-cells expanded immediately after exercise have increased anti-tumor activity compared to TCR-γδ T-cells expanded at rest and during the early (1 h-Post) stage of exercise recovery, and that the exercise effects are dependent on both β_1-AR and β_2-AR signaling.

Exercise Increases TCR-γδ T-Cell Cytotoxic Activity Against U266 Target Cells Through NKG2D Dependent Signaling

A greater proportion of TCR-γδ T-cells expanded Post-Ex displayed an NKG2D+/CD62L– phenotype compared to those expanded at Pre-Ex. We, therefore, examined the effects of blocking the NKG2D receptor on TCR-γδ T-cells prior to performing the *in vitro* cytotoxicity assay against U266 and K562 tumor cells. NKG2D blockade on Pre-Ex expanded TCR-γδ T-cells did not alter cytotoxic activity against U266 cells ($p > 0.05$) but the enhanced cytotoxic effect of TCR-γδ T-cells expanded Post-Ex was abrogated by NKG2D blockade ($p < 0.05$; **Figure 5B**). Blocking NKG2D had no impact on the exercise-induced increase in TCR-γδ T-cell cytotoxicity against K562 tumor cells (data not shown). Tellingly, the U266 cell line had a greater surface expression of the NKG2D ligands MICA/MICB, ULBP-1, and ULBP-3 compared to K562 cells (**Figure 5A**).

DISCUSSION

TCR-γδ T-cells have emerged as an important subset of effector lymphocytes in allo-HCT and adoptive transfer immunotherapy due to their ability to attack a wide range of solid and hematological tumors without causing GvHD. However, the low frequency of TCR-γδ T-cells in the peripheral blood of healthy donors limits their therapeutic potential. We have demonstrated that systemic β-AR activation, using acute dynamic exercise as an experimental model, mobilizes TCR-γδ T-cells to the peripheral blood and, for the first time here, augments their *ex vivo* expansion and anti-tumor activity. These adjuvant effects of exercise were associated with certain phenotypic shifts and found to be largely dependent on β_2-AR signaling, as they were abrogated by administering a $\beta_1 + \beta_2$-AR antagonist (nadolol) but not a β_1-antagonist (bisoprolol) prior to exercise. These findings highlight the β_2-AR as a potential therapeutic target to mobilize TCR-γδ T-cells in healthy alloHCT donors and to also increase the potency of TCR-γδ T-cell therapeutics.

Prior studies have demonstrated that systemic β-AR activation using either exercise or isoproterenol infusion, increases the number of circulating TCR-γδ T-cells 2–4-fold (12, 14). We have shown previously that exercise has potent adjuvant effects on the mobilization and *ex vivo* manufacture of viral specific T-cells and were interested to evaluate whether these findings extend to TCR-γδ T-cells also (21–23). This is particularly pertinent as TCR-γδ T-cell reconstitution after alloHCT has been associated with improved leukemia free survival and protection against GvHD (4–6). The *ex vivo* manufacture and adoptive transfer of TCR-γδ T-cells are being applied to elicit GvT effects in alloHCT recipients and in the treatment of solid tumors such as renal cell carcinoma, melanoma, lung cancer, and neuroblastoma (7). We determined that just 30-min of intensity-controlled exercise increased the numbers of TCR-γδ T-cells in peripheral blood almost 3-fold ($\sim\Delta$ 73 cells/μL). This allowed us to manufacture 2-times more TCR-γδ T-cells

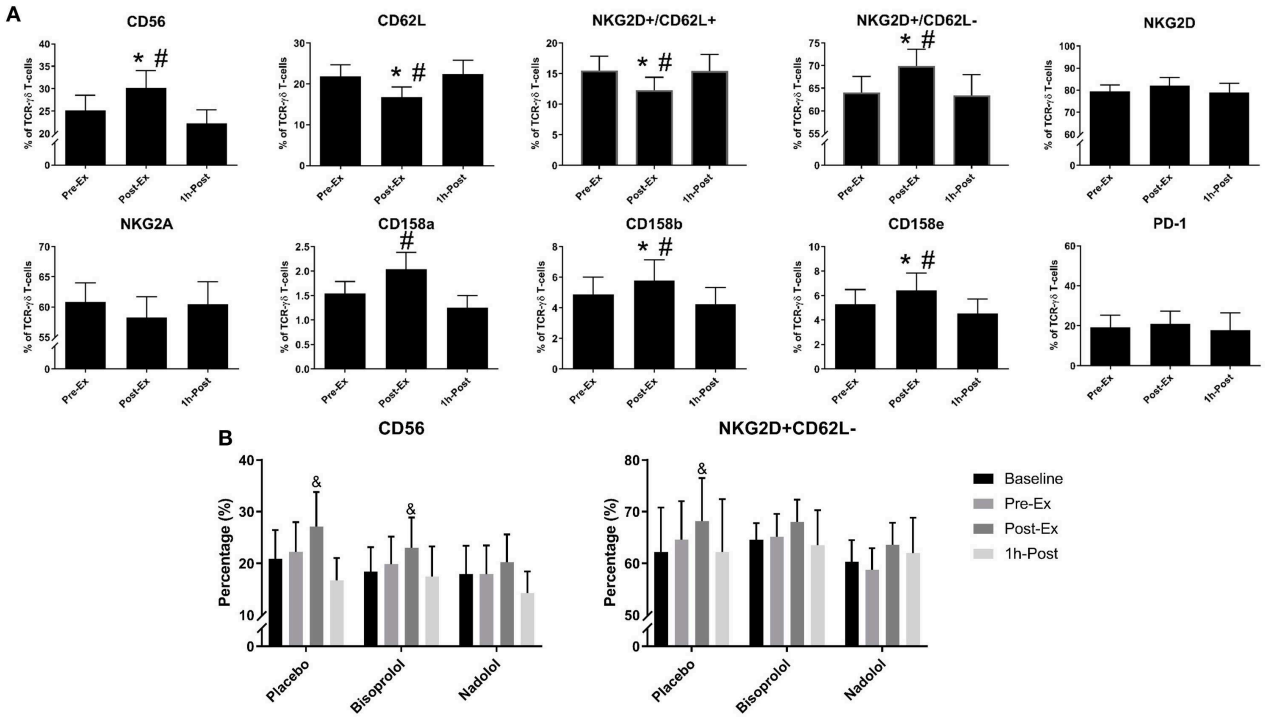

FIGURE 3 | Exercise alters the surface phenotypes of *ex vivo* expanded TCR-γδ T-cells. **(A)** The percentage of CD56+, CD62L+, NKG2D+/CD62L+, NKG2D+/CD62L–, NKG2D+, NKG2A+, CD158a+, CD158b+, CD158e+, and PD-1+ cells among total TCR-γδ T-cells after 14-days expansion ($n = 14$). **(B)** The effects of administering a placebo, bisoprolol, or nadolol prior to exercise on the proportions of CD56+ and NKG2D+/CD62L– cells among total TCR-γδ T-cells after 14-days expansion ($n = 6$). Values are mean ± SE. Significant differences from baseline, Pre-Ex, and 1 h-Post are indicated by &,*, and #, respectively ($p < 0.05$).

from blood samples collected during exercise compared to rest. Moreover, the TCR-γδ T-cells expanded after exercise had a greater surface expression of several activating receptors, a lowered expression of inhibitory receptors, and were found to have superior cytolytic activity *in vitro* against various tumor targets than TCR-γδ T-cells expanded at rest. The limited therapeutic application of TCR-γδ T-cells to date has been attributed to low circulating numbers in healthy transplant donors (1–5% of blood lymphocytes) (8). This results in low numbers of TCR-γδ T-cells in peripheral blood stem cell grafts of G-CSF mobilized donors, which could be partially responsible for poor TCR-γδ T-cell reconstitution in alloHCT patients posttransplant (4, 24). Using systemic β-AR activation to enrich G-CSF mobilized peripheral blood stem cell grafts with TCR-γδ T-cells could also improve *ex vivo* graft engineering methods such as TCR-αβ+CD19 depletion (25), which are designed to protect against GvHD and EBV-induced lymphoproliferative disease but retain TCR-γδ T-cells and NK-cells in the graft to maintain anti-tumor activity. This could help overcome some reported limitations with this method such as graft failure and poor immune reconstitution, which leads to an increased incidence of relapse and infection (26). Moreover, although ZOL+IL-2 has been used to expand TCR-γδ T-cells (Vδ2 subset) *in vitro* and *in vivo*, TCR-γδ T-cells respond poorly to ZOL+IL-2 in some patients and donors (8, 10, 27–30). The current findings indicate that systemic β-AR activation is a simple, economical, and effective adjuvant for the potential enrichment of peripheral blood stem cell grafts with TCR-γδ T-cells, and also for increasing their responsiveness to exogenous cytokines and phosphoantigens such as ZOL+IL-2. This could be effective, not only for the *ex vivo* manufacture of TCR-γδ T-cell products shown here, but also for expanding TCR-γδ T-cells *in vivo* following alloHCT using subcutaneous ZOL+IL-2 injections.

Our finding that the adjuvant effects of exercise are largely dependent on β_2-AR signaling has important practical applications as it might allow us to further optimize potential pharmaceutical interventions for mobilizing and expanding TCR-γδ T-cells in healthy donors. Administering a preferential β_1-AR antagonist (e.g., bisoprolol) prior to exercise or isoproterenol infusion is likely to provide the required β_2-AR stimulation to mobilize and activate TCR-γδ T-cells without causing sustained elevations in heart rate and systolic blood pressure, which is predominantly a β_1-AR mediated effect (31). Indeed, we found that both bisoprolol and nadolol blunted the exercise-induced increases in heart rate and blood pressure but the adjuvant effects of exercise were still apparent in the bisoprolol trial. This finding likely excludes increases in hemodynamic shear stress as a potential mechanism for the adjuvant effects of exercise on TCR-γδ T-cell mobilization and *ex vivo* expansion. Bisoprolol did, however, blunt the effects of exercise on the cytotoxic capabilities of the expanded TCR-γδ T-cell product suggesting a role for both β_1-ARs and β_2-ARs in improving the function of

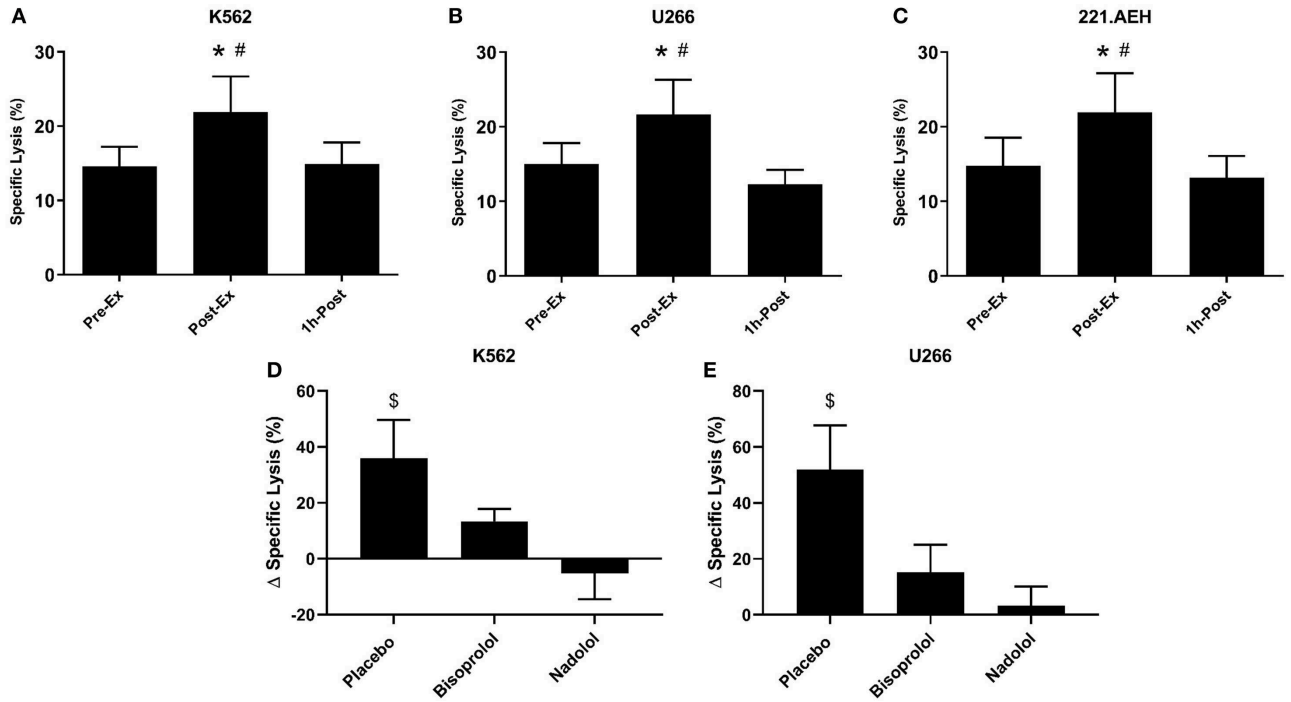

FIGURE 4 | Exercise augments the anti-tumor activity of *ex vivo* expanded TCR-γδ T-cells in a manner that is dependent on both β_1 and β_2-AR signaling. The percentage of K562 **(A)**, U266 **(B)**, and 221.AEH **(C)** target cells killed by the expanded TCR-γδ T-cells at an E:T ratio of 10:1 following 14-days expansion with ZOL+IL-2 ($n = 14$). The effects of placebo, bisoprolol, and nadolol on the exercise-induced changes in specific lysis against K562 **(D)** and U266 **(E)** target cells following *ex vivo* expansion ($n = 6$). Values are mean ± SE. Differences from Pre-Ex are indicated by * and differences from 1 h-Post are indicated by #, $p < 0.05$. Differences from the nadolol trial are indicated by $, $p < 0.05$.

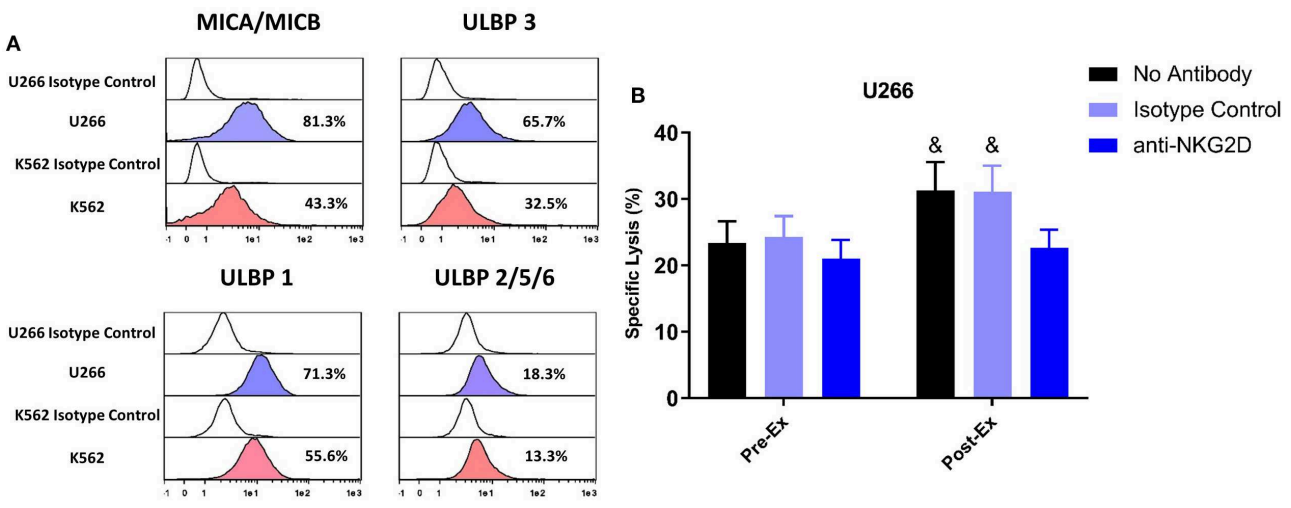

FIGURE 5 | Enhanced cytotoxic effect of exercise expanded TCR-γδ T-cells against U266 cells is dependent on NKG2D signaling. **(A)** The expression of NKG2D ligands, MICA/MICB, ULBP 3, ULBP 1, and ULBP 2/5/6 on U266 and K562 target cell lines. **(B)** The percentage of U266 cells killed by Pre-Ex and Post-Ex expanded TCR-γδ T-cells under 3 different conditions: no antibody (media), isotype control (REA), and anti-NKG2D. Values are mean ± SE. Differences from Post-Ex anit-NKG2D condition are indicated by &, $p < 0.05$.

ex vivo expanded TCR-γδ T-cells. An important observation was the augmented *ex vivo* expansion of the TCR-γδ T-cells expanded from blood collected 1 h after exercise cessation compared to rest. As the numbers of TCR-γδ T-cells in blood at this time were lower than at rest, this indicates that the adjuvant effects of exercise are not merely due to increased numbers of TCR-γδ T-cells within a fixed volume of blood.

Previous studies have shown that ZOL+IL-2 expands a TCR-γδ T-cell product with a high surface expression of the activating receptors NKG2D, TRAIL, DNAM-1, an increased expression of perforin and granzyme-B, and transforms the cells to an effector/central memory phenotype (8, 10, 32). Regardless of whether blood samples were collected at rest, during, or in the recovery phase of exercise, the 14-day *ex vivo* expansion with ZOL+IL-2 generated a cell product that was >98% pure for CD3+ T-cells. This expanded cell product consisted primarily of CD3+/CD4–/CD8– Vγ9Vδ2 T-cells with few CD8+ and CD4+ T-cells and almost no NK-cells (<1%). Similarly, administering nadolol or bisoprolol prior to exercise had no impact on the purity of the expanded TCR-γδ T-cell product. However, we did find some phenotypic differences in the TCR-γδ T-cell products expanded from exercised compared to resting blood. Notably, greater proportions of NKG2D+/CD62L−, CD56+, CD158a+, CD158b+, and CD158e+ and decreased proportions of NKG2A+ and CD62L+ cells were found among the Vγ9Vδ2+ T-cells expanded after exercise. As TCR-γδ T-cells recognize stress-associated antigens such as MICA/B and nectin-like-5 via NKG2D and DNAM-1, respectively (33), it is possible that these phenotypic changes on the expanded cell product with exercise are responsible for the augmented cytotoxic effects seen against the K562, U266, and 221.AEH cell lines *in vitro*. Indeed, although expression of the activating receptor NKG2D was not upregulated by exercise on the expanded TCR-γδ T-cells, blocking NKG2D *in vitro* abrogated the enhanced cytotoxic effects of the TCR-γδ T-cells expanded after exercise against U266 target cells. This indicates that exercise evokes phenotypic shifts (mainly a downregulation of inhibitory receptors) that allow activation signals via NKG2D to be more dominant. However, blocking NKG2D did not eliminate the enhancing effects of exercise on the cytotoxic effects of TCR-γδ T-cells against the K562 target cell line. This could be due to our U266 target cells expressing higher levels of the NKG2D ligands MICA/MICB ULBP-1 and ULBP-3 than the K562 cells, corroborating what has been published previously (34, 35). Moreover, nadolol prevented some of the phenotypic shifts seen with exercise (e.g., CD56+ and NKG2D+/CD62L–) concomitantly with an abrogation of the exercise-induced improvements in TCR-γδ T-cell cytotoxicity. It remains possible that the enhanced cytotoxic effects of TCR-γδ T-cells against K562 target cells with exercise are due to phenotypic shifts we did not capture in our study. Also, because we only tested the effects of β-AR blockade on a subgroup of participants, this might explain why nadolol did not abrogate all of the phenotypic changes observed during the main exercise trial to a level that reached statistical significance.

Exercise is known to preferentially mobilize TCR-γδ T-cells with a differentiated phenotype, increasing proportions of effector memory (EM), CD45RA+ EM (EMRA), and central memory (CM) cells among total TCR-γδ T-cells in blood (16, 36, 37). However, expanding TCR-γδ T-cells *ex vivo* overrode these phenotypic shifts of exercise, as similar proportions of naïve (∼5%), EM (∼71%), CM (∼21%), and EMRA (∼3%) cells were found among the expanded Vγ9Vδ2+ T-cells regardless of whether blood samples were collected before, during, or in the recovery phase of exercise. Previous studies have shown that IPP and Zoledronate stimulation causes a shift toward an EM phenotype in expanded Vγ9Vδ2+ T-cells and these cells have enhanced cytotoxic activity and increased IFN-γ release in response to activation (8, 10, 38, 39).

A limitation of the present study is that we only attempted to expand Vγ9Vδ2+ and not Vδ1+ T-cells with exercise. Although Vγ9Vδ2+ T-cells are the most abundant subset of TCR-γδ T-cells in blood, the Vδ1+ subset is known to play a prominent role in anti-tumor immunity and in the resolution of viral infections such as cytomegalovirus (40). We did not expect to find increased numbers of Vδ1+ T-cells in our expanded products as this subset of TCR-γδ T-cells do not respond to aminobisphosphonates. There are methods for the *ex vivo* expansion and adoptive transfer of Vδ1+ cells has been used in the treatment of multiple myeloma (41), colon cancer (42), B-cell chronic lymphocytic leukemia (43), and glioblastoma (44), but it remains to be seen if systemic β-AR activation can augment the *ex vivo* manufacture of this cell type also. It is also possible that the adjuvant effects of exercise on the *ex vivo* expansion of TCR-γδ T-cells are monocyte-dependent. Previous studies have shown that removing monocytes from culture results in no expansion of TCR-γδ T-cells when stimulated with ZOL+IL-2 (45). When aminobiphosphates such as ZOL are taken up by monocytes, they block farnesyl pyrophosphate synthase (FPPS) resulting in an intracellular accumulation of isopentenyl phosphate (IPP) via the mevalonate pathway. Subsequent cell-to-cell contact then triggers the activation and expansion of Vγ9Vδ2 T-cells (46). Exercise is known to cause proportional and phenotypic changes within the blood monocyte population (18, 47–50) and it is possible that these are driving the adjuvant effects of exercise on the *ex vivo* expansion and increased cytotoxicity of TCR-γδ T-cells. Specifically, exercise increases the proportions and absolute number of non-classical monocytes, which release higher levels of pro inflammatory cytokines (e.g., TNF-α and IL-18) that are essential for the activation and expansion of Vγ9Vδ2 T-cells (51). Moreover, the activation of Vγ9Vδ2 T-cells by ZOL and IPP requires expression of butyrophilin BTN3A molecules on monocytes (52), which could also be affected by exercise. Future studies should determine the role monocytes play in activating and expanding TCR-γδ T-cells after exercise. It will also be important to determine if the TCR-γδ T-cells expanded with systemic β-AR activation persist following adoptive transfer and exert improved anti-tumor effects *in vivo*.

In summary, this is the first study to show that systemic β-AR activation augments the *ex vivo* expansion and anti-tumor cytotoxicity of Vγ9Vδ2 T-cells in healthy humans. We have also demonstrated that these effects are largely mediated by catecholamine signaling through the β_2-AR subtype and exercise-induced phenotypic shifts among the expanded Vγ9Vδ2 T-cells that promote a dominant activating signal through the NKG2D receptor. Future studies should determine if targeted β_1-AR and/or β_2-AR activation in allogeneic donors can generate superior G-CSF mobilized peripheral stem cell grafts and increase

the potency of TCR-γδ T-cell therapeutics to elicit more positive outcomes in alloHCT patients and patients with solid tumors.

DATA AVAILABILITY STATEMENT

The datasets generated for this study are available on request to the corresponding author.

ETHICS STATEMENT

The studies involving human participants were reviewed and approved by Committee for the Protection of Human Participants (CPHS) at the University of Houston. The patients/participants provided their written informed consent to participate in this study.

AUTHOR CONTRIBUTIONS

RS, CB, RB, and FB developed the theoretical framework, working hypotheses, and designed the study. FB, AB, and NA performed the laboratory experiments and analyzed results. FB, RS, AB, CB, EK, RB, CP, and DO'C interpreted data. FB and RS wrote the manuscript with contributions from AB, CB, EK, DO'C, CP, and RB. The statistical analyses were performed by FB and DO'C. The overall study was supervised by RS.

FUNDING

This work was supported by NASA Grants NNX12AB48G, NNX16AB29G, and NNX16AG02G and NIH Grant R21 CA197527-01A1.

REFERENCES

1. Lawand M, Dechanet-Merville J, Dieu-Nosjean MC. Key features of gamma-delta T-cell subsets in human diseases and their immunotherapeutic implications. *Front Immunol.* (2017) 8:761. doi: 10.3389/fimmu.2017.00761
2. Kabelitz D, Kalyan S, Oberg HH, Wesch D. Human Vdelta2 vs. non-Vdelta2 gammadelta T cells in antitumor immunity. *Oncoimmunology.* (2013) 2:e23304. doi: 10.4161/onci.23304
3. Vantourout P, Hayday A. Six-of-the-best: unique contributions of gammadelta T cells to immunology. *Nat Rev Immunol.* (2013) 13:88–100. doi: 10.1038/nri3384
4. Perko R, Kang G, Sunkara A, Leung W, Thomas PG, Dallas MH. γδ T cell reconstitution is associated with fewer infections and improved event-free survival after hematopoietic stem cell transplantation for pediatric leukemia. *Biol Blood Marrow Transplant.* (2015) 21:130–6. doi: 10.1016/j.bbmt.2014.09.027
5. Hu Y, Cui Q, Luo C, Luo Y, Shi J, Huang H. A promising sword of tomorrow: human gammadelta T cell strategies reconcile allo-HSCT complications. *Blood Rev.* (2016) 30:179–88. doi: 10.1016/j.blre.2015.11.002
6. Godder KT, Henslee-Downey PJ, Mehta J, Park BS, Chiang KY, Abhyankar S, et al. Long term disease-free survival in acute leukemia patients recovering with increased gammadelta T cells after partially mismatched related donor bone marrow transplantation. *Bone Marrow Transplant.* (2007) 39:751–7. doi: 10.1038/sj.bmt.1705650
7. Hoeres T, Smetak M, Pretscher D, Wilhelm M. Improving the efficiency of Vγ9Vδ2 T-cell immunotherapy in cancer. *Front Immunol.* (2018) 9:800. doi: 10.3389/fimmu.2018.00800
8. Kondo M, Izumi T, Fujieda N, Kondo A, Morishita T, Matsushita H, et al. Expansion of human peripheral blood gammadelta T cells using zoledronate. *J Vis Exp.* (2011) 55:3182. doi: 10.3791/3182
9. Bertaina A, Zorzoli A, Petretto A, Barbarito G, Inglese E, Merli P, et al. Zoledronic acid boosts gammadelta T-cell activity in children receiving alphabeta(+) T and CD19(+) cell-depleted grafts from an HLA-haplo-identical donor. *Oncoimmunology.* (2017) 6:e1216291. doi: 10.1080/2162402X.2016.1216291
10. Kondo M, Sakuta K, Noguchi A, Ariyoshi N, Sato K, Sato S, et al. Zoledronate facilitates large-scale *ex vivo* expansion of functional gammadelta T cells from cancer patients for use in adoptive immunotherapy. *Cytotherapy.* (2008) 10:842–56. doi: 10.1080/14653240802419328
11. Pressey JG, Adams J, Harkins L, Kelly D, You Z, Lamb LSJr. *In vivo* expansion and activation of gammadelta T cells as immunotherapy for refractory neuroblastoma: a phase 1 study. *Medicine.* (2016) 95:e4909. doi: 10.1097/MD.0000000000004909
12. Anane LH, Edwards KM, Burns VE, Drayson MT, Riddell NE, van Zanten JJ, et al. Mobilization of gammadelta T lymphocytes in response to psychological stress, exercise, and beta-agonist infusion. *Brain Behav Immun.* (2009) 23:823–9. doi: 10.1016/j.bbi.2009.03.003
13. Gustafson MP, DiCostanzo AC, Wheatley CM, Kim CH, Bornschlegl S, Gastineau DA, et al. A systems biology approach to investigating the influence of exercise and fitness on the composition of leukocytes in peripheral blood. *J Immunother Cancer.* (2017) 5:30. doi: 10.1186/s40425-017-0231-8
14. Pistillo M, Bigley AB, Spielmann G, LaVoy EC, Morrison MR, Kunz H, et al. The effects of age and viral serology on gammadelta T-cell numbers and exercise responsiveness in humans. *Cell Immunol.* (2013) 284:91–7. doi: 10.1016/j.cellimm.2013.07.009
15. Jackson AS, Blair SN, Mahar MT, Wier LT, Ross RM, Stuteville JE. Prediction of functional aerobic capacity without exercise testing. *Med Sci Sports Exerc.* (1990) 22:863–70. doi: 10.1249/00005768-199012000-00021
16. Bigley AB, Rezvani K, Chew C, Sekine T, Pistillo M, Crucian B, et al. Acute exercise preferentially redeploys NK-cells with a highly-differentiated phenotype and augments cytotoxicity against lymphoma and multiple myeloma target cells. *Brain Behav Immun.* (2014) 39:160–71. doi: 10.1016/j.bbi.2013.10.030
17. Weltman A. *The Blood Lactate Response to Exercise*. Champaign, IL: Human Kinetics (1995).
18. Rooney BV, Bigley AB, LaVoy EC, Laughlin M, Pedlar C, Simpson RJ. Lymphocytes and monocytes egress peripheral blood within minutes after cessation of steady state exercise: a detailed temporal analysis of leukocyte extravasation. *Physiol Behav.* (2018) 194:260–7. doi: 10.1016/j.physbeh.2018.06.008
19. Lee N, Goodlett DR, Ishitani A, Marquardt H, Geraghty DE. HLA-E surface expression depends on binding of TAP-dependent peptides derived from certain HLA class I signal sequences. *J Immunol.* (1998) 160:4951–60.
20. Bigley AB, Agha NH, Baker FL, Spielmann G, Kunz HE, Mylabathula PL, et al. NK-cell function is impaired during long-duration spaceflight. *J Appl Physiol.* (2018) 126:842–53. doi: 10.1152/japplphysiol.00761.2018
21. Kunz HE, Spielmann G, Agha NH, O'Connor DP, Bollard CM, Simpson RJ. A single exercise bout augments adenovirus-specific T-cell mobilization and function. *Physiol Behav.* (2018) 194:56–65. doi: 10.1016/j.physbeh.2018.04.035
22. Simpson RJ, Bigley AB, Agha N, Hanley PJ, Bollard CM. Mobilizing immune cells with exercise for cancer immunotherapy. *Exerc Sport Sci Rev.* (2017) 45:163–72. doi: 10.1249/JES.0000000000000114
23. Spielmann G, Bollard CM, Kunz H, Hanley PJ, Simpson RJ. A single exercise bout enhances the manufacture of viral-specific T-cells from healthy donors: implications for allogeneic adoptive transfer immunotherapy. *Sci Rep.* (2016) 6:25852. doi: 10.1038/srep25852
24. Airoldi I, Bertaina A, Prigione I, Zorzoli A, Pagliara D, Cocco C, et al. gammadelta T-cell reconstitution after HLA-haploidentical hematopoietic transplantation depleted of TCR-alphabeta+/CD19+ lymphocytes. *Blood.* (2015) 125:2349–58. doi: 10.1182/blood-2014-09-599423
25. Locatelli F, Lucarelli B, Merli P. Current and future approaches to treat graft failure after allogeneic hematopoietic stem cell transplantation. *Expert Opin Pharmacother.* (2014) 15:23–36. doi: 10.1517/14656566.2014.852537

26. Lo Presti E, Corsale AM, Dieli F, Meraviglia S. γδ cell-based immunotherapy for cancer. *Expert Opin Biol Ther*. (2019) 19:887–95. doi: 10.1080/14712598.2019.1634050
27. Kunzmann V, Bauer E, Feurle J, Weissinger F, Tony HP, Wilhelm M. Stimulation of gammadelta T cells by aminobisphosphonates and induction of antiplasma cell activity in multiple myeloma. *Blood*. (2000) 96:384–92. doi: 10.1182/blood.V96.2.384.013k07_384_392
28. Salot S, Bercegeay S, Dreno B, Saiagh S, Scaglione V, Bonnafous C, et al. Large scale expansion of Vgamma9Vdelta2 T lymphocytes from human peripheral blood mononuclear cells after a positive selection using MACS "TCR gamma/delta+ T cell isolation kit". *J Immunol Methods*. (2009) 347:12–8. doi: 10.1016/j.jim.2009.05.006
29. Wilhelm M, Kunzmann V, Eckstein S, Reimer P, Weissinger F, Ruediger T, et al. Gammadelta T cells for immune therapy of patients with lymphoid malignancies. *Blood*. (2003) 102:200–6. doi: 10.1182/blood-2002-12-3665
30. Wilhelm M, Smetak M, Schaefer-Eckart K, Kimmel B, Birkmann J, Einsele H, et al. Successful adoptive transfer and *in vivo* expansion of haploidentical gammadelta T cells. *J Transl Med*. (2014) 12:45. doi: 10.1186/1479-5876-12-45
31. Wheeldon NM, McDevitt DG, Lipworth BJ. The effects of lower than conventional doses of oral nadolol on relative beta 1/beta 2-adrenoceptor blockade. *Br J Clin Pharmacol*. (1994) 38:103–8. doi: 10.1111/j.1365-2125.1994.tb04332.x
32. Dokouhaki P, Schuh NW, Joe B, Allen CA, Der SD, Tsao MS, et al. NKG2D regulates production of soluble TRAIL by *ex vivo* expanded human gammadelta T cells. *Eur J Immunol*. (2013) 43:3175–82. doi: 10.1002/eji.201243150
33. Lafont V, Sanchez F, Laprevotte E, Michaud HA, Gros L, Eliaou JF, et al. Plasticity of gammadelta T cells: impact on the anti-tumor response. *Front Immunol*. (2014) 5:622. doi: 10.3389/fimmu.2014.00622
34. Girlanda S, Fortis C, Belloni D, Ferrero E, Ticozzi P, Sciorati C, et al. MICA expressed by multiple myeloma and monoclonal gammopathy of undetermined significance plasma cells costimulates pamidronate-activated γδ lymphocytes. *Cancer Res*. (2005) 65:7502–8. doi: 10.1158/0008-5472.CAN-05-0731
35. Martin-Antonio B, Najjar A, Robinson SN, Chew C, Li S, Yvon E, et al. Transmissible cytotoxicity of multiple myeloma cells by cord blood-derived NK cells is mediated by vesicle trafficking. *Cell Death Differ*. (2014) 22:96. doi: 10.1038/cdd.2014.120
36. Anane LH, Edwards KM, Burns VE, Zanten JJ, Drayson MT, Bosch JA. Phenotypic characterization of gammadelta T cells mobilized in response to acute psychological stress. *Brain Behav Immun*. (2010) 24:608–14. doi: 10.1016/j.bbi.2010.01.002
37. Campbell JP, Riddell NE, Burns VE, Turner M, van Zanten JJ, Drayson MT, et al. Acute exercise mobilises CD8+ T lymphocytes exhibiting an effector-memory phenotype. *Brain Behav Immun*. (2009) 23:767–75. doi: 10.1016/j.bbi.2009.02.011
38. Dieli F, Poccia F, Lipp M, Sireci G, Caccamo N, Di Sano C, et al. Differentiation of effector/memory Vdelta2 T cells and migratory routes in lymph nodes or inflammatory sites. *J Exp Med*. (2003) 198:391–7. doi: 10.1084/jem.20030235
39. Pauza CD, Liou ML, Lahusen T, Xiao L, Lapidus RG, Cairo C, et al. γδ T cell therapy for cancer: it is good to be local. *Front Immunol*. (2018) 9:1305. doi: 10.3389/fimmu.2018.01305
40. Couzi L, Pitard V, Moreau JF, Merville P, Dechanet-Merville J. Direct and indirect effects of cytomegalovirus-induced gammadelta T cells after kidney transplantation. *Front Immunol*. (2015) 6:3. doi: 10.3389/fimmu.2015.00003
41. Knight A, Mackinnon S, Lowdell MW. Human Vdelta1 gamma-delta T cells exert potent specific cytotoxicity against primary multiple myeloma cells. *Cytotherapy*. (2012) 14:1110–8. doi: 10.3109/14653249.2012.700766
42. Wu D, Wu P, Wu X, Ye J, Wang Z, Zhao S, et al. *Ex vivo* expanded human circulating Vdelta1 gammadeltaT cells exhibit favorable therapeutic potential for colon cancer. *Oncoimmunology*. (2015) 4:e992749. doi: 10.4161/2162402X.2014.992749
43. Siegers GM, Dhamko H, Wang XH, Mathieson AM, Kosaka Y, Felizardo TC, et al. Human Vdelta1 gammadelta T cells expanded from peripheral blood exhibit specific cytotoxicity against B-cell chronic lymphocytic leukemia-derived cells. *Cytotherapy*. (2011) 13:753–64. doi: 10.3109/14653249.2011.553595
44. Knight A, Arnouk H, Britt W, Gillespie GY, Cloud GA, Harkins L, et al. CMV-independent lysis of glioblastoma by *ex vivo* expanded/activated Vdelta1+ gammadelta T cells. *PLoS ONE*. (2013) 8:e68729. doi: 10.1371/journal.pone.0068729
45. Miyagawa F, Tanaka Y, Yamashita S, Minato N. Essential requirement of antigen presentation by monocyte lineage cells for the activation of primary human γδ T cells by aminobisphosphonate antigen. *J Immunol*. (2001) 166:5508–14. doi: 10.4049/jimmunol.166.9.5508
46. Roelofs AJ, Jauhiainen M, Monkkonen H, Rogers MJ, Monkkonen J, Thompson K. Peripheral blood monocytes are responsible for gammadelta T cell activation induced by zoledronic acid through accumulation of IPP/DMAPP. *Br J Haematol*. (2009) 144:245–50. doi: 10.1111/j.1365-2141.2008.07435.x
47. Campbell JP, Turner JE. Debunking the myth of exercise-induced immune suppression: redefining the impact of exercise on immunological health across the lifespan. *Front Immunol*. (2018) 9:648. doi: 10.3389/fimmu.2018.00648
48. Graff RM, Kunz HE, Agha NH, Baker FL, Laughlin M, Bigley AB, et al. β2-adrenergic receptor signaling mediates the preferential mobilization of differentiated subsets of CD8+ T-cells, NK-cells and non-classical monocytes in response to acute exercise in humans. *Brain Behav Immun*. (2018) 74:143–53. doi: 10.1016/j.bbi.2018.08.017
49. LaVoy EC, Bollard CM, Hanley PJ, O'Connor DP, Lowder TW, Bosch JA, et al. A single bout of dynamic exercise by healthy adults enhances the generation of monocyte-derived-dendritic cells. *Cell Immunol*. (2015) 295:52–9. doi: 10.1016/j.cellimm.2015.02.007
50. Simpson RJ, Kunz H, Agha N, Graff R. Exercise and the regulation of immune functions. *Prog Mol Biol Transl Sci*. (2015) 135:355–80. doi: 10.1016/bs.pmbts.2015.08.001
51. Nussbaumer O, Gruenbacher G, Gander H, Komuczki J, Rahm A, Thurnher M. Essential requirements of zoledronate-induced cytokine and gammadelta T cell proliferative responses. *J Immunol*. (2013) 191:1346–55. doi: 10.4049/jimmunol.1300603
52. Kabelitz D, Lettau M, Janssen O. Immunosurveillance by human gammadelta T lymphocytes: the emerging role of butyrophilins. *F1000Res*. (2017) 6:782. doi: 10.12688/f1000research.11057.1

Conflict of Interest: The authors declare that the research was conducted in the absence of any commercial or financial relationships that could be construed as a potential conflict of interest.

frontiers in Immunology

ORIGINAL RESEARCH
published: 12 May 2020
doi: 10.3389/fimmu.2020.00699

Immune Modulation Properties of Zoledronic Acid on TcRγδ T-Lymphocytes After TcRαβ/CD19-Depleted Haploidentical Stem Cell Transplantation: An analysis on 46 Pediatric Patients Affected by Acute Leukemia

Pietro Merli[1], Mattia Algeri[1], Federica Galaverna[1], Giuseppe Maria Milano[1], Valentina Bertaina[1], Simone Biagini[1], Elia Girolami[1], Giuseppe Palumbo[1], Matilde Sinibaldi[1], Marco Becilli[1], Giovanna Leone[2], Emilia Boccieri[1], Lavinia Grapulin[3], Stefania Gaspari[1], Irma Airoldi[4], Luisa Strocchio[1], Daria Pagliara[1] and Franco Locatelli[1,5]*

[1] Department of Pediatric Hematology and Oncology and of Cell and Gene Therapy, Scientific Institute for Research and Healthcare (IRCCS), Bambino Gesù Childrens' Hospital, Rome, Italy, [2] Transfusion Unit, Department of Laboratories, Scientific Institute for Research and Healthcare (IRCCS), Bambino Gesù Childrens' Hospital, Rome, Italy, [3] Department of Radiology and Radiotherapy, Sapienza University, Rome, Italy, [4] Stem Cell Laboratory and Cell Therapy Center, Giannina Gaslini Institute (IRCCS), Genoa, Italy, [5] Sapienza, University of Rome, Rome, Italy

OPEN ACCESS

Edited by:
Bruno Silva-Santos,
Universidade de Lisboa, Portugal

Reviewed by:
Matthias Eberl,
Cardiff University, United Kingdom
Emmanuel Scotet,
Institut National de la Santé et de la Recherche Médicale (INSERM), France

***Correspondence:**
Pietro Merli
pietro.merli@opbg.net

Specialty section:
This article was submitted to T Cell Biology, a section of the journal Frontiers in Immunology

Received: 19 February 2020
Accepted: 27 March 2020
Published: 12 May 2020

Citation:
Merli P, Algeri M, Galaverna F, Milano GM, Bertaina V, Biagini S, Girolami E, Palumbo G, Sinibaldi M, Becilli M, Leone G, Boccieri E, Grapulin L, Gaspari S, Airoldi I, Strocchio L, Pagliara D and Locatelli F (2020) Immune Modulation Properties of Zoledronic Acid on TcRγδ T-Lymphocytes After TcRαβ/CD19-Depleted Haploidentical Stem Cell Transplantation: An analysis on 46 Pediatric Patients Affected by Acute Leukemia. Front. Immunol. 11:699. doi: 10.3389/fimmu.2020.00699

TcRαβ/CD19-cell depleted HLA-haploidentical hematopoietic stem cell transplantation (haplo-HSCT) represents a promising new platform for children affected by acute leukemia in need of an allograft and lacking a matched donor, disease recurrence being the main cause of treatment failure. The use of zoledronic acid to enhance TcRγδ+ lymphocyte function after TcRαβ/CD19-cell depleted haplo-HSCT was tested in an open-label, feasibility, proof-of-principle study. Forty-six children affected by high-risk acute leukemia underwent haplo-HSCT after removal of TcRαβ+ and CD19+ B lymphocytes. No post-transplant pharmacological graft-versus-host disease (GvHD) prophylaxis was given. Zoledronic acid was administered monthly at a dose of 0.05 mg/kg/dose (maximum dose 4 mg), starting from day +20 after transplantation. A total of 139 infusions were administered, with a mean of 3 infusions per patient. No severe adverse event was observed. Common side effects were represented by asymptomatic hypocalcemia and acute phase reactions (including fever, chills, malaise, and/or arthralgia) within 24–48 h from zoledronic acid infusion. The cumulative incidence of acute and chronic GvHD was 17.3% (all grade I-II) and 4.8% (all limited), respectively. Patients given 3 or more infusions of zoledronic acid had a lower incidence of both acute GvHD (8.8 vs. 41.6%, $p = 0.015$) and chronic GvHD (0 vs. 22.2%, $p = 0.006$). Transplant-related mortality (TRM) and relapse incidence at 3 years were 4.3 and 30.4%, respectively. Patients receiving repeated infusions of zoledronic acid had a lower TRM as compared to those receiving 1 or 2 administration of the drug (0 vs. 16.7%, $p = 0.01$). Five-year overall survival (OS) and disease-free survival (DFS) for the whole cohort were 67.2 and 65.2%, respectively, with

a trend toward a better OS for patients receiving 3 or more infusions (73.1 vs. 50.0%, $p = 0.05$). The probability of GvHD/relapse-free survival was significantly worse in patients receiving 1–2 infusions of zoledonic acid than in those given ≥3 infusions (33.3 vs. 70.6%, respectively, $p = 0.006$). Multivariable analysis showed an independent positive effect on outcome given by repeated infusions of zoledronic acid (HR 0.27, $p = 0.03$). These data indicate that the use of zoledronic acid after TcRαβ/CD19-cell depleted haploHSCT is safe and may result in a lower incidence of acute GvHD, chronic GvHD, and TRM.

Keywords: TcRγδ+ lymphocytes, zoledronic acid, TcRαβ/CD19 cell depleted haploidentical stem cell transplantation, acute leukemia, children

INTRODUCTION

Hematopoietic stem cell transplantation (HSCT) is, so far, the best curative option for a number of malignant disorders (1, 2). However, up to 30% of patients lack both a HLA-identical sibling or an alternative donor [i.e., HLA-Matched Unrelated Donor (MUD) or Unrelated Donor Umbilical Cord Blood (UD-UCB)] (3). Thus, HSCT from an HLA-haploidentical relative (haplo-HSCT) represents a very promising option, since it owns particular features, including applicability for virtually all patients, choice of best donor from a panel of potential candidates, immediate accessibility to the transplant procedure, and easy access to donors in case adoptive cell therapies as are required after transplantation (3). However, compared to other types of allograft, haplo-HSCT has been hampered by a delayed immune reconstitution (4, 5), which, in turn, influences the risk of both post-transplant infections and, most importantly, relapse incidence (6, 7). Since it has been demonstrated that specific innate immunity cell subpopulations [e.g., NK (8) and TcRγδ T cells (9)] may influence transplant outcome, we and other groups recently developed a new method of graft manipulation (i.e., TcRαβ/CD19 negative selective depletion) (10–13), which allows to retain large numbers of mature, ready-to-kill effector cells, namely NK and TcRγδ lymphocytes, in the final product. TcRγδ cells are a non-alloreactive, "innate-like," T lymphocyte subpopulation (normally accounting for 1–10% of circulating T lymphocytes) capable of recognizing targets in an MHC-independent manner (through several activating receptors, like γδ-TcR, NKG2D, and TLRs) and displaying different functions, including anti-infective and anti-tumor activity (14, 15). We have recently reported the largest pediatric cohort receiving this kind of transplant, clearly showing that this approach represents a suitable alternative for children affected by acute leukemia, with outcomes comparable to those of HLA-matched donor HSCT recipients (13).

Preclinical data showed that bisphosphonates, such as pamidronate and zoledronate, commonly used to treat bone diseases and hypercalcemia in multiple myeloma, can mediate the improvement of TcRγδ-mediated tumor cells killing capacity (16, 17). Such an effect is obtained thanks to the activation of a particular subset of TcRγδ cells, through the accumulation of phosphoantigens (18) and, to a lesser extent, the sensitization of tumor target cells (19).

In an attempt to reduce the relapse incidence and the risk of severe infections in high risk-patients given TcRαβ/CD19-cell depleted haploHSCT, we explored the administration of zoledronic acid in the post-transplant period (20). We previously reported detailed cytofluorimetric, functional, and proteomic analysis of TcRγδ cells of patients treated with this strategy, showing that zoledronate administration promotes γδ T-cell differentiation and cytotoxicity (20). Here we report the long-term outcomes of 46 patients treated with zoledronic acid after TcRαβ/CD19-depleted haploHSCT.

PATIENTS AND METHODS

Patients

Patients aged 0.3 to 21 years, affected by acute leukemia, who were in need of an allograft while lacking an HLA-matched related or unrelated donor between January 1st, 2013 and September 26th, 2016 at IRCCS Ospedale Pediatrico Bambino Gesù in Rome, were considered eligible. All patients or legal guardians provided written informed consent, and the research was conducted under a Hospital Ethical Committee- approved protocol, in accordance with the Declaration of Helsinki.

Transplantation Procedure

All the 46 enrolled patients received a fully myeloablative conditioning regimen, which was based on the use of total body irradiation (TBI) in 37 (80%) children and chemo-based in 9 patients (20%) (details are reported in the **Supplementary Material**). Pre-transplantation rabbit anti-T lymphocyte globulin (ATLG, Grafalon®, Neovii) was administered, at a dose of 4 mg/kg/day for 3 consecutive days (days−5 to−3), in order to prevent both graft failure and graft-versus-host disease (GvHD), through *in vivo* T-cell depletion and/or modulation of bidirectional alloreactivity. On day−1, children were also given rituximab 200 mg/m^2 for *in vivo* donor and recipient B-cell depletion to reduce the risk of Epstein-Barr virus (EBV)-related post-transplantation lymphoproliferative disorders (PTLD). No patient was given any post-transplant pharmacologic GvHD prophylaxis.

The donor was chosen according to immune-genetic criteria, giving priority to natural killer (NK) alloreactivity (evaluated according to the killer immunoglobulin-like receptor (KIR)-KIR ligand model), NK cell B haplotype, and higher B content, as previously described (10, 21). The donor was a parent

for all patients but one, who was transplanted from her HLA-haploidentical brother. Granulocyte colony-stimulating factor (G-CSF) at a dose of 10–12 μg/kg/day was administered by subcutaneous injection to all donors to mobilize in peripheral blood hematopoietic stem cells from day−5 until leukapheresis (day−1). Ten donors (21.7%) with circulating CD34+ cell count <0.04 x 10^9/L on day−2 also received a single-dose of plerixafor (240 μg/kg) 6–9 h before cell collection. Graft manipulation was performed using the CliniMACS device as previously described (22).

Zoledronic Acid Administration

Zoledronic acid was administered monthly at a dose of 0.05 mg/kg/dose (maximal single dose 4 mg) over 1 h, starting after: i) achievement of stable donor engraftment, and ii) at least day +20 from transplantation. The dose was based on literature data about zoledronate use in pediatric bone diseases (23). Since this was an open-label, feasibility, proof-of-principle study, the number of scheduled doses was not fixed; patients continued to receive monthly infusions of up to 5 consecutive doses, unless an event (i.e., side effects related to the drug, disease relapse, severe infections, hospitalization for any cause, patient/parents refusal) occurred. We opted to administer multiple infusions of zoledronic acid, based on current literature data indicating that *in vivo* activation of TcRγδ T-cells in response to the drug is a transient phenomenon (24). Oral calcitriol, together with calcium supplementation, was administered for 7–10 days after zoledronate infusion, in order to prevent/treat hypocalcemia. Zoledronic acid was administered either in the inpatient or in the outpatient unit.

Statistical Analysis

Quantitative variables were reported as median value and range; categorical variables were expressed as absolute value and percentage. Clinical characteristics of patients were compared using the Chi-square test or Fisher's exact test for categorical variables, while the Mann-Whitney rank sum test or the Student's *T*-test were used for continuous variables as appropriate (25). The time to neutrophil engraftment was defined as time from HSCT to the first of 3 consecutive days with an absolute neutrophil count equal to or greater than 0.5×10^9 per liter, and the time to platelet engraftment as time from HSCT to the first of 7 consecutive days with an unsupported platelet count equal to or greater than 20×10^9 per liter.

Patients surviving for more than 7 and 100 days after transplantation were considered evaluable for acute and chronic GvHD (aGvHD, cGvHD) occurrence, respectively. Severity of aGvHD and cGvHD was assessed according to Glucksberg and Shulman criteria (26, 27).

Overall survival (OS), disease-free survival (DFS), GvHD/relapse-free survival (GRFS), transplant-related mortality (TRM), aGvHD, cGvHD, and relapse incidence (RI) were estimated from the date of transplantation to the date of an event or last follow-up. Probabilities of OS, DFS, and GRFS were calculated according to the Kaplan and Meier method (28). TRM, aGvHD, cGvHD, and RI were calculated as cumulative incidence curves in order to adjust the estimates for the appropriate competing risks (29). All results were expressed as probability or cumulative incidence (%) and 95% confidence interval (95% CI) (30).

The significance of differences between OS, DFS, and GRFS was estimated by the log–rank test (Mantel–Cox), while Gray's test was used to assess, in univariate analyses, differences between cumulative incidences (31). Multivariate analysis was performed using the Cox proportional hazard regression model (30). *P*-values < 0.05 were considered to be statistically significant.

Statistical analysis was performed using EZR version 1.32 (Saitama Medical Centre, Jichi Medical University), which is a graphical user interface for R (The R Foundation for Statistical Computing, Vienna, Austria) (32).

RESULTS

Patients

Forty-six patients affected by acute leukemia received a TcRαβ/CD19-cell depleted peripheral blood stem cell allograft from an HLA-haploidentical relative in the study period at IRCCS Ospedale Pediatrico Bambino Gesù, Rome. **Table 1** reports patient demographic and disease characteristics, and transplant details. Twenty-six patients had B-cell precursor acute lymphoblastic leukemia (BCP-ALL), 7 T-cell lineage ALL (T-ALL), and 11 acute myeloid leukemia (AML), while 2 patients were affected by mixed phenotype acute leukemia (MPAL). Seven patients had previously received a first HSCT. Two patients were not in morphological complete remission at time of transplantation.

Graft Composition and Hematopoietic Recovery

All children received $< 1 \times 10^5$ TcRαβ cells per kg of recipient body weight (median 0.04×10^6/kg; range 0.001–0.099), with a median Log depletion of 3.93 (range 3.42–5.42), while the median number of TcRγδ cells infused was 7.7×10^6 per kg (range 0.8–42.7) (details of graft composition are reported in **Table 1**). The median number of infused CD34+ cells per kg was 15.4×10^6 (range 6.5–40.6) (median CD34+ stem cell recovery 91.25%; range 71.67–100), while that of B cells was 0.03×10^6/kg (range 0.001–0.18) (median Log depletion of 3.42; range 2.93–4.50).

All patients achieved engraftment; the median time to neutrophil engraftment was 14.5 days (range 8–21), whereas the median time to platelet recovery was 11 days (range 8–27). Monitoring of donor-recipient chimerism performed to hypervariable regions of human DNA confirmed the engraftment of donor hematopoiesis in all patients.

Zoledronic Acid Infusions and Adverse Reactions

The 46 patients received a total of 139 zoledronic acid infusions, with a mean of 3 infusions per patient (range 1–6). Specifically, 4 patients received a single infusion, 8 patients received 2 infusions, 20 were given 3 infusions, 12 received 4 infusions, while one patient each received 5 and 6 infusions (because of physician decision, based on good tolerability and positive effect on bone metabolism parameters). Treatment started at a median of 39 days (range 20–79). Ten patients (21.7%) experienced an acute phase reaction, including fever, chills, malaise, arthralgia, and/or

TABLE 1 | Patient demographic, disease characteristics, and transplant details.

	Number	Percentage (%)	Median	Range
Total	46	100		
Gender				
Male	33	72		
Female	13	28		
Age at diagnosis, years			9.2	0.6–22
Age at transplant, years			10.9	1–22.2
Disease				
BCP-ALL	26	57		
T-ALL	7	15		
AML	11	24		
MPAL	2	4		
Phase of disease				
CR1	13	28		
CR2	23	50		
>CR2	8	18		
Active disease	2	4		
Genetic abnormalities				
t(9;22)	2	4		
Complex karyotype	2	4		
FLT3-ITD	2	4		
Cytogenetic abnormalities involving 11q23*	3	7		
Previous HSCT	7	15		
Conditioning regimen				
TBI-based	37	80		
Chemo-based	9	20		
Cell dose infused				
CD34+ × 10^6/kg			15.4	6.5–40.6
TCRαβ+ × 10^6/kg			0.04	0.001–0.099
TCRγδ+ × 10^6/kg			7.7	0.8–42.7
NK+ × 10^6/kg			23.3	2.0–141.6
CD20+ × 10^6/kg			0.03	0.001–0.18
Donor Characteristics				
Age (years)			39	21–56
Type of donor				
Mother	27	59		
Father	18	39		
Brother	1	2		
Sex mismatch (F->M)	23	50		
NK alloreactivity (KIR-KIR-L model)	19	41		
KIR genotype B/X	36	78		

*1 case each of t(6;11), t(9;11) and t(10;11).

transient skin rash, within 24–48 h after the first administration. Five patients (10.8%) had a transient decrease in the WBC or platelet count. All patients experienced a reduction of calcium serum levels; however, only one episode of symptomatic hypocalcemia (at first administration) occurred and was rapidly corrected with parenteral calcium supplementation. One patient (2%) presented asymptomatic hypokaliemia. No other adverse event was recorded; in particular, we did not observe any case of osteonecrosis.

TcRγδ T-Cells After Zoledronic Acid Infusion

As already reported (13, 16), TcRγδ T-cells represented the main T cell population in the first weeks after TcRαβ/CD19-depleted haploidentical HSCT. This predominance of TcRγδ T-cells was observed also in zoledronate-treated patients. Subsequently, TcRαβ T-lymphocytes progressively increased over time, exceeding the percentage of TcRγδ T-cells before the third month after transplantation (data not shown). Interestingly, as already shown (20), in patients given zoledronic acid a progressive decrease in the percentage and absolute number of TcRγδ T-cells was observed, thus suggesting that repeated infusions of zoledronic acid do not induce persistence of this cell subset (**Figure 1A**). No significant difference in the number of circulating TcRγδ T-cells between patients receiving ≥3 infusions of zoledronic acid as compared to those given 1 or 2 infusion was found, although there was a trend toward a higher reduction at 3 months after HSCT in the first group (**Figure 1B**).

Graft-*versus*-Host Disease

Skin-only aGvHD was observed in 8 children after zoledronic acid infusion, with 3 patients experiencing overall grade I and 5 patient developing grade II aGvHD, the cumulative incidence of aGvHD being 17.3% (95% confidence interval (CI) 5.6–27.6) (**Figure 2A**). Grade I aGvHD was treated with sole topical steroid application, while patients with grade II aGvHD received systemic corticosteroids with or without extracorporeal photopheresis (ECP), with complete resolution in all cases. Two out of the 42 evaluable patients developed limited cGvHD, with a cumulative incidence of 4.8% (95% CI 0–11.2) (**Figure 3A**).

Notably, patients given 3 or more infusions of zoledronate had a lower incidence of both acute and chronic GvHD. In detail, patients receiving either ≥3 doses or 1–2 doses of zoledronic acid had a cumulative incidence of aGvHD of 8.8% (95% CI 0–17.9) and 41.6% (95% CI 5.9–63.8), respectively ($p = 0.015$) (**Figure 2B**).

Since the 2 patients experiencing cGvHD received <3 infusions of zoledronic acid, the cumulative incidence of cGvHD in patients receiving 3 or more infusions of zoledronate compared to those who received 1 or 2 infusions was 0 and 22.2% (95% CI 0–45.1), respectively ($p = 0.006$) (**Figure 3B**).

Infections

In terms of early virus reactivation, cytomegalovirus (CMV) DNAemia was recorded in 15 patients, with a cumulative incidence of 30.4% (95% CI 15.7–42.5). However, none progressed to CMV disease thanks to the administration of pre-emptive treatment with ganciclovir. Regarding EBV, no EBV-associated PTLD occurred in our cohort. Nine patients experienced Adenovirus infection (cumulative incidence 19.5%; 95% CI 7.2–30.2); in one case the infection was not controlled by pharmacological therapy, leading to a disseminated infection that ultimately resulted in the patient's death. Three patients

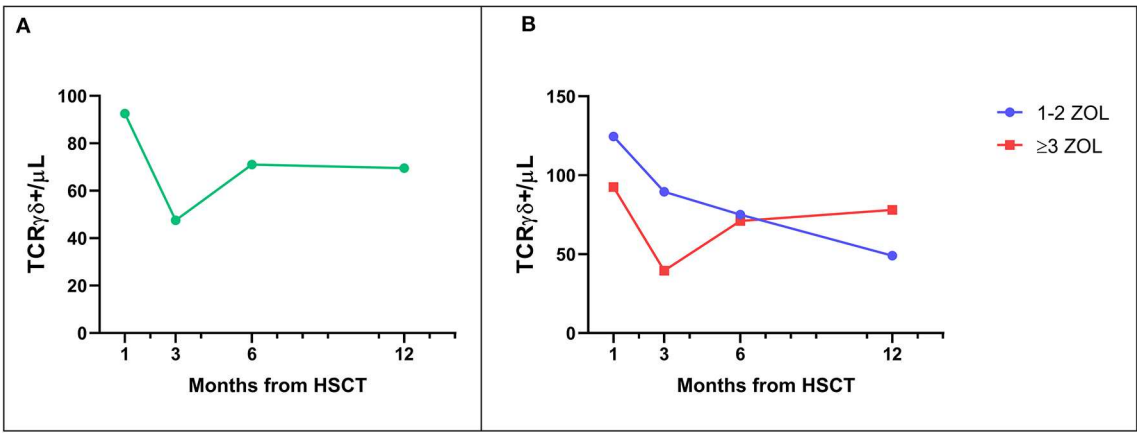

FIGURE 1 | (A) Median number of TcRγδ T-cells in the peripheral blood of patients receiving zoledronic acid after TcRαβ/CD19-depleted haploHSCT. **(B)** Median number of TcRγδ T-cells in the peripheral blood of patients receiving either 1–2 or 3–6 infusions of zoledronic acid (ZOL).

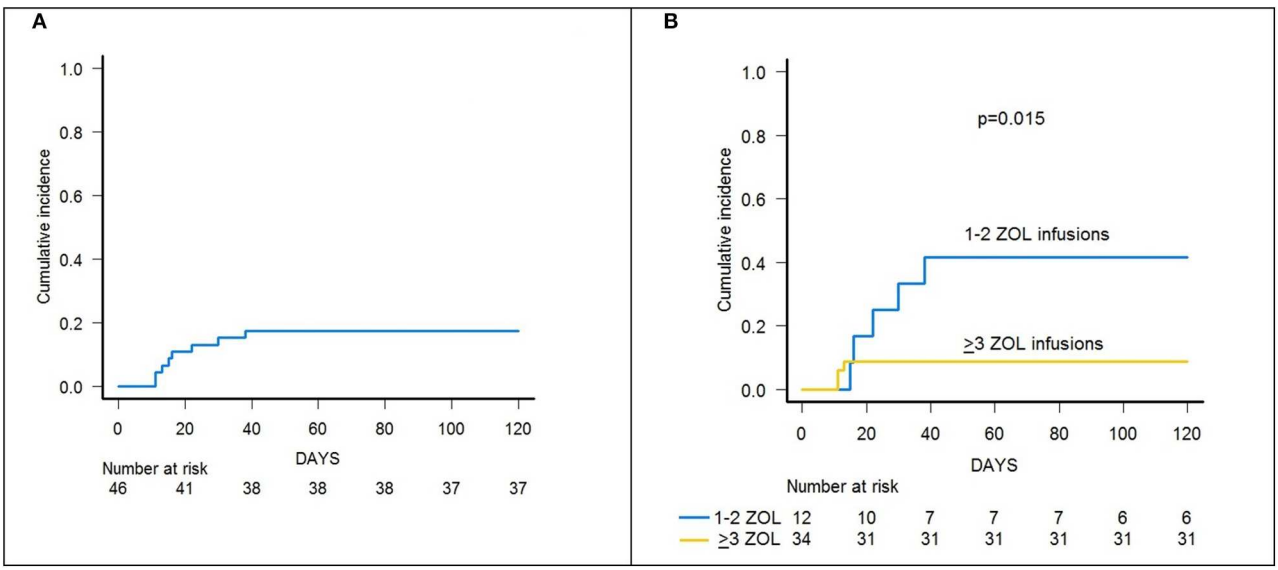

FIGURE 2 | (A) Cumulative incidence of acute GvHD (all grades) of the whole cohort of 46 patients. **(B)** Cumulative incidence of acute GvHD (all grades) in patients receiving either 1–2 or 3–6 infusions of zoledronic acid (ZOL).

developed bacterial infection (2 Gram-positive and 1 Gram-negative sepsis) (cumulative incidence 6.5%; 95% CI 0–13.4), controlled by large-spectrum antibiotic therapy. Finally, one patient suffered from a fatal *Aspergillus flavus* infection. The number of zoledronic acid infusion did not affect the incidence of viral, bacterial, or fungal infection. However, there was a trend toward a lower incidence of CMV infection in patients given 3–6 infusions (26.4 vs. 41.6% for patient receiving less administrations), but the difference was not statistically significant.

Relapse and Transplant-Related Mortality

Fourteen patients relapsed at a median time of 194 days after HSCT (range 81–1,081), the cumulative incidence of relapse being 30.4% (95% CI 17.8–44.1). It did not differ between patients receiving 1–2 infusions of zoledronic acid and patients receiving 3–6 administrations (33.3 vs. 29.4%, p = n.s.), although there was a trend toward reduction of relapse for patients receiving 4–6 zoledronate doses as compared to those receiving 1–3 infusions (37.5 vs. 14.3%, $p = 0.11$) (**Supplementary Figure 2**). Time to first zoledronic acid infusion was comparable between relapsed and disease-free patients (median 39 vs. 42.5 days, p = n.s.). Moreover, time to relapse was comparable between relapsed patients receiving 1–2 zoledronic acid infusions and those receiving 3–6 administrations. Finally, the proportion of children receiving 3–6 infusions was comparable between the subgroup of patients in first complete remission (CR) and those in second CR/other disease *status* (p = n.s.). As already reported

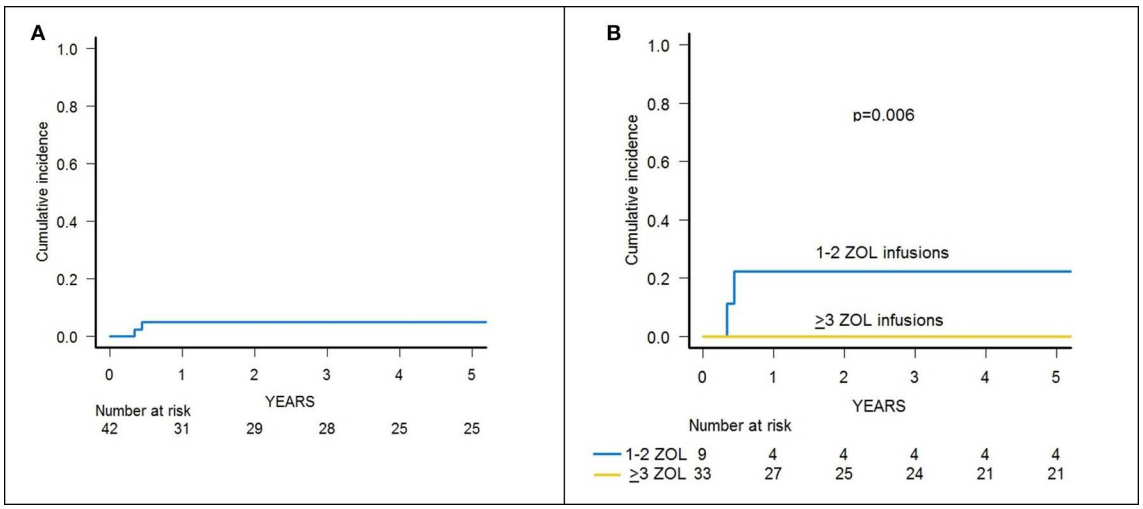

FIGURE 3 | (A) Cumulative incidence of chronic GvHD of the whole cohort of 46 patients. **(B)** Cumulative incidence of chronic GvHD in patients receiving either 1–2 or 3–6 infusions of zoledronic acid (ZOL).

(13), the use of TBI in the conditioning regimen was associated with a reduced incidence of relapse (21.6 vs. 66.7%, $p = 0.01$).

Since two patients died due to infections, the 3-year cumulative incidence of TRM was 4.3% (95% CI 0.8–13.2) (**Supplementary Figure 1**). A significantly lower TRM was observed for patients who received 3–6 infusions of zoledronic acid in comparison with those given 2 or less administrations (0 vs. 16.7%, $p = 0.01$) (**Figure 4**).

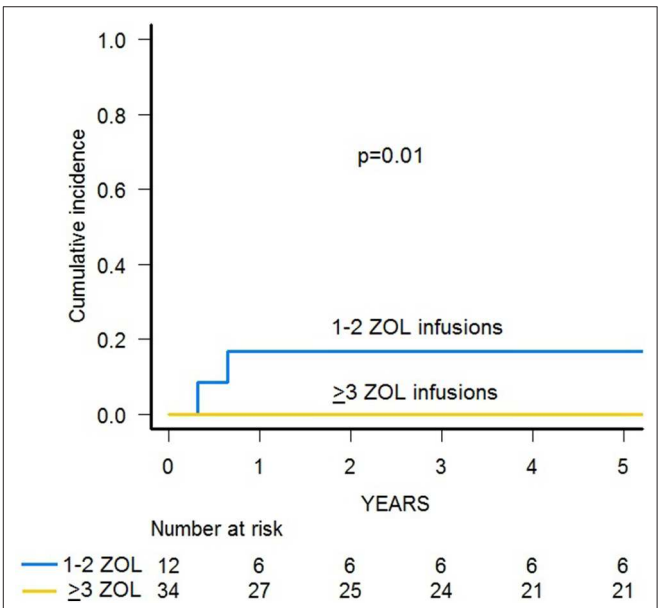

FIGURE 4 | TRM of patients receiving either 1–2 or 3–6 infusions of zoledronic acid (ZOL).

Survival Outcomes

With a median follow-up of 70.4 months (range 39.8–84.0), 31 patients are alive, and the 5-year probability of OS was 67.2% (95% CI 51.5–78.7) (**Figure 5A**). Since 14 patients relapsed, the 5-year probability of DFS was 65.2 (95% CI 49.6–77.0) (**Supplementary Figure 3A**). Five-year probability of GRFS was 60.9 (95% CI 45.3–73.3) (**Figure 6A**). As previously demonstrated in this setting (13), the use of a TBI-based conditioning resulted in an improved outcome. Indeed, DFS was 73.0% (95% CI 55.6–84.4) and 33.3% (95% CI 7.8–62.3) in patients who either did or did not receive TBI, respectively ($p = 0.02$; **Figure 7**); OS was 75.7% (95% CI 58.5–86.5) and 44.0% (95% CI 13.6–71.9) for these 2 groups ($p = 0.10$).

A trend toward higher survival estimates was observed in patients given 3 or more infusions as compared to those receiving 1–2 infusions, suggesting a possible influence of repeated administrations of zoledronic acid on outcome, although the difference was not statistically significant. In detail, OS was 73.1% (95% CI 54.7–85.1) for patients who received more than 2 infusions vs. 50% (95% CI 20.8–73.6) for those who received 1–2 infusions ($p = 0.05$) (**Figure 5B**), while DFS was 70.6% (95% CI 55.2–83.0) vs. 50.0% (95% CI 20.8–73.6) for patients given 3 or more infusions and those receiving 2 or less infusions, respectively (p = n.s.) (**Supplementary Figure 3B**). Notably, when stratified according to the conditioning regimen employed (TBI-based vs. chemo-based), the effect of repeated infusions of zoledronic acid was more evident, with the best OS obtained by patients who received both TBI and more than 2 zoledronic acid infusions (80.8%, 95% CI 59.8–91.5) (**Figure 8**). Moreover, in multivariable analysis model including these 2 variables, together with age at transplant and type of disease (ALL vs. AML), the repeated infusions of zoledronic acid showed an independent positive effect on OS (**Table 2**). GRFS differed significantly between patients receiving 1–2 infusion of zoledonic acid (33.3%, 95% CI 10.3–58.8) or ≥3 infusions (70.6%, 95% CI 52.2–83.0) ($p = 0.006$) (**Figure 6B**).

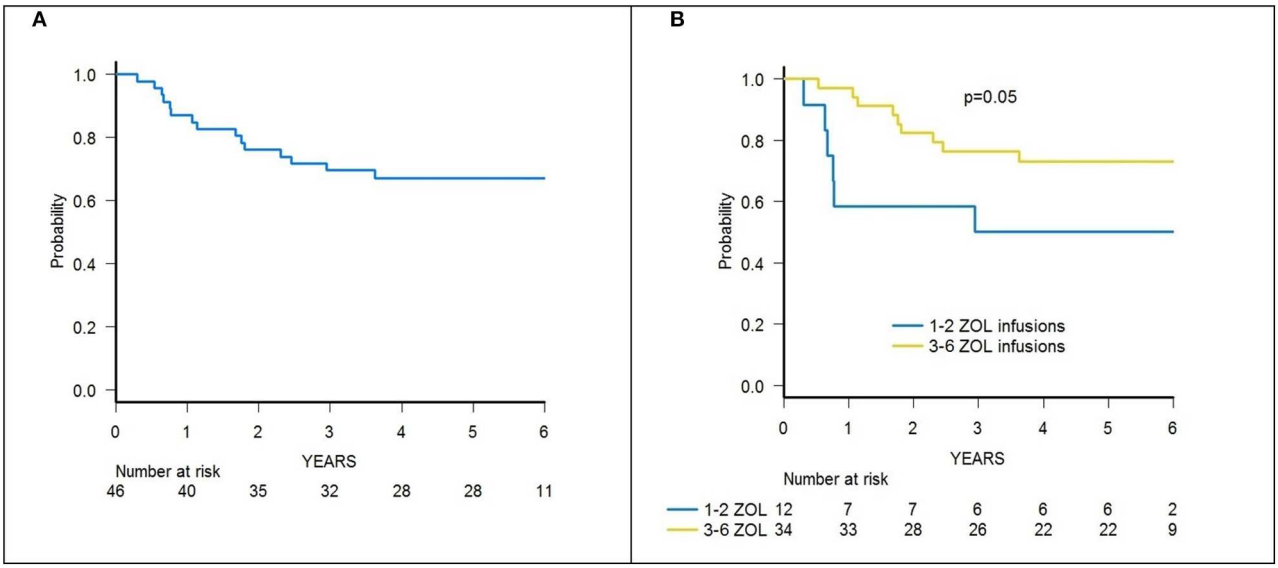

FIGURE 5 | (A) OS of the whole cohort of 46 patients. **(B)** OS of patients receiving either 1–2 or 3–6 infusions of zoledronic acid (ZOL).

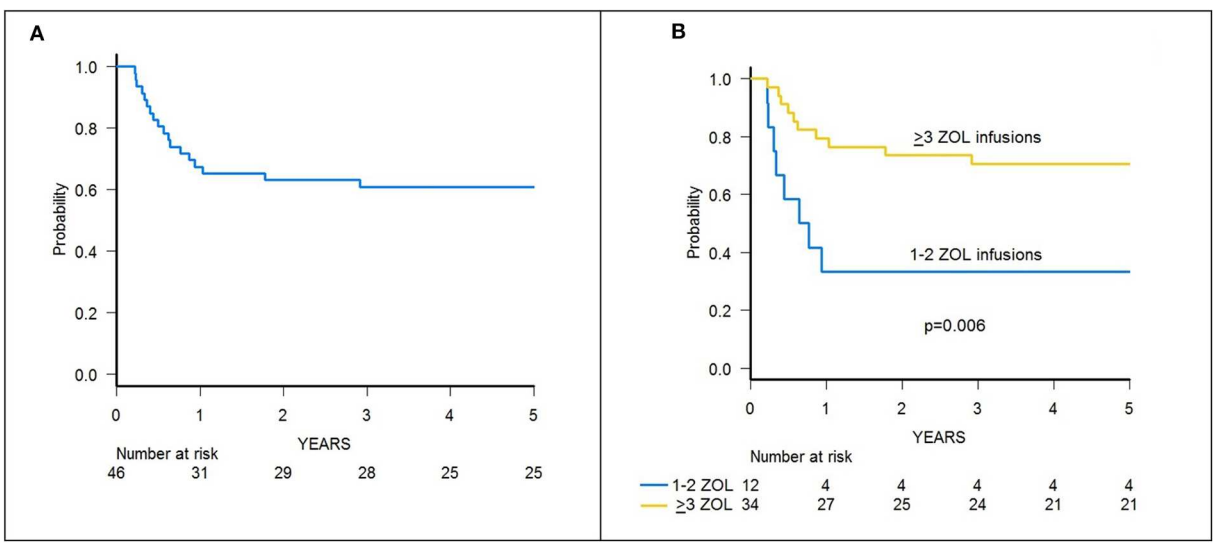

FIGURE 6 | (A) GRFS of the whole cohort of 46 patients. **(B)** GRFS of patients receiving either 1–2 or ≥3 infusions of zoledronic acid (ZOL).

Outcome was not influenced by the number of TcRγδ cells infused with the graft (data not shown), nor by other factors, including age at transplant, type of leukemia (myeloid, T or B lineage, or MPAL), disease *status* at HSCT, NK alloreactivity, B-content score, or graft composition (data not shown).

DISCUSSION

Despite major improvements in T-cell depleted haploHSCT, disease relapse remains the main cause of treatment failure in acute leukemias (13); thus, strategies aimed at reducing leukemia recurrence are needed. TcRγδ T-lymphocytes are a subpopulation of T cells with features between innate and adaptive immunity endowed with notable properties (lysis of infected or stressed cells and cytokine and chemokine production among the others) through which they give unique contributions to immune reactions (33). Several studies have demonstrated the cytotoxic activity of TcRγδ T-cells against hematologic malignancies both *in vitro* (34) and *in vivo* (35), through direct recognition (i.e., in a MHC-independent way) of targets present on leukemia cells (36). Thus, not surprisingly, a faster immune reconstitution of this subset has been associated with an improved DFS after allogeneic HSCT in patients with either ALL or AML (9, 37, 38). In particular, seminal works by Lamb and colleagues

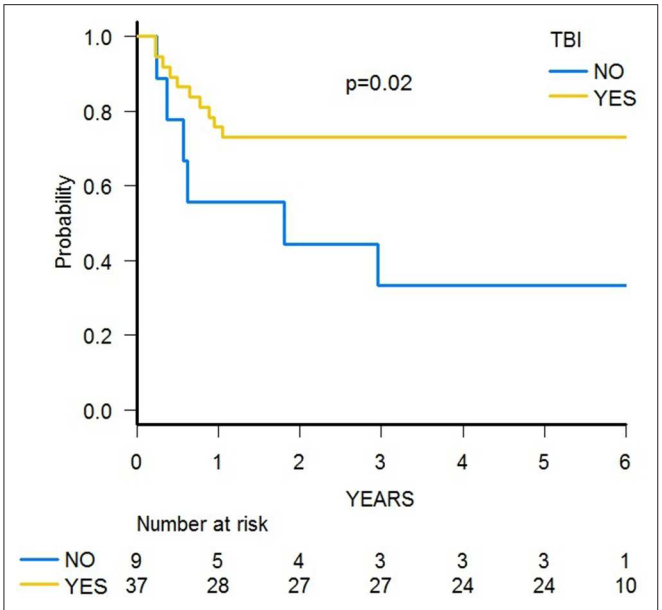

FIGURE 7 | DFS probability of patients receiving a TBI-based or a chemo-based conditioning regimen.

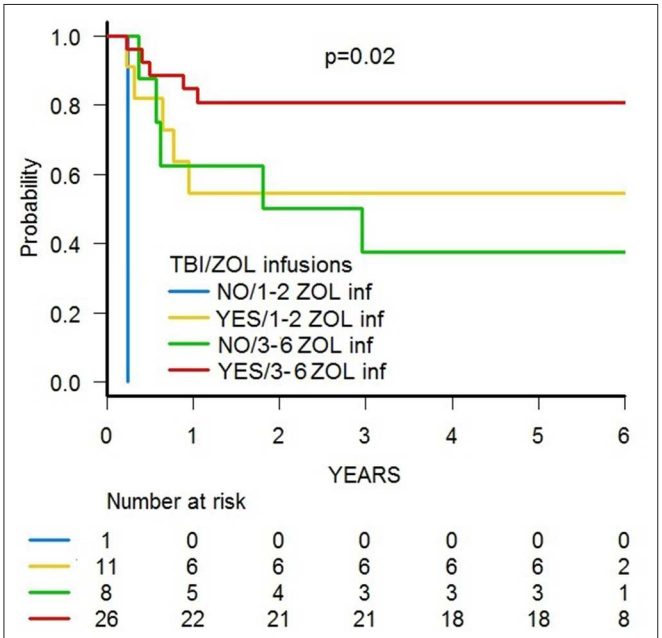

FIGURE 8 | OS of patients stratified according to (i) the conditioning regimen used and (ii) the number of zoledronic acid (ZOL) infusion received after HSCT.

in T-cell depleted HSCT from partially mismatched related donors demonstrated that accelerated TcRγδ T-cell recovery was associated with improved DFS (9, 37), mainly due to a decreased relapse incidence (39).

Kunzmann and colleagues first reported the activation and expansion of TcRγδ T-cells following the administration of aminobisphosphonates (17). The authors provided *in vitro* evidence that the proliferative response of TcRγδ T-cells to bisphosphonates was IL-2 dependent, whereas their activation occurred in the absence of cytokines (40). It has been shown that nitrogen-containing bisphosphonates, such as zoledronic acid, cause the inhibition of farnesyl diphosphate synthase in tumor cell lines, which leads to the accumulation of isopentenyl pyrophosphate (IPP), a type of non-peptidic-phosphorylated metabolite (nPAgs), which indirectly activates γδ T cell (41, 42). What still remains unclear is the precise mechanism by which TcRγδ T-cells are activated by nPAgs, although the γδ-TcR appears to undergo a conformational change or clustering of the butyrophilin family member 3A1 (BTN3A1) molecule (18). Although zoledronic acid increases the cytotoxic capacity of both principal subsets of TcRγδ T-cells (i.e., Vδ1 and Vδ2 (33)), Vδ2 T cells are more prone to this effect (20).

TABLE 2 | OS multivariable analysis model.

Variable	Hazard ratio	Lower 95% CI	Upper 95% CI	*p*-value
Use of TBI during conditioning regimen	0.277	0.074	1.035	0.056
Zoledronic Acid infusions > 2	0.273	0.082	0.905	0.033
Age at HSCT (< or > 10.9 years)	0.366	0.107	1.255	0.110
Disease (ALL vs. AML)	2.65	0.458	14.510	0.260

As detailed in recently published studies (12, 22), TcRαβ/CD19-depletion of G-CSF mobilized PBSC of haploidentical donors is an effective manipulation strategy, able to efficiently remove TcRαβ lymphocytes while retaining in the graft high numbers of effector cells, namely mature NK and TcRγδ T-cells. We characterized, by means of immunophenotypic and functional assays, the immune reconstitution of TcRγδ T-lymphocyte after this type of T-cell depleted haploHSCT (16), demonstrating that: i) TcRγδ T-cells are the predominant T-cell population in the early post-transplantation period, mainly deriving from cells infused with the graft; ii) these cells expand *in vivo* after transplantation; iii) they display a cytotoxic phenotype and degranulate when challenged with primary acute myeloid and lymphoid leukemia blasts; and iv) Vδ2 cells more efficiently lyse primary lymphoid and myeloid blasts *in vitro* after their exposure to zoledronic acid. Thus, this transplant platform constitutes the ideal setting to test the immune-modulatory properties of *in vivo* administration of aminobisphosphonates. Indeed, zoledronic acid has been previously demonstrated to be safe in pediatric age in studies on osteopenia (43) and, more importantly, at escalating doses (up to 4 mg/m^2), in patients affected by recurrent/refractory neuroblastoma (44). Moreover, the use of bisphosphonates in HSCT recipients ameliorates osteoporosis, a well-known complication of transplantation (45). Indeed, the Australasian Leukemia and Lymphoma Group showed that post-transplant administration of zoledronate, based on a risk-adapted algorithm, minimizes bone loss (46).

We previously reported biological characterization, as well as short-term clinical data [median follow-up of surviving patients

was 7.5 months (range 2.5–15) as compared to 70.4 months in the present study], of 43 patients receiving zoledronic acid after TcRαβ/CD19-depleted haploHSCT (20).

Our findings confirm that multiple infusions of zoledronic acid (up to 6 administrations) in children after HSCT, starting even a few weeks after the infusion of HSC, are well-tolerated and safe. In particular, no serious adverse event was recorded (specifically no cases of osteonecrosis of the jaw), as previously reported by Dieli in adults affected by prostate cancer (24) and by the aforementioned study of Russell in neuroblastoma patients (44). Moreover, the drug was safely administered in an outpatient setting, even in children aged 1 year or less.

As already reported (13), despite the lack of any pharmacological post-transplant prophylaxis, in our study the incidence of both acute and chronic GvHD was limited (with no patient experiencing grade III-IV acute or extensive chronic GvHD), much lower than that of other similar case series (47) or other type of graft manipulation, such as CD3/CD19-depletion (48). Of note, none of the patients experienced *de novo* onset or worsening of previously developed aGvHD, supporting the hypothesis that γδ T-lymphocytes do not cause GvHD (34). Moreover, our findings showing that patients receiving multiple infusions of zoledronic acid have a reduced incidence of both acute and chronic GvHD are of particular interest. Indeed, this is the first experience (20) of such an induced effect *in vivo* and deserves further investigation. Immunoregulatory properties of TcRγδ T-cells were first described by Patel and colleagues (49) and are now beginning to be investigated. Notably, Drobyski and colleagues noted that, in mice, activated TcRγδ T-cells are capable of modulating the ability of MHC-incompatible TcRαβ T-cells to cause GvHD after HSCT (50). Both Vδ1 and Vδ2 subsets may display regulatory properties, depending on different settings. Moreover, stimulation with pyrophosphates can induce regulatory capacities on Vδ2 T cells a few days after initial stimulation (51). In particular, IPP-stimulated Vδ2 T lymphocytes can inhibit the proliferation of CD4+ and CD8+ αβ T cells in response to strong recall antigens (52). Interestingly, strong co-stimulatory antigen-processing cell (APC) signals (i.e., acute GvHD initiating condition) seem to play an important role in the induction of these suppressive properties. The mechanisms of suppression by TcRγδ T-cells are still not clear; while some authors identified TGFβ, IL-10, and other suppressive cytokines as mediators of these effects (53), other data suggested that cell-to-cell interactions, via CD80, CD86, and PDL-1 expressed on Vδ2 T lymphocytes, are necessary to achieve suppression of other cell populations (54). Another unresolved issue is the lack of defined regulatory γδ T-cell phenotype (51), although CD39 (55) and latency-associated peptide (a membrane-bound TGF-β1) (56) have been identified as putative markers; thus, further studies are needed to address this question.

The cumulative incidence of TRM in our study cohort was remarkably low (4.3%), with 2 patients dying due to infection. Repeated infusions of zoledronic acid seems to also have a role in reducing TRM, since we recorded no infectious deaths in children who received more than 2 administrations. The well-known anti-infectious role of TcRγδ T-cells has been very recently demonstrated by Perko and colleagues in children after HSCT (38). Indeed, using a logistic regression model, they showed that the higher the number of TcRγδ T-cells after HSCT, the lower the risk of infection, which results in an improved EFS. However, because of the limited number of patients per cohort, subanalysis on different types of donors (siblings, MUDs, haploidentical relatives, and umbilical cord blood) failed to demonstrate a similar effect in any single subgroup. In our study, repeated infusions of zoledronic acid did not affect the incidence of infections of either viral, bacterial, or fungal origin. However, patients receiving multiple infusions had a reduced, although not statistically significant, cumulative incidence of CMV infection. Given the low number of patients enrolled in this study, it is possible that the number of events was not sufficient to highlight such an effect.

The OS estimate observed in our study (without any difference between ALL, either of T or B lineage, AML patients), in line with our recently published cohort (13), is higher than that reported in other pediatric trials of CD34 selected (57, 58) or CD3/CD19-depleted haploidentical HSCT (48), suggesting a favorable impact of TcRγδ T-cells on outcome. Outcome data were also similar to those reported by Maschan et al., who used the same type of graft manipulation, although with different study population and donors (47), making comparison difficult to interpret. Smetak and colleagues studied a different method of T-cell depletion, namely based on CD4+ and CD8+ depletion, able to leave in the graft innate lymphocytes such as TcRγδ T cells and NK cells (59). Despite similar depletion capacity, other authors noted that the B-cell content of the graft was high, raising concerns about the risk of EBV-associated PTLD (60).

We previously demonstrated that the use of TBI in the conditioning regimen positively influenced the outcome in this setting, probably due to a potent antileukemia effect, compensating for the lack of TcRαβ cell–mediated GvL effect (13). Here, we show that patients receiving more than 2 infusions of zoledronic acid seem to have an improved OS, although the difference did not reach the statistical significance level. However, when stratified according to the type of conditioning regimen employed, the independent beneficial effect of zoledronic acid on OS became evident, as also highlighted by multivariable analysis. As zoledronic acid improves cytotoxicity of TcRγδ T-cells, the initial hypothesis was that multiple infusions could reduce RI. However, due to the limited number of patients enrolled and events observed, it was not possible to draw any firm conclusion; in particular, we were not able to highlight a significant reduction of RI. Since time to relapse and disease status were comparable between patients receiving 1–2 or 3–6 infusions of zoledronic acid, the trend toward a better outcome of patients receiving multiple infusions does not seem to be due to the fact that those patients had longer DFS allowing for multiple infusions nor because they had a less aggressive disease.

We were not able to demonstrate an association between an increased number of TcRγδ T-cells after HSCT and an improved outcome (data not shown), as demonstrated by Lamb *et al.* (9, 37). A possible explanation for these apparently discordant findings can be given by the observation that, as shown by our data, the percentage and absolute number of TcRγδ T-lymphocytes, and especially of the Vδ2 subset,

decrease over time after prolonged exposure to zoledronic acid (20). This phenomenon, in contrast with the first *in vitro* observations by Kunzmann (40), was previously proven by Dieli and coauthors in patients treated with zoledronic acid for hormone-refractory prostate cancer (24) and by Kalyan and colleagues in post-menopausal women treated with bisphosphonates for osteoporosis (61). These authors demonstrated an inhibitory effect on TcRγδ T-cells produced by neutrophils upon bisphosphonate uptake through the production of reactive oxygen species (62). Although the use of IL-2 could improve proliferation of TcRγδ T-lymphocytes (24), we decided not to administer this cytokine because of a possible increase in the risk of GvHD (63).

The main limitations of this study include: i) the lack of a control arm and ii) a variability of the administration schedule, this limiting the possibility to draw firm conclusions on the number and timing of zoledronic acid administration. Finally, we did not systematically collect data on bone metabolism pre and post zoledronic acid infusions. Since it is well-known that patients undergoing HSCT suffer from osteopenia (64), data on bone metabolism after zoledronic acid administration could help guide post-transplant supportive therapies.

In conclusion, our data indicate that the infusion of zoledronic acid after TcRαβ/CD19-depleted haploidentical HSCT is safe. Three or more infusions of zoledronic acid result in a lower incidence of both acute and chronic GvHD and lower TRM. Moreover, they had an independent effect in ameliorating the outcome. Further investigation (a non-randomized prospective trial is currently ongoing at Wisconsin University, ClinicalTrials.gov Identifier: NCT02508038), namely a randomized-controlled trial, is needed to confirm these data.

DATA AVAILABILITY STATEMENT

The datasets generated for this study are available on request to the corresponding author.

ETHICS STATEMENT

The study involving human participants was reviewed and approved by the Ethical Committee of Bambino Gesù Children's Hospital. Written informed consent to participate in this study was provided by the participants' legal guardian/next of kin.

AUTHOR CONTRIBUTIONS

PM, MA, FG, GM, GP, LS, DP, and FL designed the study, analyzed data, and wrote the paper. VB, SB, EG, MS, and IA performed graft manipulation, characterized the graft, and edited the paper. PM, MA, FG, GM, MB, GL, EB, LG, SG, DP, and FL treated patients, collected data, analyzed data, and edited the paper. All authors approved the final version of the paper.

FUNDING

This work was partly supported by grants from: AIRC (Associazione Italiana Ricerca sul Cancro, Investigator Grant-ID 21724), Ministero della Salute (Ricerca Finalizzata to FL), and Ministero dell'Istruzione, Università e Ricerca (MIUR, Project PRIN 2017-ID 2017WC8499-to FL).

SUPPLEMENTARY MATERIAL

The Supplementary Material for this article can be found online at: https://www.frontiersin.org/articles/10.3389/fimmu.2020.00699/full#supplementary-material

Supplementary Figure 1 | Cumulative incidence of relapse and TRM of the whole cohort of 46 patients.

Supplementary Figure 2 | Cumulative incidence of relapse of patients receiving either 1–3 or 4–6 infusions of zoledronic acid (ZOL).

Supplementary Figure 3 | DFS of the whole cohort of 46 patients. B. DFS of patients receiving either 1-2 or 3-6 infusions of zoledronic acid (ZOL).

REFERENCES

1. Copelan EA. Hematopoietic stem-cell transplantation. *N Engl J Med*. (2006) 354:1813–26. doi: 10.1056/NEJMra052638
2. Locatelli F, Giorgiani G, Di-Cesare-Merlone A, Merli P, Sparta V, Moretta F. The changing role of stem cell transplantation in childhood. *Bone Marrow Transplant*. (2008) 41(Suppl. 2):S3–7. doi: 10.1038/bmt.2008.45
3. Reisner Y, Hagin D, Martelli MF. Haploidentical hematopoietic transplantation: current status and future perspectives. *Blood*. (2011) 118:6006–17. doi: 10.1182/blood-2011–07-338822
4. Oevermann L, Lang P, Feuchtinger T, Schumm M, Teltschik HM, Schlegel P, et al. Immune reconstitution and strategies for rebuilding the immune system after haploidentical stem cell transplantation. *Ann N Y Acad Sci*. (2012) 1266:161–70. doi: 10.1111/j.1749–6632.2012.06606.x
5. de Koning C, Plantinga M, Besseling P, Boelens JJ, Nierkens S. Immune reconstitution after allogeneic hematopoietic cell transplantation in children. *Biol Blood Marrow Transplant*. (2016) 22:195–206. doi: 10.1016/j.bbmt.2015.08.028
6. Bayraktar UD, Milton DR, Guindani M, Rondon G, Chen J, Al-Atrash G, et al. Optimal threshold and time of absolute lymphocyte count assessment for outcome prediction after bone marrow transplantation. *Biol Blood Marrow Transplant*. (2015) 22:505–13. doi: 10.1016/j.bbmt.2015.10.020
7. Platzbecker U, Ehninger G, Bornhauser M. Allogeneic transplantation of CD34+ selected hematopoietic cells–clinical problems and current challenges. *Leuk Lymphoma*. (2004) 45:447–53 doi: 10.1080/10428190310001615684
8. Ruggeri L, Capanni M, Urbani E, Perruccio K, Shlomchik WD, Tosti A, et al. Effectiveness of donor natural killer cell alloreactivity in mismatched hematopoietic transplants. *Science*. (2002) 295:2097–100. doi: 10.1126/science.1068440
9. Godder KT, Henslee-Downey PJ, Mehta J, Park BS, Chiang KY, Abhyankar S, et al. Long term disease-free survival in acute leukemia patients recovering with increased gammadelta T cells after partially mismatched related donor bone marrow transplantation. *Bone Marrow Transplant*. (2007) 39:751–7. doi: 10.1038/sj.bmt.1705650
10. Bertaina A, Merli P, Rutella S, Pagliara D, Bernardo ME, Masetti R, et al. HLA-haploidentical stem cell transplantation after removal of αβ+ T and B-cells in children with non-malignant disorders. *Blood*. (2014) 124:822–6. doi: 10.1182/blood-2014–03-563817

11. Chaleff S, Otto M, Barfield RC, Leimig T, Iyengar R, Martin J, et al. A large-scale method for the selective depletion of alphabeta T lymphocytes from PBSC for allogeneic transplantation. *Cytotherapy*. (2007) 9:746–54. doi: 10.1080/14653240701644000
12. Schumm M, Lang P, Bethge W, Faul C, Feuchtinger T, Pfeiffer M, et al. Depletion of T-cell receptor alpha/beta and CD19 positive cells from apheresis products with the CliniMACS device. *Cytotherapy*. (2013) 15:1253–8. doi: 10.1016/j.jcyt.2013.05.014
13. Locatelli F, Merli P, Pagliara D, Li Pira G, Falco M, Pende D, et al. Outcome of children with acute leukemia given HLA-haploidentical HSCT after alphabeta T-cell and B-cell depletion. *Blood*. (2017) 130:677–85. doi: 10.1182/blood-2017–04-779769
14. Bonneville M, O'Brien RL, Born WK. Gammadelta T cell effector functions: a blend of innate programming and acquired plasticity. *Nat Rev Immunol*. (2010) 10:467–78. doi: 10.1038/nri2781
15. Locatelli F, Merli P, Rutella S. At the Bedside: innate immunity as an immunotherapy tool for hematological malignancies. *J Leukoc Biol*. (2013) 94:1141–57. doi: 10.1189/jlb.0613343
16. Airoldi I, Bertaina A, Prigione I, Zorzoli A, Pagliara D, Cocco C, et al. gammadelta T-cell reconstitution after HLA-haploidentical hematopoietic transplantation depleted of TCR-alphabeta+/CD19+ lymphocytes. *Blood*. (2015) 125:2349–58. doi: 10.1182/blood-2014–09-599423
17. Kunzmann V, Bauer E, Wilhelm M. Gamma/delta T-cell stimulation by pamidronate. *N Engl J Med*. (1999) 340:737–8. doi: 10.1056/NEJM199903043400914
18. Gu S, Nawrocka W, Adams EJ. Sensing of pyrophosphate metabolites by Vgamma9Vdelta2 T cells. *Front Immunol*. (2014) 5:688. doi: 10.3389/fimmu.2014.00688
19. Nishio N, Fujita M, Tanaka Y, Maki H, Zhang R, Hirosawa T, et al. Zoledronate sensitizes neuroblastoma-derived tumor-initiating cells to cytolysis mediated by human gammadelta T cells. *J Immunother*. (2012) 35:598–606. doi: 10.1097/CJI.0b013e31826a745a
20. Bertaina A, Zorzoli A, Petretto A, Barbarito G, Inglese E, Merli P, et al. Zoledronic acid boosts γδ T-cell activity in children receiving αβ+ T and CD19+ cell depleted grafts from an HLA-haploidentical donor. *Oncoimmunology*. (2016) 27:e1216291. doi: 10.1080/2162402X.2016.1216291
21. Moretta L, Locatelli F, Pende D, Marcenaro E, Mingari MC, Moretta A. Killer Ig-like receptor-mediated control of natural killer cell alloreactivity in haploidentical hematopoietic stem cell transplantation. *Blood*. (2011) 117:764–71. doi: 10.1182/blood-2010–08-264085
22. Li Pira G, Malaspina D, Girolami E, Biagini S, Cicchetti E, Conflitti G, et al. Selective depletion of alphabeta T cells and B cells for human leukocyte antigen-haploidentical hematopoietic stem cell transplantation. A three-year flow-up of procedure efficiency. *Biol Blood Marrow Transplant*. (2016) 22:2056–64. doi: 10.1016/j.bbmt.2016.08.006
23. Ooi HL, Briody J, Biggin A, Cowell CT, Munns CF. Intravenous zoledronic Acid given every 6 months in childhood osteoporosis. *Horm Res Paediatr*. (2013) 80:179–84. doi: 10.1159/000354303
24. Dieli F, Vermijlen D, Fulfaro F, Caccamo N, Meraviglia S, Cicero G, et al. Targeting human {gamma}delta} T cells with zoledronate and interleukin-2 for immunotherapy of hormone-refractory prostate cancer. *Cancer Res*. (2007) 67:7450–7. doi: 10.1158/0008–5472.CAN-07–0199
25. Byar DP. Identification of prognostic factorsm, in *Cancer clinical trials*, eds Buyse ME, Staquet MJ, Sylvester RJ (New York, NY: Oxford University Press) (1988) 423–43.
26. Glucksberg H, Storb R, Fefer A, Buckner CD, Neiman PE, Clift RA, et al. Clinical manifestations of graft-versus-host disease in human recipients of marrow from HL-A-matched sibling donors. *Transplantation*. (1974) 18:295–304. doi: 10.1097/00007890–197410000-00001
27. Shulman HM, Sullivan KM, Weiden PL, McDonald GB, Striker GE, Sale GE, et al. Chronic graft-versus-host syndrome in man. A long-term clinicopathologic study of 20 Seattle patients. *Am J Med*. (1980) 69:204–17. doi: 10.1016/0002–9343(80)90380–0
28. Kaplan E, Meier P. Non parametric estimation from incomplete observations. *J Am Stat Assoc*. (1958) 53:457–81. doi: 10.1080/01621459.1958.10501452
29. Gooley TA, Leisenring W, Crowley J, Storer BE. Estimation of failure probabilities in the presence of competing risks: new representations of old estimators. *Stat Med*. (1999) 18:695–706.
30. lein JP, Rizzo JD, Zhang MJ, Keiding N. Statistical methods for the analysis and presentation of the results of bone marrow transplants. part I: unadjusted analysis. *Bone Marrow Transplant*. (2001) 28:909–15. doi: 10.1038/sj.bmt.1703260
31. Gray R. A class of K-sample tests for comparing the cumulative incidence of a competing risk. *Ann Stat*. (1988) 16:1141–54. doi: 10.1214/aos/1176350951
32. Kanda Y. Investigation of the freely available easy-to-use software 'EZR' for medical statistics. *Bone Marrow Transplant*. (2013) 48:452–8. doi: 10.1038/bmt.2012.244
33. Vantourout P, Hayday A. Six-of-the-best: unique contributions of γδ T cells to immunology. *Nat Rev Immunol*. (2013) 13:88–100. doi: 10.1038/nri3384
34. Lamb LS Jr, Musk P, Ye Z, van Rhee F, Geier SS, Tong JJ, et al. Human gammadelta(+) T lymphocytes have *in vitro* graft vs leukemia activity in the absence of an allogeneic response. *Bone Marrow Transplant*. (2001) 27:601–6. doi: 10.1038/sj.bmt.1702830
35. Wilhelm M, Kunzmann V, Eckstein S, Reimer P, Weissinger F, Ruediger T, et al. Gammadelta T cells for immune therapy of patients with lymphoid malignancies. *Blood*. (2003) 102:200–6. doi: 10.1182/blood-2002–12-3665
36. Born WK, Kemal Aydintug M, O'Brien RL. Diversity of γδ T-cell antigens. *Cell Mol Immunol*. (2013) 10:13–20. doi: 10.1038/cmi.2012.45
37. Lamb LS Jr, Henslee-Downey PJ, Parrish RS, Godder K, Thompson J, Lee C, et al. Increased frequency of TCR gamma delta + T cells in disease-free survivors following T cell-depleted, partially mismatched, related donor bone marrow transplantation for leukemia. *J Hematother*. (1996) 5:503–9. doi: 10.1089/scd.1.1996.5.503
38. Perko R, Kang G, Sunkara A, Leung W, Thomas PG, Dallas MH. Gamma delta T cell reconstitution is associated with fewer infections and improved event-free survival after hematopoietic stem cell transplantation for pediatric leukemia. *Biol Blood Marrow Transplant*. (2015) 21:130–6. doi: 10.1016/j.bbmt.2014.09.027
39. Lamb LS, Jr. Gee AP, Hazlett LJ, Musk P, Parrish RS, O'Hanlon TP, et al. Influence of T cell depletion method on circulating gammadelta T cell reconstitution and potential role in the graft-versus-leukemia effect. *Cytotherapy*. (1999) 1:7–19 doi: 10.1080/0032472031000141295
40. Kunzmann V, Bauer E, Feurle J, Weissinger F, Tony HP, Wilhelm M. Stimulation of gammadelta T cells by aminobisphosphonates and induction of antiplasma cell activity in multiple myeloma. *Blood*. (2000) 96:384–92. doi: 10.1182/blood.V96.2.384
41. Gober HJ, Kistowska M, Angman L, Jeno P, Mori L, de Libero G. Human T cell receptor gammadelta cells recognize endogenous mevalonate metabolites in tumor cells. *J Exp Med*. (2003) 197:163–8. doi: 10.1084/jem.20021500
42. Idrees AS, Sugie T, Inoue C, Murata-Hirai K, Okamura H, Morita CT et al. Comparison of gammadelta T cell responses and farnesyl diphosphate synthase inhibition in tumor cells pretreated with zoledronic acid. *Cancer Sci*. (2013) 104:536–42. doi: 10.1111/cas.12124
43. Simm PJ, Johannesen J, Briody J, McQuade M, Hsu B, Bridge C, et al. Zoledronic acid improves bone mineral density, reduces bone turnover and improves skeletal architecture over 2 years of treatment in children with secondary osteoporosis. *Bone*. (2011) 49:939–43. doi: 10.1016/j.bone.2011.07.031
44. Russell HV, Groshen SG, Ara T, DeClerck YA, Hawkins R, Jackson HA, et al. A phase I study of zoledronic acid and low-dose cyclophosphamide in recurrent/refractory neuroblastoma: a new approaches to neuroblastoma therapy (NANT) study. *Pediatr Blood Cancer*. (2011) 57:275–82. doi: 10.1002/pbc.22821
45. McClune BL, Polgreen LE, Burmeister LA, Blaes AH, Mulrooney DA, Burns LJ, et al. Screening, prevention and management of osteoporosis and bone loss in adult and pediatric hematopoietic cell transplant recipients. *Bone Marrow Transplant*. (2011) 46:1–9. doi: 10.1038/bmt.2010.198
46. Grigg A, Butcher B, Khodr B, Bajel A, Hertzberg M, Patil S, et al. An individualised risk-adapted protocol of pre- and post transplant zoledronic acid reduces bone loss after allogeneic stem cell transplantation: results of a phase II prospective trial. *Bone Marrow Transplant*. (2017) 52:1288–93. doi: 10.1038/bmt.2017.108
47. Maschan M, Shelikhova L, Ilushina M, Kurnikova E, Boyakova E, Balashov D, et al. TCR-alpha/beta and CD19 depletion and treosulfan-based conditioning regimen in unrelated and haploidentical transplantation

in children with acute myeloid leukemia. *Bone Marrow Transplant*. (2016) 51:668–74. doi: 10.1038/bmt.2015.343
48. Lang P, Teltschik HM, Feuchtinger T, Muller I, Pfeiffer M, Schumm M, et al. Transplantation of CD3/CD19 depleted allografts from haploidentical family donors in paediatric leukaemia. *Br J Haematol*. (2014) 165:688–98. doi: 10.1111/bjh.12810
49. Patel SS, Wacholtz MC, Duby AD, Thiele DL, Lipsky PE. Analysis of the functional capabilities of CD3+CD4-CD8- and CD3+CD4+CD8+ human T cell clones. *J Immunol*. (1989) 143:1108–17.
50. Drobyski WR, Vodanovic-Jankovic S, Klein J. Adoptively transferred gamma delta T cells indirectly regulate murine graft-versus-host reactivity following donor leukocyte infusion therapy in mice. *J Immunol*. (2000) 165:1634–40. doi: 10.4049/jimmunol.165.3.1634
51. Wesch D, Peters C, Siegers GM. Human gamma delta T regulatory cells in cancer: fact or fiction? *Front Immunol*. (2014) 5:598. doi: 10.3389/fimmu.2014.00598
52. Traxlmayr MW, Wesch D, Dohnal AM, Funovics P, Fischer MB, Kabelitz D, et al. Immune suppression by gammadelta T-cells as a potential regulatory mechanism after cancer vaccination with IL-12 secreting dendritic cells. *J Immunother*. (2010) 33:40–52. doi: 10.1097/CJI.0b013e3181b51447
53. Kuhl AA, Pawlowski NN, Grollich K, Blessenohl M, Westermann J, Zeitz M, et al. Human peripheral gammadelta T cells possess regulatory potential. *Immunology*. (2009) 128:580–8. doi: 10.1111/j.1365–2567.2009.03162.x
54. Peters C, Oberg HH, Kabelitz D, Wesch D. Phenotype and regulation of immunosuppressive Vδ2-expressing γδ T cells. *Cell Mol Life Sci*. (2014) 71:1943–60. doi: 10.1007/s00018–013-1467–1
55. Otsuka A, Hanakawa S, Miyachi Y, Kabashima K. CD39: a new surface marker of mouse regulatory γδ T cells. *J Allergy Clin Immunol*. (2013) 132:1448–51. doi: 10.1016/j.jaci.2013.05.037
56. Rezende RM, da Cunha AP, Kuhn C, Rubino S, M'Hamdi H, Gabriely G, et al. Identification and characterization of latency-associated peptide-expressing gammadelta T cells. *Nat Commun*. (2015) 6:8726. doi: 10.1038/ncomms9726
57. Klingebiel T, Cornish J, Labopin M, Locatelli F, Darbyshire P, Handgretinger R, et al. Results and factors influencing outcome after fully haploidentical hematopoietic stem cell transplantation in children with very high-risk acute lymphoblastic leukemia: impact of center size: an analysis on behalf of the acute leukemia and pediatric disease working parties of the European blood and marrow transplant group. *Blood*. (2010) 115:3437–46. doi: 10.1182/blood-2009–03-207001
58. Marks DI, Khattry N, Cummins M, Goulden N, Green A, Harvey J, et al. Haploidentical stem cell transplantation for children with acute leukaemia. *Br J Haematol*. (2006) 134:196–201. doi: 10.1111/j.1365–2141.2006.06140.x
59. Smetak M, Kimmel B, Birkmann J, Schaefer-Eckart K, Einsele H, Wilhelm M, et al. Clinical-scale single-step CD4(+) and CD8(+) cell depletion for donor innate lymphocyte infusion (DILI). *Bone Marrow Transplant*. (2008) 41:643–50. doi: 10.1038/sj.bmt.1705942
60. Lamb LS Jr, Sande J. B-cell enrichment and infusion in CD4+/CD8+ T-cell depleted products for donor innate immune lymphocyte infusion: is risk of EBV-associated lymphocyte post transplantation lymphoproliferative disease a concern? *Bone Marrow Transplant*. (2008) 41:995–6. doi: 10.1038/bmt.2008.17
61. Kalyan S, Quabius ES, Wiltfang J, Monig H, Kabelitz D. Can peripheral blood gammadelta T cells predict osteonecrosis of the jaw? An immunological perspective on the adverse drug effects of aminobisphosphonate therapy. *J Bone Miner Res*. (2013) 28:728–35. doi: 10.1002/jbmr.1769
62. Kalyan S, Chandrasekaran V, Quabius ES, Lindhorst TK, Kabelitz D. Neutrophil uptake of nitrogen-bisphosphonates leads to the suppression of human peripheral blood gammadelta T cells. *Cell Mol Life Sci*. (2014) 71:2335–46. doi: 10.1007/s00018–013-1495-x
63. Lucarelli B, Merli P, Bertaina V, Locatelli F. Strategies to accelerate immune recovery after allogeneic hematopoietic stem cell transplantation. *Expert Rev Clin Immunol*. (2016) 12:343–58. doi: 10.1586/1744666X.2016.1123091
64. Mostoufi-Moab S, Ginsberg JP, Bunin N, Zemel B, Shults J, Leonard MB. Bone density and structure in long-term survivors of pediatric allogeneic hematopoietic stem cell transplantation. *J Bone Miner Res*. (2012) 27:760–9. doi: 10.1002/jbmr.1499

Conflict of Interest: The authors declare that the research was conducted in the absence of any commercial or financial relationships that could be construed as a potential conflict of interest.

frontiers in Immunology

REVIEW
published: 22 May 2020
doi: 10.3389/fimmu.2020.00992

Emerging Challenges of Preclinical Models of Anti-tumor Immunotherapeutic Strategies Utilizing Vγ9Vδ2 T Cells

Noémie Joalland[1,2] *and Emmanuel Scotet*[1,2]*

[1] Université de Nantes, INSERM, CNRS, CRCINA, Nantes, France, [2] LabEx IGO "Immunotherapy, Graft, Oncology", Nantes, France

Despite recent advances, the eradication of cancers still represents a challenge which justifies the exploration of additional therapeutic strategies such as immunotherapies, including adoptive cell transfers. Human peripheral Vγ9Vδ2 T cells, which constitute a major transitional immunity lymphocyte subset, represent attractive candidates because of their broad and efficient anti-tumor functions, as well as their lack of alloreactivity and easy handling. Vγ9Vδ2 T cells act like immune cell stress sensors that can, in a tightly controlled manner but through yet incompletely understood mechanisms, detect subtle changes of levels of phosphorylated metabolites of isoprenoid synthesis pathways. Consequently, various anti-tumor immunotherapeutic strategies have been proposed to enhance their reactivity and cytotoxicity, as well as to reduce the deleterious events. In this review, we expose these advances based on different strategies and their validation in preclinical models. Importantly, we next discuss advantages and limits of each approach, by highlighting the importance of the use of relevant preclinical model for evaluation of safety and efficacy. Finally, we propose novel perspectives and strategies that should be explored using these models for therapeutic improvements.

Keywords: human Vγ9Vδ2 T lymphocytes, cancer, functions, immunotherapy, preclinical models

OPEN ACCESS

Edited by:
Dieter Kabelitz,
University of Kiel, Germany

Reviewed by:
Serena Meraviglia,
University of Palermo, Italy
Thomas H. Winkler,
University of Erlangen Nuremberg, Germany

***Correspondence:**
Emmanuel Scotet
emmanuel.scotet@inserm.fr

Specialty section:
This article was submitted to T Cell Biology, a section of the journal Frontiers in Immunology

Received: *14 February 2020*
Accepted: *27 April 2020*
Published: *22 May 2020*

Citation:
Joalland N and Scotet E (2020) Emerging Challenges of Preclinical Models of Anti-tumor Immunotherapeutic Strategies Utilizing Vγ9Vδ2 T Cells. Front. Immunol. 11:992. doi: 10.3389/fimmu.2020.00992

BIOLOGY AND ANTI-TUMOR FUNCTIONS OF HUMAN Vγ9Vδ2 T CELLS

The complex immune system orchestrates with molecular and cellular components that act concomitantly or sequentially to sense and to eliminate potential exogenous and endogenous threats. In vertebrates, the innate immunity is the first germline-encoded and older evolutionary defense strategy that contributes to a rapid, but poorly specific, reactivity that also remains essential for recruiting immune cells and establishing a physical and chemical barrier. A major hallmark of the adaptive immunity, that is associated to immunological memory and next takes place after this initial process, is the extreme specificity against particular antigenic structures. This slower, but highly potent, immune reactivity axis is made up of the two mainT and B lymphocyte effector subsets. Recently, a growing class of additional cellular contributors, that express either TCR (*T Cell Receptor*) or BCR (*B Cell Receptor*) molecules and share phenotypical and functional characteristics from both systems has been identified. They have been differentially named as transitional immunity, unconventional or innate-*like* effectors. Most well-described cell subsets

that fall at this interface between innate and adaptive immunities are NKT (*Natural Killer T*), MAIT (*Mucosal Associated Invariant T*) and γδ T cells (1). This latter T cell subset expresses a heterodimeric TCR composed of γ and δ chains, named as opposed to α and β chains, associated to the CD3 signaling complex (2, 3). It is important to note that, although γδ T cell subsets are present in most vertebrates, there is little conservation of γ and δ TCR chains and reactivities between species. This has been evidenced by genetic studies indicating a high heterogeneity between murine and primate TCR genes (4, 5).

For the sake of clarity, we propose to focus this present review on human γδ T cell biology, and more precisely, the human Vγ9Vδ2 T cell subset, as well as their therapeutic targeting in preclinical cancer models. The γδ TCR is composed from a limited number of γ and δ chains (<15 Vγ and Vδ gene segments) but this low combinatorial diversity is efficiently counterbalanced by both an elevated junctional diversity and pairing assembly restrictions to finally produce an extremely diverse γδ TCR. In humans, γδ T cells are distributed into four major subsets, which have been identified according to the expression of δ chain segments, as $V\delta1^+$, $V\delta2^+$, $V\delta3^+$, and $V\delta5^+$ populations (6). Following ontogeny, most γδ T cell subsets naturally exhibit a preferential tropism for particular tissues/organs, through yet unclear mechanisms. As a typical example of this preferential localization, human Vγ9Vδ2 T cells [using the nomenclature of Lefranc & Rabbitts (7)] constitute a major subset in adult peripheral blood (8, 9). Vγ9Vδ2T cells represent prototypical immune sensors of cellular stress activated under various pathological contexts, such as infections and cancer. The species-specific antigenic activation of Vγ9Vδ2 T cells is a contact- and a TCR-dependent process. It is important to note that this activation is not restricted by either conventional MHC class I or II molecules, thus theoretically minimizing the risk of alloreactive reactions for allogeneic Vγ9Vδ2 T cell-therapies (e.g., GVHD, *graft vs. host disease*). This antigenic activation process implicates mandatory small phosphorylated carbohydrate metabolites (hereafter called phosphoantigens, PAg), such as IPP (*Isopentenyl PyroPhosphate*), which endogenous (MEV mammalian mevalonate pathway), or exogenous (MEP microbial pathway) expression might be altered in some pathological contexts (e.g., cancer, infections). Recent studies have shown that PAg levels are sensed through mechanisms involving both BTN2A1 and BTN3A1 butyrophilins (BTN) expressed by target cells (10–12). Accordingly, pharmacological compounds that inhibit the synthesis (i.e., statins) or the degradation (i.e., aminobisphosphonates, alkylamines) of PAg in mammalian cells can block, or induce, the antigenic activation of Vγ9Vδ2 T cells, respectively (13, 14). Importantly, this *Self*-reactive nature of Vγ9Vδ2 T cells needs to be tightly regulated by a set of various molecules [see (15) and (16), for recent reviews], such as adhesion molecules (i.e., CD54), activating (i.e., NKG2D) or inhibiting (i.e., CD94/NKG2A,) NKR (*Natural Killer Receptors*), FcR (*Fc Receptor*) (i.e., FcRγIIIA/CD16), Nectin/Nectin-*like* (i.e., CD226), TLR (*Toll-like Receptor*) (i.e., TLR4), cytokine receptors (i.e., IL (*interleukin*)-15R, IL-21R), and immune checkpoint inhibitors (i.e., PD-1, *programmed cell death protein 1*). Hence, numerous Vδ2 T cell dysfunctions in cancer indications (e.g., hypo-reactivity, exhaustion) have been associated to altered expression profiles of these molecules. In this exquisite sensing process, Vγ9Vδ2 T cells integrate activatory and inhibitory signals to rapidly deliver strong functional responses such as proliferation, cytolysis (through perforin/granzyme-, TRAIL (*TNF-related apoptosis inducing ligand*)-, CD95-pathways) and cytokines (i.e., TNF (*Tumor Necrosis Factor*)-α, IFN (*Interferon*)-γ)/chemokines (i.e., CCL3, *Chemokine (C-C motif) ligand 3*)/anti-microbial factors (i.e., granulysin)/epithelial growth factors (i.e., KGF, *Keratinocyte Growth Factor*) release. These latter functions are also linked to their capacity to help other immune effectors and induce the maturation of antigen-presenting cells, including themselves (9). Finally, as for most lymphocyte subsets, the migration of Vγ9Vδ2 T cells is tightly controlled by a set of chemoattractant factors, such as chemokine receptors. Their expression regulates Vγ9Vδ2 T cell trafficking during physiological and inflammatory conditions (e.g., CCR5, *Chemokine (C-C motif) Receptor 5*), a process that is proposed to be of particular importance for tumor addressing and infiltration *in vivo*.

For a long time, a set of compelling *in vitro* studies evidenced the natural reactivity of human Vγ9Vδ2 T cells against a broad range of human tumor cell lines and normal cells infected by a variety of viruses, parasites and bacteria (17–19). With respect to transformed cells, the range of cell lines recognized by Vγ9Vδ2 T cells, initially thought to be primarily restricted to hematopoietic tumors (20, 21), was next extended to several solid tumors, such as renal and colon carcinomas (22–24). Importantly, this vision has been next modified by the availability of aminobisphophonates (e.g., pamidronate, zoledronate) and synthetic PAg (e.g., BrHPP, *BromoHydrin Pyrophosphate*) that can further help sensitizing a broad variety of cells to Vγ9Vδ2 T cell sensing and elimination. Like for most γδ T cell subsets, *in vitro* studies showed that Vγ9Vδ2 T cells are able to directly kill target cells and express pro-inflammatory cytokines that can be also involved in the clearance of tumor cells (25, 26). Altogether, these *in vitro* observations supported a natural implication of Vγ9Vδ2 T cells in protective anti-tumor immunity. Based on initial results indicating an altered tumor growth control in TCR δ^{neg} mice (27), several *in vivo* studies showed that transferred allogeneic Vγ9Vδ2 T cells can reach and infiltrate tumor site and display a strong anti-tumor activity as evidenced by significant clinical benefits (e.g., survival, tumor growth) (28, 29). The implication of Vγ9Vδ2T cells in the anti-tumor immune reactivity is supported by the fact that infiltrating γδ T cells are considered as a favorable cancer prognosis marker for several cancers (30, 31), Vδ2 T cells infiltrating tumors were detected in various types of cancer. However, their precise physiological role might vary from one condition to another, mainly due the heterogeneity of the tumor microenvironment which can modulate their functions as well as their functional plasticity (30, 31).

RATIONALE FOR HARNESSING Vγ9Vδ2 T CELLS IN CANCER IMMUNOTHERAPY

Human Vγ9Vδ2 T cells should be considered as attractive immune effectors of high therapeutic potential for the main following reasons:

1. Inter-individual conservation and elevated frequency in the peripheral blood of human adults;
2. Antigenic specificity linked to cell stress-associated molecules whose expression is frequently dysregulated in cancer cells;
3. Clinical-grade synthetic agonist molecules, such as aminobisphosphonates and PAg, that specifically induce activation, expansion and sensitization of human tumor cells;
4. Simple handling and elevated in/ex vivo expansion index;
5. Absence of alloreactivity (no MHC class I/II restrictions);
6. Capacity to reach and infiltrate tumors;
7. Direct and indirect cytotoxic activities against tumor cells, through the secretion of lytic molecules and pro-inflammatory cytokines.

SUCCESSES AND LIMITATIONS OF Vγ9Vδ2 T CELL CANCER IMMUNOTHERAPIES

Several types of immunotherapies that aim at helping the immune system to better react against tumor cells, are used to treat cancer. They include immune checkpoint inhibitors, monoclonal antibodies and immune cell therapy. In this latter category, active and passive immunotherapies are distinguished, according to the approaches developed for inducing Vγ9Vδ2 T cell activation and expansion.

Regarding active immunotherapies, several strategies have been considered to obtain *in vivo* activation of Vγ9Vδ2 T cell effectors induced following administration(s) of specific clinical-grade agonist molecules, such as PAg or aminobisphophonates, together with pro-proliferating cytokines (e.g., IL-2) (32, 33). These approaches originated from initial observations describing increased frequencies of peripheral Vγ9Vδ2 T cells in hematological cancer patients treated with pamidronate (34). In patients with non-Hodgkin's lymphoma or multiple myeloma, systemic administrations of both pamidronate with IL-2 were tolerated by patients and induced expansions of endogenous peripheral Vγ9Vδ2 T cells, accompanied by partial remissions of cancer in some patients (35). Next, this strategy was applied to solid tumors (i.e., non-hormonal prostate cancer) and showed that activation of Vγ9Vδ2 T cells *in vivo* was associated with the development of a pro-inflammatory(IFN-γ) responses (36). Following these first encouraging results, several clinical trials have been conducted in patients with renal cell carcinoma or bone metastases deriving from breast or prostate cancers (32, 33). These studies have demonstrated therapeutic responses such as stabilized diseases and partial remissions in some patients (37–39). More recently, the efficacy of this strategy was improved in patients with malignant hemopathies receiving haploidentical donor lymphocyte infusion (40). Importantly, the majority of treated patients in these trials experienced mild side effects (i.e., flu-*like* syndrome), likely associated to IL-2, thus confirming the reduced toxicity of this strategy. To further improve its specificity, synthetic PAg compounds have been produced at a clinical grade (i.e., BrHPP) and tested *in vivo*. In metastatic renal cell carcinoma patients who received repeated infusions of BrHPP and IL-2, potent Vγ9Vδ2 T cell expansions with moderate clinical activities were observed (41). These phase I/0 clinical assays showed a satisfactory feasibility of this approach, with a reduced toxicity (mainly due to IL-2) and excellent Vγ9Vδ2 T cell expansion rates, but modest clinical efficacies, that might have been complicated by the bad clinical condition of cancer patients. Further studies, including assays in monkeys, next pointed out potential issues such as the progressive exhaustion of Vγ9Vδ2 T cells (i.e., tachyphylaxis), altered immune status, activation contexts and tissue homing, that should be solved to improve the therapeutic efficacy of this strategy in cancer treatment (42).

Passive immunotherapies, which are based on *ex vivo* PBL(*Peripheral Blood Lymphocytes*)-Vγ9Vδ2 T cell expansions and cell transfer(s) have been tested in renal carcinoma patients with reduced toxicity by low therapeutic efficacy (43). Next, several clinical trials have been carried out in patients with circulating or solid cancers, who have been treated by adoptive transfer of autologous Vγ9Vδ2 T cells, amplified *ex vivo*, associated with IL-2 and zoledronate (32, 33). In general, these studies indicated a good feasibility but a low, although promising, therapeutic efficacy of this therapy as evidenced by some partial/complete cancer remissions. Clinical trials of adoptive transfer of allogeneic Vγ9Vδ2 T cells are currently underway. Recently, a case report of a patient with a stage IV cholangiocarcinoma showing recurrent mediastinal lymph node metastasis after liver transplantation was published. This patient received consecutive infusions of allogeneic Vγ9Vδ2 T cells which have been expanded from PBMC (*Peripheral Blood Mononuclear Cells*) of a healthy donor. No adverse effects were detected and a significant clinical response, with no detectable peritoneal lymph node metastasis, was reported at the end of treatment (44). Improved strategies for redirecting immune cell effectors to target cells expressing γδ T cell tumor antigens are being generated and tested for therapy (45). Thanks to the significant advance of genetic engineering and transduction approaches, the efficient expression of natural or optimized TCR (e.g., γδ TCR) can be realized in lymphocytes (46). The clinical-grade production of these engineered effectors [e.g., CAR (*Chimeric Antigen Receptor*) γδ T cells] has recently been validated and is currently being tested in patients with leukemia or multiple myeloma (33, 46).

Though promising (e.g., feasibility, safety), the results of these clinical trials, though exploratory or phase 0/I only, stressed the urgent need of developing new Vγ9Vδ2 T cell-immunotherapies (e.g., combined therapies) and optimizing their use (e.g., clinical positioning) to significantly improve their clinical efficacy in circulating and solid oncological indications. The achievement of this ambitious goal should require the use of robust physiological preclinical models *in vivo* for assessing both the feasibility and efficacy parameters of these strategies.

IMPLEMENTATION OF PRECLINICAL CANCER MODELS AND Vγ9Vδ2 IMMUNOTHERAPIES

A substantial number of preclinical *in vivo* cancer models, including, for some of them, Vγ9Vδ2 T cell immunotherapies, have been carried out using heterotopic mouse models established with subcutaneous injections of cultured human tumor cell lines. Among various advantages, these approaches allow a fast and easy monitoring of tumor growth by physical measurement of tumor volume (47). However, these fast growing models, also generally used for non-Vγ9Vδ2 T cell therapies, rarely faithfully recapitulate the complexity and heterogeneity of human oncological disease (e.g., origin of tumor cells, nature of the environment), also because of the large number of cells implanted in this particular localization (48, 49). Another problem is linked to their limited ability to disseminate (e.g., metastasis). To address this problem, it is important to orthotopically implant tumor cells (i.e., corresponding anatomical position) and, if possible, in a minimal quantity to further mimic the first stages of tumor development and its natural dissemination, according to the organ of origin (**Figure 1**). Importantly, the growing tumor should be characterized using various approaches such as imaging, histology or analysis of the phenotype of tumor cells to accurately determine the relevance of this model *in vivo* (50–52).

An indisputable tool for creating preclinical murine models representative of human pathology, not to mention therapies subsequently used, is the graft of explanted tumor samples from cancer patients. Two main strategies have been proposed: (i) the administration of dissociated and cultured tumor cells or (ii) the implantation of tumor fragments (hereafter called PDX, *patient-derived xenograft*) (**Figure 1**). These human tumors can heterotypically or orthotopically engrafted in immunodeficient mice, such as NSG (*NOD.Cg-PrkdcscidIl2rgtm1Wjl/SzJl*), with engraftment rates (40–95%) related to the presence of stroma. In the case of dissociated and cultured primary tumor cells, all these preparation steps might affect their phenotype and promote the biased growth of particular tumor variants. This issue can be addressed using tumor fragments (53) but the implantation of such large PDX is rarely possible in orthotopic because of size or surgical issues (e.g., intracerebral glioblastoma) (**Figure 1**). The engraftment and the growth of PDX often take 2–4 months, which can vary by tumor type, implant location, and the strain of immunodeficient mice utilized. This long duration parameter, further complicated by the necessity to divide and to re-implant small fragments of grafted PDX, strongly limits the use of PDX models and its interest for establishing robust, homogeneous and reliable tumor mouse models (i.e., progressive loss of tumor heterogeneity and replacement of the human microenvironment disappears by a murine stroma) (53).

In the absence of relevant and robust *in vitro* tumor models, including the promising, but currently developed spheroid/organoid/3D tumor systems, the development of novel therapies still requires assessment steps in preclinical animal models before being proposed for therapy. Their use is expected to help predict selected therapeutic effects and analyze selected parameters such as feasibility, side effects and toxicity. In particular with regard to human Vγ9Vδ2 T cells, it is not possible to use syngeneic murine models due to the lack of counterpart of this lymphocyte subset in mice and its species specificity (4, 5). Mostly due to an elevated cost of care, non-human primates, which also contain PAg-reactive γδ T cells, are ill-developed for cancer therapy studies. Highly immunodeficient mice, such as nude or NSG mice, represent the most relevant strains of choice for developing human cancer and immunotherapy models. However, the downside is that most of these immunodeficient mouse models are not relevant for analyzing the contribution of the tumor environment and immune system components to the anti-tumor efficacy of immunotherapies. Rebuilding human immune system in mice remains possible, thanks to the systemic injection of human PBMC in irradiated mice (54). However, this approach might generate strong xenogeneic reaction against the host, which limits the relevance and the operational time window for using these humanized animal models. In addition, the management and reproducibility of these sophisticated models remains complicated. Right now, the mostly developed method

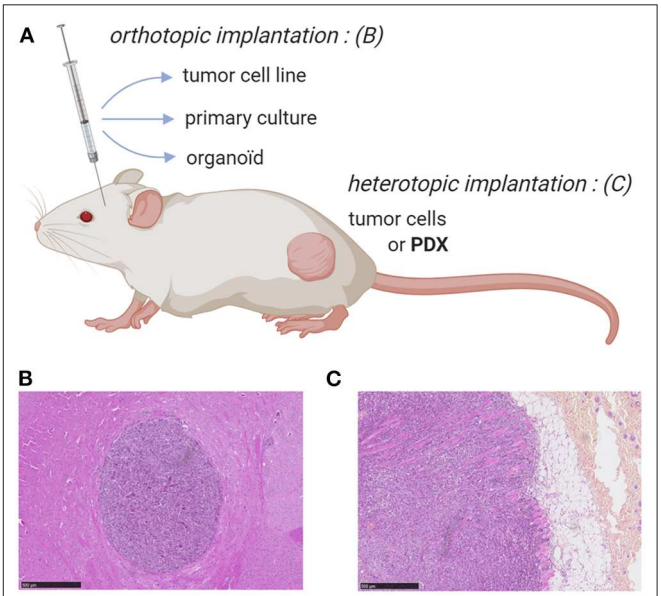

FIGURE 1 | Mouse models for ortho- or heterotopic administrations of human tumor cells. **(A)** Schematic representation of human tumor cell implantation strategies in immunodeficient mouse (e.g., NSG). Human tumor cells from either cell lines, primary/organoid cultures or patient-derived xenograft can be implanted orthotopically or heterotopically, respectively. **(B,C)** Immunohistochemistry (hematoxylin and eosin stainings) of orthtopic (brain) implantation of cells from a primary culture of human glioblastoma (GBM-1) **(B)** and heterotopic (subcutaneous) implantation of human prostate cancer cells (PC-3 cell line) **(C)**. Bars: 500 μm. NJ & ES, unpublished work.

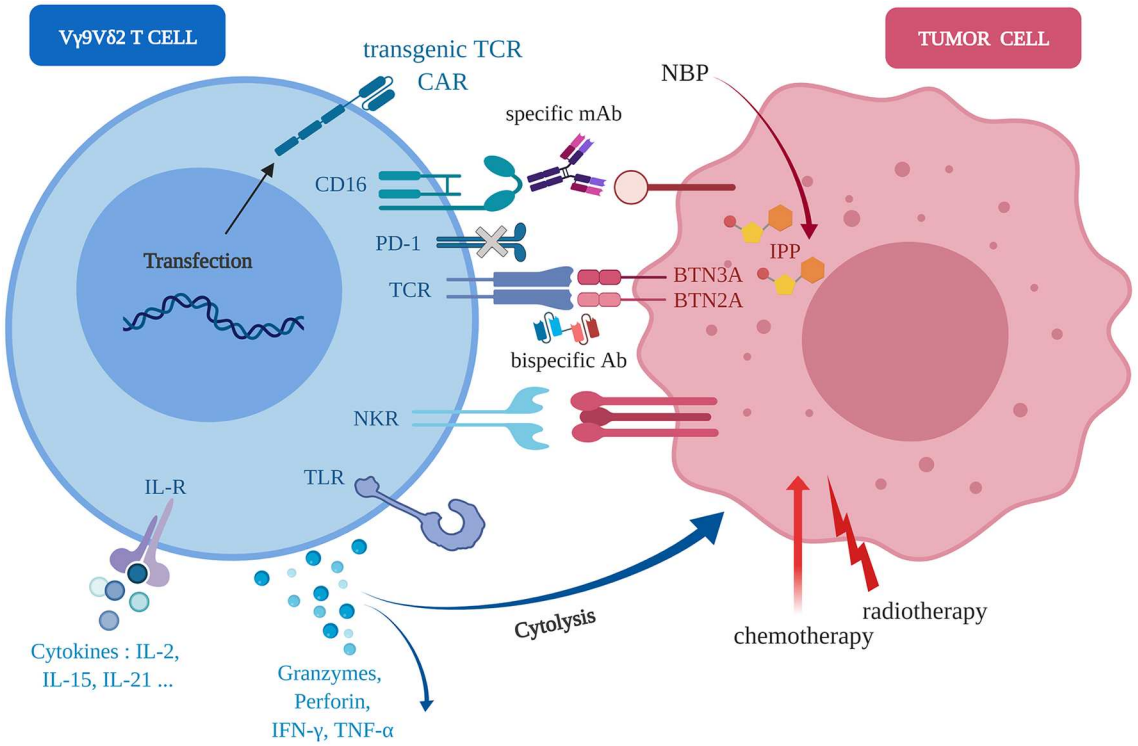

FIGURE 2 | Molecular axes foroptimization(s) of anti-tumor Vγ9Vδ2 immunotherapies. Human Vγ9Vδ2 T cells (*left, blue*) can sense human tumor cells (*right, red*) of diverse tissular origins, in independent or cooperative manners, through various molecular pathways implicating wild-type or engineered TCR, NKR, FcR/CD16, TLR, CAR. Following activation, the direct (cytolysis) and indirect (e.g., pro-inflammatory cytokines release) anti-tumor reactivity might be enhanced by either agonist compounds, such as aminobisphosphonates (NBP), standard chemo-radiotherapies or environment factors, such as cytokines (e.g., IL-21).

of humanization remains the injection/grafting of human tumor cells into immunodeficient mice.

PATHS FOR THE DEVELOPMENT OF IMPROVED Vγ9Vδ2 IMMUNOTHERAPIES USING PRECLINICAL MODELS

Various preclinical strategies are currently developed to assess the therapeutic potential of novel optimized Vγ9Vδ2 immunotherapies targeting various pathways (which are summarized in **Figure 2**). In particular, several research and clinical groups aim at proposing immunotherapeutic strategies to enhance the reactivity and the cytolytic activity of human Vγ9Vδ2 T cells against tumor cells (16). Of note, the routes for treatment administration in preclinical models should be carefully selected. Most clinical treatments are either orally or systemically administered which might significantly contribute to an increased toxicity or alow therapeutic efficiency (e.g., low specificity). An increasing number of studies evidenced the benefits of local administrations for limiting the systemic toxicity while increasing therapeutic doses (55, 56). These principles should be applied, if clinically possible, for the adoptive transfer(s) of Vγ9Vδ2 T cells.

Following an initial assessment *in vitro*, both orthotopic and heterotopic preclinical models of human tumors from various types of tissues, have been implemented in mice and used for the following Vγ9Vδ2 T cell immunotherapy optimizations (**Figure 2**):

- Natural reactivity of allogeneic Vγ9Vδ2 T cells against some tumor cell types. For example, some human mesenchymal GBM cells naturally overexpress NKG2D ligands that induce a natural Vγ9Vδ2 T cell reactivity leading to the elimination of tumor cells *in vivo* (57);
- Transfer(s) of human Vγ9Vδ2 T cells combined to agonist compounds (e.g., aminobisphosphonate compounds) administration(s) to further increase the recognition of tumor cells by Vγ9Vδ2 T cells (47). These therapeutic components can be injected either systemically (e.g., intravenously) or close to the tumor sites (for solid tumors) in orthotopic models (50, 52);
- Transfer(s) of human Vγ9Vδ2 T cells combined to radio-chemotherapies. This strategy relies on the observations that these first-line standard treatments are proposed for most cancer indications and could promote cell stress events that could increase the reactivity of Vγ9Vδ2 T cells against human tumor cells (58–60);

- Transfer(s) of human Vγ9Vδ2 T cells combined to antibodies directed against inhibitory immune checkpoint molecules (e.g., PD-1) (61) or ADCC (*Antibody-Dependent Cellular Cytotoxicity*)-triggering molecules molecules (e.g., FcγRIIIA/CD16) (62, 63);
- Bispecific antibodies which are generated under various molecular formats and have a dual specificity for a selected tumor antigen (targeting) and for the Vγ9Vδ2 TCR (activation) (64).
- Agonist antibodies targeting Vγ9Vδ2 T cell activation molecules (e.g., ectodomain of BTN3A1) to induce a PAg-independent, but TCR-specific, reactivity of Vγ9Vδ2 T cells against tumor cells (65);
- Selected cytokines that can enhance the cytotoxic potential of Vγ9Vδ2 T cells, such as IL-21 (51, 66), or boost their proliferation during *ex vivo* amplification before adoptive transfer, such as IL-15 associated to Vitamin C (67).

CONCLUDING REMARKS

In terms of phenotype and functions, the human Vγ9Vδ2 T cell subset represents a unique and highly attractive T cell population for designing efficient cancer immunotherapies. However, initial clinical trials targeting this subset yielded mixed results with both encouraging (e.g., good feasibility, weak toxicity) and disappointing observations (e.g., modest clinical efficacy), that could be attributed to inappropriately designed strategies or incorrect therapeutic settings. Nonetheless, these studies clearly met on the urgent need for proposing improved therapies, an objective that should be achieved through the development of more relevant and physiological preclinical models. Although first *in vivo* models have been proposed decades ago, with a major bias toward rodents (ie. mouse), their use for designing Vγ9Vδ2 T cell-immunotherapies has long been severely hampered by the strict species-specific restrictions of this primate subset. However, the research in this field widely accelerated in the past years thanks to the emergence and development of immunodeficient murine strains as well as improved grafting, mouse humanization and high-dimension detection/"big data" analysis approaches. Importantly, animal-free *in vitro* models (e.g., spheroids, organoids) are currently developed and should also be used soon in this process. Altogether, these elements should accelerate the entry of this research field within a novel dimension, which should be evidenced by an increased number of successful immunotherapeutic trials in cancer patients.

AUTHOR CONTRIBUTIONS

NJ and ES contributed to the writing process, prepared the manuscript, and approved the final version.

FUNDING

This work was supported by grants from INSERM, CNRS, Université de Nantes, Fondation pour la Recherche Médicale (FRM DEQ20170839118), Ligue Contre le Cancer AO GO2019 (Côtes d'Armor, Loire-Atlantique), Association pour la Recherche contre le Cancer (PJA20191209404). This work was realized in the context of the LabEX IGO program, supported by the National Research Agency Investissements d'Avenir via the program ANR-11-LABX-0016-01.

ACKNOWLEDGMENTS

The authors thank the staff of the cellular and tissular imaging core (MicroPICell) and the animal facilities (UTE) from SFR F. Bonamy, Nantes University, for their help and expert assistance.

REFERENCES

1. Dranoff G. Cytokines in cancer pathogenesis and cancer therapy. *Nat Rev Cancer.* (2004) 4:11–22. doi: 10.1038/nrc1252
2. Brenner MB, McLean J, Dialynas DP, Strominger JL, Smith JA, Owen FL, et al. Identification of a putative second T-cell receptor. *Nature.* (1986) 322:145–9. doi: 10.1038/322145a0
3. Saito H, Kranz DM, Takagaki Y, Hayday AC, Eisen HN, Tonegawa S. Complete primary structure of a heterodimeric T-cell receptor deduced from cDNA sequences. *Nature.* (1984) 309:757–62. doi: 10.1038/309757a0
4. Kazen AR, Adams EJ. Evolution of the VD and J gene segments used in the primate $\gamma\delta$ T-cell receptor reveals a dichotomy of conservation and diversity. *Proc Natl Acad Sci USA.* (2011) 108:E332–40. doi: 10.1073/pnas.1105105108
5. Sturm E, Bontrop RE, Vreugdenhil RJ, Otting N, Bolhuis RL. T-cell receptor gamma/delta: comparison of gene configurations and function between humans and chimpanzees. *Immunogenetics.* (1992) 36:294–301. doi: 10.1007/BF00215657
6. Zhao Y, Niu C, Cui J. Gamma-delta (γδ) T cells: friend or foe in cancer development? *J Transl Med.* (2018) 16:3. doi: 10.1186/s12967-018-1491-x
7. Lefranc MP, Rabbitts TH. A nomenclature to fit the organization of the human T-cell receptor γ and δ genes. *Res Immunol.* (1990) 141:615–8. doi: 10.1016/0923-2494(90)90068-A
8. Pauza CD, Cairo C. Evolution and function of the TCR Vgamma9 chain repertoire: it's good to be public. *Cell Immunol.* (2015) 296:22–30. doi: 10.1016/j.cellimm.2015.02.010
9. Vantourout P, Hayday A. Six-of-the-best: unique contributions of γδ T cells to immunology. *Nat Rev Immunol.* (2013) 13:88–100. doi: 10.1038/nri3384
10. Rigau M, Ostrouska S, Fulford TS, Johnson DN, Woods K, Ruan Z, et al. Butyrophilin 2A1 is essential for phosphoantigen reactivity by γδ T cells. *Science.* (2020) 367:eaay5516. doi: 10.1126/science.aay5516
11. Karunakaran MM, Willcox CR, Salim M, Paletta D, Fichtner AS, Noll A, et al. Butyrophilin-2A1 directly binds germline-encoded regions of the Vγ9Vδ2 TCR and is essential for phosphoantigen sensing. *Immunity.* (2020) 52:487–98.e6. doi: 10.1016/j.immuni.2020.02.014
12. Boutin L, Scotet E. Towards deciphering the hidden mechanisms that contribute to the antigenic activation process of human Vγ9Vδ2 T cells. *Front Immunol.* (2018) 9:828. doi: 10.3389/fimmu.2018.00828
13. Coppens I. Targeting lipid biosynthesis and salvage in apicomplexan parasites for improved chemotherapies. *Nat Rev Microbiol.* (2013) 11:823–35. doi: 10.1038/nrmicro3139
14. Thompson K, Rogers MJ. Statins prevent bisphosphonate-induced γ,δ-T-cell proliferation and activation in vitro. *J Bone Miner Res Off J Am Soc Bone Miner Res.* (2004) 19:278–88. doi: 10.1359/JBMR.0301230

15. Ribeiro ST, Ribot JC, Silva-Santos B. Five layers of receptor signaling in γδ T-cell differentiation and activation. *Front Immunol.* (2015) 6:15. doi: 10.3389/fimmu.2015.00015
16. Hoeres T, Smetak M, Pretscher D, Wilhelm M. Improving the efficiency of Vγ9Vδ2 T-cell immunotherapy in cancer. *Front Immunol.* (2018) 9:800. doi: 10.3389/fimmu.2018.00800
17. Gober H-J, Kistowska M, Angman L, Jenö P, Mori L, De Libero G. Human T cell receptor $\gamma\delta$ cells recognize endogenous mevalonate metabolites in tumor cells. *J Exp Med.* (2003) 197:163–8. doi: 10.1084/jem.20021500
18. Harly C, Peigné C-M, Scotet E. Molecules and mechanisms implicated in the peculiar antigenic activation process of human Vγ9Vδ2 T cells. *Front Immunol.* (2014) 5:657. doi: 10.3389/fimmu.2014.00657
19. Silva-Santos B, Serre K, Norell H. γδ T cells in cancer. *Nat Rev Immunol.* (2015) 15:683–91. doi: 10.1038/nri3904
20. Kunzmann V, Bauer E, Feurle J, Weissinger F, Tony HP, Wilhelm M. Stimulation of gammadelta T cells by aminobisphosphonates and induction of antiplasma cell activity in multiple myeloma. *Blood.* (2000) 96:384–92. doi: 10.1182/blood.V96.2.384.013k07_384_392
21. Sturm E, Braakman E, Fisch P, Vreugdenhil RJ, Sondel P, Bolhuis RL. Human Vγ9-Vδ2 T cell receptor-gamma delta lymphocytes show specificity to Daudi Burkitt's lymphoma cells. *J Immunol Baltim Md.* (1990) 145:3202–8.
22. Kobayashi H, Tanaka Y, Yagi J, Toma H, Uchiyama T. Gamma/delta T cells provide innate immunity against renal cell carcinoma. *Cancer Immunol Immunother CII.* (2001) 50:115–24. doi: 10.1007/s002620100173
23. Viey E, Fromont G, Escudier B, Morel Y, Da Rocha S, Chouaib S, et al. Phosphostim-activated $\gamma\delta$ T cells kill autologous metastatic renal cell carcinoma. *J Immunol Baltim Md 1950.* (2005) 174:1338–47. doi: 10.4049/jimmunol.174.3.1338
24. Corvaisier M, Moreau-Aubry A, Diez E, Bennouna J, Mosnier J-F, Scotet E, et al. Vγ9Vδ2 T cell response to colon carcinoma cells. *J Immunol Baltim Md 1950.* (2005) 175:5481–8. doi: 10.4049/jimmunol.175.8.5481
25. Dunne MR, Mangan BA, Madrigal-Estebas L, Doherty DG. Preferential Th1 cytokine profile of phosphoantigen-stimulated human Vγ9Vδ2 T cells. *Mediators Inflamm.* (2010) 2010:704941. doi: 10.1155/2010/704941
26. García VE, Sieling PA, Gong J, Barnes PF, Uyemura K, Tanaka Y, et al. Single-cell cytokine analysis of gamma delta T cell responses to nonpeptide mycobacterial antigens. *J Immunol Baltim Md 1950.* (1997) 159:1328–35.
27. Girardi M, Glusac E, Filler RB, Roberts SJ, Propperova I, Lewis J, et al. The distinct contributions of murine T cell receptor (TCR)γδ+ and TCRαβ+ T cells to different stages of chemically induced skin cancer. *J Exp Med.* (2003) 198:747–55. doi: 10.1084/jem.20021282
28. Kabelitz D, Wesch D, Pitters E, Zöller M. Characterization of tumor reactivity of human Vγ9Vδ2$\gamma\delta$ T cells in vitro and in SCID mice in vivo. *J Immunol Baltim Md 1950.* (2004) 173:6767–76. doi: 10.4049/jimmunol.173.11.6767
29. Zheng BJ, Chan KW, Im S, Chua D, Sham JS, Tin PC, et al. Anti-tumor effects of human peripheral $\gamma\delta$ T cells in a mouse tumor model. *Int J Cancer.* (2001) 92:421–5. doi: 10.1002/ijc.1198
30. Gentles AJ, Newman AM, Liu CL, Bratman SV, Feng W, Kim D, et al. The prognostic landscape of genes and infiltrating immune cells across human cancers. *Nat Med.* (2015) 21:938–45. doi: 10.1038/nm.3909
31. Lo Presti E, Dieli F, Meraviglia S. Tumor-infiltrating γδ T lymphocytes: pathogenic role, clinical significance, and differential programing in the tumor microenvironment. *Front Immunol.* (2014) 5:607. doi: 10.3389/fimmu.2014.00607
32. Fournié J-J, Sicard H, Poupot M, Bezombes C, Blanc A, Romagné F, et al. What lessons can be learned from γδ T cell-based cancer immunotherapy trials? *Cell Mol Immunol.* (2013) 10:35–41. doi: 10.1038/cmi.2012.39
33. Sebestyen Z, Prinz I, Déchanet-Merville J, Silva-Santos B, Kuball J. Translating gammadelta (γδ) T cells and their receptors into cancer cell therapies. *Nat Rev Drug Discov.* (2019) 19:169–84. doi: 10.1038/s41573-019-0038-z
34. Kunzmann V, Bauer E, Wilhelm M. γ/δ T-cell stimulation by pamidronate. *N Engl J Med.* (1999) 340:737–8. doi: 10.1056/NEJM199903043400914
35. Wilhelm M, Kunzmann V, Eckstein S, Reimer P, Weissinger F, Ruediger T, et al. $\gamma\delta$ T cells for immune therapy of patients with lymphoid malignancies. *Blood.* (2003) 102:200–6. doi: 10.1182/blood-2002-12-3665
36. Dieli F, Gebbia N, Poccia F, Caccamo N, Montesano C, Fulfaro F, et al. Induction of $\gamma\delta$ T-lymphocyte effector functions by bisphosphonate zoledronic acid in cancer patients in vivo. *Blood.* (2003) 102:2310–1. doi: 10.1182/blood-2003-05-1655
37. Dieli F, Vermijlen D, Fulfaro F, Caccamo N, Meraviglia S, Cicero G, et al. Targeting human $\gamma\delta$ T cells with zoledronate and interleukin-2 for immunotherapy of hormone-refractory prostate cancer. *Cancer Res.* (2007) 67:7450–7. doi: 10.1158/0008-5472.CAN-07-0199
38. Lang JM, Kaikobad MR, Wallace M, Staab MJ, Horvath DL, Wilding G, et al. Pilot trial of interleukin-2 and zoledronic acid to augment γδ T cells as treatment for patients with refractory renal cell carcinoma. *Cancer Immunol Immunother CII.* (2011) 60:1447–60. doi: 10.1007/s00262-011-1049-8
39. Meraviglia S, Eberl M, Vermijlen D, Todaro M, Buccheri S, Cicero G, et al. In vivo manipulation of Vγ9Vδ2 T cells with zoledronate and low-dose interleukin-2 for immunotherapy of advanced breast cancer patients. *Clin Exp Immunol.* (2010) 161:290–7. doi: 10.1111/j.1365-2249.2010.04167.x
40. Wilhelm M, Smetak M, Schaefer-Eckart K, Kimmel B, Birkmann J, Einsele H, et al. Successful adoptive transfer and in vivo expansion of haploidentical γδ T cells. *J Transl Med.* (2014) 12:45. doi: 10.1186/1479-5876-12-45
41. Bennouna J, Levy V, Sicard H, Senellart H, Audrain M, Hiret S, et al. Phase I study of bromohydrin pyrophosphate (BrHPP, IPH 1101), a Vγ9Vδ2 T lymphocyte agonist in patients with solid tumors. *Cancer Immunol Immunother CII.* (2010) 59:1521–30. doi: 10.1007/s00262-010-0879-0
42. Sicard H, Ingoure S, Luciani B, Serraz C, Fournié J-J, Bonneville M, et al. In vivo immunomanipulation of Vγ9Vδ2 T cells with a synthetic phosphoantigen in a preclinical nonhuman primate model. *J Immunol Baltim Md 1950.* (2005) 175:5471–80. doi: 10.4049/jimmunol.175.8.5471
43. Kobayashi H, Tanaka Y, Yagi J, Osaka Y, Nakazawa H, Uchiyama T, et al. Safety profile and anti-tumor effects of adoptive immunotherapy using gamma-delta T cells against advanced renal cell carcinoma: a pilot study. *Cancer Immunol Immunother CII.* (2007) 56:469–76. doi: 10.1007/s00262-006-0199-6
44. Alnaggar M, Xu Y, Li J, He J, Chen J, Li M, et al. Allogenic Vγ9Vδ2 T cell as new potential immunotherapy drug for solid tumor: a case study for cholangiocarcinoma. *J Immunother Cancer.* (2019) 7:36. doi: 10.1186/s40425-019-0501-8
45. Fisher JP, Heuijerjans J, Yan M, Gustafsson K, Anderson J. γδ T cells for cancer immunotherapy: a systematic review of clinical trials. *Oncoimmunology.* (2014) 3:e27572. doi: 10.4161/onci.27572
46. Straetemans T, Kierkels GJJ, Doorn R, Jansen K, Heijhuurs S, Dos Santos JM, et al. GMP-grade manufacturing of T cells engineered to express a defined γδTCR. *Front Immunol.* (2018) 9:1062. doi: 10.3389/fimmu.2018.01062
47. Santolaria T, Robard M, Léger A, Catros V, Bonneville M, Scotet E. Repeated systemic administrations of both aminobisphosphonates and human Vγ9Vδ2 T cells efficiently control tumor development in vivo. *J Immunol Baltim Md 1950.* (2013) 191:1993–2000. doi: 10.4049/jimmunol.1300255
48. Perrin S. Preclinical research: make mouse studies work. *Nature.* (2014) 507:423–5. doi: 10.1038/507423a
49. Wege AK. Humanized mouse models for the preclinical assessment of cancer immunotherapy. *BioDrugs Clin Immunother Biopharm Gene Ther.* (2018) 32:245–66. doi: 10.1007/s40259-018-0275-4
50. Jarry U, Chauvin C, Joalland N, Léger A, Minault S, Robard M, et al. Stereotaxic administrations of allogeneic human Vγ9Vδ2 T cells efficiently control the development of human glioblastoma brain tumors. *Oncoimmunology.* (2016) 5:e1168554. doi: 10.1080/2162402X.2016.1168554
51. Joalland N, Chauvin C, Oliver L, Vallette FM, Pecqueur C, Jarry U, et al. IL-21 increases the reactivity of allogeneic human Vγ9Vδ2 T cells against primary glioblastoma tumors. *J Immunother Hagerstown Md 1997.* (2018) 41:224–31. doi: 10.1097/CJI.0000000000000225
52. Joalland N, Lafrance L, Oullier T, Marionneau-Lambot S, Loussouarn D, Jarry U, et al. Combined chemotherapy and allogeneic human Vγ9Vδ2 T lymphocyte-immunotherapies efficiently control the development of human epithelial ovarian cancer cells in vivo. *Oncoimmunology.* (2019) 8:e1649971. doi: 10.1080/2162402X.2019.1649971
53. Jung J, Seol HS, Chang S. The generation and application of patient-derived xenograft model for cancer research. *Cancer Res Treat Off J Korean Cancer Assoc.* (2018) 50:1–10. doi: 10.4143/crt.2017.307

54. Morton JJ, Bird G, Refaeli Y, Jimeno A. Humanized mouse xenograft models: narrowing the tumor-microenvironment gap. *Cancer Res.* (2016) 76:6153–8. doi: 10.1158/0008-5472.CAN-16-1260
55. Pauza CD, Liou M-L, Lahusen T, Xiao L, Lapidus RG, Cairo C, et al. Gamma delta T cell therapy for cancer: it is good to be local. *Front Immunol.* (2018) 9:1305. doi: 10.3389/fimmu.2018.01305
56. Yuasa T, Sato K, Ashihara E, Takeuchi M, Maita S, Tsuchiya N, et al. Intravesical administration of $\gamma\delta$ T cells successfully prevents the growth of bladder cancer in the murine model. *Cancer Immunol Immunother CII.* (2009) 58:493–502. doi: 10.1007/s00262-008-0571-9
57. Chauvin C, Joalland N, Perroteau J, Jarry U, Lafrance L, Willem C, et al. NKG2D controls natural reactivity of Vγ9Vδ2 T lymphocytes against mesenchymal glioblastoma cells. *Clin Cancer Res Off J Am Assoc Cancer Res.* (2019) 25:7218–28. doi: 10.1158/1078-0432.CCR-19-0375
58. Chitadze G, Lettau M, Luecke S, Wang T, Janssen O, Fürst D, et al. NKG2D- and T-cell receptor-dependent lysis of malignant glioma cell lines by human γδ T cells: modulation by temozolomide and A disintegrin and metalloproteases 10 and 17 inhibitors. *Oncoimmunology.* (2016) 5:e1093276. doi: 10.1080/2162402X.2015.1093276
59. Todaro M, Orlando V, Cicero G, Caccamo N, Meraviglia S, Stassi G, et al. Chemotherapy sensitizes colon cancer initiating cells to Vγ9Vδ2 T cell-mediated cytotoxicity. *PLoS ONE.* (2013) 8:e65145. doi: 10.1371/journal.pone.0065145
60. Zoine JT, Knight KA, Fleischer LC, Sutton KS, Goldsmith KC, Doering CB, et al. Ex vivo expanded patient-derived γδ T-cell immunotherapy enhances neuroblastoma tumor regression in a murine model. *Oncoimmunology.* (2019) 8:1593804. doi: 10.1080/2162402X.2019.1593804
61. Rossi C, Gravelle P, Decaup E, Bordenave J, Poupot M, Tosolini M, et al. Boosting γδ T cell-mediated antibody-dependent cellular cytotoxicity by PD-1 blockade in follicular lymphoma. *Oncoimmunology.* (2019) 8:1554175. doi: 10.1080/2162402X.2018.1554175
62. Capietto A-H, Martinet L, Fournié J-J. Stimulated γδ T cells increase the in vivo efficacy of trastuzumab in HER-2+ breast cancer. *J Immunol Baltim Md 1950.* (2011) 187:1031–8. doi: 10.4049/jimmunol.1100681
63. Gertner-Dardenne J, Bonnafous C, Bezombes C, Capietto A-H, Scaglione V, Ingoure S, et al. Bromohydrin pyrophosphate enhances antibody-dependent cell-mediated cytotoxicity induced by therapeutic antibodies. *Blood.* (2009) 113:4875–84. doi: 10.1182/blood-2008-08-172296
64. de Bruin RCG, Veluchamy JP, Lougheed SM, Schneiders FL, Lopez-Lastra S, Lameris R, et al. A bispecific nanobody approach to leverage the potent and widely applicable tumor cytolytic capacity of Vγ9Vδ2-T cells. *Oncoimmunology.* (2017) 7:e1375641. doi: 10.1080/2162402X.2017.1375641
65. Benyamine A, Le Roy A, Mamessier E, Gertner-Dardenne J, Castanier C, Orlanducci F, et al. BTN3A molecules considerably improve Vγ9Vδ2T cells-based immunotherapy in acute myeloid leukemia. *Oncoimmunology.* (2016) 5:e1146843. doi: 10.1080/2162402X.2016.1146843
66. Thedrez A, Harly C, Morice A, Salot S, Bonneville M, Scotet E. IL-21-mediated potentiation of antitumor cytolytic and proinflammatory responses of human Vγ9Vδ2 T cells for adoptive immunotherapy. *J Immunol Baltim Md 1950.* (2009) 182:3423–31. doi: 10.4049/jimmunol.0803068
67. Kouakanou L, Xu Y, Peters C, He J, Wu Y, Yin Z, et al. Vitamin C promotes the proliferation and effector functions of human γδ T cells. *Cell Mol Immunol.* (2019) 17:462–73. doi: 10.1038/s41423-019-0247-8

Conflict of Interest: The authors declare that the research was conducted in the absence of any commercial or financial relationships that could be construed as a potential conflict of interest.

frontiers in Immunology

ORIGINAL RESEARCH
published: 19 June 2020
doi: 10.3389/fimmu.2020.01287

Aberrantly Expressed Embryonic Protein NODAL Alters Breast Cancer Cell Susceptibility to γδ T Cell Cytotoxicity

Gabrielle M. Siegers[1], Indrani Dutta[1], Eun Young Kang[2], Jing Huang[1], Martin Köbel[2] and Lynne-Marie Postovit[1,3]*

[1] Department of Oncology, University of Alberta, Edmonton, AB, Canada, [2] Department of Pathology and Laboratory Medicine, Foothills Medical Centre, University of Calgary, Calgary, AB, Canada, [3] Department of Biomedical and Molecular Sciences, Queen's University, Kingston, ON, Canada

Gamma delta (γδ) T cells kill transformed cells, and increased circulating γδ T cells levels correlate with improved outcome in cancer patients; however, their function within the breast tumor microenvironment (TME) remains controversial. As tumors progress, they begin to express stem-cell associated proteins, concomitant with the emergence of therapy resistant metastatic disease. For example, invasive breast cancers often secrete the embryonic morphogen, NODAL. NODAL has been shown to promote angiogenesis, therapy resistance and metastasis in breast cancers. However, to date, little is known about how this secreted protein may interact with cells in the TME. Herein we explore how NODAL in the TME may influence γδ T cell function. We have assessed the proximity of γδ T cells to NODAL in a cohort of triple negative breast tumors. In all cases in which γδ T cells could be identified in these tumors, γδ T cells were found in close proximity to NODAL-expressing tumor cells. Migration of γδ and αβ T cells was similar toward MDA-MB-231 cells in which NODAL had been knocked down (shN) and MDA-MB-231 scrambled control cells (shC). Furthermore, Vδ1 γδ T cells did not migrate preferentially toward conditioned medium from these cell lines. While 24-h exposure to NODAL did not impact CD69, PD-1, or T cell antigen receptor (TCR) expression on γδ T cells, long term exposure resulted in decreased Vδ2 TCR expression. Maturation of γδ T cells was not significantly influenced by NODAL stimulation. While neither short- nor long-term NODAL stimulation impacted the ability of γδ T cells to kill MCF-7 breast cancer cells, the absence of NODAL resulted in greater sensitivity of targets to γδ T cell cytotoxicity, while overexpression of NODAL conferred resistance. This appeared to be at least in part due to an inverse correlation between NODAL and surface MICA/B expression on breast cancer target lines. As such, it appears that NODAL may play a role in strategies employed by breast cancer cells to evade γδ T cell targeting, and this should be considered in the development of safe and effective γδ T cell immunotherapies.

Keywords: gamma delta T cells, gammadelta, NODAL, triple negative breast cancer, invasive ductal carcinoma, MICA, tumor evasion

OPEN ACCESS

Edited by:
Ilan Bank,
Sheba Medical Center, Israel

Reviewed by:
Elena Lo Presti,
University of Palermo, Italy
David L. Wiest,
Fox Chase Cancer Center,
United States

****Correspondence:***
Gabrielle M. Siegers
siegers@ualberta.ca

Specialty section:
This article was submitted to T Cell Biology, a section of the journal Frontiers in Immunology

Received: *20 March 2020*
Accepted: *21 May 2020*
Published: *19 June 2020*

Citation:
Siegers GM, Dutta I, Kang EY, Huang J, Köbel M and Postovit L-M (2020) Aberrantly Expressed Embryonic Protein NODAL Alters Breast Cancer Cell Susceptibility to γδ T Cell Cytotoxicity. Front. Immunol. 11:1287. doi: 10.3389/fimmu.2020.01287

INTRODUCTION

Breast cancer is the most common women's cancer in Canada with 27 400 expected diagnoses and a projected mortality rate of 6.1% of all cancer deaths in 2020 (1). Mortality is often due to treatment resistance, leading to recurrence and metastatic spread (2).

Immunotherapy using conventional or chimeric antigen receptor-transduced (CAR) T cells is on the cutting edge of advancement in cancer therapeutics (3, 4). However, γδ T cell immunotherapy constitutes an exciting alternative, offering several advantages over the use of conventional αβ T cells. Most importantly γδ T cells are broadly reactive to cancer cells but are not typically MHC-restricted, and thus do not cause graft-vs. host disease (5, 6). Their potent anti-cancer activity and excellent safety profile (7), combined with their non-reliance on tumor mutational loads (8), and improved expansion protocols (9–13) are catapulting γδ T cells into the limelight (14, 15).

Gamma delta T cells kill a wide range of malignancies (6). Their role in breast cancer has been recently reviewed (16). Specific to breast cancer, expanded γδ T cells kill MDA-MB-231, MCF-7 and T47D breast cancer cell lines (17–22). In a phase I clinical trial testing γδ T cell agonist Zoledronate in combination with IL-2 in advanced metastatic breast cancer patients, a significant positive correlation between peripheral γδ T cell numbers and clinical outcome was observed (23). Migration of infused γδ T cells to breast cancer tumors and metastases has been evidenced in both xenograft models (24) and patients (25).

While γδ T cell frequency in blood correlates with positive outcome (23), their prognostic value in breast tumors is unclear. In a comprehensive study including over 18,000 human tumors across 25 cancers, γδ T cell tumor infiltrating lymphocytes (TIL) were the most significant positive prognostic factor (26), although it has since been shown that the CIBERSORT algorithm used in this analysis could not properly discriminate γδ T cells from CD4+ and CD8+ T cells or NK cells; an optimized deconvolution that can reliably identify Vγ9Vδ2 TIL has now been reported (8). The authors of this study focussed on acute myeloid and chronic lymphocytic leukemias, colorectal and prostate cancers, confirming that γδ T cell TIL associate with positive patient outcome, but they did not reassess outcomes for breast cancer patients, which would be of great interest here (8). While a 2012 study proposed that γδ T cells are negative prognosticators in human breast cancer (27), a more recent investigation of TIL in breast cancer using various unbiased *in silico* approaches found that higher levels of γδ T cells correlated with better outcomes (28). In all cases, correlations were identified, but causality not determined.

Later studies have delved more deeply into the presence of γδ T cells infiltrating triple negative breast cancers (TNBC), revealing increased presence of γδ T cells compared to fibroadenomas or breast tissues from healthy individuals, suggesting active infiltration of γδ T cells into tumors (29), and that infiltrating γδ T cells are likely active (30).

The seemingly paradoxical data on γδ T cells in breast cancer highlight the importance of determining the role of γδ T cell TIL before γδ T cells are further developed as a cellular immunotherapy for breast cancer. Indeed, researchers now recognize the importance of determining how the TME influences the function of γδ T cells [reviewed in (31)]. We recently investigated γδ T cell function under hypoxia, a biophysical condition present in many tumors, and discovered that while γδ T cells were activated under low oxygen, breast tumor cells shed MICA to evade detection by γδ T cells (22).

NODAL is an embryonic morphogen secreted by tumor cells in the TME, whose aberrant expression is induced under hypoxia (32). NODAL has been correlated with breast cancer progression, and functionally promotes angiogenesis, invasion, tumor growth and metastasis, irrespective of ER, PR or HER2 status (33–36). NODAL promotes tumor growth in Nude mice bearing a partial immune system, but this effect diminishes when more immunodeficient models are used (33), suggesting a role for NODAL in immune evasion.

Thus, we decided to investigate whether γδ T cells can be found in proximity to NODAL expressing breast tumor cells in TNBC cases and, if so, what impact NODAL may have on γδ T cell function.

MATERIALS AND METHODS

Ethics Statement

This study was carried out in accordance with the recommendations of the Research Ethics Guidelines, Health Research Ethics Board of Alberta—Cancer Committee with written informed consent from all subjects. All subjects gave written informed consent in accordance with the Declaration of Helsinki. The protocol was approved by the Health Research Ethics Board of Alberta—Cancer Committee.

Patients and Tissues

We assessed 20 surgically resected triple negative breast tumors from cancer patients diagnosed at the Cross Cancer Institute, Edmonton, AB in 2017. Patient and tumor characteristics are listed in **Table 1**.

Immunohistochemistry

We performed anti-human T cell antigen receptor (TCR)δ staining as reported (22, 37); however, we modified the protocol

Abbreviations: αβTc, αβ T cells; bp, band pass; BrCa, breast cancer; CAIX, carbonic anhydrase IX; CalAM, Calcein AM; CTV, Cell Trace Violet; ER, estrogen receptor; E:T, effector:target ratio; FACS, fluorescence acquired cell sorting; FBS, fetal bovine serum; FMO, fluorescence minus one; γδ T cells, gamma delta T cells; H&E, hematoxylin and eosin; HRP, horseradish peroxidase; IDC, invasive ductal carcinoma; IHC, immunohistochemistry; IL, interleukin; lp, long pass; mAb, monoclonal antibody; MACS, magnetic cell sorting; MBC, medullary breast cancer; MICA, MHC class I polypeptide-related sequence A; MFI, median fluorescence intensity; NKG2D, natural killer group 2, member D; PBMCs, peripheral blood mononuclear cells; PBS, phosphate buffered saline; PIC, protease and phosphatase inhibitor cocktail; rhNODAL, recombinant human NODAL; shC, scrambled control; shN, NODAL knockdown BrCa; spon, spontaneous release; TBST, tris-buffered saline plus 0.05% Tween-20; TCR, T cell antigen receptor; TGFβ, transforming growth factor β; TIL, tumor infiltrating lymphocytes; TME, tumor microenvironment; TNBC, triple negative breast cancer; ZA, Zombie Aqua fixable viability dye; ZNIR, Zombie Near Infrared fixable viability dye.

TABLE 1 | Characteristics of triple negative breast cancer cohort.

	n (% of 20 cases)	*n* (% of 9 cases with γδ TIL)
Age at diagnosis—Median (range)	67.5 (48–91)	63.6 (50–91)
Histology		
Invasive ductal carcinoma (IDC)	14 (70)	5 (56)
Multifocal IDC	5 (25)	3 (33)
Apocrine carcinoma	1 (5)	1 (11)
IDC size (cm)—Median (range)	1.7 (0.6–5.5)	1.1 (0.6–5.5)
Not specified	7 (35)	2 (22)
<2	7 (35)	4 (44)
2–5	5 (25)	2 (22)
>5	1 (5)	1 (11)
Tumor grade		
Not specified	1 (5)	
2/3	2 (10)	1 (11)
3/3	17 (85)	8 (89)
Tumor stage		
Not specified	2 (10)	
1	7 (35)	4 (44)
2	7 (35)	3 (33)
3	2 (10)	1 (11)
4	2 (10)	1 (11)
Lymph node status		
Positive	9 (45)	3 (33)
Negative	11 (55)	6 (67)
Deceased as of February 2020	4 (20)	1 (11)

such as to perform dual staining for TCRδ and CAIX using the EnVision G12 Doublestain System, rabbit/mouse (Agilent Technologies Canada, Mississauga, ON, Canada). Briefly, 4 μm serial sections from formalin-fixed paraffin-embedded tumors were melted at 60°C for a minimum of 10 min on a slide warmer followed by de-paraffinization using fresh Citrus Clearing Solvent (Richard Allan Scientific Reagents, Kalamazoo, MI, USA). Hydration of sections was achieved with a series of graded ethanol (100, 95, 70, 60%) followed by brief incubation in water, then tris-buffered saline plus 0.05% Tween-20 (TBST). Target retrieval solution pH 9 (DAKO North America, Carpinteria, CA, USA) was utilized for antigen retrieval at 100°C for 20 min. After cooling to room temperature, tissues were circled with an ImmEdge pen (Vector Laboratories, Burlingame, CA, USA) and blocking and staining steps were performed as per the manufacturer's instructions. Primary antibody dilutions were 1:150 mouse monoclonal anti-human TCRδ antibody (clone H-41, Santa Cruz Biotechnology, Dallas, TX, USA) and 1:50 dilution of rabbit monoclonal anti-human CAIX [clone EPR4151(2), abcam, Cambridge, MA, USA] or corresponding isotype control diluted to the same antibody concentration. We included known positive controls and isotype controls with each batch for quality control. DAB chromogen bound anti-mouse HRP to indicate TCRδ-positive cells in brown; CAIX-positive cells were stained with permanent red chromogen. After staining with primary and secondary antibodies, we counterstained with Haematoxylin (DAKO), slides were rinsed in water and then dehydrated using a graded ethanol series (60, 70, 95, 100%). Slides were then cleared with Citrus Clearing Solvent, dried and coverslips mounted with VectaMount permanent mounting medium (Vector Laboratories). Serial sections were stained for NODAL as previously published (33).

Assessment of γδ T Cell Infiltration and Localization With Respect to NODAL and CAIX

Light microscopy and semi-quantitative scoring were performed by two pathologists. The entirety of each slide was assessed. Scores for CAIX were 0, absent; 1, weak and/or very focal staining; 2, strong but focal or moderate intensity; and 3, strong and extensive staining, as per our previous publication (22). The score reflects the intensity of staining observed in the majority of cells. NODAL was scored in the same manner on serial sections from the same cases. TCRδ staining was categorized as absent or present; when scored present, TCRδ+ cells were further identified as focal or diffuse. Only TCRδ+ cells within peri- and intratumoral stroma were considered. Co-localization between TCRδ+ cells and CAIX or TCRδ+ cells and NODAL was deemed positive or negative based on staining overlap. Proximity was defined as $< 50\,\mu m$ distance. Representative images were taken from a Nikon DS-U3 camera on Nikon eclipse 80i microscrope at 400 x (500 px bar = 40 μm). The Venn diagram in **Figure 1F** was created using a free online tool created by Dr. Tim Hulsen at http://www.biovenn.nl/venndiagram.tk/create.php, ©2003–2008.

Primary γδ T Cells

Primary human γδ T cells were derived from healthy donor blood as described (10). In brief, peripheral blood mononuclear cells were isolated and cultured in media containing 1 μg/ml Concanavalin A and 10 ng/ml IL-2 and IL-4. T cells expanded together for 6–8 days, and then conventional αβTc were depleted by magnetic cell separation. For Vδ1 cultures used in migration assays, Vδ2 T cells were depleted from mixed T cells at the same time as αβTc [1 μl anti-TCRαβ PE (Biolegend) plus 0.5 μl anti-TCRVδ2 PE (Miltenyi Biotec) per million cells, followed by anti-PE beads, (Miltenyi Biotec)], and cells were supplemented with conditioned medium after depletion. Viability and fold expansion were routinely assessed *via* Trypan Blue exclusion and cell counting. When fed, cells were diluted to one million cells/ml with complete medium (RPMI 1640 with 10% FBS, heat-inactivated, 1 × MEM NEAA, 10 mM HEPES, 1 mM sodium pyruvate, 50 U/ml penicillin–streptomycin, and 2 mM L-glutamine—all from Invitrogen™, Thermo Fisher Scientific, Waltham, Massachusetts, USA) supplemented with 10 ng/ml IL-2 and IL-4. Subset composition and γδ T cell culture purities are provided in **Table S1**.

Breast Cancer Cell Lines

Breast cancer target cell lines included MCF-7, T47D, and MDA-MB-231, all cultured in RPMI medium containing 10% FBS. MDA-MB-231 NODAL knockdown (shN) and scrambled

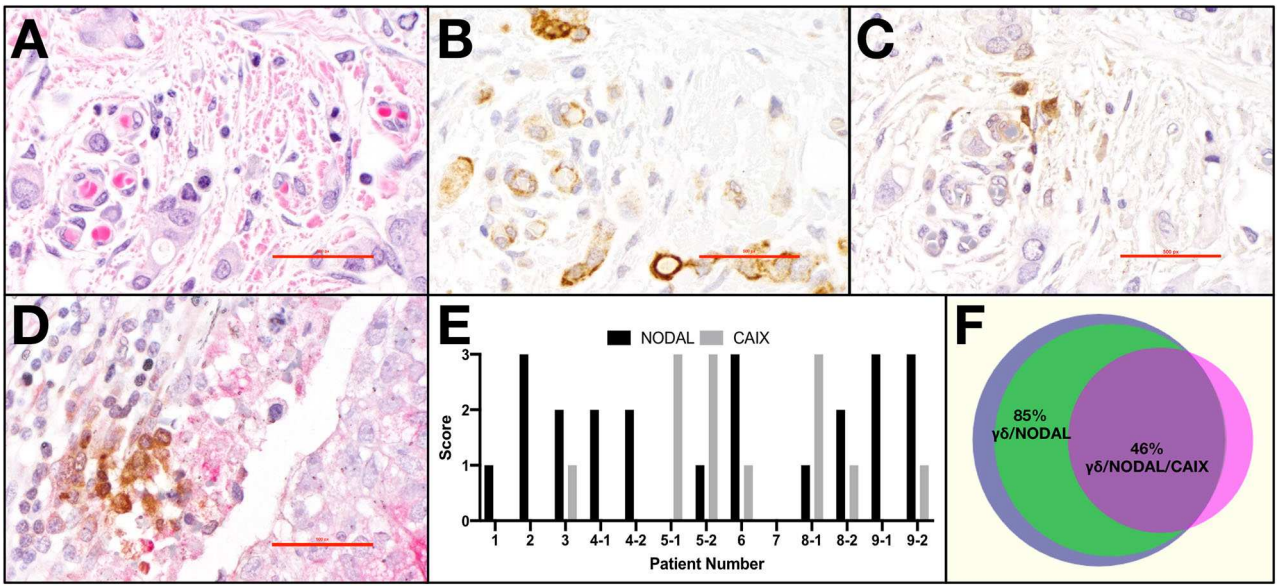

FIGURE 1 | γδ T cells and NODAL are co-localized in breast tumor tissues from patients. Representative example of paraffin-embedded serial sections from a triple negative breast tumor stained via immunohistochemistry for **(A)** H&E with hematoxylin staining nuclei dark blue-purple and eosin indicating cytoplasm in pink, **(B)** NODAL indicated by brown DAB staining, **(C)** TCRδ also stained brown with DAB, **(D)** Representative example of TCRδ (brown) found in a CAIX-positive region, stained pink with permanent red dye; scale bar = 40 μm. **(E)** Scoring for NODAL and CAIX expression in tumor sections in which γδ T cells were identified. Cases in which more than one slide was positive for TCRδ are indicated with −1, −2 designations. **(F)** Venn diagram depicting co-localization of γδ T cells (blue), NODAL (green), and CAIX (fuchsia). Percent overlaps are indicated.

control (shC) cell lines as well as T47D NODAL overexpresser (NOE) and empty vector (EV) control lines were established and characterized in our lab (33). They were cultured in RPMI containing 10% FBS and supplemented with 500 ng/ml Puromycin.

In vitro Migration Assays (35)

For the experiment shown in **Figure 3A**, 60,000 MDA-MB-231 shN or shC cells in 600 μl complete medium were plated in the lower chamber of transwell plates (Corning #3421, 6.5 mm diameter inserts, 5.0 μm pore size, tissue culture treated) and allowed to adhere overnight. 20,000 αβ or γδ T cells in 100 μl serum free medium were plated in the top chamber and incubated for 3 h. Transwells were then washed in PBS, and then fixed in cold methanol for 15 min. After three washes in PBS, filters were carefully excised, placed on microscope slides (J. Melvin Freed, Frosted, Cat# 7,525 MF) and one drop DAPI mounting medium (Molecular Probes Prolong Gold antifade P36935) applied before placement of coverslips. Slides were stored at 4 degrees in the dark until visualization. 600 μl conditioned medium from MDA-MB-231 shN or shC cells was placed in lower chamber. Biological replicates shown in **Figure 3B** were done as follows: 50,000 Vδ1 γδ T cells in 100 μl serum free medium were plated in the top chamber and incubated for 3 h. Washing and fixing of membrane was done as described above.

Images were acquired on the Zeiss Axio Observer Z1 microscope such that all fields of view were stitched together to obtain an image of the entire transwell insert.

Image Analysis

Images of migrated cells as identified by their DAPI-stained nuclei were analyzed using MetaXpress 6.0 software. Regions of interest (ROI) on 16-bit images were traced to encompass the entire filter; exemptions were drawn and subtracted to remove bubbles from the analysis. The value for net ROI, in pixels, was divided by one million. The net ROI was divided by one million to obtain a number below 100; this step is reflected in the 10^{-6} in the units. The Top Hat morphology filter (15–20 pixel diameter circle) was applied to remove artifacts. Nuclei with 10 −20 μm width displaying 10,000–15,000 intensity above background were considered to identify cells and were counted. True cells were defined with area ≤ 299 pixels. The total nuclei counted on the entire ROI from the insert were then divided by the ROI to achieve the # cells/pixel ($x10^{-6}$) as depicted in the graphs. This was done to normalize the cell count to the area analyzed, to prevent skewing of results due to potential differences in excised filters or from loss of area due to bubbles.

NODAL Stimulations

Unless otherwise stated, cells were stimulated with 100 ng/ml recombinant human NODAL protein (R&D Systems, catalog number 3218-ND/CF) for 4 h (cytotoxicity assays), 24 h or 4–10 days as indicated. Controls were NODAL vehicle control (NVC, 4 mM HCl in dH_2O), 1.7 ng/ml carrier-free recombinant human TGF-β1 (BioLegend), 5 μg/ml anti-CD3 antibody (BioLegend, clone OKT3) or 200 μM pervanadate (4.1 μl 50 mM sodium orthovanadate, 1.2 μl 30% H_2O_2 plus 4.7 μl PBS per ml cell suspension).

P19 Cell Stimulations

P19 mouse embryonal carcinoma cells were cultured and used periodically to verify the activity of recombinant human NODAL used in some assays. P19 cells were cultured in Alpha Minimum Essential Medium with ribonucleosides and deoxyribonucleosides, 7.5% bovine calf serum and 2.5% fetal bovine serum. P19 cells were seeded in 6 wells plate with 200,000 cells/well and grown in media with serum. The next day, media containing 10 μM SB431542 to suppress phosphoSMAD signals was added and incubated overnight. On the third day, the cells were washed with warm serum-free Alpha Minimum Essential medium and treated with rhNODAL 100 ng/mL (R&D system, cat#3218-ND/CF) for 1 hr at 37°C with 5% CO_2 supplementation. After 1 h of treatment, cells were lysed and stored at −20°C for further western blotting analysis.

Western Blotting

Cell lysates were prepared by adding M-PER Mammalian Protein Extraction Reagent containing Halt™ Protease and Phosphatase Inhibitor (both from Thermo Fisher Scientific) at 10 μl lysis buffer per million γδ T cells or 10 μl lysis buffer per 0.28 million target cells followed by 10 min incubation at room temperature. Cell lysates were then centrifuged for 15 min at 13,000 rpm at 4°C, after which supernatants were collected and 5 × reducing sample buffer [0.0625 M Tris/HCl pH6.8, 2% SDS, 20% glycerol, 0.05% β-mercaptoethanol, 0.025% (w/v) Bromophenol Blue] was added. Samples were boiled for 5 min and briefly centrifuged in a benchtop centrifuge before running on 10% SDS-PAGE gels. The mixed MW program on the Trans-Blot Turbo Transfer System (Bio-Rad, Mississauga, ON, Canada) was used to transfer proteins onto Immobilon-FL PVDF membranes (Millipore). Membranes were blocked for 40 min in 3% milk in TBST, followed by primary antibody incubation overnight at 4°C. Membranes were then washed and incubated with the corresponding species-specific HRP-labeled secondary antibody for 1 h, followed by further washing and finally detection using Clarity™ Western ECL Substrate (Bio-Rad). Primary antibody baths were prepared using PBS containing 2% bovine serum albumin and 0.05% sodium azide at the following dilutions: 1:3,000 mouse anti-human β-Actin (Santa Cruz, Danvers, MA, USA, clone C4); 1:2,000 rabbit anti-human β-Actin (Cell Signaling Technologies, Danvers, MA, USA); 1:2500 mouse anti-human NODAL (R&D Systems, clone 784410), 1:1000 anti-phospho-Smad2 (Cell Signaling, clone 138D4). Secondary antibodies were diluted in 3% milk in TBST (Tris buffered saline with Tween, 20mM Tris, 150 mM NaCl, 0.1% Tween 20) 1:10,000 goat anti-mouse IgG HRP (Bio-Rad); 1:20,000 goat anti-rabbit IgG HRP (Bio-Rad). The presence of multiple bands in some NODAL blots reflects different NODAL species corresponding to pro-NODAL, as well as processed NODAL (glycosylated/sialylated), and differ depending on cell type and conditions (33).

Quantification of Bands on Western Blots

FIJI software (ImageJ Version 2.0.0-rc-15/1.49 m) was used to measure band intensities for phosphoSMAD2, Nodal and β-actin on 8-bit converted grayscale images using consistent rectangular regions of interest. Measured values for bands and background (region of same size beneath each band) were subtracted from 255, then net values for protein bands of interest and loading control bands (actin) were obtained by subtracting background values. Then, the ratios of the net protein bands to net loading control bands were calculated. Microsoft Excel version 15.3 (Microsoft, Redmond,WA, USA) was used for calculations.

Flow Cytometry

γδ T Cell Immunophenotyping (9, 10, 38)

Live γδ T cells were gated on forward- and side-scatter properties and live/dead ZA staining. We used fluorescence minus one controls to set gates. Samples were acquired on BD FACS CantoII or Fortessa SORP X20 analyzers. Data were analyzed using FlowJo™ software version 10.6.0 for Mac (Becton Dickinson & Company, Ashland, OR, USA). In cases where Vδ1 + Vδ2 combined gates are indicated (**Figure 3A**, **Figures S3A–C**), the FlowJo tool "make or gate" under the Boolean dropdown menu was used to combine these gates.

Antibodies

For surface marker staining of γδ T cells, the following anti-human antibodies from BioLegend (unless otherwise indicated) were employed: TCRγδ PE (clone B1, 1:25); TCRγδ PE (Miltenyi, clone REA591, 1:10); TCRγδ BV421(clone B1, 1:10); TCR Vδ1 FITC (Miltenyi, clone REA173, 1:10); TCR Vδ2 PE (Miltenyi, clone 123R3, 1:100); TCR Vδ2 PerCP (clone B6, 1:25); CD27 AF700 (clone M-T271, 1:25); CD27 APC (clone M-T271, 1:25); CD45RA FITC (clone HI100, 1:25); CD69 AF700 (clone FN50, 1:4); CTLA-4 APC (clone L3D10, 5 μl); and PD-1 BV421 (clone EH12.2H7, 1:20).

For breast cancer cell line surface staining, anti-human MICA/B PE (clone 6D4, 0.1 μg); ULBP-2,5,6 (R&D systems, clone 165,903, 0.2 μg); ULBP-3 (R&D systems, clone 166,510, 0.04 μg); ULBP-4 (R&D systems, clone 709,116, 0.1 μg).

Surface Marker Staining

γδ T cells and breast cancer cell lines were re-suspended at 10 × 10^6 cells/ml and stained with Zombie Aqua fixable viability dye in PBS (ZA, BioLegend) at a dilution of 1 μl/10^6 cells for 15–30 min at room temperature in the dark. For γδ T cell staining, cells were stained directly with fluorochrome-conjugated antibodies diluted in FACS buffer [PBS containing 1% FBS and 2 mM EDTA (Invitrogen)] as indicated above. For the target breast cancer cell lines, cells were re-suspended at 10 × 10^6 cells/ml and blocked with FACS buffer containing 50 μl/ml Trustain FcX (BioLegend) and incubated on ice for 30 min. Following blocking, cells were centrifuged and supernatants were removed such that 10 μl FACS buffer plus block remained. Antibodies and FACS buffer were added to 20 μl total volume, and cells incubated on ice 15–20 min followed by washing. Cells were then fixed in FACS buffer containing 2% paraformaldehyde (Sigma-Aldrich), stored at 4°C and acquired within 1 week.

Cell Trace Violet Proliferation Assay

γδ T cells were labeled as per the manufacturer's instructions with 1 μM Cell Trace Violet (Invitrogen), cultured for the indicated

length of time, and were washed and re-suspended in FACS buffer prior to flow acquisition. Proliferation modeling was performed and statistics generated using FlowJo™ software, version 10.5.3.

Flow Cytometer Specifications

Cell samples were analyzed on a FACS CANTO II (Becton Dickinson, Mississauga ON) equipped with: an air-cooled 405-nm solid state diode, 30 mW fiber power output violet laser, with 450/50 and 510/50 band pass (BP) (502 long pass (LP) detector); a 488-nm solid state, 20-mW blue laser with 530/30 Bp (502 LP), 585/42 BP (556 LP), 670 LP (655 LP), and 780/60 BP (735 LP) filters; and a 633-nm HeNe, 17-mW red laser with 660/20 BP and 780/60 BO (735 LP) filters. Calibration was performed with CS&T beads (Becton Dickenson, Mississauga ON). Live singlets were gated based on forward and side-scatter properties and absence of fixable viability dye staining. Fluorescence minus one (FMO) controls were used to set gates. Analysis was performed using FlowJo™ software version 10.6.0.

Fluorescence-Based Blocking/Cytotoxicity Assays (10)

Target Cell Labeling With Calcein AM

As per the manufacturer's instructions, target cells were labeled with 5 μM Calcein AM (CalAM, Invitrogen/Thermo Fisher Scientific). Cells were diluted to 30,000 cells/100 μl medium for cytotoxicity assays. For blocking assays, 4 μg blocking antibody (MICA/B, Biolegend, clone 6D4) was added to 400 μl cell suspension for each test in Eppendorf tubes, and from this, 100 μl/well was plated in a 96-well round-bottomed plate in triplicate and incubated at 37°C, 5% CO_2 for 30 min. Mouse IgG (Sigma-Aldrich) was used as a control. Effector γδ T cells were re-suspended at a dilution of 6×10^6 cells/ml in complete medium, then further diluted and added to target cells in 100 μl volumes to achieve the indicated effector:target (E:T) ratios; blocking assays were done at 20:1. Effectors and targets were incubated together at 37°C, 5% CO_2 for 4 hr. Experimental controls were untreated and mouse IgG-treated cells (for the blocking assay). For CalAM fluorescence detection, plates were centrifuged and supernatants transferred to fresh 96-well plates (Costar, black plate, clear, flat bottom) and readings taken on a fluorimeter (FLUOstar Omega, BMG labtech). Controls were CalAM-labeled target cells incubated alone (spon = spontaneous release) and 0.05% Triton-X-100 (Thermo Fisher Scientific)-treated cells (max = maximum release). Percent lysis was calculated: [(test – spon)/(max – spon)] × 100%.

Flow Cytometric Cytotoxicity Assay (38)

Targets were labeled with 1 μM Cell Trace Violet 1 day prior to the assay. Targets were harvested and re-suspended in complete medium at 30,000/100 μl and plated 100 μl/well in a 96-well round-bottom plate. γδ T cells (effectors) were harvested and cell densities adjusted for each E:T ratio (1:1, 5:1,10:1, 20:1). Leftover γδ T cells were used for unstained, CTV only and Calcein AM Red Orange only staining controls. 100 μl effectors were added to targets and 100 μl/well media was added to target only wells; they were then incubated for 4 h at 37°C, 5% CO_2. One Calcein AM Red Orange stock vial was reconstituted in 20 μl DMSO followed by further 1:5000 dilution in DMSO. Next, Calcein AM was diluted 1:100 in PBS. The 96-well plate containing effectors and targets was then centrifuged, pellets were re-suspended in 200 μl Calcein AM in PBS, and incubated at room temperature for 15 min in the dark. Finally, the plate was spun again, supernatants removed and pellets re-suspended in 200 μl FACs buffer [PBS containing 1% FBS and 2 mM EDTA (Invitrogen)]. Counting beads (Precision Count Beads™, Biolegend, Catalog # 424,902) were diluted 1:4 in FACs buffer and transferred to FACS tubes (200 μl/sample) on ice to which 200 μl cell suspensions were added prior to acquisition on the Fortessa X-20.

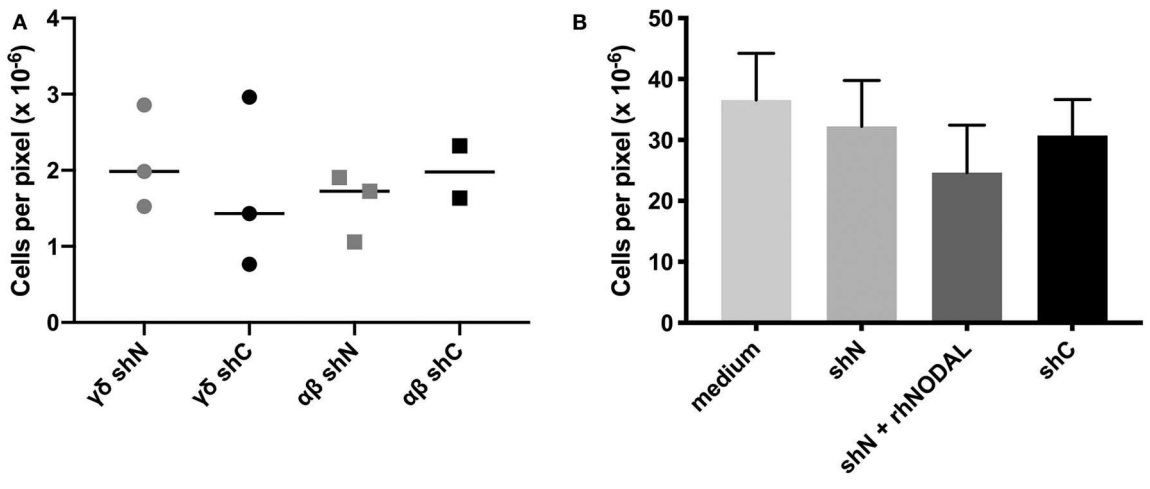

FIGURE 2 | The NODAL-positive breast cancer cell secretome has no influence on γδ T cell migration. **(A)** No significant difference in migration of αβ and γδ T cells toward shN and shC plated in complete medium with 20,000 T cells in the top and 60,000 MDA-MB-231 cells in complete medium in the bottom chamber. Individual technical replicates are shown. **(B)** Compiled data from four independent Vδ1 migration assays toward medium or conditioned medium without or containing recombinant human NODAL (rhNODAL). Error bars are SEM.

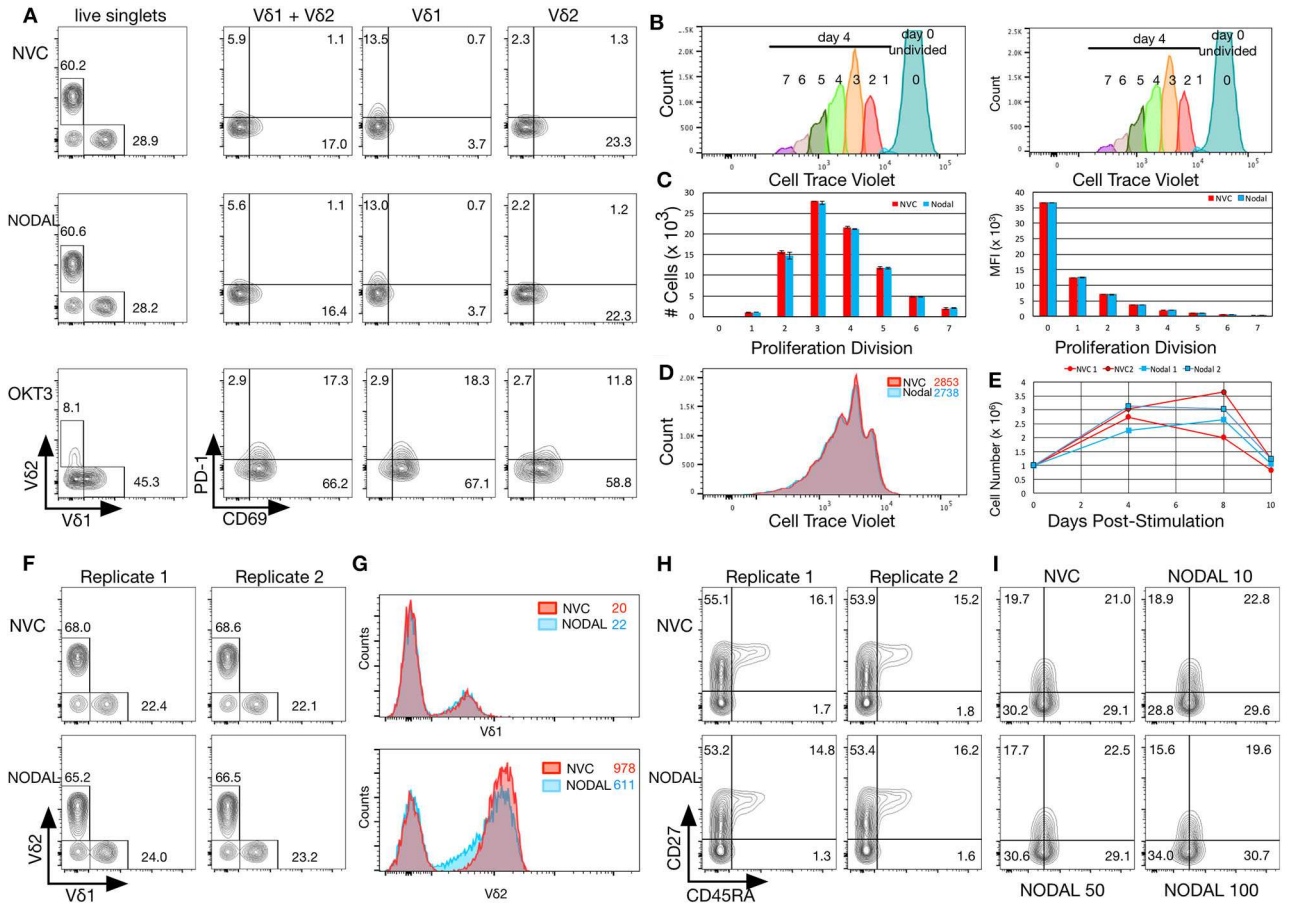

FIGURE 3 | NODAL stimulation has no impact on activation markers, proliferation or maturation of γδ T cells but longer term exposure to NODAL results in decreased Vδ2 TCR surface expression. **(A)**, γδ T cells were subject to 24 h 100 ng/ml NODAL stimulation, and then surface expression of Vδ1 and Vδ2 TCR, PD-1, and CD69 were assessed *via* flow cytometry. NVC, NODAL vehicle control; anti-CD3 (OKT3) stimulation was done as a positive control for activation markers. This is a representative example of $n = 3$ independent experiments. **(B)**, Long term NODAL stimulation has no impact on γδ T cell proliferation. γδ T cells from the same culture as in A were labeled with Cell Trace Violet, then stimulated one time with NODAL vehicle control (NVC) or 100 ng/ml recombinant human NODAL. Flow cytometry was performed on days 0, 4, 8, and 10. Proliferation modeling analyses for the day 4 time point are shown. **(C)**, Cell numbers and median fluorescence intensities (MFI) of proliferation divisions for the experiment shown in B are shown; $n = 2$ technical replicates, error bars are SD. **(D)**, A representative example of histogram overlays from the day 4 time point of the experiment shown in B and C; MFIs are indicated. **(E)**, Cell counts on days 0, 4, 8, and 10 are plotted here for the two technical replicates done in the experiment shown in **(B–D)**. No significant differences were observed. **(F)**, Ten days after NODAL stimulation, cells cultured in parallel with the experiment in B-E were stained for Vδ1 and Vδ2 TCR expression; results from two technical replicates are shown. **(G)**, Histogram overlays and MFIs of TCR expression for representative examples from the experiment shown in **(F)**. **(H)**, For the experiment shown in **(F,G)**, maturation was assessed *via* CD45RA and CD27 staining; both technical replicates are shown. **(I)**, Maturation assessment after stimulating γδ T cells for 4 days with 10, 50, or 100 ng/ml recombinant human NODAL.

Statistics

Microsoft® Excel for Mac Version 15.30 was employed for paired 2-tailed Student's *t*-tests (**Figure S3E**). All other statistics were done using GraphPad Prism Version 8.2.1: Kruskal-Wallis and Dunn's multiple comparisons tests when Shapiro-Wilk normality tests failed because N was too small [(**Figures S2A,C,D**); one-way ANOVA analysis and Tukey's multiple comparisons (**Figures 2A,B**, **Figure S2B**)]; and two-way ANOVA with Bonferroni's pairwise multiple comparison *post-hoc* tests (**Figure 4**, **Figure S4**). The significance threshold was set at $P < 0.05$; asterisks indicate degrees of significance as indicated in the figure legends. Simple linear regression analyses were applied to data shown in **Figures 5C–E**, **Figure S4P**. The correlation matrix in **Figure 5F** shows calculated Pearson's correlation coefficients; the determined *P*-values were one-tailed.

RESULTS

γδ T Cells Are Found in Areas in Which NODAL Is Expressed in Triple Negative Breast Tumors

Previously, we determined that γδ T cells are enriched in areas of hypoxia, as indicated by expression of carbonic anhydrase IX (CAIX), in estrogen receptor positive (ER+) breast tumors (22). We thus extended our studies to primary tumor tissues

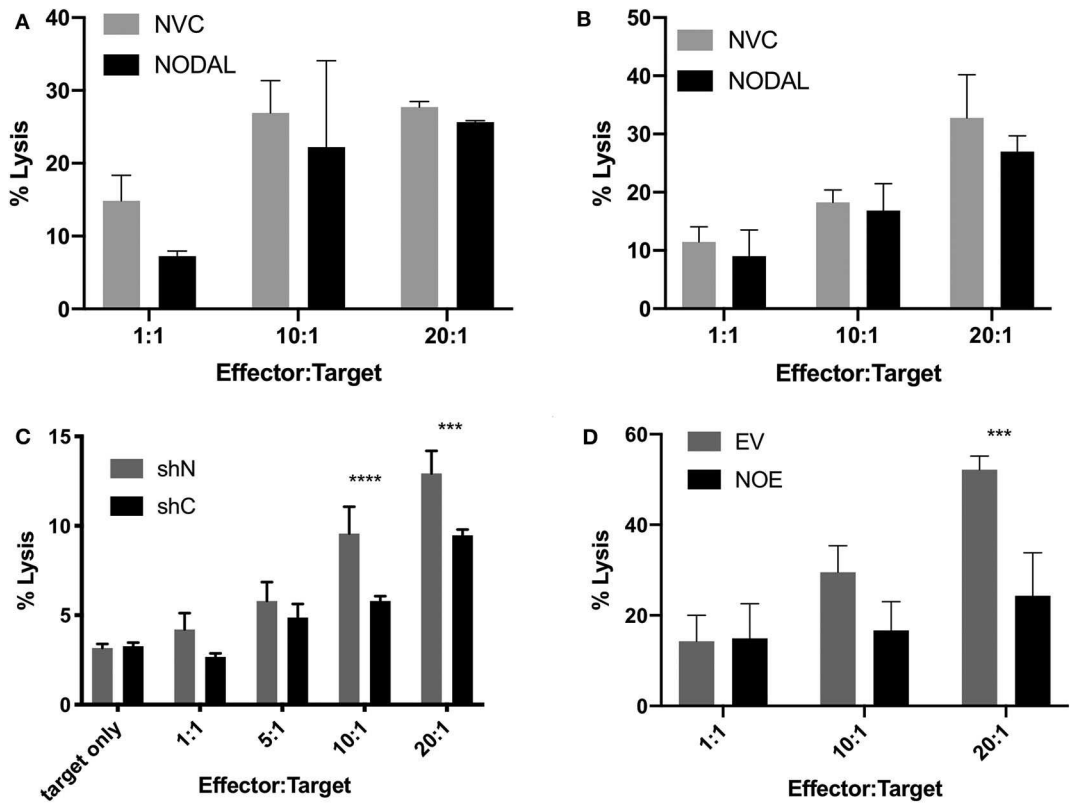

FIGURE 4 | NODAL expression inversely correlates with susceptibility of breast cancer cells to γδ T cell cytotoxicity. **(A)**, NODAL stimulation during a 4-h Calcein AM-release cytotoxicity assay does not impact γδ T cell cytotoxicity against MCF-7 cells. NVC, NODAL vehicle control; $n = 3$ independent experiments. **(B)**, Long term NODAL stimulation has no impact on γδ T cell cytotoxicity against MCF-7 cells. γδ T cells were stimulated one time with NODAL vehicle control (NVC) or 100 ng/ml recombinant human NODAL, then 9 days later were co-incubated for 4 h with Calcein-AM labeled MCF-7 target cells at the indicated Effector:Target (E:T) ratio. **(C)**, Representative example in which day 21 γδ T cells and shC or shN MDA-MB-231 target lines were co-incubated for 4 h at the indicated E:T, and acquired *via* flow cytometry. ***$P = 0.0002$, ****$P < 0.0001$; $n = 6$ independent experiments. **(D)**, Overexpressing NODAL in T47D cells (NOE) confers significantly greater resistance to γδ T cell cytotoxicity as shown in a Calcein AM-release cytotoxicity assay; EV = empty vector control; A, B, D, Calcein AM assays; ***$P = 0.0007$; representative of $n = 4$ independent experiments. **(A–D)** Error bars are SD (3 technical replicates). *P*-values were calculated with 2 way ANOVA followed by Bonferroni multiple comparisons analysis.

from a cohort of TNBC patients (**Table 1**) from which we stained serial sections of up to four different pieces of TNBC tumors from each patient (case). Representative examples are shown (**Figures 1A–D**). The hematoxylin and eosin (H&E) image depicts the invasive front of a triple negative breast carcinoma with large pleomorphic tumor cells showing intimate relationship to the stromal and immune microenvironment (**Figure 1A**). The tumor cells show strong cytoplasmic NODAL expression (**Figure 1B**). Scattered γδ T cells are seen in the vicinity of invasive tumor cell clusters (**Figure 1C**). Other examples from a different case are shown in **Figures S1A–C**. An image of γδ T cells in a CAIX-positive region from a third case are also shown (**Figure 1D**). We found γδ T cells in 45% (9/20) of cases studied on 13/39 slides. Scores for expression of NODAL and CAIX on these 13 slides are shown (**Figure 1E**).

In all cases in which both NODAL and γδ T cells could be detected, γδ T cells were found in close proximity to NODAL-expressing tumor cells; proximity was defined by a distance of $< 50\,\mu m$. NODAL expression was observed in 78% of cases (7/9) and 85% of slides (11/13, **Figure 1F**). γδ T cells were found in regions of CAIX positivity in 100% of cases in which CAIX staining was evident (44%, 4/9 cases; 7/13 slides). Of seven slides from four patient tumors where CAIX and γδ T cell infiltration were both evident, in six (86%) they were co-localized, also with NODAL (46%, 6/13). It should be noted that γδ T cells were also found in areas in which neither NODAL nor CAIX were present. On all slides in which NODAL and CAIX were detected, regardless of γδ T cell infiltration, they were co-localized.

While this patient cohort is small and not powered enough to perform statistics, there appears to be no correlation of γδ T cell infiltration with patient age, invasive ductal carcinoma (IDC) size, grade, stage, or lymph node status (**Table 1**). Of the nine patients whose tumors contained γδ T cells, one had

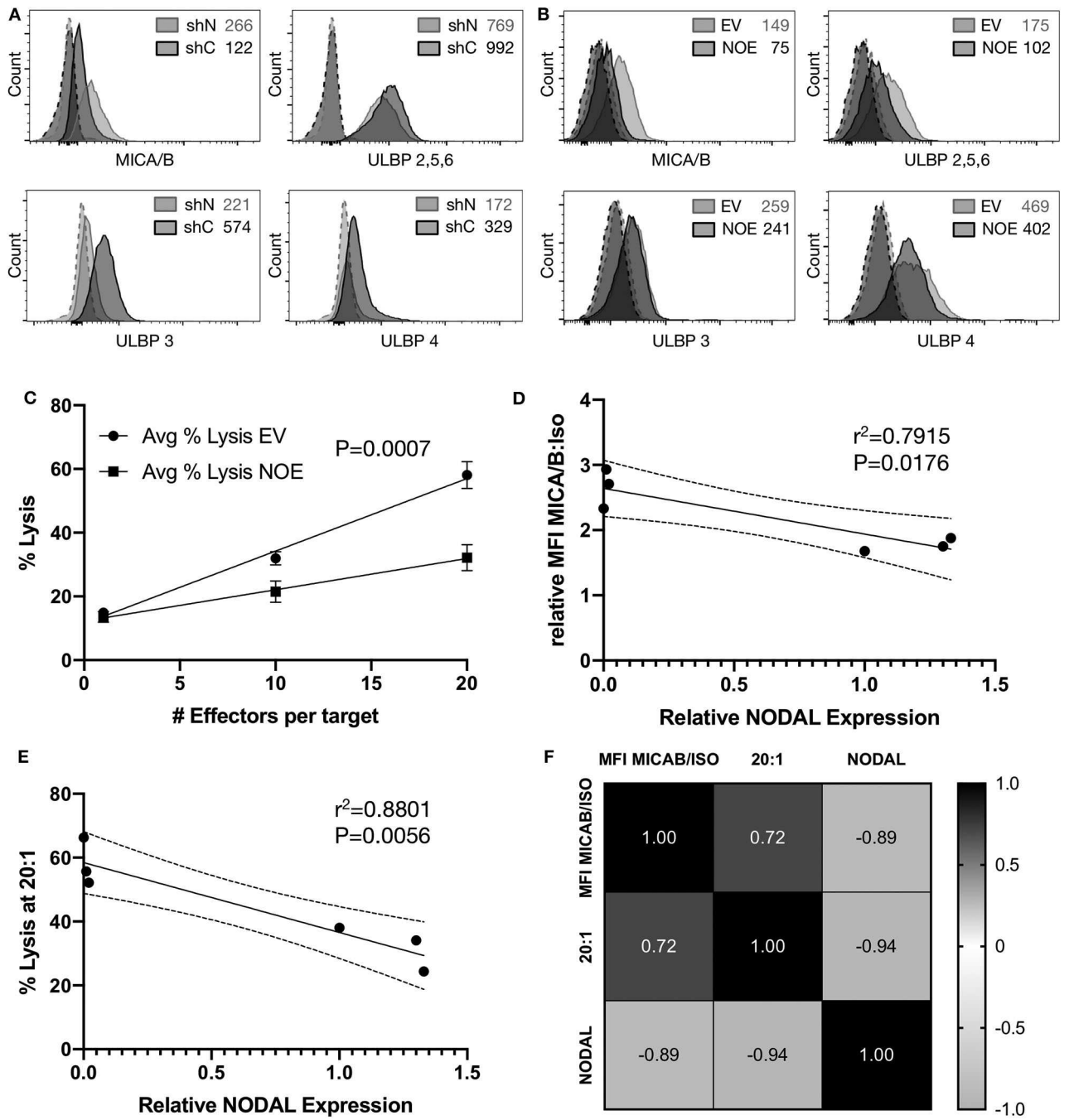

FIGURE 5 | Surface expression of MICA/B is inversely correlated to NODAL expression. **(A)**, Representative examples of MICA/B, ULBP2/5/6, ULBP3, and ULBP4 tumor antigen surface expression on shC and shN MDA-MB-231 cells. Dashed lines are isotope controls. Median fluorescence intensity (MFI) values are indicated. **(B)**, Representative examples of MICA/B, ULBP2/5/6, ULBP3, and ULBP4 tumor surface antigen expression on T47D EV and NOE cells. Dashed lines are isotope controls. Median fluorescence intensity (MFI) values are indicated. **(C)**, Linear regression analysis on data from cytotoxicity assays shown in 4D, S4K,L. Avg = average. **(D)**, Relative ratios of MFI for MICA/B stained cells over isotype controls were plotted against relative NODAL expression as determined by densitometry on protein expression in lysates from matched cells shown in **Figure S4O**. **(E)**, Average percent lysis at 20:1 effector:target ratio from experiments shown in 4D, S4K,L were plotted against relative NODAL expression as determined by densitometry shown in **Figure S4O**. **(F)**, Correlation matrix showing Pearson's correlation coefficients from multiple variables analysis of percent lysis at 20:1, relative NODAL and MICA/B expression from experiments shown in **Figure 4D**, **Figures S4K,L**.

passed away as of February 2020 (11%); three of the eleven patients whose tumors lacked γδ T cells (27%) are deceased. Since NODAL is correlated with breast cancer progression, (36) and we found γδ T cells in close proximity to NODAL-expressing tumor cells, we decided to investigate the impact of NODAL on γδ T cells.

NODAL Stimulation of γδ T Cells Does Not Alter Their Migration

Since chemotaxis is a major regulator of TME composition, we wanted to see whether NODAL had an influence on the migration of γδ T cells. In transwell assays, we tested migration of both αβ and γδ T cells toward MDA-MB-231 cells in which NODAL had been knocked down (γδ shN) compared to those in which NODAL was expressed (γδ shC) and observed no difference in the number of migrating cells (**Figure 2A**). A representative image of a transwell filter with migrated cells before, during and after processing for quantification is shown in **Figures S2A–D**, respectively. Since Vδ1 cells are often found within solid tumors (39) and investigators recently reported a majority of Vδ1 γδ T cell TIL in TNBC specifically, we enriched for Vδ1 γδ T cells and determined that they did not migrate preferentially toward conditioned medium from NODAL-expressing or NODAL knockdown cells. While the addition of recombinant human NODAL (rhNODAL) seemed to decrease migration somewhat, this difference was not significant. Compiled data from four independent migration assays with Vδ1 cells from four different donors are shown in **Figure 2B**. Results from the individual experiments in the compiled **Figure 2B** can be found in **Figures S2E–H**. Verification of NODAL expression in shN and shC cells used to produce conditioned medium for migration experiments can be found in **Figures S2I,J**.

NODAL Stimulation Does Not Impact Activation Marker Expression, Proliferation or Maturation Profiles of γδ T Cells, but Longer Stimulation Time Results in Decreased Vδ2 TCR Expression

Compared to vehicle control, exposure to 100 ng/ml rhNODAL for 24 h had no impact on expression of Vδ1 or Vδ2 TCR, CD69, or PD-1 on the surface of primary human γδ T cells cultured for 14 days (**Figure 3A**). CTLA-4 was not detectible on these cells (data not shown). The Vδ1 + Vδ2 populations shown are a combination of those two individually gated cell types, combined using the FlowJo Boolean "make or gate." Since the anti-Vδ2 TCR antibody outcompetes pan-γδ TCR antibody for binding, we do not show results for pan-γδ TCR staining (which would not include Vδ2 cells), but rather chose to combine Vδ1 and Vδ2 as indicated. Stimulation with OKT3, an anti-CD3 antibody, was included as a positive control for activation marker expression. As expected, both Vδ1 and Vδ2 TCRs were downregulated upon anti-CD3 stimulation; however, Vδ2 surface expression decreased more dramatically. Interestingly, Vδ1 appeared to have more basal PD-1 expression than Vδ2; in contrast, Vδ2 expressed more CD69 (**Figure 3A**, top panel, compare NVC Vδ1 and Vδ2 plots). Fluorescence minus one gating controls are shown in **Figure S3A**. These results were consistent with two other biological replicates done with γδ T cells from different donors; one other example is shown in **Figures S3B,C**.

To assess longer term impact of NODAL on γδ T cells, cells were labeled with Cell Trace Violet (CTV) and followed for 10 days. Samples were taken on days 0, 4, 8, and 10 for flow cytometric analysis. Proliferation modeling of data acquired on day 4 indicated no differences in proliferation between NVC and NODAL stimulated cells (**Figures 3B–D**), with proliferation indices averaging 1.81±0.01 and 1.815 ± 0.015, respectively. Cell counts for all of the time points for both technical replicates are shown in **Figure 3E**. Proliferation was measured via cell counting in a similar manner for three other cultures from two other donors (**Figures S3D–F**), with only one experiment showing some evidence of decreased proliferation of NODAL-treated cells 2 and 7 days post-stimulation but not at the end of culture (**Figure S3D**). In parallel, with the same γδ T cell culture used in **Figures 3A–E**, but left unlabeled, cells were stimulated with NODAL or NVC and then stained for flow cytometric assessment of Vδ1 and Vδ2 TCRs as well as maturation markers CD45RA and CD27. Proportions of Vδ1 and Vδ2 T cells were unaffected by NODAL stimulation (**Figure 3F**), and Vδ1 TCR expression levels remained unchanged (**Figure 3G** top panel); however, Vδ2 TCR expression levels decreased (**Figure 3G** bottom panel). This appears to occur as early as 4 days post-stimulation (**Figure S3G**). Maturation did not appear to be affected by long term NODAL stimulation (**Figure 3H**, FMOs in **Figure S3I**). Maturation was similarly unaffected in two other γδ T cell cultures subjected to a similar assessment (**Figure 3I**, **Figure S3J**), although perhaps there was a trend toward greater conversion of $CD45RA^{-}CD27^{+}$ central memory (CM) cells to $CD45RA^{-}CD27^{-}$ effector memory (EM) cells with higher NODAL doses after 4 days: at 10 ng/ml, CM/EM was 18.9/28.8 and at 100 ng/ml this was 15.6/34.0 (**Figure 3I**, FMOs in **Figure S3K**). An example of another 10-day NODAL stimulation is also shown, although it should be noted that cell viability for this culture by day 22 was no longer optimal and it appears that slightly more naïve cells were present in the NODAL-stimulated culture (**Figure S3J**).

NODAL Expression Is Inversely Proportional to γδ T Cell Cytotoxicity

Since NODAL is correlated with a poor prognosis in breast cancer, and prognosis is also associated with immune evasion, we chose to investigate whether NODAL is implicated in this resistance. Neither short- nor long-term stimulation of γδ T cells with exogenous recombinant human NODAL had any impact on γδ T cell cytotoxicity against MCF-7 breast cancer cells as shown in Calcein AM release assays (**Figures 4A,B**, **Figures S4A–D**). We then went on to investigate whether expression of NODAL in cancer cells could confer resistance, which constitutes a more physiologically relevant scenario, particularly since NODAL becomes upregulated under hypoxic conditions often found in tumors (32). For this, we made use of MDA-MB-231 NODAL knockdown and scrambled control cell lines as targets (35). Since these cell lines express GFP, which is not compatible with Calcein AM release assays, we turned to flow cytometric cytotoxicity assays to determine susceptibility of the lines to γδ T cell cytotoxicity. Indeed, we discovered that loss of NODAL confers susceptibility to γδ T cell killing, which is most significant at 10:1 and 20:1 effector:target ratios (**Figure 4C**, **Figures S4E–I**). We next utilized T47D cells [which have little endogenous NODAL

expression (32)] transduced with an empty vector (EV) or a NODAL overexpression construct (NOE) as targets in our Calcein AM release cytotoxicity assays and found that NODAL overexpression confers resistance to γδ cell killing on T47D cells, again most prominently displayed at higher effector:target ratios of 10:1 and 20:1 (**Figure 4D**, **Figures S4J–L**). Verification of relative NODAL expression levels in these cell lines is depicted in **Figure S4O**. We plotted average percent lysis values for the 20:1 effector:target ratio for cytotoxicity assays shown in **Figures 4C,D**, **Figures S4H,I,L,K**—for which matched NODAL expression levels had been determined in **Figure S4O**—and performed linear regression analyses. The slope of the line of best fit was −21.33 and although the low r^2 value of 0.3500 and position of data points outside the 95% confidence intervals indicated a poor fit, a significant negative association between % lysis and NODAL expression was nevertheless revealed (**Figure S4P**, $P = 0.0427$).

Surface Expression of MICA/B Is Inversely Correlated to NODAL Expression

Flow cytometric assessment of the tumor surface antigens MICA/B, and UL-16 binding proteins (ULBP) 2–6 on shN and shC cells revealed that shN typically have higher surface MICA/B levels (**Figure 5A**, **Figures S5A–C**), but lower levels of all ULBPs tested compared to shC cells (**Figure 5A**). Similar analyses showed that the control EV line expressed higher levels of MICA/B (**Figure 5B**, **Figures S5D–F**), ULBP 2,5,6 and ULBP4 than NOE cells. Levels of ULBP3 were comparable on both lines (**Figure 5B**). As such, it appears that MICA/B surface expression and thus target cell susceptibility to γδ T cell cytotoxicity is inversely proportional to NODAL expression. We then blocked MICA/B on EV and NOE targets prior to cytotoxicity assays. Blocking EV with anti-MICA/B antibody reduced lysis down to a similar level to that of NOE targets (**Figures S4M,N**, compare EV MICA/B with NOE IgG), while blocking MICA/B on NOE targets had less impact than MICA/B blocking on EV (**Figures S4M,N**, compare IgG and MICA/B on EV and NOE). Linear regression analysis on averages from three independent cytotoxicity assays combined (**Figure 4C**, **Figures S4K,L**) indicated significantly decreased susceptibility to γδ T cell lysis of T47D NOE compared to EV targets (**Figure 5C**, $p = 0.0007$). After plotting relative MICA/B MFI over NODAL expression for the T47D EV and NOE cells used in **Figure 5C**, we performed simple linear regression. Narrowing this analysis to only T47D cells yielded a line of best fit with $r^2 = 0.7915$ and a slope significantly different from 0 (**Figure 5D**, $P = 0.0176$). The same analysis of percent lysis at 20:1 vs. relative NODAL expression yielded a P-value of 0.0056 and $r^2 = 0.8801$ (**Figure 5E**). Finally, analysis of percent lysis at 20:1, together with relative NODAL and MICA/B expression, yielded Pearson's correlation coefficients displayed in a matrix in which strong positive correlations were found between percent lysis and MICA/B expression ($r = 0.72$, $P = 0.054$) and negative correlations between percent lysis and NODAL expression ($r = -0.94$, $P = 0.003$) as well as NODAL and MICA/B expression (**Figure 5F**, $r = -0.89$, $P = 0.009$).

DISCUSSION

Alternative therapies for TNBC are in great demand (40) and the impact of the TME on γδ T cells is of great interest to those wishing to further develop γδ T cell immunotherapy (31). For example, altered tumor cell metabolism was addressed in a recent study describing harmful effects of LDL cholesterol on Vδ2 γδ T cell cytokine production and cytotoxicity against MDA-MB-231 *in vitro* and *in vivo*, which may well occur in the TME (41). We previously found that while hypoxia activates γδ T cells, at the same time low oxygen serves to downregulate surface expression and/or increase shedding of MICA by breast cancer cell lines leading to less efficient target cell recognition (22). Since NODAL is induced by hypoxia (32) and is correlated with breast cancer progression (42), we chose to investigate these particular elements of the TME and their influence on γδ T cell function.

We obtained formalin-fixed paraffin-embedded sections from twenty TNBC cases from which, in some cases, we could access slides from different parts of the same tumor. Gamma delta T cells were not equally distributed among these slides; in other words, the presence of γδ T cells in one section did not predict their presence in other tumor sections from another part of the same patient tumor, underlining the heterogeneity of tumors and infiltrating lymphocytes (8). As this was a relatively small cohort of patient tumors, we could not apply statistics to infer prognostic value of γδ TIL; however, there were enough examples of γδ T cell proximity to NODAL-expressing tumor cells to warrant further investigation of the potential impact of NODAL on γδ T cell function.

Hidalgo et al. (29) carefully assessed localization of γδ T cell TIL in a cohort of 26 TNBC tumors, comparing 14 IDC to 12 medullary breast cancer (MBC) cases. They found that most γδ T cells were in the tumor stroma in IDCs, but that in individual cases the cells could be found both in parenchyma and stroma (29). More recent pathological assessments of breast tumors no longer classify malignancies as MBCs, but rather TNBC cases are designated IDCs; as such, we cannot confirm Hidalgo's comparison. We can confirm, however, that γδ T cells could be found in close proximity to tumor cells, some of which expressed NODAL, but that most γδ T cells were localized in the adjacent tumor stroma. Since NODAL is a secreted protein, which would not be captured by IHC, it is reasonable to infer that the NODAL produced by tumor cells would come into contact with γδ T cells in the TME.

We looked for these effects by stimulating one time with exogenously administered rhNODAL and harvesting cells at various time points to determine functional outcome of this stimulus. While in many of our functional assays there appeared to be no significant influence of NODAL on γδ T cells, there were a few exceptions.

Although statistical analysis of compiled Vδ1 T cell migration assays did not yield significant differences, there was a trend toward lesser migration of these cells in the presence of rhNODAL (**Figure 2B**, **Figures S2E–H**) that may have become more clear had we altered incubation times for these assays. We also recognize that the presence of γδ T cells near NODAL-expressing tumor cells suggests that, if there is an inhibitory

effect of NODAL on γδ T cell migration to the tumor, γδ T cells are able to overcome this, at least partially. Further exploration into chemokine receptor expression on γδ T cells after NODAL stimulation may be warranted. It should also be noted that the activity of rhNODAL was assessed periodically *via* P19 assays to ensure that the lack of response we observed in our assays was not due to lack of rhNODAL activity (**Figure S6**).

Vδ2 cells expressed CD69 after anti-CD3 stimulation, which has been found by others to indicate activation in the form of degranulation and production of proinflammatory cytokines (43), whereas Vδ1 cells upregulated PD-1. Such subset-specific responses to anti-CD3 stimulation are reminiscent of the work of Kress et al. (44) who stimulated Vδ1 and Vδ2 cells with PMA/Ionomycin or LPS and measured resulting gene expression changes in the two subsets, which were considerable, with ∼50% being subset specific. Unfortunately, access to the complete gene lists is no longer available online; as such, we were unable to determine whether CD69 or PD-1 were assessed in their analyses. While no noticeable TCR downregulation had occurred at 24 h post-NODAL stimulation (**Figure 3A**), 4 days later, Vδ2 TCR internalization was evident (**Figure S3H**), which was also seen in other experiments at 10 days post-stimulation (**Figure 3G**, **Figure S3I**). Typically, the TCR is internalized upon TCR stimulation, as seen in **Figure 3A** after exposure to anti-CD3, and so this decreased receptor expression indicates some form of activation that we have, as of yet, been unable to pinpoint. Vδ1 TCR expression remained unchanged. Such differential responses of Vδ1 and Vδ2 subsets to stimuli, which we can assess with our polyclonal γδ T cell cultures, may prove useful in the development of subset-specific γδ T cell immunotherapies. One limitation of our study was our use of activated expanding primary γδ T cells, which may have masked subtle effects of NODAL stimulation. In future studies, "untouched" γδ T cells could be used in stimulation assays and also extended to additional readouts such as cytokine release and CD107a degranulation assays.

Most γδ T cell immunotherapy development currently focusses on Vδ2 cells, yet Vδ1 cells are often found in solid tumors. In a very early study utilizing frozen sections from five breast carcinomas, Bank et al. (19) found both Vδ1 and Vδ2 γδ T cell TIL, with slightly higher prevalence of Vδ2 cells, but their cohort was small. In contrast, Peng et al. (45) generated tumor-derived TILs from breast, prostate and melanoma tumors, finding greater numbers of Vδ1 than Vδ2 γδ T cell TIL derived from the epithelial malignancies (breast and prostate), but not in cultures derived from melanoma. While the authors went on to show immunosuppressive qualities of Vδ1 TIL-derived γδ T cells, these assays were conducted only after expansion of cells in high levels of IL-2; considering the inherent plasticity of γδ T cells (46), these immunosuppressive effects may well have been induced by culture conditions and may not reflect the activity of the cells *in situ*.

In contrast, the activity of γδ T cell TIL in TNBC *in situ* has been painstakingly investigated in a recently published study in which γδ T cells were identified in frozen TNBC tumor sections from nine patients, isolated by laser capture microdissection and subjected to single cell sequencing analysis. These analyses confirmed a polyclonal population of γδ T cells had infiltrated TNBC tumors and that these expressed CD69 and the pro-inflammatory cytokines IFNγ and TNFα; only a minor fraction (<20%) expressed IL-17 (30). Since different combinations of TCRγ and TCRδ chains confer distinct antigen recognition capabilities (30), if the response of γδ T cells to NODAL stimulation is TCR dependent, effects on individual clones would have been lost in our current analyses. As such, a study of the impact of NODAL on clonal populations may be of interest, or single cell RNAseq (39) could be employed to tease out individual responses. This was beyond the scope of our current study, but could be considered moving forward.

While NODAL belongs to the TGF-β family, we did not observe the effects reported by Peters et al. (17) with respect to enhancement of γδ T cell cytotoxic activity. In contrast, we found no impact on cytotoxic activity upon addition of rhNODAL to our cytotoxicity assays (**Figure 4A**) or with longer-term γδ T cell stimulation prior to co-culture with targets (**Figure 4B**), although considering the shift from CM to EM observed after 4 days of NODAL stimulation (**Figure 3B**), this may have been evident had we assessed cytotoxicity after 4 days instead of 10 days, since by 10 days NODAL stimulation there was no difference in maturation status of γδ T cells compared to control NVC-stimulated cells (**Figure 3I**).

We found that the ability of target cells to produce NODAL decreases their susceptibility to γδ T cell killing (**Figures 4C,D**, **Figures S4E–N,P**). Previous work from our laboratory documented variable endogenous NODAL levels across breast cancer cell lines, and that MDA-MB-231 cells express more NODAL than T47D (42), which we have confirmed (**Figure S4O**). Furthermore, the MDA-MB-231 shN NODAL knockdown cells produce more NODAL than T47D EV cells (**Figure S4O** compare lanes 1, 3 and 5 with relative intensities for shN of 0.6, 0.3, and 0.2 to lanes 8, 10, 12, and 14 for EV, all 0). Linear regression analysis of percent lysis from cytotoxicity experiments performed with six different donor cultures vs. NODAL expression in 231 shN/shC and T47D EV/NOE targets revealed a significant negative correlation between NODAL expression and susceptibility to γδ T cell killing (**Figure S4P**). The data points are more closely clustered when applied only to T47D EV/NOE (**Figure 5E**), yet the slopes of the lines from these two analyses are nearly the same (−21.33 and −21.9).

There is a significant inverse correlation of NODAL with MICA/B on the tumor cell surface (**Figures 5A,B,D,F**). Blocking EV with anti-MICA/B antibody reduced lysis down to a similar level to that of NOE targets, suggesting that this is indeed an important mechanism by which γδ T cells recognize and target T47D breast cancer cells (**Figures S4M,N**); however, the greater resistance of MDA-MB-231 compared to T47D cannot be solely attributed to NODAL, and we unfortunately did not measure matched MICA/B expression levels for shN and shC targets concurrent with our cytotoxicity assays. MICA shedding played a significant role in the evasion of breast cancer cell lines to γδ T cell killing under hypoxia in our previous study (22). Altogether, our work confirms the findings of Aggarwal et al. (18) who showed that susceptibility of breast cancer cells to killing by Vδ2 γδ T cells was dependent on MICA/B surface levels.

Considering that our assays were performed with primary γδ T cells expanded from many different donors (**Table S1**), which is expected to confer a great deal of inter-donor variability, we observed a remarkable negative correlation between the lysis of T47D targets and their expression of NODAL (**Figures 5E,F**). A very strong negative correlation between MICA/B and NODAL expression was also evident (**Figures 5D,F**). Thus, NODAL perhaps mediates tumor cell escape by somehow regulating expression of surface MICA, the exact mechanism of which remains to be determined. The interaction of NODAL with γδ T cells in the TME may well comprise another example of the tissue sensing adaptate function of γδ T cells (15), the understanding of which deserves further attention to optimize their clinical potential.

DATA AVAILABILITY STATEMENT

All datasets presented in this study are included in the article/**Supplementary Material**.

ETHICS STATEMENT

The studies involving human participants were reviewed and approved by Research Ethics Guidelines, Health Research Ethics Board of Alberta—Cancer Committee. The patients/participants provided their written informed consent to participate in this study.

AUTHOR CONTRIBUTIONS

GS and L-MP contributed to research design. GS and ID conducted experiments. Data analysis was carried out by GS, ID, EK, JH, and MK. GS wrote the manuscript. All authors provided feedback and approved the final version.

FUNDING

This work has been funded by the London Regional Cancer Program, London, ON (Translational Breast Cancer Research Unit Postdoctoral award to GS), the Cancer Research Society (CRSOG2013 to L-MP and GS) and the Canadian Breast Cancer Foundation (L-MP). Support was also provided by the Sawin-Baldwin Chair in Ovarian Cancer, Dr. Anthony Noujaim Legacy Oncology Chair, and Alberta Innovates Health Solutions Translational Health Chair to L-MP. ID has been supported by the Queen Elizabeth II Graduate Scholarship, the University of Alberta Doctoral Recruitment Scholarship and the Alberta Cancer Foundation Antoine Noujaim Scholarship. JH was supported by an Alberta Innovates HYRS program summer studentship.

ACKNOWLEDGMENTS

Flow cytometry was performed at the University of Alberta, Faculty of Medicine and Dentistry Flow Cytometry Facility, which received financial support from the Faculty of Medicine and Dentistry and the Canadian Foundation for Innovation awards to contributing investigators. We would like to thank Dr. Raymond Lai for helping us to obtain tumor sections from the TNBC cohort, Guihua Zhang for NODAL IHC staining and Dylan Dieters-Castator for advice and assistance with preparation of conditioned medium from MDA-MB-231 shN and shC cell lines.

SUPPLEMENTARY MATERIAL

The Supplementary Material for this article can be found online at: https://www.frontiersin.org/articles/10.3389/fimmu.2020.01287/full#supplementary-material

REFERENCES

1. Brenner DR, Weir HK, Demers AA, Ellison LF, Louzado C, Shaw A, et al. Projected estimates of cancer in Canada in 2020. *CMAJ*. (2020) 192:E199–205. doi: 10.1503/cmaj.191292
2. Geng SQ, Alexandrou AT, Li JJ. Breast cancer stem cells: multiple capacities in tumor metastasis. *Cancer Lett*. (2014) 349:1–7. doi: 10.1016/j.canlet.2014.03.036
3. Couzin-Frankel J. Breakthrough of the year 2013. Cancer immunotherapy. *Science*. (2013) 342:1432–3. doi: 10.1126/science.342.6165.1432
4. Connor S. *Cancer Treatment Trials Using Patient's Own Cells to Destroy Solid Tumours 'Will Begin Within a Year'*. London: The Independent (2016).
5. Godder KT, Henslee-Downey PJ, Mehta J, Park BS, Chiang KY, Abhyankar S, et al. Long term disease-free survival in acute leukemia patients recovering with increased gammadelta T cells after partially mismatched related donor bone marrow transplantation. *Bone Marrow Transplant*. (2007) 39:751–7. doi: 10.1038/sj.bmt.1705650
6. Silva-Santos B, Serre K, Norell H. γδ T cells in cancer. *Nat Rev Immunol*. (2015) 15:683–91. doi: 10.1038/nri3904
7. Fisher JP, Heuijerjans J, Yan M, Gustafsson K, Anderson J. γδ T cells for cancer immunotherapy: a systematic review of clinical trials. *Oncoimmunology*. (2014) 3:e27572. doi: 10.4161/onci.27572
8. Tosolini M, Pont F, Poupot M, Vergez F, Nicolau-Travers ML, Vermijlen D, et al. Assessment of tumor-infiltrating TCRVγ9Vδ2 γδ lymphocyte abundance by deconvolution of human cancers microarrays. *Oncoimmunology*. (2017) 6:e1284723. doi: 10.1080/2162402X.2017.1284723
9. Siegers GM, Felizardo TC, Mathieson AM, Kosaka Y, Wang XH, Medin JA, et al. Anti-leukemia activity of *in vitro*-expanded human gamma delta T cells in a xenogeneic Ph+ leukemia model. *PLoS ONE*. (2011) 6:e16700. doi: 10.1371/journal.pone.0016700
10. Siegers GM, Ribot EJ, Keating A, Foster PJ. Extensive expansion of primary human gamma delta T cells generates cytotoxic effector memory cells that can be labeled with Feraheme for cellular MRI. *Cancer Immunol Immunother*. (2013) 62:571–83. doi: 10.1007/s00262-012-1353-y
11. Polito VA, Cristantielli R, Weber G, Del Bufalo F, Belardinilli T, Arnone CM, et al. Universal ready-to-use immunotherapeutic approach for the treatment of cancer: expanded and activated polyclonal γδ memory T cells. *Front Immunol*. (2019) 10:2717. doi: 10.3389/fimmu.2019.02717
12. Almeida AR, Correia DV, Fernandes-Platzgummer A, da Silva CL, da Silva MG, Anjos DR, et al. Delta one T cells for immunotherapy of chronic lymphocytic leukemia: clinical-grade expansion/differentiation and preclinical proof of concept. *Clin Cancer Res*. (2016) 22:5795–804. doi: 10.1158/1078-0432.CCR-16-0597

13. Deniger DC, Maiti SN, Mi T, Switzer KC, Ramachandran V, Hurton LV, et al. Activating and propagating polyclonal gamma delta T cells with broad specificity for malignancies. *Clin Cancer Res*. (2014) 20:5708–19. doi: 10.1158/1078-0432.CCR-13-3451
14. Siegers GM, Lamb LS Jr. Cytotoxic and regulatory properties of circulating Vdelta1+ gammadelta T cells: a new player on the cell therapy field? *Mol Ther*. (2014) 22:1416–22. doi: 10.1038/mt.2014.104
15. Hayday AC. γδ T cell update: adaptate orchestrators of immune surveillance. *J Immunol*. (2019) 203:311–20. doi: 10.4049/jimmunol.1800934
16. Morrow ES, Roseweir A, Edwards J. The role of gamma delta T lymphocytes in breast cancer: a review. *Transl Res*. (2019) 203:88–96. doi: 10.1016/j.trsl.2018.08.005
17. Peters C, Meyer A, Kouakanou L, Feder J, Schricker T, Lettau M, et al. TGF-β enhances the cytotoxic activity of Vdelta2 T cells. *Oncoimmunology*. (2019) 8:e1522471. doi: 10.1080/2162402X.2018.1522471
18. Aggarwal R, Lu J, Kanji S, Das M, Joseph M, Lustberg MB, et al. Human Vγ2Vδ2 T cells limit breast cancer growth by modulating cell survival-, apoptosis-related molecules and microenvironment in tumors. *Int J Cancer*. (2013) 133:2133–44. doi: 10.1002/ijc.28217
19. Bank I, Book M, Huszar M, Baram Y, Schnirer I, Brenner H. V delta 2+ gamma delta T lymphocytes are cytotoxic to the MCF 7 breast carcinoma cell line and can be detected among the T cells that infiltrate breast tumors. *Clin Immunol Immunopathol*. (1993) 67:17–24. doi: 10.1006/clin.1993.1040
20. Guo BL, Liu Z, Aldrich WA, Lopez RD. Innate anti-breast cancer immunity of apoptosis-resistant human gammadelta-T cells. *Breast Cancer Res Treat*. (2005) 93:169–75. doi: 10.1007/s10549-005-4792-8
21. Dutta I, Postovit LM, Siegers GM. Apoptosis induced via gamma delta T cell antigen receptor "blocking" antibodies: a cautionary tale. *Front Immunol*. (2017) 8:776. doi: 10.3389/fimmu.2017.00776
22. Siegers GM, Dutta I, Lai R, Postovit LM. Functional plasticity of gamma delta T cells and breast tumor targets in hypoxia. *Front Immunol*. (2018) 9:1367. doi: 10.3389/fimmu.2018.01367
23. Meraviglia S, Eberl M, Vermijlen D, Todaro M, Buccheri S, Cicero G, et al. *In vivo* manipulation of Vγ9Vδ2 T cells with zoledronate and low-dose interleukin-2 for immunotherapy of advanced breast cancer patients. *Clin Exp Immunol*. (2010) 161:290–7. doi: 10.1111/j.1365-2249.2010.04167.x
24. Beck BH, Kim HG, Kim H, Samuel S, Liu Z, Shrestha R, et al. Adoptively transferred *ex vivo* expanded γδ-T cells mediate *in vivo* antitumor activity in preclinical mouse models of breast cancer. *Breast Cancer Res Treat*. (2010) 122:135–44. doi: 10.1007/s10549-009-0527-6
25. Nicol AJ, Tokuyama H, Mattarollo SR, Hagi T, Suzuki K, Yokokawa K, et al. Clinical evaluation of autologous gamma delta T cell-based immunotherapy for metastatic solid tumours. *Br J Cancer*. (2011) 105:778–86. doi: 10.1038/bjc.2011.293
26. Gentles AJ, Newman AM, Liu CL, Bratman SV, Feng W, Kim D, et al. The prognostic landscape of genes and infiltrating immune cells across human cancers. *Nat Med*. (2015) 21:938–45. doi: 10.1038/nm.3909
27. Ma C, Zhang Q, Ye J, Wang F, Zhang Y, Wevers E, et al. Tumor-infiltrating gammadelta T lymphocytes predict clinical outcome in human breast cancer. *J Immunol*. (2012) 189:5029–36. doi: 10.4049/jimmunol.1201892
28. Bense RD, Sotiriou C, Piccart-Gebhart MJ, Haanen J, van Vugt M, de Vries EGE, et al. Relevance of tumor-infiltrating immune cell composition and functionality for disease outcome in breast cancer. *J Natl Cancer Inst*. (2017) 109:djw192. doi: 10.1093/jnci/djw192
29. Hidalgo JV, Bronsert P, Orlowska-Volk M, Diaz LB, Stickeler E, Werner M, et al. Histological analysis of γδ T lymphocytes infiltrating human triple-negative breast carcinomas. *Front Immunol*. (2014) 5:632. doi: 10.3389/fimmu.2014.00632
30. Janssen A, Villacorta Hidalgo J, Beringer DX, van Dooremalen S, Fernando F, van Diest E, et al. γδ T-cell receptors derived from breast cancer-infiltrating T lymphocytes mediate antitumor reactivity. *Cancer Immunol Res*. (2020) 8:530–43. doi: 10.1158/2326-6066.CIR-19-0513
31. Lo Presti E, Pizzolato G, Corsale AM, Caccamo N, Sireci G, Dieli F, et al. γδ T cells and tumor microenvironment: from immunosurveillance to tumor evasion. *Front Immunol*. (2018) 9:1395. doi: 10.3389/fimmu.2018.01395
32. Quail DF, Taylor MJ, Walsh LA, Dieters-Castator D, Das P, Jewer M, et al. Low oxygen levels induce the expression of the embryonic morphogen Nodal. *Mol Biol Cell*. (2011) 22:4809–21. doi: 10.1091/mbc.e11-03-0263
33. Quail DF, Walsh LA, Zhang G, Findlay SD, Moreno J, Fung L, et al. Embryonic protein nodal promotes breast cancer vascularization. *Cancer Res*. (2012) 72:3851–63. doi: 10.1158/0008-5472.CAN-11-3951
34. Quail DF, Siegers GM, Jewer M, Postovit LM. Nodal signalling in embryogenesis and tumourigenesis. *Int J Biochem Cell Biol*. (2013) 45:885–98. doi: 10.1016/j.biocel.2012.12.021
35. Quail DF, Zhang G, Findlay SD, Hess DA, Postovit LM. Nodal promotes invasive phenotypes via a mitogen-activated protein kinase-dependent pathway. *Oncogene*. (2014) 33:461–73. doi: 10.1038/onc.2012.608
36. Strizzi L, Hardy KM, Margaryan NV, Hillman DW, Seftor EA, Chen B, et al. Potential for the embryonic morphogen Nodal as a prognostic and predictive biomarker in breast cancer. *Breast Cancer Res*. (2012) 14:R75. doi: 10.1186/bcr3185
37. Jungbluth AA, Frosina D, Fayad M, Pulitzer MP, Dogan A, Busam KJ, et al. Immunohistochemical Detection of γ/δ T Lymphocytes in Formalin-fixed Paraffin-embedded Tissues. *Appl Immunohistochem Mol Morphol*. (2019) 27:581–3. doi: 10.1097/PAI.0000000000000650
38. Siegers GM, Dhamko H, Wang XH, Mathieson AM, Kosaka Y, Felizardo TC, et al. Human Vδ1 γ T cells expanded from peripheral blood exhibit specific cytotoxicity against B-cell chronic lymphocytic leukemia-derived cells. *Cytotherapy*. (2011) 13:753–64. doi: 10.3109/14653249.2011.553595
39. Pizzolato G, Kaminski H, Tosolini M, Franchini DM, Pont F, Martins F, et al. Single-cell RNA sequencing unveils the shared and the distinct cytotoxic hallmarks of human TCRVδ1 and TCRVδ2 γδ T lymphocytes. *Proc Natl Acad Sci USA*. (2019) 116:11906–15. doi: 10.1073/pnas.1818488116
40. Blackley EF, Loi S. Targeting immune pathways in breast cancer: review of the prognostic utility of TILs in early stage triple negative breast cancer (TNBC). *Breast*. (2019) 48(Suppl. 1):S44–8. doi: 10.1016/S0960-9776(19)31122-1
41. Rodrigues NV, Correia DV, Mensurado S, Nobrega-Pereira S, deBarros A, Kyle-Cezar F, et al. Low-Density lipoprotein uptake inhibits the activation and antitumor functions of human Vγ9Vδ2 T Cells. *Cancer Immunol Res*. (2018) 6:448–57. doi: 10.1158/2326-6066.CIR-17-0327
42. Quail DF, Zhang G, Walsh LA, Siegers GM, Dieters-Castator DZ, Findlay SD, et al. Embryonic morphogen nodal promotes breast cancer growth and progression. *PLoS ONE*. (2012) 7:e48237. doi: 10.1371/journal.pone.0048237
43. Harly C, Guillaume Y, Nedellec S, Peigne CM, Monkkonen H, Monkkonen J, et al. Key implication of CD277/butyrophilin-3 (BTN3A) in cellular stress sensing by a major human γδ T-cell subset. *Blood*. (2012) 120:2269–79. doi: 10.1182/blood-2012-05-430470
44. Kress E, Hedges JF, Jutila MA. Distinct gene expression in human Vδ1 and Vδ2 γδ T cells following non-TCR agonist stimulation. *Mol Immunol*. (2006) 43:2002–11. doi: 10.1016/j.molimm.2005.11.011
45. Peng G, Wang HY, Peng W, Kiniwa Y, Seo KH, Wang RF. Tumor-infiltrating gammadelta T cells suppress T and dendritic cell function via mechanisms controlled by a unique toll-like receptor signaling pathway. *Immunity*. (2007) 27:334–48. doi: 10.1016/j.immuni.2007.05.020
46. Lafont V, Sanchez F, Laprevotte E, Michaud HA, Gros L, Eliaou JF, et al. Plasticity of γδ T cells: impact on the anti-tumor response. *Front Immunol*. (2014) 5:622. doi: 10.3389/fimmu.2014.00622

Conflict of Interest: The authors declare that the research was conducted in the absence of any commercial or financial relationships that could be construed as a potential conflict of interest.

frontiers in Immunology

ORIGINAL RESEARCH
published: 30 June 2020
doi: 10.3389/fimmu.2020.01328

Galectin-3 Released by Pancreatic Ductal Adenocarcinoma Suppresses γδ T Cell Proliferation but Not Their Cytotoxicity

Daniel Gonnermann[1†], Hans-Heinrich Oberg[1†], Marcus Lettau[1], Matthias Peipp[2], Dirk Bauerschlag[3], Susanne Sebens[4], Dieter Kabelitz[1] and Daniela Wesch[1]*

[1] Institute of Immunology, University Hospital Schleswig-Holstein (UKSH) and Christian-Albrechts University (CAU) of Kiel, Kiel, Germany, [2] Division of Stem Cell Transplantation and Immunotherapy, Department of Medicine II, UKSH, CAU Kiel, Kiel, Germany, [3] Department of Gynecology and Obstetrics, UKSH, Kiel, Kiel, Germany, [4] Institute for Experimental Cancer Research, UKSH, CAU Kiel, Kiel, Germany

OPEN ACCESS

Edited by:
Nadia Caccamo,
University of Palermo, Italy

Reviewed by:
Jean Jacques Fournie,
INSERM U1037 Centre de Recherche en Cancérologie de Toulouse, France
Julie Ribot,
Universidade de Lisboa, Portugal

***Correspondence:**
Daniela Wesch
daniela.wesch@uksh.de

[†] These authors share first authorship

Specialty section:
This article was submitted to T Cell Biology, a section of the journal Frontiers in Immunology

Received: 18 March 2020
Accepted: 26 May 2020
Published: 30 June 2020

Citation:
Gonnermann D, Oberg H-H, Lettau M, Peipp M, Bauerschlag D, Sebens S, Kabelitz D and Wesch D (2020) Galectin-3 Released by Pancreatic Ductal Adenocarcinoma Suppresses γδ T Cell Proliferation but Not Their Cytotoxicity. Front. Immunol. 11:1328. doi: 10.3389/fimmu.2020.01328

Pancreatic ductal adenocarcinoma (PDAC) is characterized by an immunosuppressive tumor microenvironment with a dense desmoplastic stroma. The expression of β-galactoside-binding protein galectin-3 is regarded as an intrinsic tumor escape mechanism for inhibition of tumor-infiltrating T cell function. In this study, we demonstrated that galectin-3 is expressed by PDAC and by γδ or αβ T cells but is only released in small amounts by either cell population. Interestingly, large amounts of galectin-3 were released during the co-culture of allogeneic *in vitro* expanded or allogeneic or autologous resting T cells with PDAC cells. By focusing on the co-culture of tumor cells and γδ T cells, we observed that knockdown of galectin-3 in tumor cells identified these cells as the source of secreted galectin-3. Galectin-3 released by tumor cells or addition of physiological concentrations of recombinant galectin-3 did neither further inhibit the impaired γδ T cell cytotoxicity against PDAC cells nor did it induce cell death of *in vitro* expanded γδ T cells. Initial proliferation of resting peripheral blood and tumor-infiltrating Vδ2-expressing γδ T cells was impaired by galectin-3 in a cell-cell-contact dependent manner. The interaction of galectin-3 with α3β1 integrin expressed by Vδ2 γδ T cells was involved in the inhibition of γδ T cell proliferation. The addition of bispecific antibodies targeting γδ T cells to PDAC cells enhanced their cytotoxic activity independent of the galectin-3 release. These results are of high relevance in the context of an *in vivo* application of bispecific antibodies which can enhance cytotoxic activity of γδ T cells against tumor cells but probably not their proliferation when galectin-3 is present. In contrast, adoptive transfer of *in vitro* expanded γδ T cells together with bispecific antibodies will enhance γδ T cell cytotoxicity and overcomes the immunosuppressive function of galectin-3.

Keywords: T cells, gammadelta T cells, pancreatic cancer, galectin-3, α3β1 integrin, bispecific antibodies, proliferation, autologous

INTRODUCTION

Galectin (gal)-3 is a member of β-galactoside-binding protein family that shares highly conserved carbohydrate recognition domains (CRD) (1, 2). The monomer gal-3 belongs to the chimera-type subgroup of the galectin family which contains one CRD that is connected to an extended non-lectin N-terminal domain. This exclusive gal-3 structure allows dimerization in the absence of binding ligands and a formation of pentamers in the presence of carbohydrate binding ligands such as N-glycans (3). As a multifunctional protein, gal-3 is involved in cell-matrix adhesion, cell proliferation, cell death, receptor turnover, and cell signaling as well as in malignant transformation depending on its subcellular localization (1–4). Gal-3 is found in the cytoplasm, shuttles between the cytoplasm and the nucleus, and can also be expressed at the cell surface or secreted into biological fluids *via* non-classical secretory pathways (3). Depending on the cellular component, gal-3 mediates both pro-and anti-apoptotic activity (5). Gal-3 overexpression as well as prominent protumorigenic effects have been shown in various tumors including pancreatic ductal adenocarcinoma (PDAC) (6). Differential expression profiling and microarray analysis revealed an enhanced gal-3 expression in the tissue of PDAC patients compared to that of chronic pancreatitis (CP) patients, and a slightly increased gal-3 expression in tissue of CP patients compared to healthy donors (7–9).

PDAC is 4th leading cancer-related death due to an aggressive growth, early metastatic dissemination and limited treatment options (10, 11). Mutations in the pro-oncogene K-Ras (rat sarcoma) together with a high Ras activity are suggested to be associated with the pathogenesis of PDAC (12, 13). An overexpression of gal-3 in pancreatic tumor tissue contributes to PDAC progression *via* gal-3 binding to retaining Ras at the plasma membrane maintaining Ras-signaling including phosphorylation of Extracellular-signal Regulated Kinases (ERK) and AKT and Ras-like (Ral) protein A activity (12–14).

In addition to the gal-3-mediated tumor transformation, gal-3 secreted by tumor cells regulates immune cell activities and contributes to immunosuppression (15). Extracellular gal-3 binds glycosylated T cell surface receptors including the receptor-linked protein tyrosine phosphatase CD45 expressed on all leukocytes, integrins like CD11a (αL integrin), CD29 (β1 integrin), and CD49c (α3 integrin) and the T cell interaction molecule CD7 (1, 16). Cross-linking glycoproteins at the T cell surface induces anergy or apoptosis (15, 17–19). Gal-3 induces anergy of CD8 T cells by distancing the T cell receptor (TCR) from the CD8 molecule, and impairs NK cell activity by inhibiting the interaction of the activating receptor natural-killer group 2, member D (NKG2D) expressed on NK cells and the heavily *O*-glycosylated tumor-derived MHC class I chain-related protein (MIC) A (15, 20, 21).

In this context, γδ T lymphocytes, which highly express NKG2D and infiltrate in PDAC tissues, are of high interest (22–25). In this study, we focused on Vδ2-expressing γδ T cells, which are specifically activated by pyrophosphate intermediates of the prokaryotic non-mevalonate pathway of cholesterol synthesis, and more importantly by dysregulated mevalonate-pathway metabolites of transformed eukaryotic cells (26, 27). Vδ2-expressing γδ T cells are a promising cell population for T cell-based immunotherapy due to their HLA-unrestricted target cell recognition and their enhanced cytotoxicity against PDAC cells after application of targeted biologicals such as bispecific antibodies (bsAb) (23, 28–30). Here, we were interested in a possible induction of anergy or apoptosis in Vδ2 γδ T cells by gal-3, which could explain the observed exhaustion of anti-tumor responses of Vδ2 γδ T cells against PDAC cells unless bsAb were applied (23, 30, 31).

Abbreviations: bsAb, bispecific antibody; BrHPP, bromohydrinpyrophosphate; CRD, conserved carbohydrate recognition domains; DC, dendritic cell; ERK, Extracellular-signal Regulated Kinases; gal-3, galectin-3; gal-9, galectin-9; HER-2, Human epidermal growth factor receptor-2; LacNAc, N-acetyl-D-lactosamine; mAb, monoclonal antibody; MICA, MHC class-I related chain A; n-BP, aminobisphosphonate; NKG2D, natural-killer group 2, member D; PDAC, pancreatic ductal adenocarcinoma; PI, propidium iodide; Ras, rat sarcoma; TCR, T cell receptor; TIL, tumor-infiltrating lymphocytes; PAg, phosphorylated antigen; PBMC, peripheral blood mononuclear cells; UKSH, University Hospital Schleswig-Holstein.

MATERIALS AND METHODS

Cohort and Ethic Statement

The Department of Transfusion Medicine of the University Hospital Schleswig-Holstein (UKSH) in Kiel, Germany, provided leukocyte concentrates from healthy adult blood donors. In addition, heparinized blood, serum samples and tumor tissue from PDAC patients were obtained from the Department of General and Thoracic Surgery (UKSH, Campus Kiel) and from the Surgery Department of the Community Hospital in Kiel distributed by the Biobank BMB-CC of the PopGen 2.0 Biobanking Network (P2N; UKSH, Campus Kiel) supervised by Dr. C. Röder (Institute for Experimental Cancer Research, Kiel, Germany). In total, 19 patients with histologically verified PDAC (stage pT2-3, pN0-2, L0-1, V0-1) were enrolled. Serum samples of 9 patients with histologically verified advanced ovarian cancer (FIGO-stage IIIA-IV) were obtained from the Department of Gynecology and Obstetrics of the UKSH in Kiel. Pathological features of all tissues were assessed according to WHO classification and UICC TNM staging. None of the patients had undergone chemo- or radiotherapy before this investigation. In accordance with the Declaration of Helsinki, written informed consent was obtained from all donors, and the research was approved by the relevant institutional review boards (Ethic Committee of the Medical Faculty of the CAU Kiel, code number: D405/10, D445/18, and A110/99).

Ex vivo Isolation of Tumor-Infiltrating Lymphocytes and Tumor Cells

Tumor tissue of PDAC patients removed during surgery was dissected in the Institute of Pathology of the UKSH, Campus Kiel. Tumor tissues (1–2 cm^3) were washed (in 10 cm dishes) with PBS to remove blood debris. Subsequently, the tumor tissues were minced into approximately 1 mm^3

pieces and treated with components A, H, and R of the Tumor Dissociation Kit (Miltenyi Biotec, Bergisch Gladbach, Germany) for 1 h at 37°C in 5 mL PBS in a Gentle MACS (Miltenyi Biotec). Digested cell suspension was then passed through a 100 μm cell strainer (Falcon, BD Biosciences), visually controlled by light microscopy and centrifuged at 481 × g for 5 min. Tumor cells as well as tumor-infiltrating cells (TIL) were isolated by Ficoll-Hypaque (Biochrom, Berlin, Germany) density gradient centrifugation. The purity of the cells was determined by staining as described in the flow cytometry section. Cells were cultured in RPMI 1640 supplemented with 2 mM L-glutamine, 25 mM HEPES, 100 U/mL penicillin, 100 μg/mL streptomycin, 10% fetal bovine serum (FBS, Thermo Fisher Scientific, Karlsruhe, Germany) [complete medium].

Ex vivo isolated tumor cells and autologous TIL were characterized phenotypically and functionally as described under flow cytometry and functional assay section.

Separation of PBMC and T Cells and Generation of Short-Term Activated T Cell Lines

Peripheral blood mononuclear cells (PBMC) were isolated from leukocyte concentrates or heparinized blood from PDAC patients by Ficoll-Hypaque (Biochrom) density gradient centrifugation. CD4 αβ T cells, CD8 αβ T cells and γδ T cells were positively separated from freshly isolated PBMC by using the magnetic cell separation system (Miltenyi Biotec). To isolate CD4 and CD8 T cells, cells were labeled directly with specific microbead-coupled mAbs (CD4 and CD8 MicroBeads, Miltenyi Biotec). To isolate γδ T cells, an indirect two-step process (anti-TCR γδ micro-Bead Kit, Miltenyi Biotec) consisting of labeling the γδ T cells with a specific hapten-coupled mAb followed by staining the cells with FITC-labeled anti-hapten microbeads were applied. The purity of the cells was >98% after their magnetic separation.

To expand short-term activated CD4 or CD8 αβ T cell lines or γδ T cell lines, 10^6 cells/mL were cultured in 24-well plates in complete medium with 50 IU/mL rIL-2 (Novartis, Basel, Switzerland) and stimulated with Activation/Expander Beads (Miltenyi Biotec) with a one bead/one cell ratio for 3–4 days for αβ T cells and 5–10 days for γδ T cells. The beads were coated with 10 μg/mL each anti-CD3 and anti-CD28 mAbs and 0.5 μg/mL anti-CD2 mAb overnight and used as T cell receptor (TCR) stimulus. Alternatively, γδ T cell lines were expanded by stimulation of PBMC with 2.5 μM aminobisphosphonate (n-BP) zoledronic acid (Novartis), which induces a selective outgrowth of Vγ9 Vδ2-expressing γδ T cells. Since resting, initially stimulated γδ T cells produced only very low amounts of IL-2, 50 IU/mL rIL-2 was added every two day. After 2 weeks, Vγ9Vδ2-expressing γδ T cell lines had a purity of 60–99% and were labeled with anti-TCRαβ mAb clone IP26 (BioLegend, San Diego, CA) and subjected to magnetic separation in order to deplete remaining αβ T cells. After αβ T cell depletion, Vγ9 Vδ2 γδ T cell lines had a purity of 98–99%.

Established Tumor Cell Lines and Cell Culture Conditions

Human PDAC cell lines Panc-1, PancTu-I, BxPC3, MiaPaCa-2, Capan-2 cells derived from primary tumors as well as Panc89 and Colo357 cells derived from a lymph node metastasis were cultured in complete medium under regular conditions (5% CO_2, humidified, 37°C) (32). The PDAC cell lines were kindly provided by Dr. C. Röder and Prof. Dr. A. Trauzold, Institute for Experimental Cancer Research, Kiel, Germany. 0.05% trypsin/0.02% EDTA was used to detach adherent PDAC cell lines from flasks. Absence of mycoplasma was routinely confirmed by RT-PCR (Venor® GEM classic, Minerva Biolabs GmbH, Germany) and genotype by short tandem repeat analysis.

Flow Cytometry

In total, 1–2 × 10^6 PBMC and *ex vivo* isolated TIL were stained by multi-color flow cytometry approach to distinguish between diverse T cell subpopulations within different $CD45^+$ leukocyte populations. Directly conjugated mAbs included PerCP-labeled anti-CD45 clone 2D1, PE-Cy7-labeled anti-pan TCRγδ clone 11F2 (both BD Biosciences, Heidelberg), AF700-labeled anti-CD3 clone SK7, BV510-labeled anti-CD4 clone OKT4, APC-Cy7-labeled anti-CD8 clone SK1 (all three, BioLegend), VioBlue-labeled anti-Vδ1 clone REA173 (Miltenyi Biotec), PE-labeled anti-Vδ2 clone B6 (BD Biosciences), and corresponding isotype controls (BD Biosciences or BioLegend).

To determine purity and expression of tumor-associated antigens such as epithelial cell adhesion molecule (EpCAM) and human epidermal growth factor receptor (HER)-2, 2 × 10^5 *ex vivo* isolated tumor cells derived from tumor tissues were stained with mAbs as follows: PerCP-labeled anti-CD45 clone 2D1 (BD Biosciences), PE-Vio770-labeled anti-HER-2 clone 24D2 and APC-labeled anti-EpCAM clone REA-125 (both from Miltenyi Biotec) followed by intracellular staining with FITC-labeled anti-pan-Cytokeratin mAb clone CK3-6H5 (Miltenyi Biotec). All *ex vivo* isolated tumor cells were pan-$Cytokeratin^+$, $EpCAM^+$ and HER-2^+, but did not express CD45. Additionally, TIL, *ex vivo* isolated tumor cells and established PDAC cell lines were also intracellularly stained with AF647-conjugated anti-gal-3 (clone M3/38) or an appropriate isotype control (an AF647-conjugated rat IgG2a mAb). Briefly, for the intracellular staining, 2–5 × 10^5 cells were washed with staining buffer, fixed and permeabilized with the Cytofix/Cytoperm kit (BD Biosciences) for 20 min following the procedures outlined by the manufacturer. Thereafter, cells were washed twice with Perm/Wash by centrifugation and stained with fluorochrome-conjugated anti-gal-3 mAb or isotype control for 30 min, washed and measured.

All samples were analyzed on a FACS Calibur and a LSR-Fortessa flow cytometer (both from BD Biosciences) using CellQuestPro, Diva 8, or FlowJo software.

Cell Death Analysis by Flow Cytometry

Cell death analysis of γδ T cells was performed by combined annexin-V FITC and propidium iodide (PI) staining. Briefly, 10^6/mL short-term activated γδ T cells were treated with medium or different concentrations (0.1 and 1 μg/mL) of gal-3 or galectin

(gal)-9 (both from BioLegend) in complete medium in 24-well plates for 24 h. After incubation, cells were washed with annexin-V binding buffer (MabTag, Friesoythe, Germany) and stained with annexin-V FITC (1:10, MabTag) and PI (2 μg/mL, Serva; Heidelberg, Germany). After two washing steps, cells were analyzed by flow cytometry, and the proportion of viable (annexin-V^- PI^-), early apoptotic cells (annexin-V^+ PI^-) and late apoptotic/necrotic cells (annexin-V^+ PI^+) was determined.

RNA Interference

In total, 1.5×10^5 PDAC cells were seeded in 12-well plates, and incubated for 24 h in cell culture medium without antibiotics. To downregulate gal-3 expression, the cells were transfected with 12 pmol gal-3 Stealth RNAi™ siRNA or non-targeting control pool (gal-3 sense; # 10620318, non-targeting gal-3 antisense; # 10620319, both Thermo Fisher Scientific) using 2 μL Lipofectamine® RNAiMAX reagent (Thermo Fisher Scientific) in 200 μL Opti-MEM medium for 10–20 min according to manufacturer's protocol. The optimal time point of downregulation was analyzed by flow cytometry and by Western blot. The lowest gal-3 expression was detected 72 h after transfection.

Functional Cell Culture Assay

In total, 1.25×10^5 PBMC of healthy donors or PDAC patients were plated in complete medium with 50 IU/mL rIL-2 in 96-round well-plates. γδ T cells within PBMC were selectively activated by 300 nM phosphorylated antigen (PAg) bromohydrinpyrophosphate (BrHPP, Innate Pharma, Marseille, France) or 2.5 μM n-BP zoledronic acid in the absence or presence of different concentrations (0.01–10 μg/mL in logarithmic steps) of gal-3 (BioLegend). IFN-γ was determined in the supernatant after 48 h using ELISA (**Supplemental Methods** and **Supplemental Figure 2**). After 6–7 days, γδ T cell proliferation was analyzed as described in the Cell proliferation assay section. Alternatively, $5–10 \times 10^3$ established PDAC cells (wild type, control or gal-3 siRNA transfected cells) were plated in 96-well flat-bottom plates in complete medium. After 24 h, 2.5×10^5 PBMC were added together with 50 IU/mL rIL-2 at an effector/target (E/T) ratio of 50:1 (PBMC/tumor cells) representing an effective E/T of 15:1–40:1 for CD3 T cells/tumor cells or of 1:4–10:1 for Vγ9Vδ2 T cells/tumor cells. The effective E/T ratio was determined by staining PBMC with anti-CD3, anti-Vγ9 and anti-Vδ2 mAb using flow cytometry. In several experiments, resting or short-term activated CD4 and CD8 positively isolated αβ T cells or γδ T cells were used as effector cells at an E/T ratio of 50:1 for resting cells or 5:1–40:1 for activated T cells. αβ T cells were stimulated with Activation/Expander Beads (Miltenyi Biotec) coated with 10 μg/mL each of anti-CD3 and anti-CD28 mAbs and 0.5 μg/mL anti-CD2 mAb as αβ TCR stimulus or with 1 μg/mL bsAb [HER2xCD3], which targets HER-2 expressed on PDAC cells to CD3-expressing T cells (23, 30). γδ T cells were cultured with 50 IU/mL IL-2 (for resting cells) and 12.5 IU/mL (for activated cells), and were stimulated by 300 nM PAg BrHPP or 2.5 μM zoledronic acid or with the tribody [$(HER2)_2$ xVγ9], which targets HER2-expressing PDAC cells to Vγ9-expressing γδ T cells (23, 30). As control, T cells were cultured and stimulated in the absence of PDAC cells. γδ T cell proliferation was analyzed after 6–7 days and αβ T cell proliferation after 3–4 days.

To analyze cell-cell contact dependency, 2×10^5 PancTu-I cells plated in 24-well plates were cocultivated with unstimulated or with PAg-stimulated short-term activated Vγ9Vδ2 γδ T cells in the presence of 12.5 IU/mL IL-2 at an E/T ratio 40:1 separated or not by a membrane with 0.4 μm pores. As control, Vγ9Vδ2 γδ T cells were cultured alone. After 24 h, gal-3 was measured in the cell culture supernatant as described in the ELISA section.

For blocking assays, 2.5×10^5 PBMC were pre-incubated in 110 μL of 10–20 μg/mL of neutralizing antibodies including anti-CD7 (clone M-T701), anti-CD11a (clone HI111), anti-CD29 (clone Mab 13), anti-CD49c (clone C3 II.I) (all from BD Biosciences) and anti-CD45 (clone HI 30, from BioLegend) as well as appropriate isotypes mIgG1 (MOPC-21, BioLegend), and rIgG2a (RTK2758, BioLegend). Alternatively, cells were pretreated with a combination of 10 μg/mL anti-CD29 mAb and 10 μg/mL anti-CD49c mAb or appropriate controls. After 2 h of incubation, 50 μL of pretreated PBMC were transferred to 5×10^3 PancTu-I cells adhered overnight and stimulated with 2.5 μM zoledronic acid and 50 IU/mL of rIL-2. γδ T cell proliferation was analyzed after 7 days.

For autologous assay system, 5×10^3 *ex vivo* isolated tumor cells of PDAC patients were plated in 96-well flat-bottom plates in complete medium. After 24 h, 2.5×10^5 autologous PBMC were added together with 50 IU/mL rIL-2 at an effector/target (E/T) ratio of 50:1 (PBMC/tumor cells) representing an effective E/T of 1:1 or 0.5:1 (Vγ9Vδ2 T cells/tumor cells). For coculturing of *ex vivo* isolated tumor cells of PDAC patients with autologous TIL, we used a lower E/T ratio. This reduced E/T ratio resulted from a low number of isolated TIL derived from 1 cm^3 PDAC tissue and from a different distribution of the cells within the tumor tissue of PDAC patients. While 40–60% expressed pan-Cytokeratin (detected as tumor cells) and 10–30% CD45 (detected as leukocytes), residual cells are tumor-associated cells, which are part of the TIL population after Ficoll-Hypaque density centrifugation of digested tumor tissue. 1.5×10^5 *ex vivo* isolated tumor cells of PDAC patients were plated in 96-well flat-bottom plates in complete medium. After 24 h, 1.5×10^3 autologous TIL were added together with 50 IU/mL rIL-2 at an effector/target (E/T) ratio of 1:4 (TIL/tumor cells) representing an effective E/T of 1:40 or 1:400 (Vγ9Vδ2 T cells/tumor cells).

Functional read out systems included a proliferation assay and measurement of gal-3 release as described as follows.

Cell Proliferation Assay

Proliferation was determined by measuring the absolute cell number of viable $CD3^+$ γδ or αβ T cells with a flow cytometric method termed standard cell dilution assay (SCDA) after 6–8 days of culture. SCDA has been reported as a precise method to specifically quantify any subset of phenotypically definable, viable cells in heterogeneous populations (33). Briefly, co-cultured T cells and tumor cells from 96-well round-bottom plates were washed and stained with fluorescein isothiocyanate (FITC)-labeled anti-CD3 mAbs (BD Biosciences, Heidelberg, Germany) or AF488-conjugated anti-Vγ9 mAb clone 7A5 (34). After one

washing step, cells were resuspended in 100 µL sample buffer containing a defined number (10^4) of APC-labeled fixed standard cells and 0.2 µg/mL PI. The standard cells were purified T cells that had been stained with APC-labeled anti-HLA class I mAb clone W6/32 and anti-TCRαβ mAb clone IP26, and fixed in 1% paraformaldehyde. The analysis on a flow cytometer allowed us to simultaneously measure the expansion of viable CD3 or Vγ9 γδ T cells (FITC$^+$ or AF488$^+$ PI$^-$ APC$^-$) and standard cells (FITC$^-$

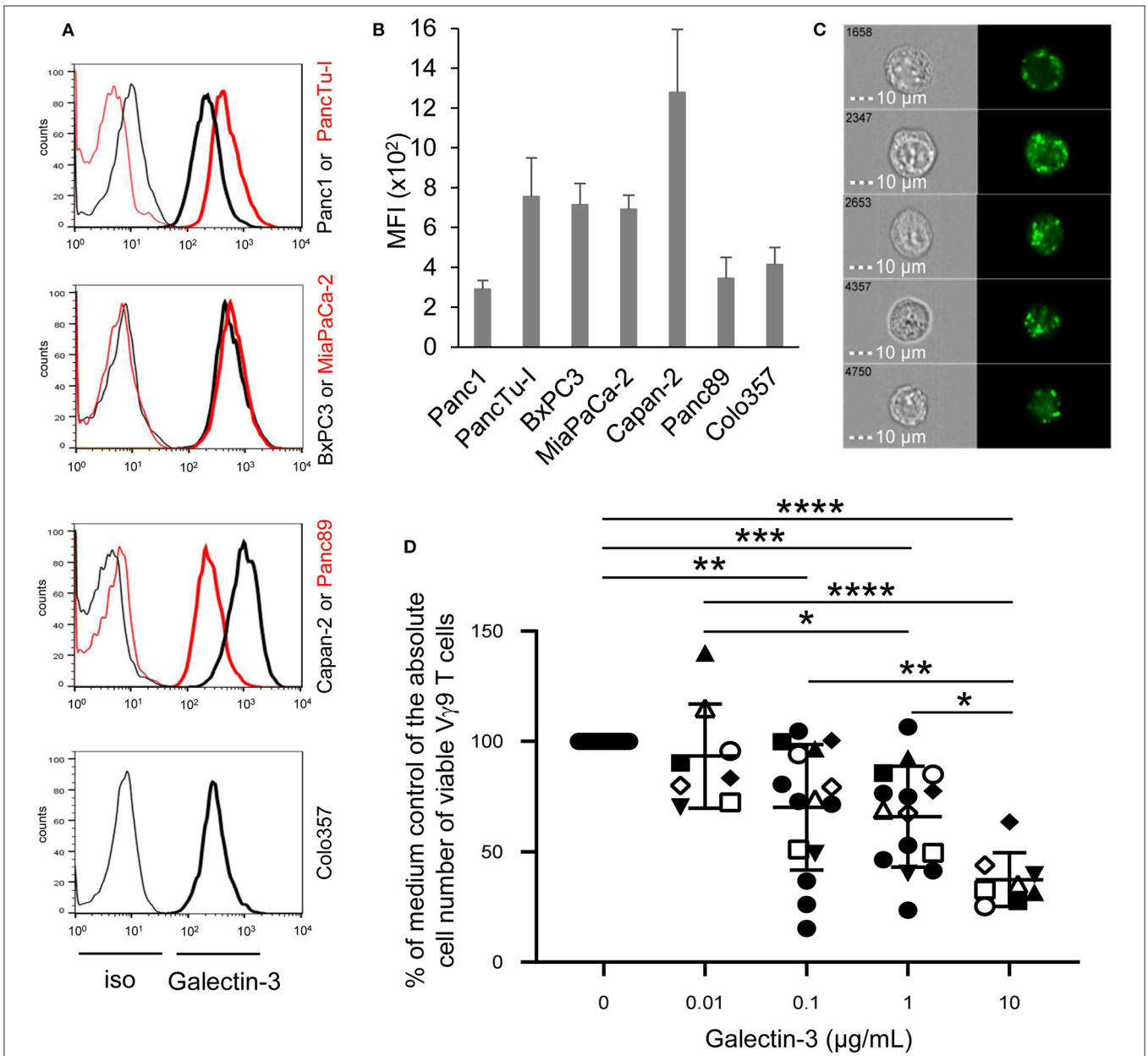

FIGURE 1 | Intracellular galectin-3 expression in PDAC cells, and effect of recombinant galectin-3 on γδ T cell proliferation. **(A)** Histograms depicted are representative results of indicated PDAC cells. Thin and bold lines represent isotype control and gal-3 expression (clone M3/38), respectively. **(B)** Median fluorescence intensity (MFI) ± SD ($n = 3$, duplicates) of gal-3 expression corrected by the MFI of the isotype control is shown for the indicated PDAC cell lines measured by FACS Calibur. **(C)** PancTu-I cells were labeled with anti-gal-3 mAb (clone Gal397) and analyzed on the ImageStream® X Mark II. Five representative cells out of 5 × 10^3 recorded cells are shown with bright field image (left side) and fluorescence image of gal-3 (right side). Scale bars represent 10 µm. **(D)** 1.25 × 10^5 PBMC of paired healthy donors ($n = 4$, different closed symbols), additional healthy donors ($n = 7$, two conc. of gal-3, closed circles) and paired PDAC patients ($n = 4$, open symbols) were stimulated with 300 nM BrHPP with the different indicated concentrations of rgal-3 and 50 IU/mL rIL-2. After 6–7 days, the absolute cell number was determined as a percentage of the medium control of the Vγ9 γδ T cells using SCDA. The mean ± SD of duplicates is shown. Statistical comparison of non-matched samples was carried out parametrically by using one-way ANOVA followed by Tukey's multiple comparison test. Significances are shown as *P*-value; $^*P < 0.05$, $^{**}P < 0.01$, $^{***}P < 0.001$, $^{****}P < 0.0001$.

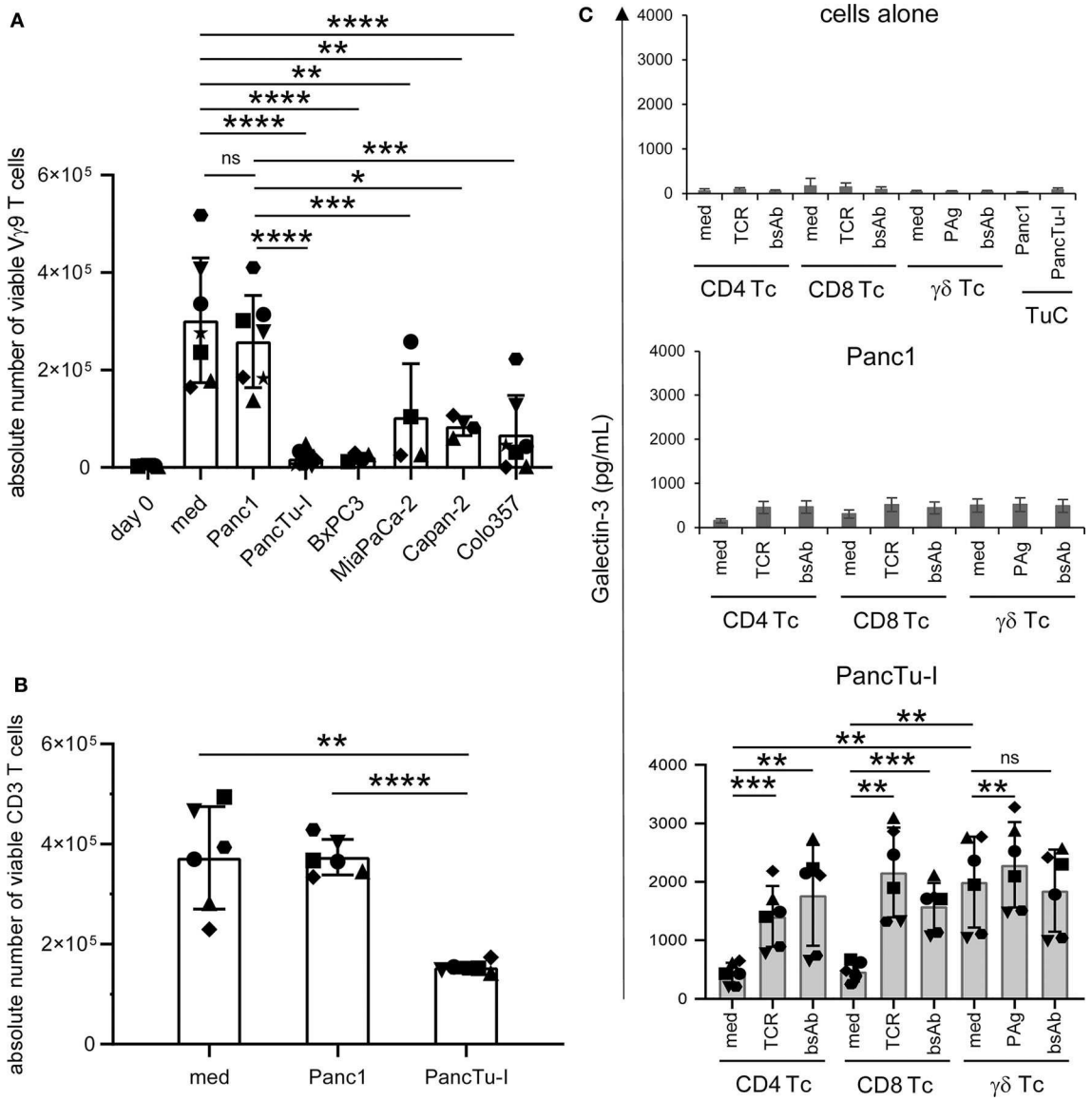

FIGURE 2 | Coculture of PDAC cells with PBMC induces galectin-3 release and inhibition of γδ T cell proliferation. **(A–C)** In total, 5×10^3 of the indicated PDAC cells were plated in complete medium. After 24 h **(A,B)** 2.5×10^5 PBMC ($n = 4$–7) or **(C)** 2×10^5 freshly isolated CD4 or CD8 αβ T cells or γδ T cells (Tc) ($n = 6$) were added or cultured alone (medium). Cells were stimulated **(A)** with 2.5 μM zoledronic acid in the presence of 50 IU/mL rIL-2, **(B)** with Activation/Expander Beads or **(C)** with Activation/Expander Beads (TCR), 300 nM BrHPP (PAg) plus rIL-2 or 1 μg/mL bsAb [HER2xCD3] for αβ T cells and [$(HER2)_2$xVγ9] plus rIL-2 for γδ T cells. **(A,B)** Vγ9 γδ T cell proliferation was determined after 6–7 days and αβ T cell proliferation after 3–4 days by SCDA. The means ± SD of duplicates are shown. **(C)** Cell culture supernatants were collected after 72 h and released gal-3 was determined by ELISA. The bars represent the mean ± SD ($n = 6$), determined in duplicates. Statistical comparison of **(A)** non-matched samples was carried out parametrically by using one-way ANOVA followed by Tukey's multiple comparison test, and of **(B,C)** matched samples also parametrically by using paired, two-tailed *t*-test. *P*-value; $^*P < 0.05$, $^{**}P < 0.01$, $^{***}P < 0.001$, $^{****}P < 0.0001$, and ns, non-significant.

or AF488$^-$ PI$^+$ APC$^+$). Based on the known number of standard cells, the absolute number of viable CD3 T cells or Vγ9 γδ T cells in a given microculture well could be determined as follows: T cell subset ratio = relative proportion of FITC$^+$ or AF488$^+$ PI$^-$ APC$^-$ stained T cells/relative proportion of FITC$^-$ or AF488$^-$ PI$^+$ APC$^+$ standard cells. The absolute number of FITC$^+$ or AF488$^+$-stained T cells can be determined by multiplying the T cell subset ratio with the number of standard cells per sample (10^4 per 100 μL), since there is a linear correlation between the T cell subset ratio and the absolute number of FITC$^+$ or AF488$^+$-stained T cells as previously described (33). All samples were analyzed on a FACS Calibur (BD Biosciences) using CellQuestPro (including Batch-Setup function). Data were transferred to MS-Excel for further analysis.

Enzyme-Linked Immunosorbent Assay

To quantify gal-3 released by PDAC cells (established cell lines or *ex vivo* isolated tumor cells) or T cells alone or after

coculture of the different cell subsets, supernatants were collected after different incubation times (24–96 h) and stored at −20°C until use. Additionally, gal-3 was determined within serum samples of PDAC patients. Gal-3 was measured by sandwich DuoSet ELISA kit (# DY1154 from R&D System, Wiesbaden, Germany) in duplicates following the procedures outlined by the manufacturer.

^{51}Cr-Release Assay

Control or gal-3 siRNA transfected PDAC cells were labeled with 50 μCi sodium ^{51}Cr and 5 × 10^3 cells were used as targets in a standard 4 h ^{51}Cr release assay with titrated numbers of short-term activated γδ T cells as effectors at an E/T ratio of 50:1, 25:1, 12.5:1, and 6.25:1. Cells were (co)cultured in medium or stimulated with the bsAb [$(HER2)_2$xVγ9] for 4 h. Supernatants were measured in a MicroBeta Trilux β-counter (PerkinElmer, Hamburg, Germany). Specific lysis was calculated as [(cpm test–cpm spontaneous)/(cpm max–cpm spontaneous)] × 100, where spontaneous release was determined in medium only and maximal release was determined in Triton-X-100 lysed target cells. Spontaneous release did not exceed 15% of the maximal release.

Imaging Flow Cytometry

The localization of proteins and their colocalization with other proteins was quantified by an ImageStream®X Mark II (Merck Millipore, Burlington, MA, USA). This device combines flow cytometry with microscopy by using a camera (with 405, 488, 562, 658, and 732 nm lasers) which takes high-resolution images of each cell in up to six fluorescence channels and analyzes up to 5,000 cells/s. To investigate the localization of gal-3 in PDAC cells, 10^6 PDAC cells were stained with 10 μg/mL anti-gal-3 mAb clone Gal397 (BioLegend) followed by 10 μg/mL AF488-conjugated goat anti-mouse secondary Ab (Thermo Fisher Scientific) according to the protocol for intracellular staining (see section flow cytometry). These images were then analyzed using the IDEAS® image analysis software.

Analysis of Synapse Formation Between Tumor Cells and T Cells

To investigate the effect of synapse formation on the localization of gal-3, PancTu-I cells were pelleted in 15 mL Eppendorf tubes and an equal number of short-term activated Vγ9Vδ2 γδ T cells as effector cells were added. After 1, 3, 5, 10, 20, or 45 min, the cell conjugates were pelleted, fixed and permeabilized with Cytofix/Cytoperm kit (BD Biosciences), and transferred to 96-well plates for staining. Thereafter, cell conjugates were stained with 10 μg/mL anti-gal-3 Ab clone M3/38 (BioLegend) followed by staining with 10 μg/mL AF555-conjugated goat anti-rat secondary Ab according to the protocol for intracellular staining. After a further washing step, cell conjugates were stained with an Ab mixture of 0.6 μg/mL APC-conjugated anti-EpCAM mAb clone REA-125 (Miltenyi) for tumor cells, 5 μg/mL BV421-conjugated anti-CD3 mAb clone UCHT-1 (BD Biosciences) for T cells, and CruzFluor-488-conjugated phalloidin (1:5000, Santa Cruz, Heidelberg) for actin-filament staining which is condensed at the immunological synapse after tumor-T cell interaction.

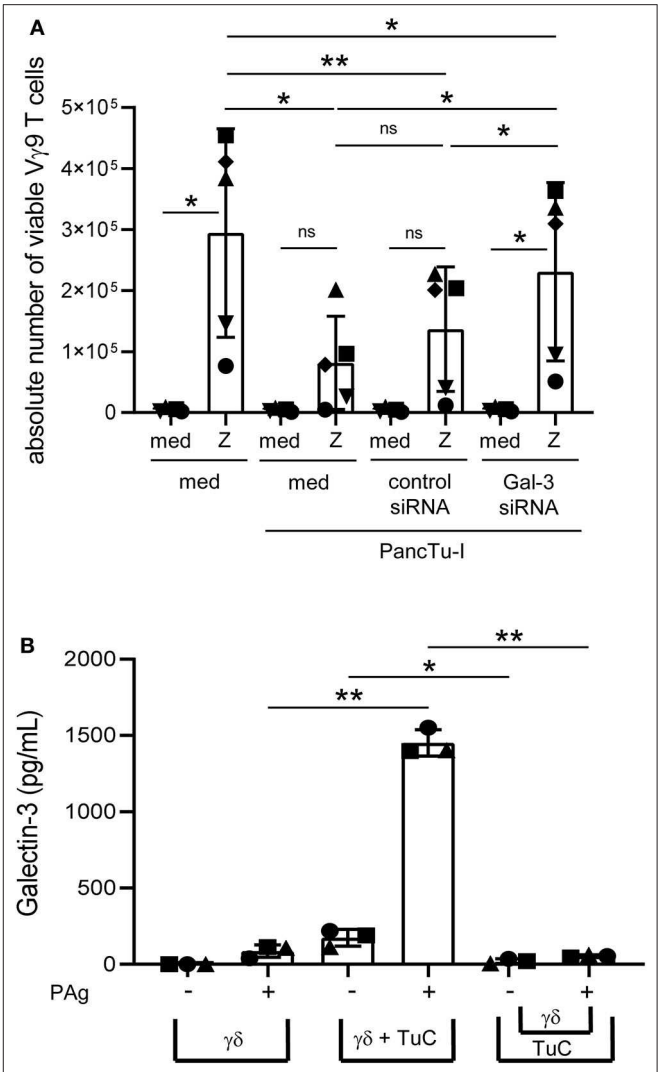

FIGURE 3 | Galectin-3 knockdown in PancTu-I cells partially restores γδ T cell proliferation within PBMC, and gal-3 release in coculture is cell contact-dependent. **(A)** In total, 5 × 10^3 PancTu-I cells left non-transfected or were transfected with either control siRNA or gal-3 siRNA and cultured in complete medium 72 h after transfection. After 24 h culture of PDAC cells, 2.5 × 10^5 PBMC were added (E/T 50:1) or cultured alone. After addition of 50 IU/mL rIL-2, cells were left unstimulated (med) or stimulated with 2.5 μM zoledronic acid (Z). After 6 days, the absolute cell number of the Vγ9 γδ T cells was determined using SCDA. The mean ± SD of duplicates from 5 donors are shown. **(B)** Short-term activated Vγ9Vδ2 T cells were cultured with 50 IU/mL rIL-2 alone and directly cocultured with 2 x 10^4 PancTu-I cells or indirectly separated by a semipermeable membrane with 0.4 μm pores of a transwell insert in 24-well plates at an E/T ratio of 40:1. Cells were left untreated or stimulated with PAg. After 24 h, gal-3 was measured in the cell culture supernatant using ELISA. The means ± SD of 3 donors are shown. **(A,B)** Statistical comparison of matched samples was carried out parametrically by using paired, two-tailed *t*-test. *P*-value; $^*P < 0.05$, $^{**}P < 0.01$, ns, not significant.

After washing, the cells were measured on ImageStream®X Mark II (Merck Millipore) and conjugates were analyzed using the IDEAS® image analysis software. Firstly, tumor-T cell conjugates

were identified *via* EpCAM, CD3, and phalloidin expression. To define the cell periphery, a peripheral mask was then generated based on the EpCAM signal, which marks the surface of the tumor cell. For this purpose, a mask was defined with the *Dilate*-function of the software that is one pixel larger than the mask of the EpCAM signal. In addition, a mask was defined with the Erode-function of the software that is six pixels smaller than the mask of the EpCAM signal. Subtraction of the *Erode*-generated mask from the *Dilate*-generated mask provided a ring-shaped peripheral mask. The peripheral mask protrudes one pixel beyond the cell and six pixels into the cell that allows the determination of the gal-3 signal in the cell periphery.

Statistical Analysis

Shapiro-Wilk normality test was applied to analyze the normal distribution assumption. The statistical analysis was assessed by using Graph Pad Prism (Graph Pad Software, Inc., La Jolla, CA, USA). The assumption of normal distribution was given in all samples [**Figures 1–4**, **7**, **8A,B** (right panel)] with the exception of parts of **Figures 5A**, **7** (γδ T cells), **8B** (left panel) as indicated in the appropriate figure legend. For parametric data of non-matched datasets, a one-way ANOVA followed by Tukey's multiple comparison test was carried out. For parametric data of matched datasets, a paired, two-tailed *t*-test was used. Non-parametric data of matched datasets were analyzed by Wilcoxon matched-pairs signed rank test. All statistical tests were two-sided and the level of significance was set at $\alpha \leq 5\%$. Tests are indicated in the figure legends where appropriate.

RESULTS

Galectin-3 as a Tumor-Suppressive Mediator of (γδ) T Cell Proliferation

Recently, we and others demonstrated that γδ T cells infiltrate the tumoral ducts of PDAC tissue (23, 24, 35). A possible reason for the weak anti-tumor response of tumor-infiltrating γδ T cells may be due to gal-3, which is described to be expressed by PDAC cells and to contribute to tumor-mediated immune suppression (13, 15). Regarding the expression of gal-3 in tumor cells, we examined PDAC cells of different origin and differentiation grade. Gal-3 was expressed very weakly in Panc1 and Panc89 cell lines derived from primary tumors as well as in Colo357 cells derived from a lymph node metastasis. Interestingly, all other primary PDAC cells expressed intracellularly gal-3 to a higher extent than Panc1, Panc89, and Colo357 cells (**Figures 1A,B**). In order to obtain further information on possible functions of gal-3, the localization of gal-3 in these PDAC cells was analyzed in more detail. PancTu-I cells which showed a high expression of gal-3 in comparison to Panc1 cells were labeled intracellularly with anti-gal-3 mAb and analyzed on an ImageStream® X Mark II. A clear cytoplasmic, vesicular localization of gal-3 was observed in all PDAC cells, also in Panc1 cells but to a much lesser extent (**Figure 1C**, data not shown). A partial colocalization of gal-3 with vesicular marker proteins such as the lysosomal membrane-associated proteins CD107a (LAMP-1) and CD63 (LAMP-3) as well as vesicle synaptosome-associated protein receptor Vti1b (expressed on vesicles of the trans-golgi network or late endosomes), respectively, was observed. The expression was found only in a small fraction of analyzed cells. However, no colocalization was found with the recycling endosomes-associated protein Rab11 (**Supplemental Figure 1**). This is in line with the described non-classical secretory pathways for gal-3. Interestingly, CD4 and CD8 TCRαβ T cells and TCRγδ T cells also showed a vesicular expression of gal-3 (data not shown).

To examine whether recombinant gal-3 has an influence on the proliferation of γδ T cells, PBMC of healthy donors and PDAC patients were stimulated with PAg BrHPP and IL-2 in the presence of different concentrations of recombinant gal-3. Whereas, BrHPP and IL-2 induced a selective outgrowth of γδ T cells within PBMC, the addition of increasing concentrations of gal-3 to stimulated γδ T cells significantly reduced their proliferation (**Figure 1D**). While the addition of 0.01 μg/mL gal-3 had no impact on γδ T cell proliferation, 0.1 and 1 μg/mL significantly impaired Vγ9Vδ2 T cell proliferation, respectively. In addition, 10 μg/mL gal-3 reduced the proliferation up to 60% compared to the medium control, suggesting a direct inhibitory effect on the proliferative capacity of γδ T cells. In contrast, the IFN-γ release after BrHPP and IL-2 stimulation was not significantly influenced in the presence of different gal-3 concentrations (**Supplemental Figure 2**).

The stimulation of PBMC with zoledronic acid induced an average 52-fold increase of the absolute cell number of viable γδ T cells within PBMC (medium) compared to day 0 (**Figure 2A**). Interestingly, coculturing these PBMC with weak gal-3 expressing Panc1 cells just leads to a minimal decrease of γδ T cell proliferation. Those primary PDAC cells, which expressed gal-3 to a higher extent, significantly suppressed γδ T cell proliferation during coculture (**Figure 2A**). Comparable results were obtained by stimulating all CD3-expressing T cells *via* their TCR. The TCR-induced CD3 T cell proliferation was not influenced by the coculture with Panc1 cells comparable to the stimulation without PDAC cells (medium), while the coculture with highly gal-3-expressing PancTu-I cells significantly reduced their proliferation (**Figure 2B**). Comparable results were obtained with other PDAC cells such as Capan-2 and BxPC3 both expressing gal-3 to a higher extent compared to Panc1 cells (data not shown). As already described, the suppression of γδ T cell proliferation in the presence of Colo357 cells is most likely due to an enhanced expression of cyclooxygenase-2 in Colo357 cells which induce prostagladin E2-mediated suppression (31, 36).

When PDAC cells or isolated T cells were cultured separately or T cells were stimulated *via* TCR or by bsAb, the release of gal-3 was weak, respectively (**Figure 2C**, upper panel, cells alone). Determination of gal-3 release in supernatants after 24, 48, and 72 h revealed the highest gal-3 release after 72 h (**Figure 2C**). Furthermore, we observed a slight increase of gal-3 secretion after coculturing the T cells with Panc1 cells (**Figure 2C**, middle panel). Interestingly, the gal-3 release significantly increased after coculture of isolated γδ T cells with PancTu-I cells compared to coculture with αβ T cells (**Figure 2C**, lower panel, medium). After polyclonal stimulation of T cells *via* the TCR or by bsAb, an enhanced gal-3 secretion was observed in the presence of PancTu-I cells (**Figure 2C**, lower panel, TCR, bsAb).

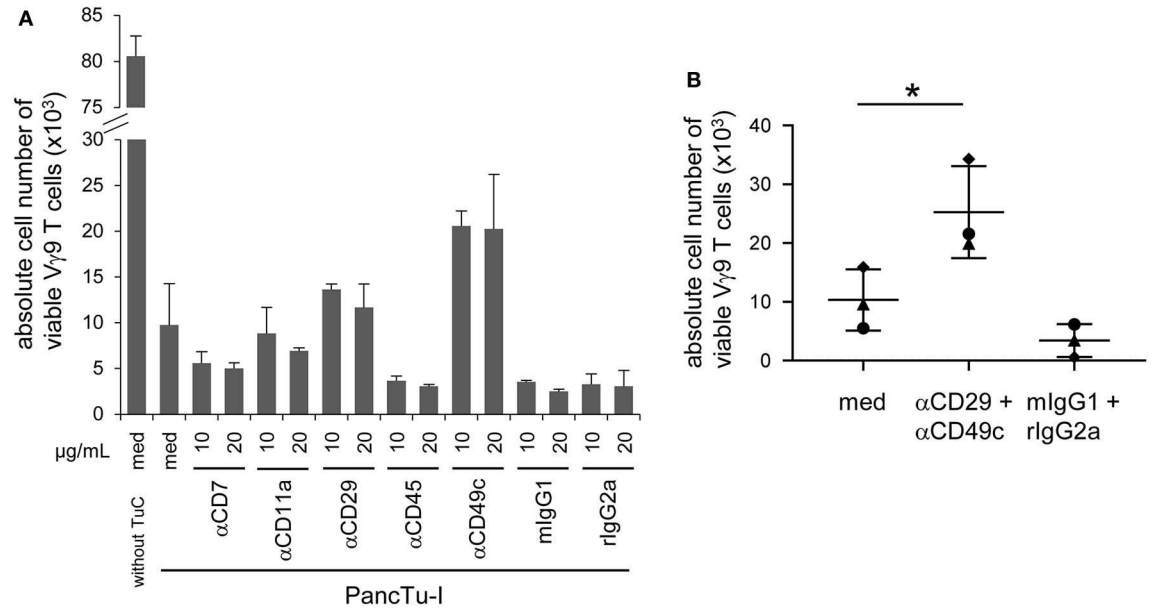

FIGURE 4 | CD49c/CD29 play a role in the galectin-3 mediated inhibition of γδ T cell proliferation within PBMC. **(A,B)** In total, 5×10^3 PancTu-I cells were seeded for 24 h. 2.5×10^5 PBMC/well were pre-incubated with **(A)** the indicated concentrations of the displayed antibodies or appropriate isotype controls or **(B)** with 10 µg/mL anti-CD29 mAb together with 10 µg/mL anti-CD49c mAb or appropriated isotype controls for 2 h. **(A,B)** Thereafter, PancTu-I cells were transferred and stimulated with 2.5 µM zoledronic acid and 50 IU/mL rIL- 2. After 7 days, the absolute cell number of Vγ9 γδ T cells was determined using SCDA. **(A)** The means ± SD of duplicates of 2 donors are shown. **(B)** Each point represents an individual donor. Statistical comparison of matched samples was carried out parametrically by using paired, two-tailed *t*-test. *P*-value; $*P < 0.05$.

Taken together, gal-3 was expressed in PDAC cells and T cells, but was released only in small amounts by either cell population. However, large amounts of gal-3 were released during coculture of T cells together with highly gal-3 expressing PDAC cells such as PancTu-I cells. PDAC cells with a high amount of gal-3 release as well as soluble recombinant gal-3 inhibited the proliferation of T cells.

Galectin-3 Released From Tumor Cells Inhibits γδ T Cell Proliferation

The release of gal-3 is drastically enhanced in the coculture of T cells and PancTu-I cells (**Figure 2C**). To examine whether the released gal-3 is responsible for the inhibition of T cell proliferation, gal-3 was knocked down by siRNA in PancTu-I cells. The functionality of different gal-3 siRNAs in PancTu-I cells was investigated on the basis of different applied concentrations and at the optimal time point using flow cytometry and Western blot analyses (**Supplemental Figure 3**). After 72 h, a knockdown of 85–90% of gal-3 expression could be shown after treatment with a concentration of 10–25 nM gal-3 siRNA in PancTu-I cells compared to control siRNA transfected cells (**Supplemental Figure 3**). Having defined the appropriate conditions, non-transfected and control or gal-3 siRNA transfected PancTu-I cells were cocultured with PBMC. After 6 days of coculture, a vigorous selective outgrowth of Vγ9 γδ T cells after stimulation with zoledronic acid compared to the control was observed by measuring absolute cell number of viable Vγ9 γδ T cells (**Figure 3A**). Because PBMCs from different donors contain varying numbers of Vγ9 Vδ2 γδ T cells, additionally, the x-fold increase of Vγ9 γδ T cells is presented (**Supplemental Figure 4A**). Non-transfected PancTu-I cells significantly inhibited the selective Vγ9 γδ T cell proliferation, while the coculture of gal-3 siRNA transfected PancTu-I cells partially, but significantly, restored the Vγ9 γδ T cell proliferation compared to the coculture with control siRNA transfected PancTu-I cells (**Figure 3A**). Similar results were obtained by applying BrHPP instead of zoledronic acid for stimulation of γδ T cell proliferation (**Supplemental Figure 4B**).

In contrast, Vγ9 γδ T cell proliferation after BrHPP or zoledronic acid stimulation of PBMC cocultured with non-transfected or control siRNA transfected Panc1 cells (with low gal-3 expression) did not differ from coculture with gal-3 siRNA transfected Panc1 cells (data not shown).

In order to induce a release of gal-3 by the PDAC cells during the coculture with T cells, soluble factors of T cells, a cell contact-dependent mechanism or both could play a role. To examine a possible cell-cell contact dependence of gal-3 release, PancTu-I cells were directly cocultured with short-term activated Vγ9Vδ2 γδ T cell lines or indirectly separated by a semipermeable membrane of a transwell insert for 24 h. When short-term activated Vγ9Vδ2 γδ T cell lines were cultured alone, only a small amount of gal-3 was released after stimulation. Release of gal-3 was significantly enhanced when cocultured with PancTu-I cells but not after separating the PDAC cells from the γδ T cell lines suggesting that the release of gal-3 is cell-cell contact-dependent (**Figure 3B**).

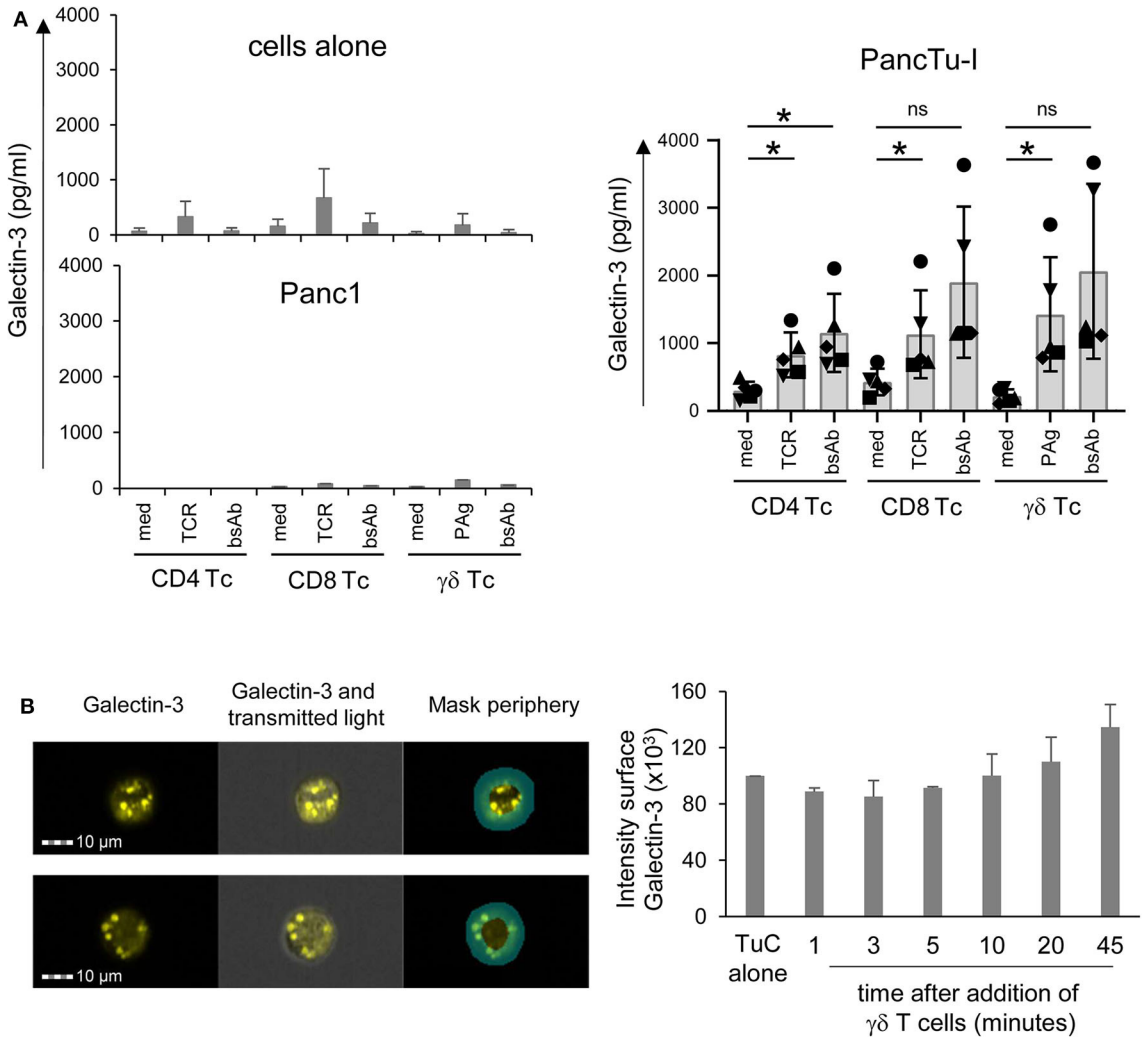

FIGURE 5 | Coculture of PancTu-I cells with activated γδ T cells increases galectin-3 release and its localization in the tumor cell periphery. **(A)** In total, 5×10^3 indicated PDAC cells were plated in complete medium. After 24 h, 2×10^5 short-term activated CD4 or CD8 αβ T cells or γδ T cells (Tc) ($n = 6$) were added or cultured alone (cells alone). Cells were stimulated with Activation/Expander Beads (TCR), 300 nM BrHPP (PAg) plus 12.5 IU/mL rIL-2 or 1 µg/mL bsAb [HER2xCD3] for αβ T cells and $[(HER2)_2xV\gamma9]$ plus 12.5 IU/mL rIL-2 for γδ T cells. Cell culture supernatants were collected after 72 h and gal-3 was determined by ELISA. The means ± SD of duplicates are shown. Statistical comparison was carried out parametrically by using paired, two-tailed *t*-test. *P*-value; $^*P < 0.05$. As samples of CD8 and γδ T cells cultured in medium in comparison to bsAb did not follow a normal distribution, a Wilcoxon non-parametric, matched-pairs signed rank test was applied, which revealed no significance (ns, non-significant). **(B)** PancTu-I cells alone or cocultured with short-term activated Vγ9 γδ T cells for the indicated time. Thereafter, cells were stained with anti-gal-3 mAb (clone Gal397) followed by secondary goat-anti-mouse Ab and anti-EpCAM mAb (clone REA-125) for tumor cells, anti-CD3 (clone UCHT-1) for T cells and phalloidin for actin-filament staining and analyzed on the ImageStream® X Mark II. The fluorescence image of gal-3 plus overlays with transmitted light image and peripheral mask of a representative PancTu-I cell with gal-3 expression predominately in the center or periphery is shown. In addition, the mean ± SD of the intensity of gal-3 expression in the periphery of PancTu-I cells after addition of γδ T cells ($n = 3$) are presented.

Similar effects were observed when using CD8 αβ T cell lines instead of γδ T cell lines or Capan-2 cells instead of PancTu-I cells (**Supplemental Figure 5**).

In sum, coculturing T cells and PDAC cells led to release of large amounts of gal-3. Knockdown of gal-3 in PDAC cells revealed that tumor cells were the source of gal-3 in coculture with T cells. The release of gal-3 by PDAC cells in coculture was dependent on cell contact with T cells, although it cannot be completely ruled out that next to direct cell contacts, soluble factors released by T cells may also be necessary to induce gal-3 release by the tumor cells.

α3β1 Integrin (CD49c/CD29) Is Involved in the Inhibition of T Cell Proliferation

Gal-3 can bind separately to various proteins expressed on T cells such as CD7, CD11a (α-L integrin), CD29 (β1 integrin), CD45 and CD49c (α3 integrin) which could be responsible for the functional interaction of T cells and PDAC cells (1, 15, 17, 37). Therefore, PBMC were pretreated with relevant

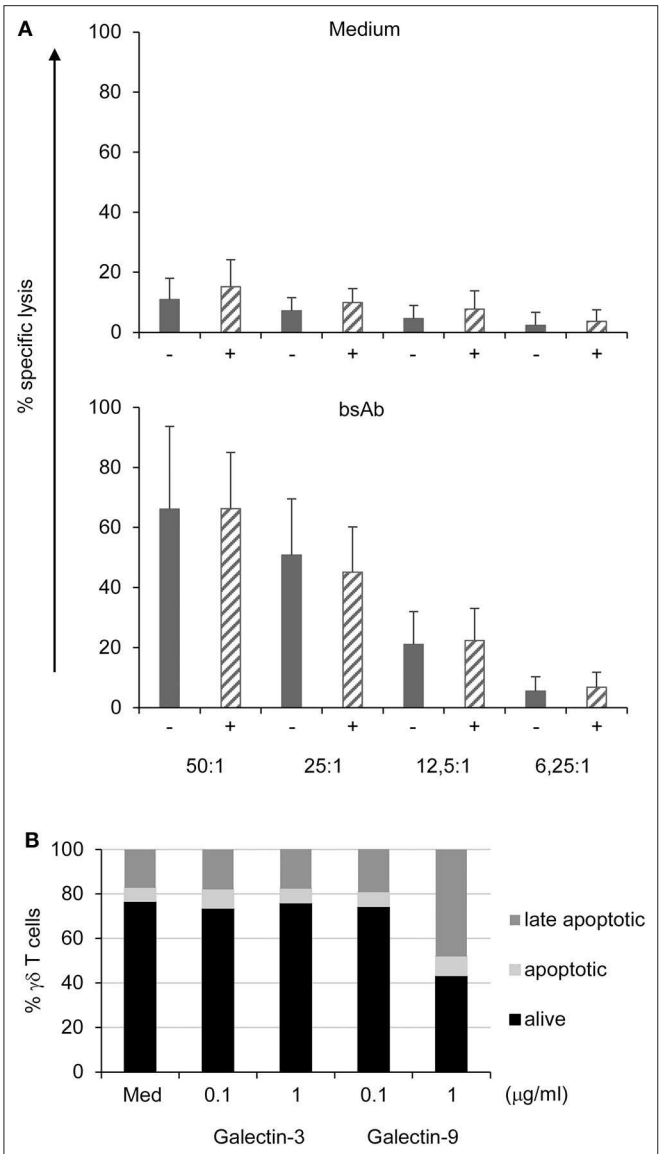

FIGURE 6 | Galectin-3 knockdown does not influence γδ T cell-mediated cytotoxicity against PDAC cells, and does not induce cell death in γδ T cells. **(A)** In total, 5×10^3 control (gray bars) or gal-3 siRNA transfected (striped bars) PancTu-I cells were labeled with ^{51}Cr and used as targets in a standard ^{51}Cr release assay. Short-term activated γδ T effector cells were titrated at the indicated E/T ratio and cultured in medium or stimulated with the bsAb [$(HER2)_2$xVγ9]. Mean values of triplicates (SD < 10%) are calculated. Mean ± SD of 3 independent experiments with 3 different donors are shown. **(B)** 10^5 short-term activated γδ T cells were treated with the indicated concentrations of gal-3 or gal-9 for 24 h. The cells were then labeled with annexin-V and propidium iodide (PI) and analyzed by flow cytometry. The proportion of alive (black bars, annexin-V$^-$ PI$^-$), early apoptotic (light gray bars, annexin-V$^+$ PI$^-$) and late apoptotic/necrotic (dark gray bars, annexin-V$^+$ PI$^+$) cells are shown as the mean value of 3 donors in 3 independent experiments. SD was <10%.

antibodies against CD7, CD11a, CD29, CD45, and CD49c or appropriate isotype controls at the indicated concentrations for 2 h, respectively. Thereafter, PBMC were stimulated with zoledronic acid combined with rIL-2 in the presence or absence of PancTu-I cells. After 6 days of culturing, γδ T cell proliferation was measured. As expected, the presence of PancTu-I cells inhibited the zoledronic acid-induced γδ T cell proliferation, and pretreatment with anti-CD7 and anti-CD45 mAbs further enhanced this inhibition (**Figure 4A**). Interestingly, only pretreatment of PBMC with anti-CD29 or anti-CD49c mAbs partially restored the proliferation of γδ T cells (**Figure 4A**). The partial restoration can be explained by the observation that antibody pretreated PBMC in the absence of cocultured PDAC cells already lead to a slight reduction of γδ T cell proliferation compared to medium only (data not shown). However, pretreatment with anti-CD49c mAb restored the γδ T cell proliferation after coculture with PDAC cells to a higher extent than pretreatment with anti-CD29 mAb suggesting that α3 integrin plays a greater role than β1 integrin (**Figure 4A**).

Interestingly, additional experiments that combined anti-CD29 and anti-CD49c mAbs also revealed only a partial but significant reconstitution of gal-3 mediated inhibition of γδ T cell proliferation (**Figure 4B**).

Taken together, gal-3-mediated Vγ9 γδ T cell inhibition by PDAC cells is partially and significantly restored by a combination of neutralizing anti-CD49c and anti-CD29 mAbs.

Enhanced Galectin-3 Release of Gal-3-Expressing PDAC Cells Cocultured With γδ T Cells

In this study, we demonstrated that gal-3 release by PDAC cells is enhanced after coculture with resting T cells compared to culture of either cell population alone. While T lymphocytes including γδ T cells in tumor patients are often suggested to be in an activated state, we examined whether the release of gal-3 differs in short-term activated T cells (**Figure 5A**) in comparison to resting T cells (**Figure 2C**). Again, when PDAC cells or short-term activated T cells were cultured in medium alone or after T cell stimulation *via* TCR or by bsAb, the release of gal-3 was very low (**Figure 5A**, upper panel, cells alone). While the coculture of short-term activated T cells with Panc1 cells revealed no increase in gal-3 release after 72 h (**Figure 5A**, lower left panel), gal-3 release was enhanced after coculturing short-term activated T cells with PancTu-I cells as well as after their stimulation *via* the TCR- or by bsAb (**Figure 5A**, right panel). In sum, we obtained similar results with short-term activated T cells compared to resting T cells.

Galectin-3 Is Relocalized Into the Cell Periphery of PDAC Cells in Coculture With T Cells

Hence, using ImageStream® X Mark II, we analyzed whether the release of gal-3 by PDAC cells was induced by the formation of an immunological synapse between interacting PDAC cells and T cells. To this end, short-term activated γδ T cells were cocultured with PancTu-I cells for 1–45 min. To distinguish between the two populations, T cells were stained with anti-CD3 mAb and PancTu-I cells with anti-EpCAM mAb. In order to demonstrate the formation of an immunological synapse, phalloidin was used

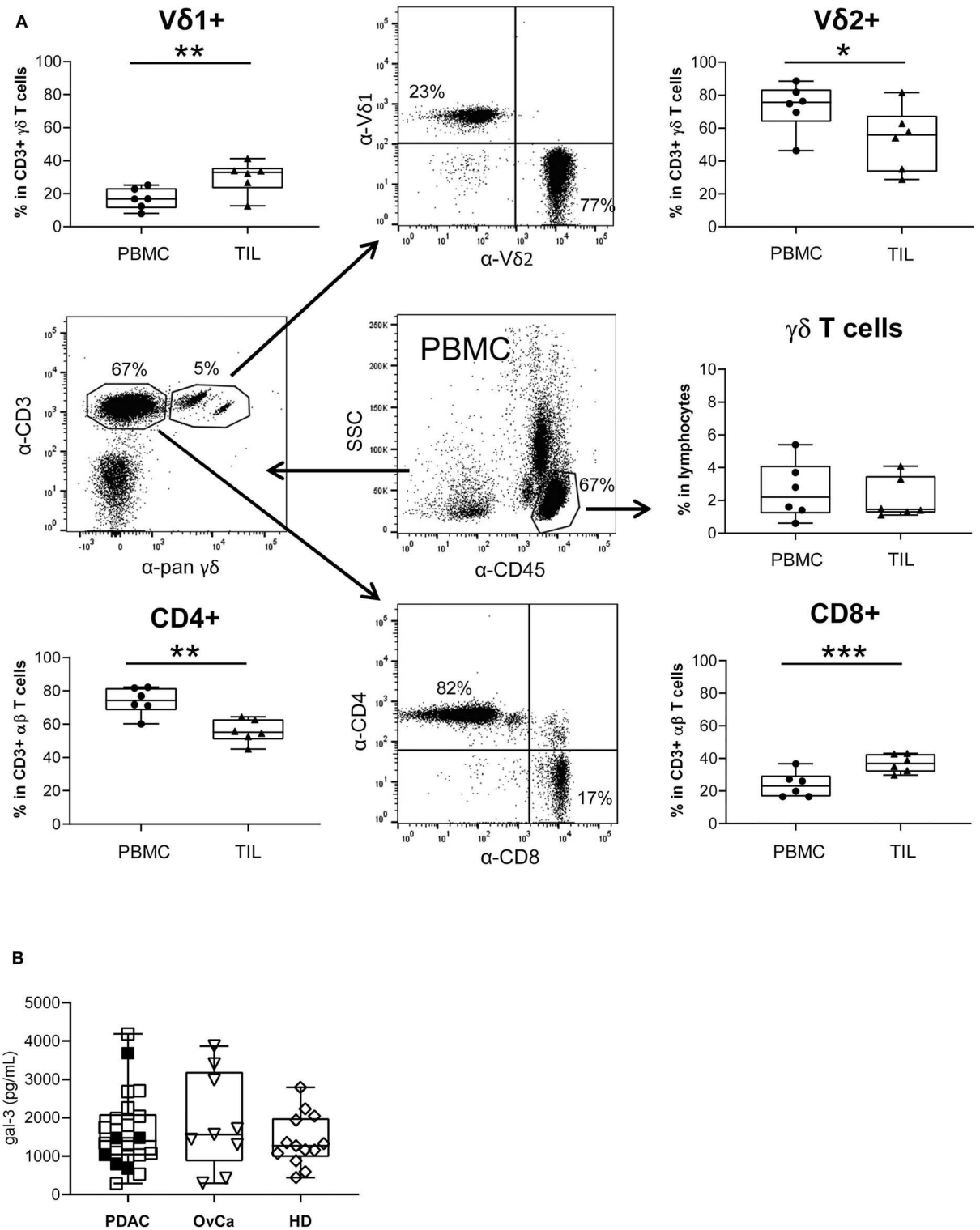

FIGURE 7 | Monitoring of T lymphocyte subsets within blood and PDAC tissue, and galectin-3 serum levels. **(A)** The relative percentage of different T cell subsets within *ex vivo* isolated PBMC and TIL of PDAC patients ($n = 6$) was determined by staining the cells with the indicated mAbs and analyzed by LSR Fortessa. A gate was set on lymphocytes based on the side scatter properties and CD45 leukocytes to analyze γδ T cells within leukocytes. To distinguish between Vδ1 and Vδ2 within the CD3/pan γδ TCR, a gate was set on CD3/pan γδ TCR-expressing T cells. For discrimination between CD4 and CD8 αβ T cells a gate was set on CD3 T cells

(Continued)

FIGURE 7 | excluding CD3/pan γδ TCR$^+$ cells. The gating strategy is shown with PBMC of one patient. Each symbol presents the data of one donor, and the lines in the boxes represent the median of different independent experiments. Statistical comparison of matched samples was carried out parametrically by using paired, two-tailed *t*-test. *P*-value; $^*P < 0.05$, $^{**}P < 0.01$, $^{***}P < 0.001$. As γδ T cell samples did not follow a normal distribution, Wilcoxon non-parametric, matched-pairs signed rank test was applied. *P*-value n.s., non-significant. **(B)** Gal-3 concentrations in serum samples from PDAC patients ($n = 22$), Ovarian cancer patients (OvCa, $n = 9$) and age-matched healthy donors (HD, $n = 13$) measured by ELISA are presented as dot plots. The filled dots are the patients presented also in **(A)**. Samples present no significant differences.

as a marker for filamentous (F)-actin. In addition, gal-3 was stained to analyze whether gal-3 is released by PDAC cells when the immunological synapse is formed (**Figure 5B**). Regardless of the time point of γδ T cell addition, <1% of the PDAC and T cells formed conjugates (data not shown). This could indicate a "kiss and run mechanism" suggesting only a short contact between PDAC and T cells. Interestingly, a different gal-3 localization was observed depending on the coculture duration (**Figure 5B**). As described in the Materials and Methods section, a peripheral ring mask, which distinguishes between cell periphery and cell center, was used to analyze the intensity of gal-3 staining. **Figure 5B** shows two representative PancTu-I cells with considerable gal-3 expression in the cell center (**Figure 5A**, upper panel) as well as in the cell periphery (**Figure 5A**, lower panel). The intensity of gal-3 expression within the peripheral mask of PancTu-I cells (Tumor cells, TuC alone, $n = 1$) and of PancTu-I cells after the indicated times of coculture with Vγ9 γδ T cells (mean of $n = 3$ donors) was calculated (**Figure 5B**). The gal-3 expression decreased slightly in the cell periphery within the first 5 min after the addition of the γδ T cells which indicates a release of gal-3. Ten minutes after γδ T cell addition, a time-dependent increase of gal-3 expression intensity in the cell periphery was detected showing up to 30% enhanced gal-3 expression intensity after 45 min in comparison to PDAC cells culture in the absence of γδ T cells. These data indicate a possible relocalization of gal-3 from cell center toward cell periphery or cell surface.

Overall, these results indicate that PDAC cells transport gal-3 in vesicles to the cell surface after having direct cell contact with γδ T cells. Consequently, gal-3 is released and inhibits γδ T cell proliferation.

Bispecific Antibody Enhanced γδ T Cell Cytotoxicity Against PDAC Cells Independent of Galectin-3 Knockdown

We next analyzed whether the γδ T cell cytotoxicity was influenced by gal-3 released by PDAC cells. Therefore, short-term activated γδ T cells were cocultured with Cr^{51}-labeled control or gal-3 siRNA transfected PDAC cells at different effector/target ratio, and cytotoxicity was analyzed using Cr^{51}-release assay.

PancTu-I and Panc1 cells were almost resistant to γδ T cell-mediated lysis unless bsAb were added to the culture [**Figure 6A** and (38)]. The addition of bsAb significantly increased the γδ T cell cytotoxicity independent of the gal-3 knockdown (striped bars) in PDAC cells (**Figure 6A**) suggesting that gal-3 did not influence γδ T cell cytotoxicity against PDAC cells. In addition, CD107a-degranulation of γδ T cells was not significantly modulated by gal-3 knockdown (**Supplemental Figure 6**).

Moreover, γδ T cell cytotoxicity was not influenced by gal-3 in the presence or absence of bsAb. BsAb enhanced the cytotoxic activity as well as the release of granzyme A and B by γδ T cells (23, 24, 29). Similar to short-term activated γδ T cells, tumor-infiltrating γδ T cells expressed high amounts of granzymes suggesting a pre-activated state of these cells (39). While preactivated γδ T cells are more susceptible to cell death, we examined whether gal-3 induces apoptosis in these cells because extracellular gal-3 has been described to mediate T cell death (16, 40). To investigate apoptosis, short-term activated γδ T cells were treated with the indicated concentration of gal-3 and gal-9 as a control for 24 h. Annexin-V served as a marker for apoptotic cells and annexin-V together with PI as markers for late apoptotic cells (**Figure 6B**). Seventy percentage of the short-term activated γδ T cells were viable (annexin-V$^-$ PI$^-$) after 24 h culture in medium, whereas 6% were apoptotic (annexin-V$^+$ PI$^-$) and 17% late apoptotic or necrotic (annexin-V$^+$ PI$^+$). The addition of gal-3 as well as gal-9 at a low concentration (0.1 μg/mL) for 24 h did not influence the viability of the short-term activated γδ T cells. Interestingly, the addition of 1 μg/mL gal-9 reduced the viability of the short-term activated T cells to 43%. In these cultures, the proportion of apoptotic cells increased to 9% and of late apoptotic cells to 48%. Taken together, in contrast to gal-9, gal-3 did not induce enhanced apoptosis in short-term activated γδ T cells.

Reduced Number of Vδ2 γδ TIL Are Suppressed in Their Proliferation by Galectin-3 Releasing Autologous PDAC Cells

In view of the gal-3 effects during the interaction of PDAC cells and T cells isolated from peripheral blood of healthy donors or PDAC patients, we speculated that the number of TIL could be reduced due to a relevant amount of soluble gal-3 present in PDAC patients.

By comparative immune profiling of TIL and PBMC of the same PDAC patients, we observed a slight decrease of the CD3 γδ T cell percentage within TIL compared to PBMC (**Figure 7A**). Additionally, we demonstrated an inversion of the Vδ1/Vδ2 T cell ratio within CD3 γδ T cells when we compared the percentage of the γδ T cell subsets of PBL and TIL from the same donor. Similar to the inversion of the Vδ1/Vδ2 T cell ratio, there was also an inversion of CD8/CD4 T cells within CD3 αβ T cells. We observed a significant increase of Vδ1 T cells and CD8 αβ T cells within TIL compared to PBMC, whereas Vδ2 TIL and the CD4 αβ TIL significantly decreased in comparison to PBMC from the same donor (**Figure 7A**). The distribution of CD8 and CD4

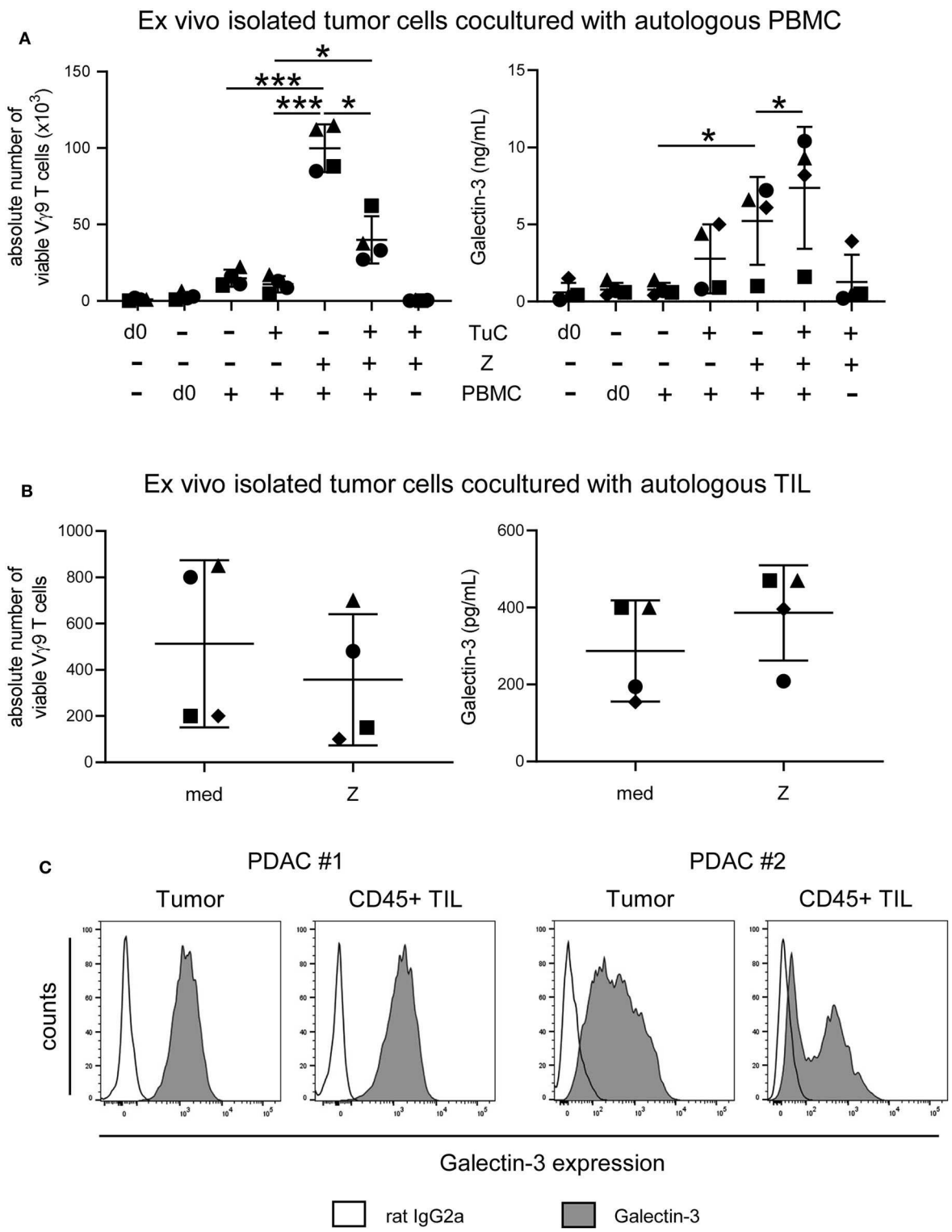

FIGURE 8 | Coculture of *ex vivo* isolated PDAC cells with autologous PBMC or TIL inhibits γδ T cell proliferation and enhances release of galectin-3. **(A)** In total, 5×10^3 or **(B)** 1.5×10^5 *ex vivo* isolated tumor cells (TuC) and **(A)** 2.5×10^5 autologous PBMC or **(B)** 1.5×10^3 autologous TIL were cultured alone or together in complete medium or were stimulated with 2.5 μM zoledronic acid with 50 IU/mL rIL-2 (Z). At day 0 and 11 days after culture, the absolute cell number of the Vγ9 γδ T cells was determined using SCDA. Cell culture supernatants were collected after 96 h and galectin-3 was determined by ELISA. Each symbol presents the data of one

(Continued)

FIGURE 8 | donor, and the lines represent the median of 4 different independent experiments. **(A)** Statistical comparison of matched samples was carried out parametrically by using paired, two-tailed *t*-test. *P*-value; $^{*}P < 0.05$, $^{***}P < 0.001$. **(B)** Wilcoxon non-parametric, matched-pairs signed rank test (left panel) or parametric, matched-pairs, two-tailed *t*-test (right panel) was carried out. Samples present no significant differences. **(C)** Histograms are showing intracellular gal-3 expression stained with anti-gal-3 Ab (gray) compared to the appropriate isotype-control (unfilled) in pan-Cytokeratin^{+} tumor cells and CD45^{+} leukocytes of 2 representative donors (PDAC #1 and #2) out of 4.

αβ T cells was calculated within the CD3 T cell populations by excluding pan γδ T cells.

Analyzing circulating gal-3 in serum of patients with PDAC or advanced ovarian cancer as well as in serum of age-matched healthy donors revealed that gal-3 concentrations did not differ between these groups (**Figure 7B**).

Since gal-3 serum levels did not differ between PDAC patients and healthy donors, we asked whether *ex vivo* isolated tumor cells release enhanced amounts of gal-3 after interaction with autologous PBMC or TIL of PDAC patients, and thereby inhibit γδ T cell proliferation. The stimulation of PBMC with zoledronic acid and IL-2 in the absence of autologous tumor cells induced a significant and selective outgrowth of Vγ9 T cells and PBMC released very low amounts of gal-3 (**Figure 8A**). By coculturing PBMC with autologous tumors cells without further stimulation, Vγ9 T cells did not proliferate, and gal-3 release was slightly enhanced in comparison to PBMC monoculture in the absence of tumor cells (**Figure 8A**). However, after stimulating the cocultured cells with zoledronic acid, γδ T cell proliferation was significantly inhibited and a significantly enhanced gal-3 release was observed (**Figure 8A**). We next asked if the proliferation of autologous γδ TIL is affected in a similar way as γδ PBMC of the same donor. Therefore, we cultured *ex vivo* isolated tumor cells with autologous TIL, which comprises tumor-associated cells, in IL-2 medium, and stimulated the culture with zoledronic acid or medium (**Figure 8B**). Interestingly, the absolute cell number of Vγ9 T cells within the TIL population was reduced after zoledronic acid stimulation and, again, we observed an increase in gal-3 release after addition of zoledronic acid to cocultured cells as well as a strong intracellular gal-3 expression in tumor cells and TIL in this autologous system (**Figures 8B,C**). Taken together, the absolute number of viable Vγ9 T cells within the TIL population was reduced comparable to the inhibition of Vγ9 γδ T cells within PBMC of the same donor after coculture with zoledronic acid-stimulated autologous tumor cells. Interestingly, zoledronic acid-stimulated autologous tumor cells cocultured with TIL released an enhanced amount of gal-3 compared to the medium control.

DISCUSSION

While an overexpression of gal-3 in PDAC tissues and a gal-3-mediated suppression of CD8 TILs have been already described, the gal-3 concentrations in the serum of pancreatic cancer patients is discussed controversially (8, 9, 41, 42). This study demonstrated that gal-3 is not increased in the serum of PDAC patients, but it is highly expressed in *ex vivo* isolated PDAC cells. In addition, gal-3 is not only expressed by PDAC cells but also by T cells within PBMC and TIL. While gal-3 is only released in small amounts by either cell population, the coculture of both populations significantly enhanced the release of gal-3. Interestingly, the stimulation of the cocultured cells further increased gal-3 release which could be of high relevance for clinical studies. Knockdown of gal-3 in PDAC cells demonstrated that PDAC cells are the main source of gal-3. Gal-3 is released by the majority of PDAC cells after interaction with T cells. It effectively inhibited T cell proliferation, but not T cell cytotoxicity regardless of presence of bsAb, which in turn potently enhanced γδ T cell cytotoxicity. We demonstrated that extracellular gal-3, released by PDAC cells after coculture with γδ T cells, binds glycosylated γδ T cell surface receptor α3β1 integrin, and contributes to inhibition of γδ T cell proliferation. This is of great interest for an *in vivo* application of PAg or zoledronic acid where the γδ T cell proliferation might be prevented if gal-3 is present.

Since the therapeutic options of PDAC treatment are very limited, and the efficacy of chemotherapeutic agents (e.g., gemcitabine) is unsatisfactory (10, 11), new therapeutic approaches including application of bsAb or silencing of gal-3 in PDAC cells could be of high clinical relevance (23, 30, 43, 44). BsAb are designed to target T cells to tumor cells, thereby enhancing T cell cytotoxicity against tumor cells. In contrast to PAg, bsAb significantly increased γδ T cell cytotoxicity against PDAC cells by inducing enhanced amounts of granzymes (23, 38). Additionally, we observed that bsAb did not further enhance gal-3 release of PDAC cells cocultured with γδ T cells, in contrast to PAg stimulation. Since the used bsAb are not designed to significantly enhance T cell proliferation, the low number of Vγ9 T cells within the tumors might be a problem. However, our preliminary results suggest that tribody [$(HER2)_2$xVγ9] can potently enhance cytotoxic activity of low numbers of Vγ9 T cells with TILs, which coexpress Vδ2 as well as Vδ1 (unpublished observation). Since Vδ1 T cells are enriched within TIL of PDAC patients, the impact of gal-3 on Vδ1 T cells is of high interest. Unfortunately, the antigens which selectively induce a Vδ1 T cell proliferation are so far unknown. Therefore, Vδ1 T cell expansion within PBMC or TIL cannot be examined.

Regarding gal-3 as a potential novel target for PDAC therapy, a transient siRNA mediated silencing of gal-3 in PDAC cells suppresses their migration and invasion decreasing β-catenin, which represents an important tumor cell invasion signal (45). In addition, silencing of gal-3 in PDAC cells inhibits their proliferation and invasion, and reduced tumor size and volume in an orthotopic PDAC mouse model (13). The reports provide clear evidence for gal-3 being an important player in PDAC progression. In our study, we focused more on the role of gal-3 in the interaction of PDAC cells and T cells with special focus on γδ T cells, which infiltrate PDAC tissues, similarly to CD8 αβ T cells (22–24, 35). All T cell subsets including αβ and γδ T cells were inhibited in their proliferation after coculture with gal-3 secreting PDAC cells, independent of

the T cell activation state. Recently, Kouo and colleagues reported about a gal-3-mediated inhibition in a CD8 T cell-based immunotherapy which aims to enhance the anti-tumor response of cytotoxic CD8 T lymphocytes. PDAC patients who respond to a granulocyte-macrophage colony-stimulating factor (GMC-SF)-secreting allogenic PDAC vaccine developed neutralizing gal-3 Ab after immunization. Gal-3 binds activated-committed CD8 T cells only in the tumor microenvironment and suppresses their anti-tumor response *via* Lymphocyte-activation gene (LAG)-3 and by inhibiting the expansion of plasmacytoid dendritic cells (42). Interestingly, gal-3 is described to contribute to a defect in cytokine-secretion by CD8 TIL which mediates an anergic state of these TIL due to defective actin rearrangement and a disturbed triggering of Lymphocyte function-associated antigen (LFA)-1 (αLβ2 integrin or CD11a/CD18) at the immunological synapse (46). In their previous publications, Demotte et al. observed a loss of colocalization of TCR and CD8 molecules on CD8 T cells that have low ability to bind tetramers and a reduced cytokine release (20, 47, 48). Galectin-glycoprotein lattices inhibited release but not intracellular cytokine expression by affecting actin regulators Coronin 1a and Cdc42 Rho GTPase and LFA-1 at the synapse (46).

Since gal-3 at physiological concentrations did not induce cell death in γδ T cells in our experiments, we hypothesized that, similar to CD8 T cells, gal-3 has an immunosuppressive function by inducing anti-proliferative signaling and consequently γδ T cell anergy. However, treatment with physiological gal-3 concentrations did not significantly modulate IFN-γ release or degranulation of γδ T cells, and the pre-treatment with lactose did not restore the gal-3-mediated inhibition of γδ T cell proliferation. Therefore, we suggest a different mechanism of gal-3 on γδ T cell proliferation (within PBMC or TIL). Knockdown of gal-3 in PDAC cells as well as neutralizing anti-CD49c CD29 (α3β1 integrin) mAbs partially restored gal-3-mediated inhibition of γδ T cell proliferation. Integrins such as LFA-1 binding to the intercellular adhesion molecule (ICAM, CD54) play an important role in the γδ T cell cytotoxicity toward PDAC cells (49). However, the role of CD49c/CD29 in the effector function of γδ T cells is less clear (50). CD49c/CD29 was expressed on the cell surface of resting γδ T cells, and was downregulated after activation (51). LFA-1, CD49a/CD29 (α1β1 integrin) and CD49c/CD29 are described to bind gal-3 (37, 52). The binding of gal-3 to CD49c/CD29 seems to be dependent on the glycosylation of the glycosyltransferase by β1,6-N-Acetylglucosaminyltransferase V (Mgat5) (53). Mgat5 is responsible for generating branched N-glycans that can be elongated with N-acetyl-D-lactosamine (LacNAc) sequences which bind the TCR. Gal-3 which also binds to LacNAc can compete with TCR binding thereby inhibiting TCR clustering (15). Knockdown of Mgat5 in mice prevents binding of gal-3 at the TCR, and improved the assembly of CD3 and TCR, and thereby T cell proliferation (54). Additionally, the interaction between poly LacNAc and gal-3 reduced the affinity of MHC class-I related chain (MIC) A to NK cell receptor Natural-killer group 2, member D (NKG2D), which impaired NK cell cytotoxicity against tumor cells (21). Beside CD49c/CD29, gal-3 can also bind to the γδ TCR or NKG2D expressed on Vδ2 γδ T cells, and thereby increase the threshold for γδ T cell activation. This results in an inhibition of T cell proliferation.

Chang et al. reported that α3β1 and α6β1 integrins mediate laminin/merosin binding and function as costimulatory molecules for human thymocyte proliferation (55). Our results suggest that the binding of gal-3 to α3β1 integrin prevents the proliferation-promoting effect of CD49c/CD29 on γδ T cells. A blockade of the gal-3 α3β1 integrin interaction mediated by applying a CD49c/CD29 mAb could also have an impact on the proliferation-promoting effect of α3β1 integrin. This fact together with binding of gal-3 to the TCR and/or NKG2D could be an explanation for the incomplete restoration of the γδ T cell proliferation after coculture with gal-3 secreting PancTu-I cells after application of a neutralizing CD49c/CD29 mAb.

For the release of gal-3 by PancTu-I cells a direct cell contact with T cells was necessary, which underscores the high importance to examine the influence of cell-cell interactions. In this study, the gal-3 intensity in the cell periphery of the PancTu-I cells was decreased 1–3 min after interaction with γδ T cells, and then increased again within the next 45 min. These data suggest that stored gal-3 can be released very rapidly by tumor cells after interaction with T cells and, thereafter, relocalization of gal-3 toward the cell periphery is required. Interestingly, very few synapses were formed between PDAC cells and γδ T cells during this process indicating that gal-3 hindered the formation of synapses between PDAC cells and T cells or a "kiss and run mechanism" is involved in which γδ T cells bind briefly to the tumor cell, kill it and move to the next tumor cell.

Since gal-3 has no signal sequence, the release *via* the endoplasmic reticulum/trans-golgi network is very unlikely (56). Furthermore, inhibitors of the classic secretory pathway such as brefeldin A and monensin did also not inhibit the gal-3 release by kidney cells suggesting that other mechanisms are involved (57). In this context, the release by proteolysis or by exosomes could be possible mechanisms. Gal-3 was already identified in exosomes of tumor cells (58). Matrix metalloproteinases-2 and−9, which both cleave gal-3, could release gal-3 bound to receptors or extracellular matrix (59, 60). Exosomes are an important component in immunological synapses between T cells and antigen-presenting cells (61). An association of gal-3 with ALIX at the immunological synapse was shown in Jurkat T cells. ALIX is a protein that is involved in the formation of exosomes (62, 63). Therefore, we analyzed the localization of gal-3 which was observed in vesicles of PDAC cells. To characterize these vesicles in more detail, the colocalization of gal-3 with the vesicular marker proteins CD107a (LAMP-1), CD63 (LAMP-3), Rab11 and Vti1b was examined. Gal-3 has been described in macrophages as a binding partner of the lysosomal membrane-associated protein CD107a (64). However, our results indicate that gal-3 did only slightly colocalize with CD107a in PDAC cells. Differences in the colocalization of gal-3 and CD107a in PDAC cells compared to macrophages may be due to different glycosylation patterns of CD107a in both cell populations. Different glycosylation patterns of CD107a associated with a change in gal-3 colocalization has been shown during the maturation of immature to mature dendritic cells (DC) (65). In addition, gal-3 slightly colocalizes with

other vesicular marker proteins such as lysosomal membrane-associated protein CD63 and vesicle synaptosome-associated protein receptor Vti1b expressed on vesicles of the trans-golgi network or late endosomes was observed in only a fraction of cells, but not with Rab11 expressed on recycling endosomes. In other studies, gal-3 was detected in exosomes from DCs as well as from bladder carcinoma cells, which suggests that the gal-3 containing vesicles in PDAC cells may contain or resemble exosomes (58, 66).

For PDAC, survival rates have not changed significantly in the recent years and also treatment with immune checkpoint inhibitors did not achieve improvements as observed in other tumor entities (67). To enhance overall responsiveness of immunotherapy, several clinical trials have started to combine treatment with immune checkpoint inhibitors together with galectin-3 inhibitor DG-MD-02 or GR-MD02 to enhance therapeutic effects in other tumor entities (42). Thus, another promising approach is the usage of bsAb which are able to restore T cell cytotoxicity against PDAC cells of previously non-reactive T cells. Our results indicate that gal-3 has an immunosuppressive function on the proliferation of circulating as well as tumor-infiltrating T cells and that T cell cytotoxicity against PDAC cells can be significantly enhanced by bsAb.

BsAb targeting γδ T cells provide a tool to enhance cytotoxic capacity of γδ T cells, and gal-3 inhibitors to overcome suppression of proliferation. Clinical studies are certainly required to further investigate the therapeutic potential of combing bsAb and galectin inhibitors.

DATA AVAILABILITY STATEMENT

The raw data supporting the conclusions of this article will be made available by the authors, without undue reservation.

ETHICS STATEMENT

In accordance with the Declaration of Helsinki, written informed consent was obtained from all donors, and the research was approved by the relevant institutional review boards (Ethic Committee of the Medical Faculty of the CAU Kiel, code number: D405/10, D445/18, and A110/99).

AUTHOR CONTRIBUTIONS

DG, H-HO, ML, and DW performed experiments. DG, H-HO, and DW designed the study with the help of DK. SS provided blood, serum, and tissue from PDAC patients. DB provided serum from advanced ovarian cancer patients. MP designed and provided the bispecific antibodies. DG and H-HO analyzed the data and designed the figures. DK, SS, DB, and MP contributed to the discussion. DW designed the project and wrote and finalized the manuscript. All authors critically reviewed the manuscript.

FUNDING

This work was supported by the Deutsche Forschungsgemeinschaft (DFG, Ka 502/16-1), DFG FOR2799 (WE 3559/6-1), and the Medical Faculty of the UKSH, Kiel.

ACKNOWLEDGMENTS

We gratefully acknowledge the biobank BMB-CCC (Dr. Christian Röder, Liane Carstensen, and Bianca Zinke, Institute for Experimental Cancer Research, Kiel, Germany) for organizing and providing blood and serum samples as well as tumor tissues from PDAC patients. The BMB-CCC is a member of the PopGen 2.0 Biobanking Network (P2N) and was funded by the German Federal Ministry of Education and Research (BMBF grant 01EY1103). Special thanks to the technical assistance of Sandra Ussat. This work forms part of DG's Ph.D. thesis.

SUPPLEMENTARY MATERIAL

The Supplementary Material for this article can be found online at: https://www.frontiersin.org/articles/10.3389/fimmu.2020.01328/full#supplementary-material

REFERENCES

1. Dumic J, Dabelic S, Flogel M. Galectin-3: an open-ended story. *Biochim Biophys Acta*. (2006) 1760:616–35. doi: 10.1016/j.bbagen.2005.12.020
2. Radosavljevic G, Volarevic V, Jovanovic I, Milovanovic M, Pejnovic N, Arsenijevic N, et al. The roles of Galectin-3 in autoimmunity and tumor progression. *Immunol Res*. (2012) 52:100–10. doi: 10.1007/s12026-012-8286-6
3. Newlaczyl AU, Yu LG. Galectin-3–a jack-of-all-trades in cancer. *Cancer Lett*. (2011) 313:123–8. doi: 10.1016/j.canlet.2011.09.003
4. Song L, Tang JW, Owusu L, Sun MZ, Wu J, Zhang J. Galectin-3 in cancer. *Clin Chim Acta*. (2014) 431:185–91. doi: 10.1016/j.cca.2014.01.019
5. Rabinovich GA, Baum LG, Tinari N, Paganelli R, Natoli C, Liu FT, et al. Galectins and their ligands: amplifiers, silencers or tuners of the inflammatory response? *Trends Immunol*. (2002) 23:313–20. doi: 10.1016/S1471-4906(02)02232-9
6. Hann A, Gruner A, Chen Y, Gress TM, Buchholz M. Comprehensive analysis of cellular galectin-3 reveals no consistent oncogenic function in pancreatic cancer cells. *PLoS ONE*. (2011) 6:e20859. doi: 10.1371/journal.pone.0020859
7. Luo Z, Wang Q, Lau WB, Lau B, Xu L, Zhao L, et al. Tumor microenvironment: the culprit for ovarian cancer metastasis? *Cancer Lett*. (2016) 377:174–82. doi: 10.1016/j.canlet.2016.04.038
8. Schaffert C, Pour PM, Chaney WG. Localization of galectin-3 in normal and diseased pancreatic tissue. *Int J Pancreatol*. (1998) 23:1–9.
9. Xie L, Ni WK, Chen XD, Xiao MB, Chen BY, He S, et al. The expressions and clinical significances of tissue and serum galectin-3 in pancreatic carcinoma. *J Cancer Res Clin Oncol*. (2012) 138:1035–43. doi: 10.1007/s00432-012-1178-2
10. Hidalgo M, Cascinu S, Kleeff J, Labianca R, Lohr JM, Neoptolemos J, et al. Addressing the challenges of pancreatic cancer: future directions for improving outcomes. *Pancreatology*. (2015) 15:8–18. doi: 10.1016/j.pan.2014.10.001
11. Siegel RL, Miller KD, Jemal A. Cancer statistics 2019. *CA Cancer J Clin*. (2019) 69:7–34. doi: 10.3322/caac.21551
12. Ji B, Tsou L, Wang H, Gaiser S, Chang DZ, Daniluk J, et al. Ras activity levels control the development of pancreatic diseases. *Gastroenterology*. (2009) 137:1072–82. doi: 10.1053/j.gastro.2009.05.052

13. Song S, Ji B, Ramachandran V, Wang H, Hafley M, Logsdon C, et al. Overexpressed galectin-3 in pancreatic cancer induces cell proliferation and invasion by binding Ras and activating Ras signaling. *PLoS ONE*. (2012) 7:e42699. doi: 10.1371/journal.pone.0042699
14. Elad-Sfadia G, Haklai R, Balan E, Kloog Y. Galectin-3 augments K-Ras activation and triggers a Ras signal that attenuates ERK but not phosphoinositide 3-kinase activity. *J Biol Chem*. (2004) 279:34922–30. doi: 10.1074/jbc.M312697200
15. Cagnoni AJ, Perez Saez JM, Rabinovich GA, Marino KV. Turning-off signaling by siglecs, selectins, and galectins: chemical inhibition of glycan-dependent interactions in Cancer. *Front Oncol*. (2016) 6:e109. doi: 10.3389/fonc.2016.00109
16. Stillman BN, Hsu DK, Pang M, Brewer CF, Johnson P, Liu FT, et al. Galectin-3 and galectin-1 bind distinct cell surface glycoprotein receptors to induce T cell death. *J Immunol*. (2006) 176:778–89. doi: 10.4049/jimmunol.176.2.778
17. Fukumori T, Takenaka Y, Yoshii T, Kim HR, Hogan V, Inohara H, et al. CD29 and CD7 mediate galectin-3-induced type II T-cell apoptosis. *Cancer Res*. (2003) 63:8302–11.
18. Peng W, Wang HY, Miyahara Y, Peng G, Wang RF. Tumor-associated galectin-3 modulates the function of tumor-reactive T cells. *Cancer Res*. (2008) 68:7228–36. doi: 10.1158/0008-5472.CAN-08-1245
19. Xue H, Liu L, Zhao Z, Zhang Z, Guan Y, Cheng H, et al. The N-terminal tail coordinates with carbohydrate recognition domain to mediate galectin-3 induced apoptosis in T cells. *Oncotarget*. (2017) 8:49824–38. doi: 10.18632/oncotarget.17760
20. Demotte N, Stroobant V, Courtoy PJ, Van Der Smissen P, Colau D, Luescher IF, et al. Restoring the association of the T cell receptor with CD8 reverses anergy in human tumor-infiltrating lymphocytes. *Immunity*. (2008) 28:414–24. doi: 10.1016/j.immuni.2008.01.011
21. Tsuboi S, Sutoh M, Hatakeyama S, Hiraoka N, Habuchi T, Horikawa Y, et al. A novel strategy for evasion of NK cell immunity by tumours expressing core2 O-glycans. *EMBO J*. (2011) 30:3173–85. doi: 10.1038/emboj.2011.215
22. Helm O, Mennrich R, Petrick D, Goebel L, Freitag-Wolf S, Roder C, et al. Comparative characterization of stroma cells and ductal epithelium in chronic pancreatitis and pancreatic ductal adenocarcinoma. *PLoS ONE*. (2014) 9:e94357. doi: 10.1371/journal.pone.0094357
23. Oberg HH, Peipp M, Kellner C, Sebens S, Krause S, Petrick D, et al. Novel bispecific antibodies increase gammadelta T-cell cytotoxicity against pancreatic cancer cells. *Cancer Res*. (2014) 74:1349–60. doi: 10.1158/0008-5472.CAN-13-0675
24. Oberg HH, Grage-Griebenow E, Adam-Klages S, Jerg E, Peipp M, Kellner C, et al. Monitoring and functional characterization of the lymphocytic compartment in pancreatic ductal adenocarcinoma patients. *Pancreatology*. (2016) 16:1069–79. doi: 10.1016/j.pan.2016.07.008
25. Wrobel P, Shojaei H, Schittek B, Gieseler F, Wollenberg B, Kalthoff H, et al. Lysis of a broad range of epithelial tumour cells by human gamma delta T cells: involvement of NKG2D ligands and T-cell receptor-versus NKG2D-dependent recognition. *Scand J Immunol*. (2007) 66:320–8. doi: 10.1111/j.1365-3083.2007.01963.x
26. Espinosa E, Belmant C, Pont F, Luciani B, Poupot R, Romagne F, et al. Chemical synthesis and biological activity of bromohydrin pyrophosphate, a potent stimulator of human gamma delta T cells. *J Biol Chem*. (2001) 276:18337–44. doi: 10.1074/jbc.M100495200
27. Gober HJ, Kistowska M, Angman L, Jeno P, Mori L, De LG. Human T cell receptor gammadelta cells recognize endogenous mevalonate metabolites in tumor cells. *J Exp Med*. (2003) 197:163–8. doi: 10.1084/jem.20021500
28. Oberg HH, Kellner C, Peipp M, Sebens S, Adam-Klages S, Gramatzki M, et al. Monitoring circulating gammadelta T cells in cancer patients to optimize gammadelta T cell-based immunotherapy. *Front Immunol*. (2014) 5:e643. doi: 10.3389/fimmu.2014.00643
29. Oberg HH, Kellner C, Gonnermann D, Peipp M, Peters C, Sebens S, et al. gammadelta T cell activation by bispecific antibodies. *Cell Immunol*. (2015) 296:41–9. doi: 10.1016/j.cellimm.2015.04.009
30. Oberg HH, Kellner C, Gonnermann D, Sebens S, Bauerschlag D, Gramatzki M, et al. Tribody [(HER2)2xCD16] is more effective than trastuzumab in enhancing γδ T cell and natural killer cell cytotoxicity against HER2-expressing Cancer Cells. *Front Immunol*. (2018) 9:e814. doi: 10.3389/fimmu.2018.00814
31. Gonnermann D, Oberg HH, Kellner C, Peipp M, Sebens S, Kabelitz D, et al. Resistance of cyclooxygenase-2 expressing pancreatic ductal adenocarcinoma cells against γδ T cell cytotoxicity. *Oncoim*. (2014) 4:e988640. doi: 10.4161/2162402X.2014.988460
32. Sipos B, Moser S, Kalthoff H, Torok V, Lohr M, Kloppel G. A comprehensive characterization of pancreatic ductal carcinoma cell lines: towards the establishment of an *in vitro* research platform. *Virchows Arch*. (2003) 442:444–52. doi: 10.1007/s00428-003-0784-4
33. Pechhold K, Pohl T, Kabelitz D. Rapid quantification of lymphocyte subsets in heterogeneous cell populations by flow cytometry. *Cytometry*. (1994) 16:152–9. doi: 10.1002/cyto.990160209
34. Janssen O, Wesselborg S, Heckl-Ostreicher B, Pechhold K, Bender A, Schondelmaier S, et al. T cell receptor/CD3-signaling induces death by apoptosis in human T cell receptor gamma delta+T cells. *J Immunol*. (1991) 146:35–9.
35. Daley D, Zambirinis CP, Seifert L, Akkad N, Mohan N, Werba G, et al. γδ T cells support pancreatic oncogenesis by restraining alphabeta T cell activation. *Cell*. (2016) 166:1485–99. doi: 10.1016/j.cell.2016.07.046
36. Tawfik D, Groth C, Gundlach JP, Peipp M, Kabelitz D, Becker T, et al. TRAIL-Receptor 4 modulates gammadelta T cell-cytotoxicity toward cancer cells. *Front Immunol*. (2019) 10:e2044. doi: 10.3389/fimmu.2019.02044
37. Fukushi J, Makagiansar IT, Stallcup WB. NG2 proteoglycan promotes endothelial cell motility and angiogenesis via engagement of galectin-3 and alpha3beta1 integrin. *Mol Biol Cell*. (2004) 15:3580–90. doi: 10.1091/mbc.e04-03-0236
38. Jonescheit H, Oberg HH, Gonnermann D, Hermes M, Sulaj V, Peters C, et al. Influence of indoleamine-2,3-dioxygenase and its metabolite kynurenine on gammadelta T cell cytotoxicity against ductal pancreatic adenocarcinoma cells. *Cells*. (2020) 9:E1140. doi: 10.3390/cells9051140
39. Oberg HH, Janitschke L, Sulaj V, Weimer J, Gonnermann D, Hedemann N, et al. Bispecific antibodies enhance tumor-infiltrating T cell cytotoxicity against autologous HER-2-expressing high-grade ovarian tumors. *J Leukoc Biol*. (2019) 9:1071–8. doi: 10.1002/JLB.5MA1119-265R
40. Yang RY, Hsu DK, Liu FT. Expression of galectin-3 modulates T-cell growth and apoptosis. *Proc Natl Acad Sci USA*. (1996) 93:6737–42. doi: 10.1073/pnas.93.13.6737
41. Gaida MM, Bach ST, Gunther F, Baseras B, Tschaharganeh DF, Welsch T, et al. Expression of galectin-3 in pancreatic ductal adenocarcinoma. *Pathol Oncol Res*. (2012) 18:299–307. doi: 10.1007/s12253-011-9444-1
42. Kouo T, Huang L, Pucsek AB, Cao M, Solt S, Armstrong T, et al. Galectin-3 shapes antitumor immune responses by suppressing CD8+ T cells via LAG-3 and inhibiting expansion of plasmacytoid dendritic cells. *Cancer Immunol Res*. (2015) 3:412–23. doi: 10.1158/2326-6066.CIR-14-0150
43. Chou FC, Chen HY, Kuo CC, Sytwu HK. Role of galectins in tumors and in clinical immunotherapy. *Int J Mol Sci*. (2018) 19:e430. doi: 10.3390/ijms19020430
44. Sun Q, Zhang Y, Liu M, Ye Z, Yu X, Xu X, et al. Prognostic and diagnostic significance of galectins in pancreatic cancer: a systematic review and meta-analysis. *Cancer Cell Int*. (2019) 19:e309. doi: 10.1186/s12935-019-1025-5
45. Kobayashi T, Shimura T, Yajima T, Kubo N, Araki K, Tsutsumi S, et al. Transient gene silencing of galectin-3 suppresses pancreatic cancer cell migration and invasion through degradation of beta-catenin. *Int J Cancer*. (2011) 129:2775–86. doi: 10.1002/ijc.25946
46. Petit AE, Demotte N, Scheid B, Wildmann C, Bigirimana R, Gordon-Alonso M, et al. A major secretory defect of tumour-infiltrating T lymphocytes due to galectin impairing LFA-1-mediated synapse completion. *Nat Commun*. (2016) 7:e12242. doi: 10.1038/ncomms12242
47. Demotte N, Wieers G, Van Der Smissen P, Moser M, Schmidt C, Thielemans K, et al. A galectin-3 ligand corrects the impaired function of human CD4 and CD8 tumor-infiltrating lymphocytes and favors tumor rejection in mice. *Cancer Res*. (2010) 70:7476–88. doi: 10.1158/0008-5472.CAN-10-0761
48. Demotte N, Bigirimana R, Wieers G, Stroobant V, Squifflet JL, Carrasco J, et al. A short treatment with galactomannan GM-CT-01 corrects the functions of freshly isolated human tumor-infiltrating lymphocytes. *Clin Cancer Res*. (2014) 20:1823–33. doi: 10.1158/1078-0432.CCR-13-2459
49. Liu Z, Guo B, Lopez RD. Expression of intercellular adhesion molecule (ICAM)-1 or ICAM-2 is critical in determining sensitivity

of pancreatic cancer cells to cytolysis by human gammadelta-T cells: implications in the design of gammadelta-T-cell-based immunotherapies for pancreatic cancer. *J Gastroenterol Hepatol*. (2009) 24:900–11. doi: 10.1111/j.1440-1746.2008.05668.x
50. Siegers GM. Integral roles for integrins in gammadelta T cell function. *Front Immunol*. (2018) 9:e521. doi: 10.3389/fimmu.2018.00521
51. Avdalovic M, Fong D, Formby B. Adhesion and costimulation of proliferative responses of human gamma delta T cells by interaction of VLA-4 and VLA-5 with fibronectin. *Immunol Lett*. (1993) 35:101–8. doi: 10.1016/0165-2478(93)90077-F
52. Ochieng J, Leite-Browning ML, Warfield P. Regulation of cellular adhesion to extracellular matrix proteins by galectin-3. *Biochem Biophys Res Commun*. (1998) 246:788–91. doi: 10.1006/bbrc.1998.8708
53. Saravanan C, Liu FT, Gipson IK, Panjwani N. Galectin-3 promotes lamellipodia formation in epithelial cells by interacting with complex N-glycans on alpha3beta1 integrin. *J Cell Sci*. (2009) 122(Pt 20):3684–93. doi: 10.1242/jcs.045674
54. Demetriou M, Granovsky M, Quaggin S, Dennis JW. Negative regulation of T-cell activation and autoimmunity by Mgat5 N-glycosylation. *Nature*. (2001) 409:733–9. doi: 10.1038/35055582
55. Chang AC, Salomon DR, Wadsworth S, Hong MJ, Mojcik CF, Otto S, et al. Alpha 3 beta 1 and alpha 6 beta 1 integrins mediate laminin/merosin binding and function as costimulatory molecules for human thymocyte proliferation. *J Immunol*. (1995) 154:500–10.
56. Sato S, Burdett I, Hughes RC. Secretion of the baby hamster kidney 30-kDa galactose-binding lectin from polarized and nonpolarized cells: a pathway independent of the endoplasmic reticulum-Golgi complex. *Exp Cell Res*. (1993) 207:8–18. doi: 10.1006/excr.1993.1157
57. Lindstedt R, Apodaca G, Barondes SH, Mostov KE, Leffler H. Apical secretion of a cytosolic protein by Madin-Darby canine kidney cells. Evidence for polarized release of an endogenous lectin by a nonclassical secretory pathway. *J Biol Chem*. (1993) 268:11750–7.
58. Welton JL, Khanna S, Giles PJ, Brennan P, Brewis IA, Staffurth J, et al. Proteomics analysis of bladder cancer exosomes. *Mol Cell Proteomics*. (2010) 9:1324–38. doi: 10.1074/mcp.M000063-MCP201
59. Ochieng J, Fridman R, Nangia-Makker P, Kleiner DE, Liotta LA, Stetler-Stevenson WG, et al. Galectin-3 is a novel substrate for human matrix metalloproteinases-2 and−9. *Biochemistry*. (1994) 33:14109–14. doi: 10.1021/bi00251a020
60. Ochieng J, Green B, Evans S, James O, Warfield P. Modulation of the biological functions of galectin-3 by matrix metalloproteinases. *Biochim Biophys Acta*. (1998) 1379:97–106. doi: 10.1016/S0304-4165(97)00086-X
61. Choudhuri K, Llodra J, Roth EW, Tsai J, Gordo S, Wucherpfennig KW, et al. Polarized release of T-cell-receptor-enriched microvesicles at the immunological synapse. *Nature*. (2014) 507:118–23. doi: 10.1038/nature12951
62. Baietti MF, Zhang Z, Mortier E, Melchior A, Degeest G, Geeraerts A, et al. Syndecan-syntenin-ALIX regulates the biogenesis of exosomes. *Nat Cell Biol*. (2012) 14:677–85. doi: 10.1038/ncb2502
63. Chen HY, Fermin A, Vardhana S, Weng IC, Lo KF, Chang EY, et al. Galectin-3 negatively regulates TCR-mediated CD4+ T-cell activation at the immunological synapse. *Proc Natl Acad Sci USA*. (2009) 106:14496–501. doi: 10.1073/pnas.0903497106
64. Dong S, Hughes RC. Macrophage surface glycoproteins binding to galectin-3 (Mac-2-antigen). *Glycoconj J*. (1997) 14:267–74.
65. Bax M, Garcia-Vallejo JJ, Jang-Lee J, North SJ, Gilmartin TJ, Hernandez G, et al. Dendritic cell maturation results in pronounced changes in glycan expression affecting recognition by siglecs and galectins. *J Immunol*. (2007) 179:8216–24. doi: 10.4049/jimmunol.179.12.8216
66. Thery C, Boussac M, Veron P, Ricciardi-Castagnoli P, Raposo G, Garin J, et al. Proteomic analysis of dendritic cell-derived exosomes: a secreted subcellular compartment distinct from apoptotic vesicles. *J Immunol*. (2001) 166:7309–18. doi: 10.4049/jimmunol.166.12.7309
67. Bisht S, Feldmann G. Novel targets in pancreatic cancer therapy - current status and ongoing translational efforts. *Oncol Res Treat*. (2018) 41:596–602. doi: 10.1159/000493437

Conflict of Interest: The authors declare that the research was conducted in the absence of any commercial or financial relationships that could be construed as a potential conflict of interest.

frontiers in Immunology

ORIGINAL RESEARCH
published: 30 June 2020
doi: 10.3389/fimmu.2020.01187

Bibliometrics Analysis of Butyrophilins as Immune Regulators [1992–2019] and Implications for Cancer Prognosis

Yixi Wang[1†], Na Zhao[2†], Xianwen Zhang[3†], Zhenhua Li[4,5,6], Zheng Liang[3], Jinrong Yang[3], Xingyu Liu[7], Yangzhe Wu[4,5,6], Kebing Chen[8], Yunfei Gao[4,5,6], Zhinan Yin[4,5,6], Xuejia Lin[4,5,6], Haibo Zhou[4], Dongbo Tian[4], Yang Cao[1*] and Jianlei Hao[4,5,6*]*

[1] Guangdong Provincial Key Laboratory of Stomatology, Guanghua School of Stomatology, Hospital of Stomatology, Sun Yat-sen University, Guangzhou, China, [2] Department of General Surgery, Tianjin Medical University General Hospital, Tianjin Medical University, Tianjin, China, [3] School of Basic Medical Sciences, Chengdu University of Traditional Chinese Medicine, Chengdu, China, [4] The Sixth Affiliated Hospital of Guangzhou Medical University, Qingyuan People's Hospital, Qingyuan, China, [5] Zhuhai Precision Medical Center, Zhuhai People's Hospital, Zhuhai Hospital Affiliated With Jinan University, Jinan University, Zhuhai, China, [6] Faculty of Medical Science, The Biomedical Translational Research Institute, Jinan University, Guangzhou, China, [7] Department of Orthodontics, Changsha Stomatological Hospital, Changsha, China, [8] Guangdong Provincial Key Laboratory of Bone and Joint Degeneration Disease, The Third Affiliated Hospital of Southern Medical University, Guangzhou, China

The butyrophilins (BTNs) represent a unique family of immunoglobulin. They were considered to be involved in milk lactation after their discovery in 1981. With the development of research, an increasing number of research revealed that BTNs play important roles in immune regulation [1992–2019]. Our research aimed to summarize the BTN research status and their relationship with lung cancers and breast cancers by bibliometrics and bioinformatics methods. Our results indicate that the researches on immune-regulatory functions of BTNs gradually developed from 1992 to 2006, whereas they increased quickly after 2007. There are international cooperations among 56 countries, of which the United States is the most active one with the highest number of studies as well as highest citations. By coauthorship and cocitation analysis, we showed that Adrian Hayday, who is active in γδ T-cell field, was an active author in BTN publications with average year of 2015 and led a subfield. By keywords co-occurrence analysis, we found that γδ T cell, which is an important cancer immune regulator, is one important hotspot. Finally, we found that several BTN members' expression levels were significantly correlated with prognosis of lung cancer and breast cancer patients. Thus, these BTNs might play immune regulatory effects and could serve as potential biomarkers for cancer.

Keywords: butyrophilin, γδ T cells, bibliometrics, VOSviewer, lung cancer, breast cancer

OPEN ACCESS

Edited by:
Jurgen Kuball,
Utrecht University, Netherlands

Reviewed by:
Christelle Harly,
INSERM U1232 Centre de Recherche en Cancérologie et Immunologie Nantes Angers (CRCINA), France
Manolo Sambucci,
Santa Lucia Foundation (IRCCS), Italy

***Correspondence:**
Dongbo Tian
qyryxnk@163.com
Yang Cao
caoyang@mail.sysu.edu.cn
Jianlei Hao
haojianlei@jnu.edu.cn

†These authors have contributed equally to this work

Specialty section:
This article was submitted to T Cell Biology, a section of the journal Frontiers in Immunology

Received: *27 February 2020*
Accepted: *13 May 2020*
Published: *30 June 2020*

Citation:
Wang Y, Zhao N, Zhang X, Li Z, Liang Z, Yang J, Liu X, Wu Y, Chen K, Gao Y, Yin Z, Lin X, Zhou H, Tian D, Cao Y and Hao J (2020) Bibliometrics Analysis of Butyrophilins as Immune Regulators [1992–2019] and Implications for Cancer Prognosis. Front. Immunol. 11:1187. doi: 10.3389/fimmu.2020.01187

INTRODUCTION

The modulatory effects of T-cell activation are significantly mediated by costimulatory molecules expressing on antigen-presenting cells. Recent discoveries show that another superfamily of immunoglobulin, the butyrophilin (BTN) family, which is similar to B7 family, has been involved in immune modulation (1). Initially, the BTN, which was discovered in 1981, was found in

milk-secreting epithelial cells and constituted the milk protein (2, 3). With the identification of additional members of this family, increasing evidence shows that BTNs play roles in immune regulation (4). To date, the human BTN superfamily has been found to include 7 BTN genes (*BTN1A1*, *BTN2A1*, *BTN2A2*, *BTN2A3*, *BTN3A1*, *BTN3A2*, *BTN3A3*), 5 BTN-like genes (*BTNL2*, *BTNL3*, *BTNL8*, *BTNL9*, *BTNL10*), and the SKINT-like factor (*SKINTL*). Twenty-one genes have been found in mice in this superfamily: *Btn1a1*, *Btn2a2*, *Btnl1*, *Btnl2*, *Btnl4*, *Btnl5*, *Btnl6*, *Btnl7*, *Btnl9*, *Btnl10*, and *Skint1*, *Skint2*, *Skint3-11* (1). Growing numbers of researches have shown that BTNs play a role in autoimmune diseases (5), infections (6), metabolic disorders (7), and cancers (8, 9) through immune stimulation and inhibition.

Despite many advances in understanding the role of BTNs, there is still a lack of global and comprehensive report that helps researchers to get a quick overview and find meaningful research directions. Bibliometrics analysis is defined to analyze the open publications in a statistical way that could summarize the current research status (10, 11) and foresee future trends quantitatively and qualitatively (12). In this research, we aimed to analyze the progression of BTN researches with the visualization techniques, VOSviewer, based on bibliometrics method and explore the relationships between BTN family members and cancers.

Members of BTN family serve as important regulators of different T-cell subsets, especially the γδ T cells, in humans and mice (4, 13, 14). Different BTN family members can stimulate corresponding γδ T-cell subsets potentially through interaction with specific T cell receptor (TCR). Previous research revealed that BTN3A1 was required in the activation of human Vγ9Vδ2 T cells (15), and BTNL3 and BTNL8 were found to bind $V\gamma4^+$ TCR (16, 17). In mice, Skint1, the new member of BTN family, was required for positive selection of $V\gamma5^+$ T cells in the embryonic thymus and contributed to normal levels of these dendritic epidermal T cells in skin, which play an important role in wound healing and preventing cancer (18, 19). BTNL1 and BTNL6 jointly regulated intestinal Vγ7 γδ T-cell function in mice, and human gut epithelial cells expressed BTNL3 and BTNL8 and stimulated Vγ4 γδ T cells (17). Moreover, γδ T cells represent a strong protective factor among leukocytes, which correlates with better prognosis of cancer (20). Collectively, these results let us hypothesize that BTNs in tumor microenvironment regulate γδ T-cell functions and serve as biomarkers for cancer prognosis.

Lung cancer is the top one cause of cancer deaths worldwide, leading to 1.6 million deaths every year (21–23). Non-small cell lung cancer (NSCLC) is the most common type of lung cancer. Lung adenocarcinoma (LUAD) and lung squamous cell carcinoma (LUSC) are two major subtypes of NSCLC, which accounts for almost 85% of cases (23). Programmed death protein 1 (PD-1) and programmed death ligand 1 (PD-L1), the two famous members of B7 family, were found to be important immune checkpoints and immunotherapy, which aimed to produce encouraging responses for NSCLC by reversing their expression levels (24–26). However, the usage of PD-1/PD-L1 inhibitors also has limitations and reality that most patients still do not benefit from their use (27). Moreover, a clinical trial showed that PD-L1 expression was not predictive of good outcomes that low expression could also observe benefit from its inhibitor treatment (28). This might be because the interaction between tumor microenvironment and immune system also involves other regulators apart from PD-1/PD-L1 axis. Thus, identification of novel predictive biomarkers and targets for therapy is important. Genome-wide analysis revealed the association between encoding BTNL2, a member of BTN family, and LUAD (29–31). Considering the TCR-specific regulatory effects of BTN family members on γδ T cells, which play critical roles in cancer, our research aimed to evaluate the prognostic values of BTNs in LUAD and LUSC, as well as breast cancer.

In this research, we summarized publications of BTNs and analyzed the publication amount, citation, coauthorship, and trends of research area. Additionally, we analyzed the expression of every BTN member in LUAD, LUSC, and breast cancer. Several BTN members showed significant correlation with overall survival (OS). These results suggested a functional role of BTNs in tumor immunity.

METHODS

Database and Search Design

We utilized Scopus (Elsevier, Amsterdam, The Netherlands), the largest abstract database of keyword searching and citation analysis coverage, as our main database (32–34). The following searching words: TITLE-ABS-KEY ("butyrophilin*") AND PUBYEAR > 1979 AND PUBYEAR < 2020 were used in Scopus. The database search was done on a single day, January 10, 2020, so as to avoid significant fluctuations in citations, as well as numbers of studies. Four hundred thirty-five studies were acquired through this step.

Titles, abstracts, and keywords of these 435 studies were screened and infiltrated manually. Full texts were further checked if necessary. The inclusion criteria were as follows: (1) a clear correlation with BTN, (2) focus on human or mice subjects, (3) not editorial notice, such as erratum, and (4) focus on immune modulation. In total, 260 studies were included after filtration by two authors independently. The publication type, annual publication numbers, and total citations were analyzed. The publication list (of the 260 articles in csv file) was used for bibliometrics analysis, and xls file is shown in the **Supplementary Table 1**.

Analysis With VOSviewer

The csv file containing these 260 studies on immune modulation in human or mouse was imported to VOSviewer to perform coauthorship, co-occurrence, and cocitation analysis.

Country Coauthorship

Country coauthorship was performed by VOSviewer in coauthorship analysis in the unit of countries. Circle labels were used to represent the country elements, which were analyzed. The areas of the circles (not the diameter) were proportional to the numbers of total publication citations of each country. The minimum number of total citations of a country was set to 4 to be shown.

Author Coauthorship

Author coauthorship was performed by VOSviewer in coauthorship analysis in the unit of authors. The circle labels represented different authors, and their area showed the total citations of each author. The minimum number of citations of an author was set to 4 to be shown.

Author Cocitation

Author cocitation was performed by VOSviewer in cocitation analysis in the unit of cited authors. The minimum number of citations of an author was set to 50 to be shown.

Author Keywords Co-occurrence Analysis

We uniformed "γδ T cells, γδT cells, gamma delta T cell, gamma delta T cells, and gamma delta T lymphocyte" to "γδ T cell." In addition, "butyrophilin-like 2" was uniformed to "btnl2" when "btnl2" was not found in the author keywords of the same publication. "Butyrophilins" was uniformed to "butyrophilin." "Butyrophilin 3a1" was uniformed to "btn3a1" when "btn3a1" was not found in the author keywords of the same publication. "T cells" and "T lymphocytes" were uniformed to "T cell." Then the csv file was imported to VOSviewer to perform co-occurrence analysis in the unit of author keywords. The minimum number of occurrences of a keyword was set to 2 to be shown. Total strength of the co-occurrence links with other keywords was calculated.

Estimation of Prognostic Values of BTN Family Members on LUAD and LUSC

The Kaplan–Meier plotter (http://kmplot.com/analysis/) was employed to perform the survival analysis of BTN family members with gene chip data in 719 patients with LUAD, 524 patients with LUSC, and 3,951 patients with breast cancer. The plotter separated patients into high and low expression groups according to the gene transcription level of each specific gene and created Kaplan–Meier plots. In the meantime, the hazard ratio (HR) with the 95% confidence interval and the log-rank *p*-value were calculated and marked on the chart. The numbers at risk of each group at different time points are displayed under the curves. When *p*-values were below 0.05, they were considered statistically significant.

RESULTS

The Publication Time and Citation of the Studies of BTNs on Immune Modulation

With the interest of human and mouse studies, the composition of the 317 studies is shown in **Figure 1A**. Studies on immune regulation in human or mouse accounted for 81.8% (260 studies). Immune-unrelated studies accounted for 18.0% (57 studies), including milk-related studies, studies on metabolism, circulation, urology, cell biology, and developmental biology. The publications (totally 260 studies, listed in the **Supplementary Table 1**) of BTNs in immune regulation in human or mouse were utilized for the following analysis. For the publication types of the 260 studies, research articles accounted for 74% (192 studies), which were the majority. Reviews accounted for 17% (45 studies), which were the second largest part. The remaining 9% were other types of documents, including book chapter (2%, five studies), notes (2%, six studies), short surveys (2%, five studies), letters (1%, three studies), and conference papers (2%, four studies).

Annual number of studies is shown in **Figure 1B**. Although the time period we searched was from 1980 to 2019, the research of BTNs in immune modulation did not arise until 1992. Generally, the annual publications could be divided into two time stages. The researches on BTNs on immune modulation increased slowly in 1992–2006, whereas they increased quickly after 2007 and reached a peak of publications in 2016.

Total citations of all BTN studies on immune modulation had fluctuations over the years (**Figure 1C**). In the first stage, two obvious peaks in 1997–2002 are shown with two highly cited articles in each year (35, 36). Total citations increased slowly during the second stage when total publications increased quickly, considering the fact that recently published papers need time to accumulate citations.

The average citation of all the studies was 37.77 times through dividing the total citation times (9,820) by 260. **Figure 1D** demonstrates the distributions of the number of citations of different ranges. One hundred sixty-one studies accounting for 61.9% were cited fewer than 20 times, of which 22 studies were not cited by any other studies. Twenty-one studies received more than 100 citations, among which the highest citation was 1,190. Among the top 15 highly cited articles, four studies were about γδ T cells (15, 18, 37, 38), including one paper about epidermal γδ T cells (18). The 15 top-cited articles are shown in **Table 1**.

The Coauthorship Analysis in the Unit of Countries

The 260 articles, studying BTNs in human and mouse, included authors from 56 countries in total. With the minimum number of documents and citations of a country was set to 4; 18 countries of these 56 countries met the thresholds.

The overlay visualization map (**Figure 2**) of country coauthorship analysis showed the coauthorship of the 18 countries, which indicated close cooperation among different countries. The United States has the highest total citations and has cooperation relationships with many countries. The map also reveals that China and South Korea are countries that started working on the immune-related functions of BTNs more recently than other countries.

Coauthorship Analysis and Cocitation Analysis

With the minimum number of documents and citations of an author was set to 4, and 34 authors met the thresholds. Five authors of them had no linkage with others. The remaining 29 authors are shown in the map (**Figure 3A**).

The overlay visualization map (**Figure 3A**) of author coauthorship analysis showed the cooperation among authors, the total citations of each author, and the average year of their publications. It revealed that Adrian Hayday was among the authors who published studies on the average year of 2015, suggesting an active researcher in BTN field.

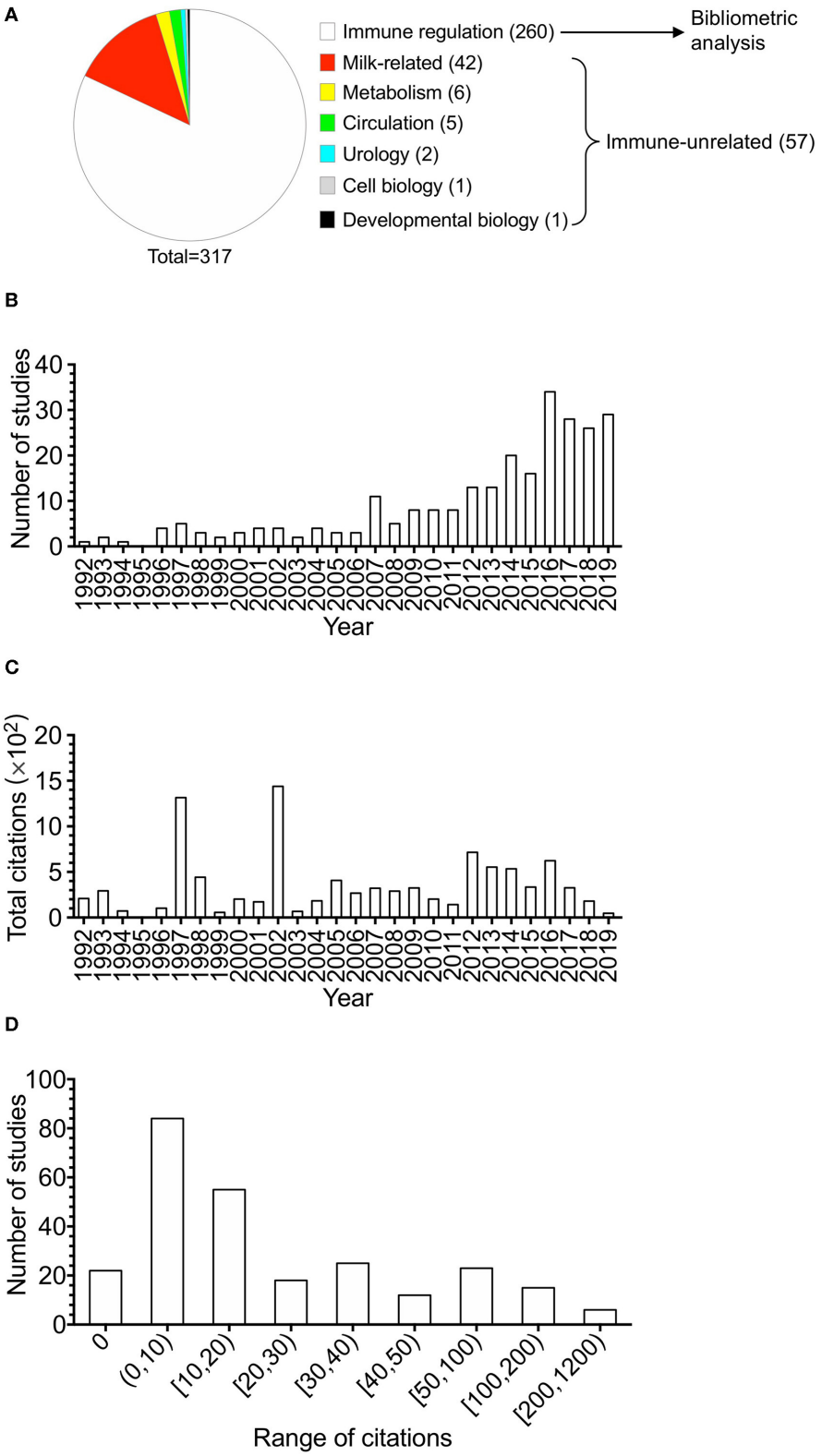

FIGURE 1 | The overview of the studies of butyrophilins on immune modulation. Studies in butyrophilins were acquired from Scopus. **(A)** The composition of the 317 studies acquired from Scopus studying human and mouse butyrophilins is shown. **(B)** The number of studies of immune-related butyrophilins for each year (from 1992 to 2019) was calculated and shown. **(C)** Annual total citations of studies every year was calculated and shown. **(D)** The article citation distributions were calculated and shown. The ranges of citation numbers were divided into 0, 0–10, 10–20, 20–30, 30–40, 40–50, 50–100, 100–200, and 200–1,200.

TABLE 1 | Top-cited articles for butyrophilins as immune regulators.

Rank	Journal	IF	NA	NC	Citations per article	Article title	Year	Authors
1	*Nature Genetics*	25.455	4	1,702	1,069	A candidate gene for familial Mediterranean fever	1997	Bernot A, et al.
					353	Sarcoidosis is associated with a truncating splice site mutation in BTNL2	2005	Valentonyte R, et al.
					166	Skint1, the prototype of a newly identified immunoglobulin superfamily gene cluster, positively selects epidermal γδ T cells	2008	Boyden LM, et al.
					114	A genome-wide association study identifies two new susceptibility loci for lung adenocarcinoma in the Japanese population	2012	Shiraishi K, et al.
2	*Nature Reviews Immunology*	44.019	1	1,190	1,190	The B7-CD28 superfamily	2002	Sharpe AH, et al.
3	*Immunity*	21.522	2	336	170	The intracellular B30.2 domain of butyrophilin 3A1 binds phosphoantigens to mediate activation of human Vγ9Vδ2T Cells	2014	Sandstrom A, et al.
					166	Coinhibitory pathways in the B7-CD28 ligand–receptor family	2016	Schildberg FA, et al.
4	*Lancet*	59.102	1	227	227	Role of human-milk lactadherin in protection against symptomatic rotavirus infection	1998	Newburg DS, et al.
5	*Blood*	16.601	1	217	217	Key implication of CD277/butyrophilin-3 (BTN3A) in cellular stress sensing by a major human γδ T-cell subset	2012	Harly C, et al.
6	*Journal of Neuroscience Research*	4.139	1	209	209	Myelin/oligodendrocyte glycoprotein is a unique member of the immunoglobulin superfamily	1992	Gardinier MV, et al.
7	*Nature Immunology*	23.530	1	198	198	Butyrophilin 3A1 binds phosphorylated antigens and stimulates human γδ T cells	2013	Vavassori S, et al.
8	*Proceedings of the National Academy of Sciences of the United States of America*	9.580	1	180	180	Myelin/oligodendrocyte glycoprotein is a member of a subset of the immunoglobulin superfamily encoded within the major histocompatibility complex	1993	Pham-Dinh D, et al.
9	*Journal of Neuroimmunology*	2.832	1	145	145	Antibodies to neuron-specific antigens in children with autism: possible cross-reaction with encephalitogenic proteins from milk, *Chlamydia pneumoniae* and *Streptococcus* group A	2002	Vojdani A, et al.
10	*Journal of Immunology*	4.718	1	126	126	BTNL2, a butyrophilin-like molecule that functions to inhibit T-cell activation	2006	Nguyen T, et al.
11	*Journal of Molecular Evolution*	1.782	1	113	113	Evolutionary study of multigenic families mapping close to the human major histocompatibility complex class I region	1993	Vernet C, et al.

NA, number of highly cited articles; NC, number of citations; IF, 2018 impact factor; Rank, rank by NC.

As for the cocitation analysis, 87 authors met the threshold with the minimum number of citations of an author set to 50. The network visualization map (**Figure 3B**) of author cocitation analysis through cited authors showed the similarities between different studies and the influence of authors.

Keywords Co-occurrence Analysis

When the minimum number of occurrences of a keyword was set to 2, 90 keywords met the threshold among the 541 keywords in total. Five keywords of them had no linkage with others. The remaining 85 keywords are shown in the map. The overlay visualization map scaled by occurrences (**Figure 4**) showed the hotspots in the field of immune modulations exerted by BTNs. As depicted in the chart, "γδ T cell" ranked one of the top keywords with the second most occurrence with the average publication year of 2017, suggesting a new hotspot in BTN field. Although "Btnl2" has significant occurrence, with average publication year of 2012, it is inclusive in BTN family. Of note, "costimulation" represents an important keyword that appeared with BTNs, with the average publication year of 2008. This is consistent with the important discoveries that emphasized the regulatory function of BTNs for αβ T cells (4, 14).

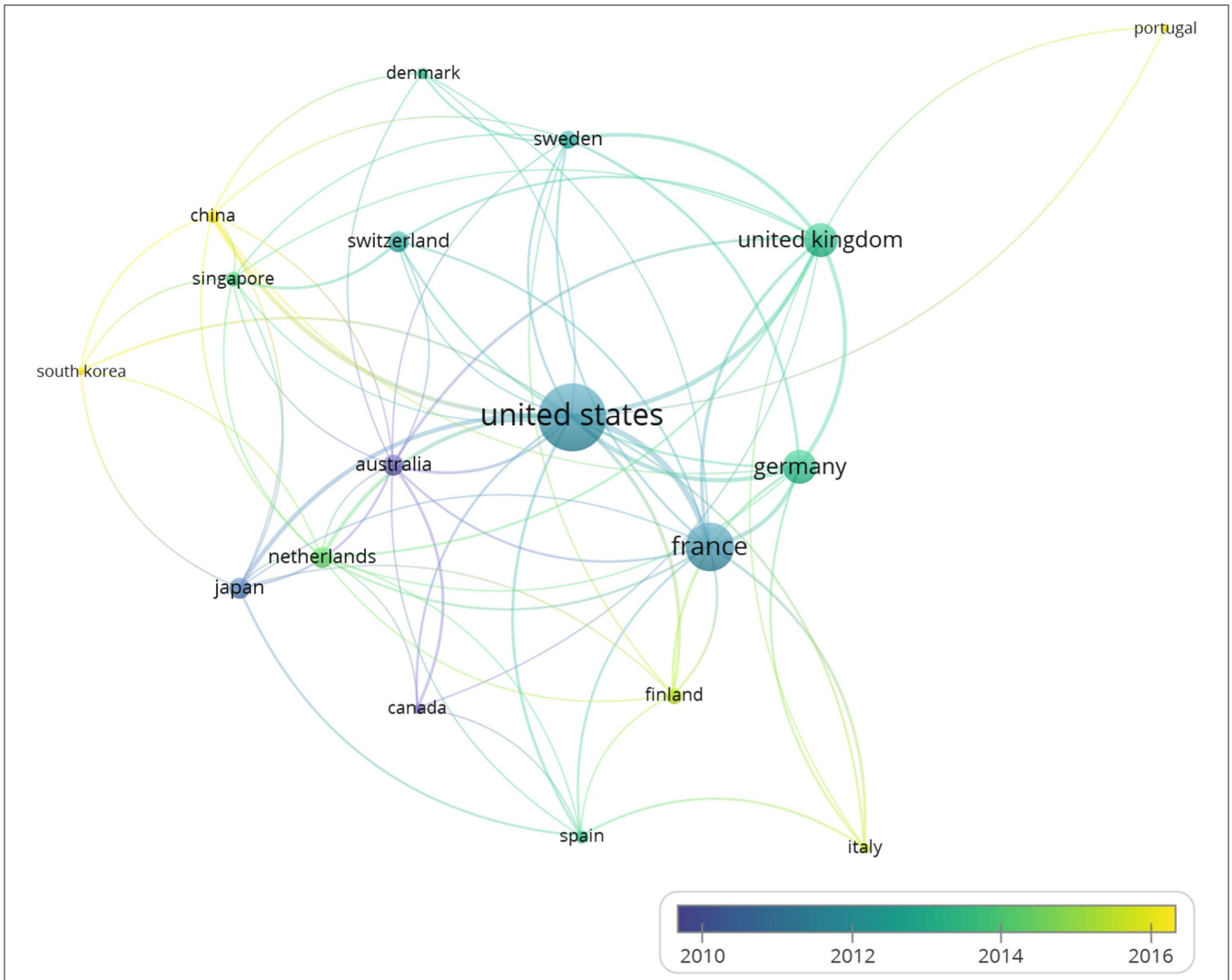

FIGURE 2 | The overlay visualization map of country coauthorship analysis. The 260 studies on immune modulation in human and mouse (listed in the **Supplementary Table 1**) were analyzed by VOSviewer, and overlay visualization map was shown. Countries were represented by circle labels. The distance between two circles indicated the relatedness of their link. The strength of the coauthor link between two countries was represented by the thickness of the connecting curve lines. The area of the circle was determined by the numbers of the total citations contained by each country. Different colors of the circles indicated the average year of the studies according to the bar on the lower right corner. Color range indicated average year of publications in each country.

The Association Between BTN Levels and Prognosis of Lung Cancer and Breast Cancer

Because of the facts that BTNs are reported to activate γδ T cells through specific TCR, and γδ T-cell number represents the best correlate of OS of a broad range of carcinomas, we analyzed correlation between the transcriptomic expression levels of BTN members with the prognosis of lung cancer and breast cancer patients. Kaplan–Meier OS survival curves of LUAD, LUSC, and breast cancer cases according to gene expression levels of BTN family members were plotted. Results showed that high expression of BTN1A1 (HR = 1.65, p = 2.1e-05), BTN2A3 (HR = 1.59, p = 9.8e-05), BTNL2 (HR = 1.33, p = 0.016), BTNL3 (HR = 1.9, p = 7.7e-08), and BTNL8 (HR = 1.32, p = 0.019) were significantly correlated with worse OS of LUAD (**Figure 5A**). However, low expressions of BTN2A1 (HR = 0.51, p = 6e-08), BTN2A2 (HR = 0.52, p = 7.2e-08), BTN3A1 (HR = 0.77, p = 0.032), BTN3A2 (HR = 0.51, p = 3.2e-08), BTN3A3 (HR = 0.48, p = 9.7e-10), and BTNL9 (HR=0.54, p = 9.1e-07) were significantly correlated with worse OS of LUAD (**Figure 5A**). Low expression of BTN3A3 (HR = 0.73, p = 0.0088) was significantly correlated with worse OS of LUSC (**Figure 5B**). These results suggested specific BTNs could serve as prognosis biomarkers for lung cancer. Because γδ T cells are involved in breast cancer (39, 40), we compared survival in high vs. low expression of BTN family in breast cancer and found low expressions of BTN1A1

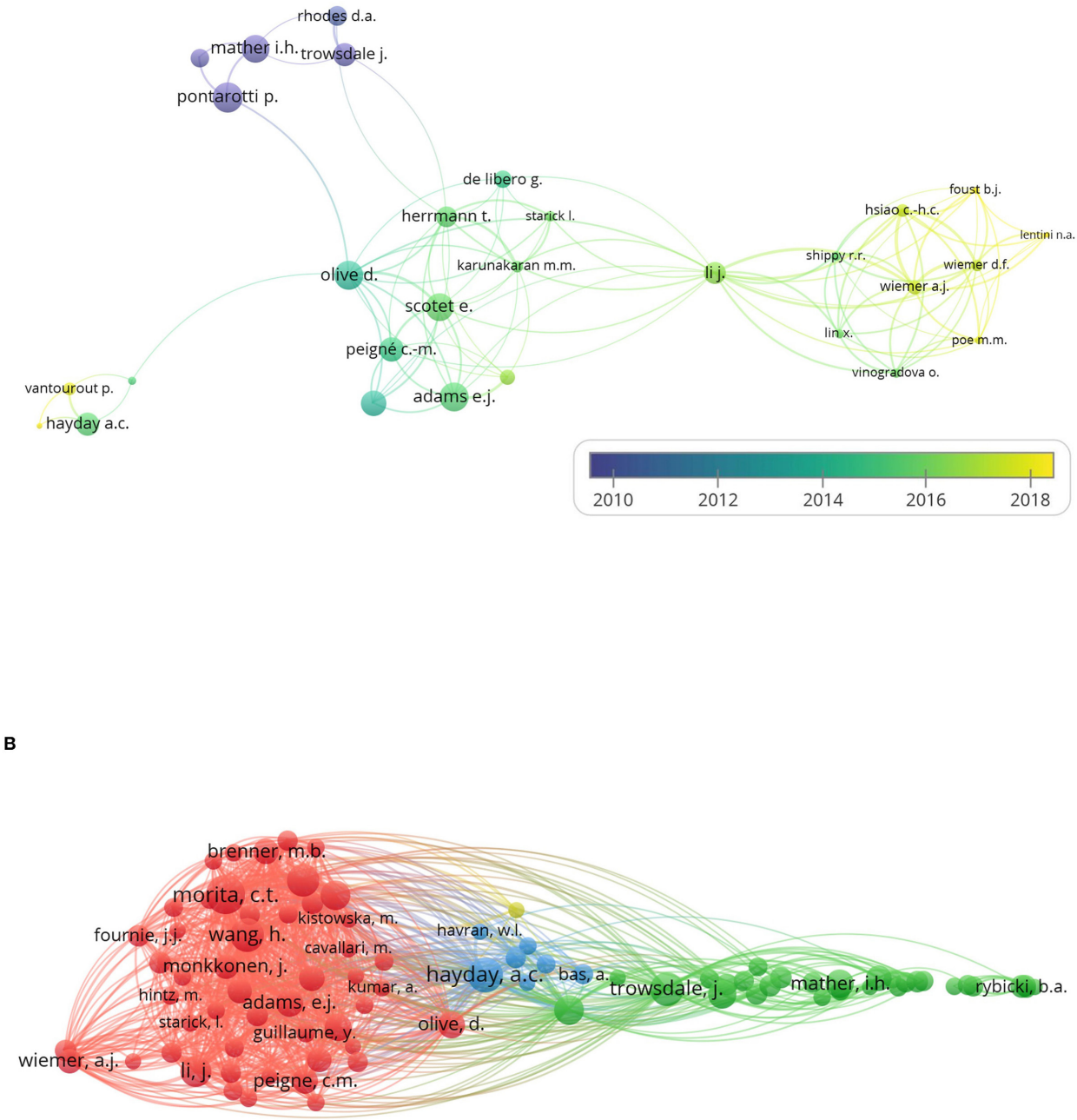

FIGURE 3 | Coauthorship analysis and cocitation analysis. The 260 studies on immune modulation in human and mouse (listed in the **Supplementary Table 1**) were analyzed by VOSviewer, and coauthorship analysis and cocitation analysis are shown. **(A)** The overlay visualization map of author coauthorship analysis. The area of the circle was determined by total citations of each author. Colors of the circles indicated the average year of the studies according to the symbol on the lower right corner. The distance between circles indicated their relatedness. The strength of the coauthor link between two countries was represented by the thickness of the connecting curve lines. **(B)** The network visualization map of author cocitation analysis. Different colors of the circles represented clusters divided by cocitations. The area of circles indicated the total citation number of each author.

(HR = 0.73, p = 1.3e-08), BTN2A1 (HR = 0.75, p = 3.7e-07), BTN2A2 (HR = 0.83, p = 0.00056), BTN2A3 (HR = 0.73, p = 2.2e-08), BTN3A1 (HR = 0.72, p = 2.3e-09), BTN3A2 (HR = 0.89, p = 0.042), BTN3A3 (HR = 0.86, p = 0.0064), BTNL2 (HR = 0.78, p = 8e-06), BTNL3 (HR = 0.71, p = 1.2e-09), and BTNL9 (HR = 0.62, p = 9.4e-10) were significantly correlated

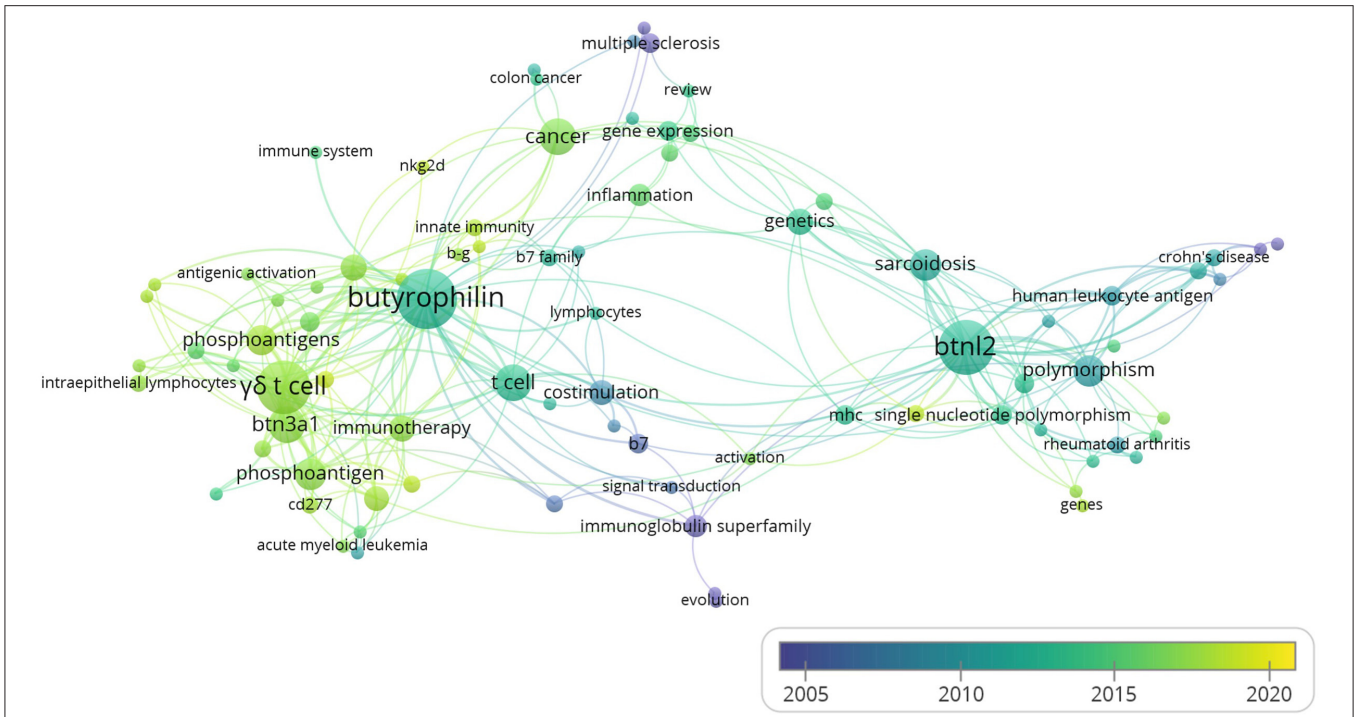

FIGURE 4 | The overlay visualization map of author keywords co-occurrence analysis. Figure was generated by VOSviewer from the data of the 260 studies on immune modulation in human or mouse (listed in the **Supplementary Table 1**). The area of the circle was determined by occurrences of each keyword. Colors of the circles indicated the average year of the keyword occurrences according to the symbol on the lower right corner.

with worse OS of breast cancer (**Figure 5C**). These collectively showed that certain BTNs serve as biomarkers for cancer and potentially therapeutic targets.

DISCUSSION

There remain notable gaps in our knowledge of the function of BTNs in immune system, although several discoveries about the modulation in T cells were found (14). The receptor of each BTN member is not well-defined, making the identification of BTN ligands a priority (14). Meantime, several studies showed that the BTNs function before identifying the structural interaction with the unknown receptors. Phosphorantigens (IPP or BrHPP) could activate human γδ T cells, whereas the mechanisms remained unclear for a long time (14). Recently, Yang et al. (41) showed that BTN3A-pAg sensing mechanism involved and triggered the inside-out signaling to activate Vγ9Vδ2 T cells, using a structural approach. Moreover, BTN2A1 was found to directly bind to Vγ9Vδ2 TCR and involved in human γδ T-cell activation (42). These studies defined BTNs as important regulators of γδ T-cell function.

Both human and mouse γδ T cells have several subsets classified by their TCR chain, and each subset of γδ T cells plays distinct roles in many diseases (43). Our previous research in mice has proven that Vγ4 γδ T cells play a protective role in tumor immunity (44, 45), whereas Vγ1 γδ T cells suppress this function via interleukin 4 (IL-4) production (46). Also, our research indicated that Vγ4 γδ T cells play a protective role in the Con A–induced hepatitis through limiting natural killer T-cell activation by secretion of IL-17 (47). Collectively, these researches indicated different γδ T-cell subsets have intrinsic functional difference. However, how these γδ T-cell subsets were regulated remains unclear. Recent research has suggested specific BTN selects or shapes specific γδ T-cell subset in its specific location and time (17), and it is critical to further characterize the interactions between γδ T cells and BTNs. Based on the facts that γδ T cells have extraordinary capacity for tumor cell killing (43) and BTNs can activate γδ T cells (17), and structure of BTNs is closely sharing the fractions of B7 family, which plays a critical role in cancer immunity (4), we postulate BTNs play potential roles in cancer immunology and may serve as biomarkers for prognosis, although the accumulated publication amount of BTNs is much less than that of PD-1.

Through survival analysis of lung cancer and breast cancer patients with mRNA expression in gene chip data of BTNs, as we expected, several BTN members were proven as playing important roles in the prognosis of LUAD, LUSC, and breast cancer. Our results showed that high expressions of BTN1A1, BTN2A3, BTNL2, BTNL3, and BTNL8 were significantly correlated with worse OS of LUAD (**Figure 5A**). However, low expressions of BTN2A1, BTN2A2, BTN3A1, BTN3A2, BTN3A3, and BTNL9 were significantly correlated with worse OS of LUAD (**Figure 5A**). Low expression of BTN3A3 was significantly correlated with worse OS of LUSC (**Figure 5B**). In breast cancer, low expressions of BTN1A1, BTN2A1, BTN2A2, BTN2A3, BTN3A1, BTN3A2, BTN3A3, BTNL2, BTNL3, and

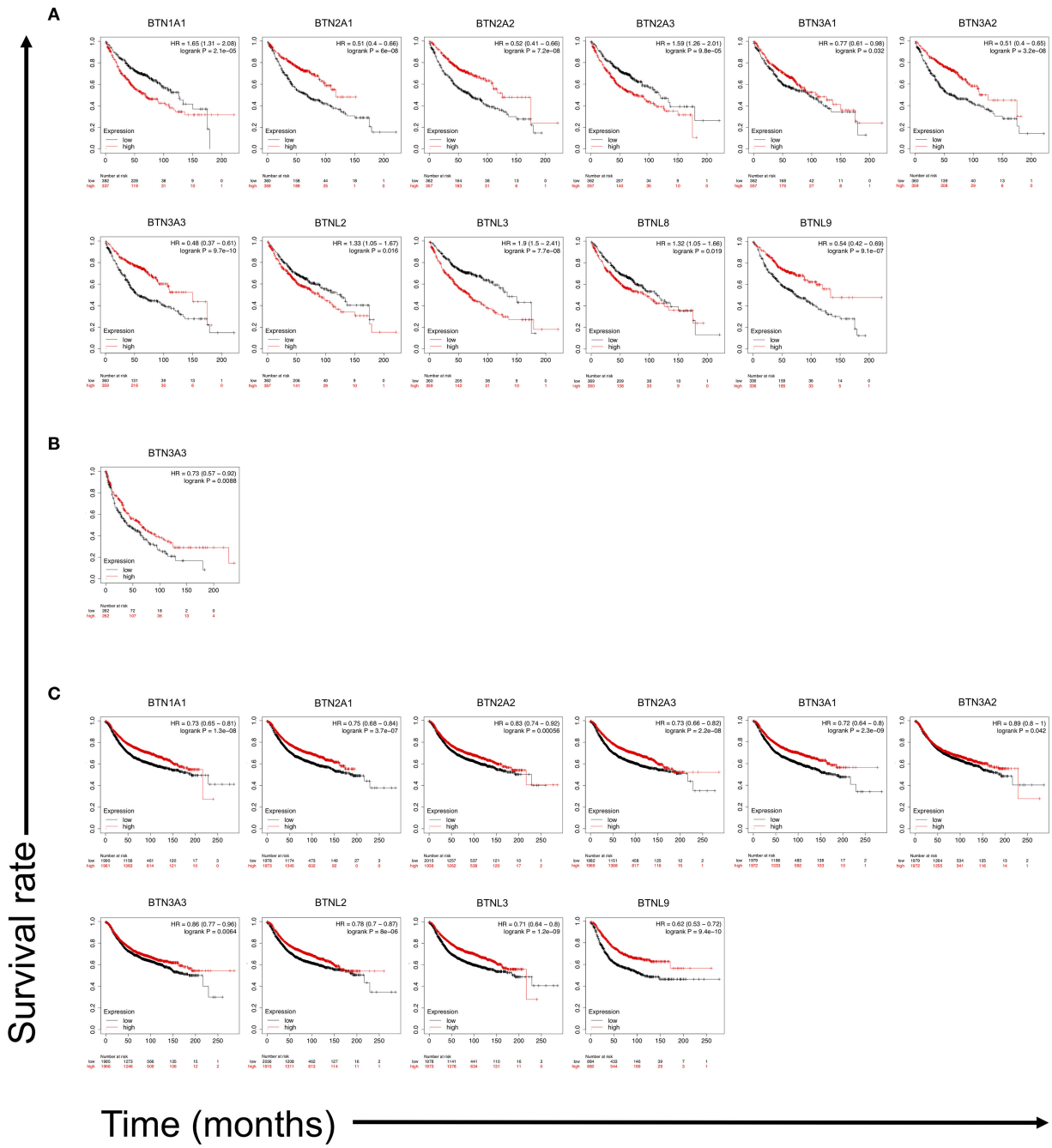

FIGURE 5 | Kaplan–Meier overall survival (OS) survival curves of LUAD and LUSC cases according to gene expression levels of butyrophilin family members. The Kaplan–Meier plotter (http://kmplot.com/analysis/) was employed to calculate survival of butyrophilin family members expression high vs. low in gene chip data on LUAD ($n = 719$), LUSC ($n = 524$), and breast cancer ($n = 3,951$) patients. **(A)** Overall survival curves of LUAD patients based on BTN1A1, BTN2A1, BTN2A2, BTN2A3, BTN3A1, BTN3A2, BTN3A3, BTNL2, BTNL3, BTNL8, and BTNL9 expression levels. **(B)** Overall survival curve of LUSC patients based on BTN3A3 expression levels. **(C)** Overall survival curve of breast cancer patients based on BTN1A1, BTN2A1, BTN2A2, BTN2A3, BTN3A1, BTN3A2, BTN3A3, BTNL2, BTNL3, and BTNL9 expression levels. Statistical difference (when log-rank $p < 0.05$) is shown. HR, hazard ratio.

BTNL9 were significantly correlated with worse OS (**Figure 5C**). These suggested a potential function of γδ T cells in cancer, which is regulated by BTNs. Currently, mechanisms of the effects are not clear; it is possible that different signal pathways are involved in specific immune microenvironment. With the impacts of Nobel Prize in 2018 (48), immune-checkpoint inhibition has been further utilized, and more researches have been done for the field. However, large amounts of people are unresponsive to immune therapy (27, 28). Based on previous research results, BTNs play important roles in cancer immunity, which might

serve as new targets or therapeutic strategies and may be effective for anti–PD-1 or anti–cytotoxic T-lymphocyte-associated protein 4–unresponsive patients.

In summary, this research focuses on the immune regulation of BTNs and their correlation with the prognosis of lung cancer patients and provides a new aspect of gene therapy or immune intervention. Further efforts are still needed in investigation of the specific BTN receptor, mechanism of BTNs instructing local immune response (especially T-cell function), and the expression pattern of BTNs.

DATA AVAILABILITY STATEMENT

All datasets generated for this study are included in the article/**Supplementary Material**.

AUTHOR CONTRIBUTIONS

YWa and XZ did the bibiometric analysis and contributed to manuscript writing. NZ did patient survival calculation. ZLi, ZLia, JY, XLiu, YWu, KC, YG, ZY, XLin, and HZ designed the research and contributed to manuscript writing. DT, YC, and JH designed the research, organized the calculations and wrote the manuscript. All authors contributed to the article and approved the submitted version.

FUNDING

This work was supported by the Grants from National Natural Science Foundation of China (81702876 to XLin, 31420103901 to ZY, 81970963 to YC, and 81630025 and 31970830 to JH), Grant from Traditional Chinese Medicine Bureau of Guangdong Province (2018071 to JH), Grant from Guangzhou Municipal Science and Technology Bureau (201906010085 to XLin and 201904010090 to JH), Grant from Health Commission of Guangdong Province (A2019520 to JH), and Grant from Department of Science and Technology of Guangdong Province (2017A030313529 to YC).

SUPPLEMENTARY MATERIAL

The Supplementary Material for this article can be found online at: https://www.frontiersin.org/articles/10.3389/fimmu.2020.01187/full#supplementary-material

REFERENCES

1. Malinowska M, Tokarz-Deptula B, Deptula W. Butyrophilins: an important new element of resistance. *Cent Eur J Immunol.* (2017) 42:399–403. doi: 10.5114/ceji.2017.72806
2. Franke WW, Heid HW, Grund C, Winter S, Freudenstein C, Schmid E, et al. Antibodies to the major insoluble milk fat globule membrane-associated protein: specific location in apical regions of lactating epithelial cells. *J Cell Biol.* (1981) 89:485–94. doi: 10.1083/jcb.89.3.485
3. Heid HW, Winter S, Bruder G, Keenan TW, Jarasch ED. Butyrophilin, an apical plasma membrane-associated glycoprotein characteristic of lactating mammary glands of diverse species. *Biochim Biophys Acta.* (1983) 728:228–38. doi: 10.1016/0005-2736(83)90476-5
4. Arnett HA, Viney JL. Immune modulation by butyrophilins. *Nat Rev Immunol.* (2014) 14:559–69. doi: 10.1038/nri3715
5. Valentonyte R, Hampe J, Huse K, Rosenstiel P, Albrecht M, Stenzel A, et al. Sarcoidosis is associated with a truncating splice site mutation in BTNL2. *Nat Genet.* (2005) 37:357–64. doi: 10.1038/ng1519
6. Newburg DS, Peterson JA, Ruiz-Palacios GM, Matson DO, Morrow AL, Shults J, et al. Role of human-milk lactadherin in protection against symptomatic rotavirus infection. *Lancet.* (1998) 351:1160–4. doi: 10.1016/S0140-6736(97)10322-1
7. Hippich M, Beyerlein A, Hagopian WA, Krischer JP, Vehik K, Knoop J, et al. Genetic contribution to the divergence in type 1 diabetes risk between children from the general population and children from affected families. *Diabetes.* (2019) 68:847–57. doi: 10.2337/db18-0882
8. Jiang Z, Liu F. Butyrophilin-Like 9 (BTNL9) suppresses invasion and correlates with favorable prognosis of uveal melanoma. *Med Sci Monit.* (2019) 25:3190–8. doi: 10.12659/MSM.914074
9. Cai P, Lu Z, Wu J, Qin X, Wang Z, Zhang Z, et al. BTN3A2 serves as a prognostic marker and favors immune infiltration in triple-negative breast cancer. *J Cell Biochem.* (2020) 121:2643–54. doi: 10.1002/jcb.29485
10. Wang Y, Wang Q, Wei X, Shao J, Zhao J, Zhang Z, et al. Global scientific trends on exosome research during 2007–2016: a bibliometric analysis. *Oncotarget.* (2017) 8:48460–70. doi: 10.18632/oncotarget.17223
11. Dabi Y, Darrigues L, Katsahian S, Azoulay D, de Antonio M, Lazzati A. Publication trends in bariatric surgery: a bibliometric study. *Obesity Surg.* (2016) 26:2691–9. doi: 10.1007/s11695-016-2160-x
12. Geaney F, Scutaru C, Kelly C, Glynn RW, Perry IJ. Type 2 diabetes research yield, 1951-2012: bibliometrics analysis and density-equalizing mapping. *PLoS ONE.* (2015) 10:e0133009. doi: 10.1371/journal.pone.0133009
13. Abeler-Dorner L, Swamy M, Williams G, Hayday AC, Bas A. Butyrophilins: an emerging family of immune regulators. *Trends Immunol.* (2012) 33:34–41. doi: 10.1016/j.it.2011.09.007
14. Rhodes DA, Reith W, Trowsdale J. Regulation of immunity by butyrophilins. *Annu Rev Immunol.* (2016) 34:151–72. doi: 10.1146/annurev-immunol-041015-055435
15. Harly C, Guillaume Y, Nedellec S, Peigne CM, Monkkonen H, Monkkonen J, et al. Key implication of CD277/butyrophilin-3 (BTN3A) in cellular stress sensing by a major human γδ T-cell subset. *Blood.* (2012) 120:2269–79. doi: 10.1182/blood-2012-05-430470
16. Willcox CR, Vantourout P, Salim M, Zlatareva I, Melandri D, Zanardo L, et al. Butyrophilin-like 3 directly binds a human Vγ4(+) T cell receptor using a modality distinct from clonally-restricted antigen. *Immunity.* (2019) 51:813–25.e814. doi: 10.1016/j.immuni.2019.09.006
17. Di Marco Barros R, Roberts NA, Dart RJ, Vantourout P, Jandke A, Nussbaumer O, et al. Epithelia use butyrophilin-like molecules to shape organ-specific γδ T cell compartments. *Cell.* (2016) 167:203–18.e217. doi: 10.1016/j.cell.2016.08.030
18. Boyden LM, Lewis JM, Barbee SD, Bas A, Girardi M, Hayday AC, et al. Skint1, the prototype of a newly identified immunoglobulin superfamily gene cluster, positively selects epidermal γδ T cells. *Nat Genet.* (2008) 40:656–62. doi: 10.1038/ng.108
19. Deng Z, Wang H, Chen Z, Wang T. Bibliometric analysis of dendritic epidermal T cell (DETC) research from 1983 to 2019. *Front Immunol.* (2020) 11:259. doi: 10.3389/fimmu.2020.00259
20. Gentles AJ, Newman AM, Liu CL, Bratman SV, Feng W, Kim D, et al. The prognostic landscape of genes and infiltrating immune cells across human cancers. *Nat Med.* (2015) 21:938–45. doi: 10.1038/nm.3909
21. Global Burden of Disease Cancer C, Fitzmaurice C, Allen C, Barber RM, Barregard L, Bhutta ZA, et al. Global, regional, and national cancer incidence, mortality, years of life lost, years lived with disability, and disability-adjusted life-years for 32 cancer groups, 1990 to 2015: a systematic analysis for the global burden of disease study. *JAMA Oncol.* (2017) 3:524–48. doi: 10.1001/jamaoncol.2016.5688

22. Torre LA, Bray F, Siegel RL, Ferlay J, Lortet-Tieulent J, Jemal A. Global cancer statistics, 2012. *CA Cancer J Clin.* (2015) 65:87–108. doi: 10.3322/caac.21262
23. Herbst RS, Morgensztern D, Boshoff C. The biology and management of non-small cell lung cancer. *Nature.* (2018) 553:446–54. doi: 10.1038/nature25183
24. Villanueva N, Bazhenova L. New strategies in immunotherapy for lung cancer: beyond PD-1/PD-L1. *Ther Adv Respir Dis.* (2018) 12:1753466618794133. doi: 10.1177/1753466618794133
25. Fehrenbacher L, Spira A, Ballinger M, Kowanetz M, Vansteenkiste J, Mazieres J, et al. Atezolizumab versus docetaxel for patients with previously treated non-small-cell lung cancer (POPLAR): a multicentre, open-label, phase 2 randomised controlled trial. *Lancet.* (2016) 387:1837–46. doi: 10.1016/S0140-6736(16)00587-0
26. Rittmeyer A, Barlesi F, Waterkamp D, Park K, Ciardiello F, von Pawel J, et al. Atezolizumab versus docetaxel in patients with previously treated non-small-cell lung cancer (OAK): a phase 3, open-label, multicentre randomised controlled trial. *Lancet.* (2017) 389:255–65. doi: 10.1016/S0140-6736(16)32517-X
27. Sacher AG, Gandhi L. Biomarkers for the clinical use of PD-1/PD-L1 inhibitors in non-small-cell lung cancer: a review. *JAMA Oncol.* (2016) 2:1217–22. doi: 10.1001/jamaoncol.2016.0639
28. Horn L, Spigel DR, Vokes EE, Holgado E, Ready N, Steins M, et al. Nivolumab versus docetaxel in previously treated patients with advanced non-small-cell lung cancer: two-year outcomes from two randomized, open-label, phase III Trials (checkMate 017 and checkMate 057). *J Clin Oncol.* (2017) 35:3924–33. doi: 10.1200/JCO.2017.74.3062
29. Seow WJ, Matsuo K, Hsiung CA, Shiraishi K, Song M, Kim HN, et al. Association between GWAS-identified lung adenocarcinoma susceptibility loci and EGFR mutations in never-smoking Asian women, and comparison with findings from Western populations. *Hum Mol Genet.* (2017) 26:454–65. doi: 10.1093/hmg/ddw414
30. Shiraishi K, Okada Y, Takahashi A, Kamatani Y, Momozawa Y, Ashikawa K, et al. Association of variations in HLA class II and other loci with susceptibility to EGFR-mutated lung adenocarcinoma. *Nat Commun.* (2016) 7:12451. doi: 10.1038/ncomms12451
31. Shiraishi K, Kunitoh H, Daigo Y, Takahashi A, Goto K, Sakamoto H, et al. A genome-wide association study identifies two new susceptibility loci for lung adenocarcinoma in the Japanese population. *Nat Genet.* (2012) 44:900–3. doi: 10.1038/ng.2353
32. Romero L, Portillo-Salido E. Trends in sigma-1 receptor research: a 25-year bibliometric analysis. *Front Pharmacol.* (2019) 10:564. doi: 10.3389/fphar.2019.00564
33. Falagas ME, Pitsouni EI, Malietzis GA, Pappas G. Comparison of pubmed, scopus, web of science, and google scholar: strengths and weaknesses. *FASEB J.* (2008) 22:338–42. doi: 10.1096/fj.07-9492LSF
34. Agarwal A, Durairajanayagam D, Tatagari S, Esteves SC, Harlev A, Henkel R, et al. Bibliometrics: tracking research impact by selecting the appropriate metrics. *Asian J Androl.* (2016) 18:296–309. doi: 10.4103/1008-682X.171582
35. French FMFC. A candidate gene for familial Mediterranean fever. *Nat Genet.* (1997) 17:25–31. doi: 10.1038/ng0997-25
36. Sharpe AH, Freeman GJ. The B7-CD28 superfamily. *Nat Rev Immunol.* (2002) 2:116–26. doi: 10.1038/nri727
37. Vavassori S, Kumar A, Wan GS, Ramanjaneyulu GS, Cavallari M, El Daker S, et al. Butyrophilin 3A1 binds phosphorylated antigens and stimulates human γδ T cells. *Nat Immunol.* (2013) 14:908–16. doi: 10.1038/ni.2665
38. Sandstrom A, Peigne CM, Leger A, Crooks JE, Konczak F, Gesnel MC, et al. The intracellular B30.2 domain of butyrophilin 3A1 binds phosphoantigens to mediate activation of human Vγ9Vδ2 T cells. *Immunity.* (2014) 40:490–500. doi: 10.1016/j.immuni.2014.03.003
39. Wu Y, Kyle-Cezar F, Woolf RT, Naceur-Lombardelli C, Owen J, Biswas D, et al. An innate-like Vδ1(+) γδ T cell compartment in the human breast is associated with remission in triple-negative breast cancer. *Sci Transl Med.* (2019) 11:eaax9364. doi: 10.1126/scitranslmed.aax9364
40. Janssen A, Villacorta Hidalgo J, Beringer DX, van Dooremalen S, Fernando F, van Diest E, et al. γδ T-cell receptors derived from breast cancer-infiltrating T lymphocytes mediate antitumor reactivity. *Cancer Immunol Res.* (2020) 8:530–43. doi: 10.1158/2326-6066.CIR-19-0513
41. Yang Y, Li L, Yuan L, Zhou X, Duan J, Xiao H, et al. A structural change in Butyrophilin upon phosphoantigen binding underlies phosphoantigen-mediated Vγ9Vδ2 T cell activation. *Immunity.* (2019) 50:1043–53.e1045. doi: 10.1016/j.immuni.2019.02.016
42. Rigau M, Ostrouska S, Fulford TS, Johnson DN, Woods K, Ruan Z, et al. Butyrophilin 2A1 is essential for phosphoantigen reactivity by γδ T cells. *Science.* (2020) 367:eaay5516. doi: 10.1126/science.aay5516
43. Carding SR, Egan PJ. γδ T cells: functional plasticity and heterogeneity. *Nat Rev Immunol.* (2002) 2:336–45. doi: 10.1038/nri797
44. He W, Hao J, Dong S, Gao Y, Tao J, Chi H, et al. Naturally activated Vγ4 γδ T cells play a protective role in tumor immunity through expression of eomesodermin. *J Immunol.* (2010) 185:126–33. doi: 10.4049/jimmunol.0903767
45. Yang Q, Liu X, Liu Q, Guan Z, Luo J, Cao G, et al. Roles of mTORC1 and mTORC2 in controlling γδ T1 and T17 differentiation and function. *Cell Death Differ.* (2020). doi: 10.1038/s41418-020-0500-9. [Epub ahead of print].
46. Hao J, Dong S, Xia S, He W, Jia H, Zhang S, et al. Regulatory role of Vγ1 γδ T cells in tumor immunity through IL-4 production. *J Immunol.* (2011) 187:4979–86. doi: 10.4049/jimmunol.1101389
47. Zhao N, Hao J, Ni Y, Luo W, Liang R, Cao G, et al. Vγ4 γδ T cell-derived IL-17A negatively regulates NKT cell function in con A-induced fulminant hepatitis. *J Immunol.* (2011) 187:5007–14. doi: 10.4049/jimmunol.1101315
48. Ledford H, Else H, Warren M. Cancer immunologists scoop medicine nobel prize. *Nature.* (2018) 562:20–1. doi: 10.1038/d41586-018-06751-0

Conflict of Interest: The authors declare that the research was conducted in the absence of any commercial or financial relationships that could be construed as a potential conflict of interest.

frontiers in Immunology

ORIGINAL RESEARCH
published: 02 July 2020
doi: 10.3389/fimmu.2020.01347

Gamma-Delta CAR-T Cells Show CAR-Directed and Independent Activity Against Leukemia

Meir Rozenbaum[1,2,3], Amilia Meir[3], Yarden Aharony[3], Orit Itzhaki[2], Jacob Schachter[2], Ilan Bank[4], Elad Jacoby[3,5,6] and Michal J. Besser[1,2,7]**

[1] Department of Clinical Microbiology and Immunology, Sackler School of Medicine, Tel Aviv University, Tel Aviv, Israel, [2] Ella Lemelbaum Institute for Immuno Oncology, Sheba Medical Center, Ramat Gan, Israel, [3] Center for Pediatric Cell Therapy, Sheba Medical Center, Tel Hashomer, Israel, [4] Rheumatology Unit, Sheba Medical Center, Tel Hashomer, Israel, [5] Division of Pediatric Hematology and Oncology, Sheba Medical Center, The Edmond and Lily Safra Children's Hospital, Tel Hashomer, Israel, [6] Department of Pediatrics, Sackler School of Medicine, Tel Aviv University, Tel Aviv, Israel, [7] Wohl Institute of Translational Medicine, Sheba Medical Center, Tel Aviv, Israel

Autologous T cells engineered to express a chimeric antigen receptor (CAR) against the CD19 antigen are in the frontline of contemporary hemato-oncology therapies, leading to high remission rates in B-cell malignancies. Although effective, major obstacles involve the complex and costly individualized manufacturing process, and CD19 target antigen loss or modulation leading to resistant and relapse following CAR therapy. A potential solution for these limitations is the use of donor-derived γδT cells as a CAR backbone. γδT cells lack allogenecity and are safely used in haploidentical transplants. Moreover, γδT cells are known to mediate natural anti-tumor responses. Here, we describe a 14-day production process initiated from peripheral-blood mononuclear cells, leading to a median 185-fold expansion of γδ T cells with high purity (>98% CD3+ and >99% γδTCR+). CAR transduction efficacy of γδ T cells was equally high when compared to standard CAR-T cells (60.5 ± 13.2 and 65.3 ± 18.3%, respectively). CD19-directed γδCAR-T cells were effective against CD19+ cell lines *in vitro* and in vivo, showing cytokine production, direct target killing, and clearance of bone marrow leukemic cells in an NSG model. Multiple injections of γδCAR-T cells and priming of mice with zoledronate lead to enhanced tumor reduction *in vivo*. Unlike standard CD19 CAR-T cells, γδCAR-T cells were able to target CD19 antigen negative leukemia cells, an effect that was enhanced after priming the cells with zoledronate. In conclusion, γδCAR-T cell production is feasible and leads to highly pure and efficient effector cells. γδCAR-T cell may provide a promising platform in the allogeneic setting, and may target leukemic cells also after antigen loss.

Keywords: gamma-delta T cells, chimeric antigen receptor, leukemia, immuno oncology, B cell malignancies

OPEN ACCESS

Edited by:
Nadia Caccamo, University of Palermo, Italy

Reviewed by:
Christelle Harly, INSERM U1232 Centre de Recherche en Cancérologie et Immunologie Nantes Angers (CRCINA), France
John-Maher, King's College London, United Kingdom

****Correspondence:***
Elad Jacoby
elad.jacoby@sheba.health.gov.il
Michal J. Besser
michal.besser@sheba.health.gov.il

Specialty section:
This article was submitted to T Cell Biology, a section of the journal Frontiers in Immunology

Received: *01 April 2020*
Accepted: *27 May 2020*
Published: *02 July 2020*

Citation:
Rozenbaum M, Meir A, Aharony Y, Itzhaki O, Schachter J, Bank I, Jacoby E and Besser MJ (2020) Gamma-Delta CAR-T Cells Show CAR-Directed and Independent Activity Against Leukemia. Front. Immunol. 11:1347. doi: 10.3389/fimmu.2020.01347

INTRODUCTION

Transduction of T cells with a chimeric-antigen receptor (CAR) enables the targeting of extracellular domains, leading to CAR-induced T cell cytotoxicity, and cytokine production, in an MHC-independent manner (1). Autologous CAR-T cells directed against the pan-B-cell antigen CD19 have been approved for acute lymphoblastic leukemia (ALL) and non-Hodgkin lymphoma

(NHL), after showing high remission rates in heavily pretreated patients, which in some may be durable (2, 3). Still, many patients do not respond to CAR-T cells or experience a relapse, through an orchestra of mechanisms including loss of transferred T cells in some patients and alterations in target antigen expression or density in others (4, 5). Thus, further multi-targeting approaches have been proposed, usually via dual CARs (5, 6), but sequential antigen loss has also been shown following CAR-mediated multi-targeting (7, 8). In addition these cellular therapies are still autologous products, necessitating complex, and individualized production associated with a significant financial burden.

Lymphocytes bearing the γδT cell receptor (γδT) are a small subset of peripheral blood cytotoxic T cells, which do not require antigenic presentation by MHC molecules for recognition and function (9, 10). *In vitro* and *in vivo* expansion of these cells is feasible, especially when exposing them to amino bisphosphonates such as zoledronate (11, 12). γδT cells are known to function across MHC-barriers, and do not cause graft-vs.-host disease (13). Moreover, anti-tumor activity has been demonstrated using expanded Vγ9Vδ2 T cells in preclinical studies and early phase clinical trials (14), though effects against ALL and NHL remain modest at most (13, 15, 16).

Since γδT cells can be safely applied in the allogeneic setting and exhibit natural anti-tumor reactivity, arming γδT cells with a CAR may provide a way to safely use allogeneic CARs and can potentially target minor clones with lower antigen density, which may not be eliminated by the standard CAR T cells. Here, we report our protocol to use γδ T lymphocytes as a platform for CAR-T cells. We show that γδCAR-T cells are effective against CD19 malignancies *in vitro* and *in vivo*, and have activity against leukemic clones lacking CD19 expression.

MATERIALS AND METHODS

Ethics

Patient material was obtained as part of a clinical trial previously reported (NCT02772198) (17, 18) and approved by the Sheba Medical Center IRB and the Israeli Ministry of Health. All animal experiments were approved by Institutional Ethical Review Process Committees and were performed under Israel Institutional Animal care and use committee approval (1131/17/ANIM).

Cell Culture

Leukemia cell lines Nalm6, CCRF-CEM, Toledo, and K562 were kindly provided by Steve Feldman, and grown in standard culture conditions, using RPMI medium supplemented with 10% fetal bovine serum (FBS), 2 mM L-Glutamate, Sodium Pyruvate, Hepes buffer 0.1 M (all from Biological Industries), and 100 U/mL penicillin and 100 μg/mL streptomycin (Sigma-Aldrich) ("target cell medium"). For activation and transduction, T cells were cultured in RPMI supplemented with 10% FBS, 2 mM L-Glu, 100 U/mL penicillin, and 100 μg/mL streptomycin and interleukin-2 (IL-2, 100 IU/ml, Novartis Proleukin) ("T cell medium"). 293T cells used for viral production were cultivated in DMEM high glucose medium supplemented with 10% FBS, 2 mM L-Glutamate, Sodium Pyruvate, Hepes buffer 0.1 M, and non-essential amino acids solution (all from Biological Industries). Alternatively, medium can be supplemented with human AB serum instead of FBS.

CAR-T Cell Production

Peripheral-blood mononuclear cells (PBMCs) were isolated using centrifugation on LymphoprepTM density gradients (Alere technologies) and were activated in T cell medium with 100 IU/ml IL2 and either OKT3 50 ng/ml (Invitrogen) for standard T cell expansion (previously published) (17), or zoledronic acid 2.94 uM (Novartis) for γδT cell expansion. On day 5 of culture, activated cells were transduced with the CD19 CAR retrovirus, based on an MSGV backbone transduced with an FMC63-CD28-CD3zeta plasmid, kindly provided by Steve Feldman. For this purpose, non-tissue culture treated 6-well-plates (Falcon) were pre-coated with 20 ug Retronectin per well (10 ug/ml, Takara-Clontech) for 3 days at 4°C followed by a 20 min incubation with a 2.5% BSA solution (Caisson labs, BSA fraction V) in PBS (Biological Industries) and a single wash with PBS. Plates were loaded with 4 ml of virus diluted 1:1 with T cell medium per well and centrifuged at 2,000 g for 2 h at 32°C. Following centrifugation, the supernatant was collected leaving only 1 ml/well. Plates were then seeded with the OKT-3 or zoledronic acid activated PBMCs, between 2 and 2.5 × 106 cell/well, centrifuged at 1,000 g for 20 min at 32°C and incubated overnight at 37°C. Un-transduced γδT cells and standard T cells were treated the same way, just without addition of virus and served as negative control. On Day 9 γδT and γδCAR-T cells underwent αβTCR+ cell depletion using MACS LD depletion magnetic columns, FcR Blocking reagent, anti-TCRa/b-Biotin, and anti-biotin MicroBeads (all from Miltenyi). The remaining γδT cells and standard CAR-T cells were further expanded in IL-2 containing T cell medium until day 13–15.

Standard CAR T cells for the clinical setting were produced the same way as standard CAR T described here, with the only differences that clinical CAR T production utilizes 300 IU/ml IL-2 (instead of 100 IU/ml), transduction is performed on day 2 (instead of day 5) and human AB serum is supplemented to the culture medium (instead of FBS) (17).

Co-culture, Cytokine Levels, and Cytotoxic Assays

Co-cultures were carried out in flat bottom 96-well-plates. For IFN-γ secretion tests T cells and targets were plated 100,000 cell/well each overnight in target cell medium. ELISA for the detection of human IFN-γ was carried out using Biolegend's Elisa MAX™ Deluxe kit. For cytotoxic assays, targets were stained by CellTrace™ Violet according to manufacturer's instructions and seeded 40,000 cells/well. T cells were then added at 160,000 cells/ml. After 2.5–3 h at 37°C, cells were collected from wells and stained for apoptosis by Annexin V-Cy5 reagent (Biovision). CellTrace positive cells were assessed for AnnexinV staining by flow cytometry.

Flow Cytometry

Flow cytometry was performed on a Beckman Coulter's Gallios. For detection of the CD19 CAR receptor we used a biotinylated

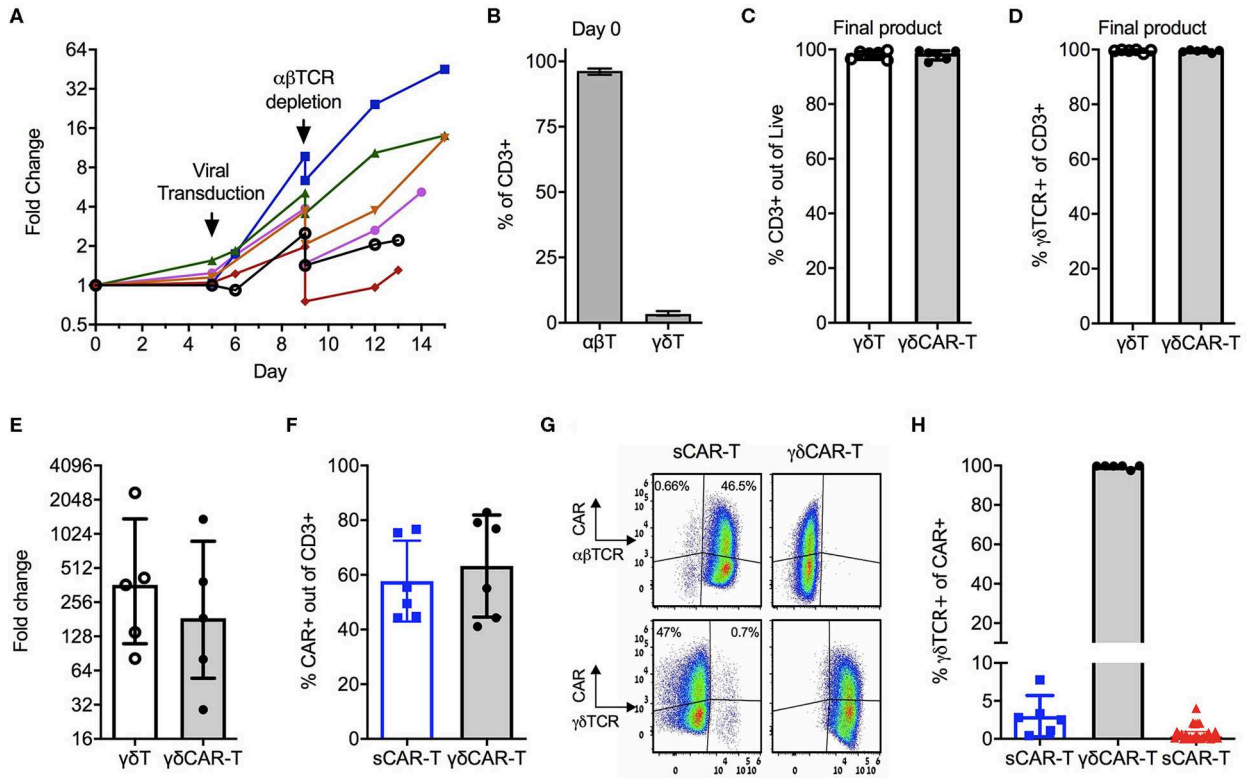

FIGURE 1 | Production of γδCAR-T cells: **(A)** Production scheme, showing total cell expansion (by fold change) along the protocol. Day 0 is the collection of blood, PBMCs isolation, and T cell activation. Each line represents a different healthy donor. **(B)** γδ-T/ αβ-T cells composition of donors' blood out of CD3 positive cells (n = 5). **(C)** CD3 positive cells in the final product of un-transduced γδ-T and transduced γδCAR-T cells (n = 6). **(D)** Purity of γδTCR+ cells in the final product of both protocols (n = 6). **(E)** γδ-T cells fold change expansion during the γδCAR-T production protocol (n = 5). **(F)** CAR transduction efficiency by flow cytometry gated on CD3 positive cells, of the standard CAR (sCAR) and γδCAR-T cell products (n = 6). **(G)** Dot plots of a representative sample showing CAR expression in γδ and αβ-T cells populations in the final product of sCAR and γδCAR-T cell protocols. **(H)** γδTCR positive cells gated on CAR positive cells in the final composition of sCAR-T cells (blue squares, n = 6), γδCAR-T cells production protocol (black circles, n = 6) and the clinically manufactured sCAR-T cells (red triangles, n = 25). Bars are at the median value, and error bars represent interquartile range.

anti-mouse FAB as a primary antibody (Jackson), Mouse Gamma Globulin as a blocking reagent (Jackson) and Anti-Biotin-Viogreen as a secondary antibody (Miltenyi). The following antibodies were used for additional staining: Anti Human CD3 – FITC, Anti Human TCRa/b-APC, Anti Human TCRg/d-PE, Anti Human CD19-PE, Anti Human CD10-PE-Cy7, Anti Human CD45 viogreen, Anti mouse CD45 APC, and for dead cell exclusion Ghost Red 780 Viability Dye (all from Miltenyi). All antibodies were incubated with samples for 20 min at 4°C. Analysis was done using the FlowJo analysis software V10.

Nalm6 CRISPR CD19 KO

We generated a Lenti virus expressing CAS9 and a sgRNA targeting CD19. The sgRNA sequence 5′-TGGAATGTTTCG GACCTAGGTGG-3′ (19) was cloned into pL-CRISPR.EFS.GFP (addgene Plasmid #57818 - Lentiviral CRISPR-Cas9 delivery for SpCas9 and sgRNA. Co-expresses eGFP via P2A cleavage site). Envelope plasmid was pMD2.G (addgene Plasmid #12259) and packaging plasmid psPAX2 (addgene Plasmid #12260). Plasmids were transfected to 293T cell line using the calcium Phosphate Profection Mammalian Transfection System (Promega cat#E1200). Viral supernatant was used for infection of Nalm6 cells with addition of Polybrene (8 ng/ml). CD19 positive cell were depleted using PE conjugated anti-CD19 antibody and anti-PE magnetic beads, on a MACS LD depletion column (Miltenyi), followed by single cell culture by plating. CD19 negative single-clones were confirmed by flow cytometry and wells were sequenced for the CD19 KO locus.

Animals and *in vivo* Models

For all *in vivo* experiments, 8–15-weeks-old NOD-SCID-IL-2Rγ- (NSG) female mice, purchased from the Jackson laboratories, were used. Mice were tail-vein injected with 1×10^6 Nalm6 cells for leukemia inoculation, followed by intravenous (IV) injections of effector cells with or without intraperitoneal (IP) injections of zoledronate (20).

Statistical Analysis

All statistical analyses were performed using the Prism v8 (GraphPad Software). Statistical comparisons between two groups were determined by two-tailed parametric or non-parametric (Mann–Whitney U-test) t-tests for unpaired data

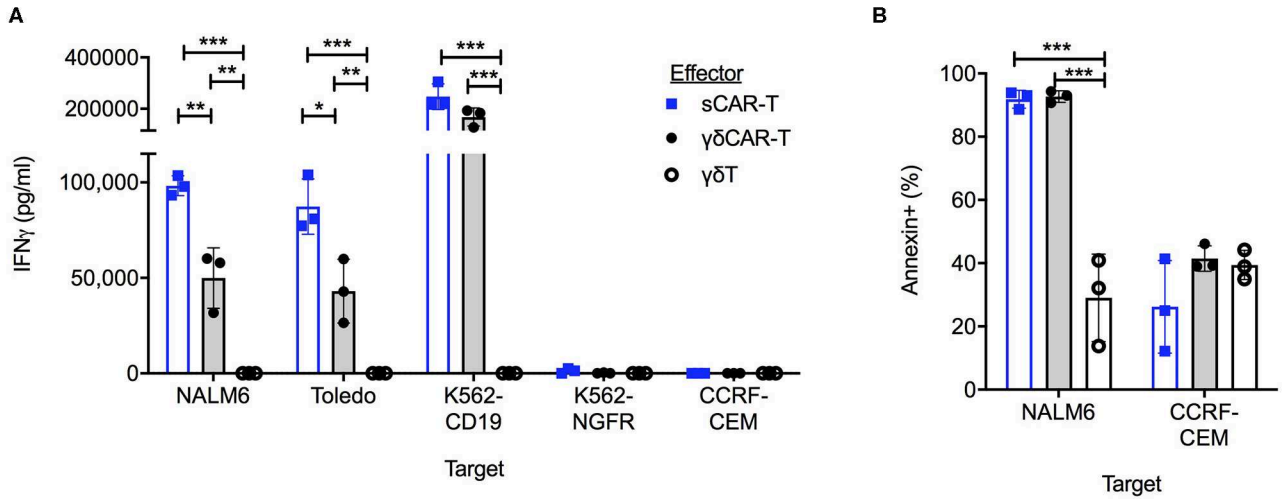

FIGURE 2 | γδCAR-T cells demonstrate CD19 target dependent activity. **(A)** IFNγ levels in co-culture medium of listed effectors with CD19 positive and negative target cells. **(B)** Cytotoxic activity of effector cells against CD19 positive Nalm6 cells and CD19 negative CCRF-CEM cells. Cell trace violette pre-stained targets were evaluated for Annexin binding by FACS analysis. Blue bars, sCAR; Gray bars, γδCAR-T; White bars, γδ-T cells. $^{*}P \leq 0.05$, $^{**}P \leq 0.01$, $^{***}P \leq 0.001$, Two tailed paired *T*-test. Error bars represent standard deviation.

or by two-tailed paired Student's *t*-tests for matched samples (produced from same donor). $P < 0.05$ were considered statistically significant.

RESULTS

Generation of Human CD19 CAR Expressing γδT Cells From Peripheral Blood

We first devised and calibrated a protocol for the generation of γδT cells expressing the CD19 CAR and depletion of αβ-TCR+ cells (**Figure 1A**). On average, γδT cells consisted of 3.4% (± 0.73%) of CD3-positive cells in the initial starting material of PBMCs (**Figure 1B**). Activation with Zoledronate on day 0 led to specific proliferation of γδT cells, whilst the total number of cell remained similar. On Day 5, cells were transduced with the CD19 CAR, followed by αβTCR+ depletion on day 9 and further proliferation of γδCAR-T for a total of 13–15 days. Un-transduced γδT cells served as control. The final products of transduced as well as un-transduced γδT cells contained 98% (±1.77%) and 98.1% (±1.49%) CD3 positive cells, respectively, with high purity of γδT cells, accounting for 99.5% (±0.5%) of the CD3+ cells ($n = 6$, **Figures 1C,D**). The median fold change of the γδT cells was 185 (range, 29–1,376) for transduced cells compared with a median of 363 (range, 81–2,350) for un-transduced γδT cells, with a variable range between different donors (**Figure 1E**, $p = 0.2$ paired *T*-test). As controls, we ran in parallel a standard CAR-T cell (sCAR-T) production for each donor, using a protocol as for the clinical setting (17), just in a smaller scale and transduction performed on day 5 instead of 2. CAR transduction efficacy ranged between 40 and 80% (**Figure 1F**), and did not differ between sCAR-T and γδCAR-T (60.5% ± 13.2 and 65.3% ± 18.3, respectively). A representative FACS dot plot is presented in **Figure 1G**. Of note, the sCAR-T cell product had also γδT cells and γδCAR-T cells (**Figures 1G,H**). We analyzed 25 infusion products administered to leukemia and lymphoma patients enrolled on a clinical trial for γδTCR expression. Final products had an average of 1.15% γδT and 0.77% γδCAR-T (**Figure 1G**). The, percentage of γδCAR-T in the final product was not associated with response (17). To summarize, using this protocol we are able to produce a pure fraction of γδT cells lacking αβ T cells, with high expression of the CD19 CAR, and this within a course of 2 weeks.

γδCAR-T Cells Show CD19 Dependent Activity Against Tumor Cell Lines

To test for the efficacy of the γδCAR-T cells in comparison to the sCAR-T cells *in vitro*, co-culture assays against CD19 positive and negative cell lines were performed. Un-transduced activated γδT cells, γδCAR-T cells, and sCAR-T cell were co-incubated with the B-ALL cell line Nalm6, the B-NHL cell line Toledo, and with K562 transduced to express CD19 (K562-CD19). Antigen-negative controls were the T-ALL cell line CCRF-CEM and K562-NGFR cell line. Testing for IFNγ secretion after over-night incubation at a T cell/target ratio of 1:1 revealed γδCAR-T cells are highly reactive against CD19 expressing tumor cells (**Figure 2A**). γδCAR-T and sCAR-T cells exhibited substantially higher levels of CD19 dependent IFNγ secretion relative to un-transduced γδT (γδCAR-T vs. γδT, $p = 0.005$, $p = 0.01$, and $p = 0.001$; sCAR-T vs. γδT, $p < 0.001$, $p < 0.001$, and $p = 0.001$, for NALM6, Toledo, and K562-CD19, respectively). The level of IFNγ in the supernatant of co-cultures with γδCAR-T cells was lower than measured in the co-culture with sCAR-T cells in the case of Nalm6 and Toledo cell lines ($p = 0.007$ and $p = 0.02$,

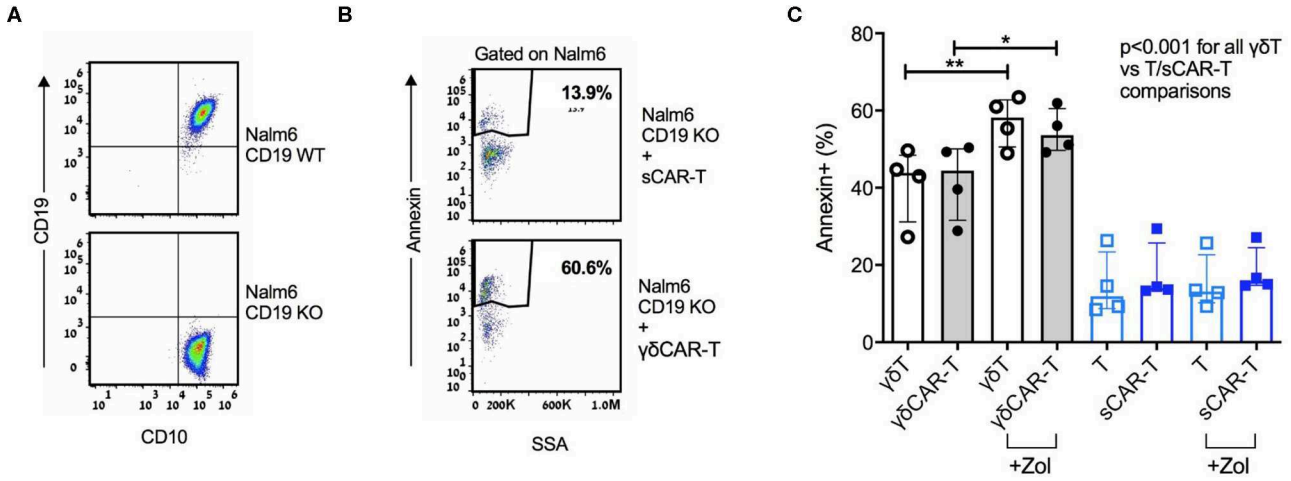

FIGURE 3 | γδCAR-T cells demonstrate activity against CD19 negative clones. **(A)** Generation of Nalm6 CD19 KO cells via CRISPR yields CD10 positive CD19 negative cells (Nalm6^{19neg}). **(B,C)** Activity of γδCAR-T cells against Nalm6^{19neg} cells is further enhanced by priming the target cells with zoledronate. **(B)** Dot plot representation showing Annexin staining of targets cells (cell-trace violet stained Nalm6^{19neg}) co-cultured with sCAR-T cells (top) or γδCAR-T cells (bottom). **(C)** Specific cytotoxicity of different effectors against Nalm6^{19neg} cells. γδ-T and γδCAR-T cells in gray bars, sT, and sCAR-T cells in blue bars. Un-transduced cells in unstained circles and CAR-T cells in filled circles. *$P \leq 0.05$, **$P \leq 0.01$, Two tailed paired *T*-test. Error bars represent interquartile range.

respectively), but not with the artificially-expressing K562-CD19 cell line ($p = 0.08$, **Figure 2A**).

In order to test for cytotoxic activity, targets were evaluated for annexin staining after a co-culture for 2.5 h at a T cell/target ratio of 5:1. Both γδCAR-T and sCAR-T cells demonstrate enhanced cytotoxic activity against the CD19 positive Nalm6, leading to 92% (±2.8%), and 93% (±1.8%) annexin expression on targets in comparison to activated γδT cells (29 ± 13.8%, $n = 3, p < 0.001$). No difference was seen in annexin expression of CD19 negative targets (**Figure 2B**).

γδCAR-T Cells Show Enhanced *in vitro* Cytotoxicity Against CD19 Negative Target Cells

A major barrier of CAR-T therapy is loss of target antigen, by various mechanisms. γδT cells are known to exert an anti-leukemic activity, especially after priming with zoledronate (13). Thus, we hypothesized that utilizing non-specific mechanisms may result in cytotoxicity also against CD19-negative targets. To further investigate this finding, we generated a CD19 knock-out B-ALL cell line Nalm6 (**Figure 3A**). γδCAR-T, γδT, sCAR-T, and un-transduced activated T cells were co-cultured with Nalm6^{19neg} for a period of 3 h at a T cell:target ratio of 4:1. Both γδT cells and γδCAR-T cells demonstrated enhanced cytotoxicity against Nalm6^{19neg} cells compared to standard T cells or sCAR-T cells (**Figures 3B,C**, $p < 0.001$ for all comparisons of γδT or γδCAR-T vs. un-transduced T or sCAR-T). Priming with Zoledronate further enhanced this effect, leading to higher target annexin expression of Nalm6^{19neg} cells incubated with γδT (57% after priming vs. 41% without zoledronate, $p = 0.007$) as well as γδCAR-T (55% after priming vs. 42% without zoledronate, $p = 0.02$, **Figure 3C**), eluding to a potential effect that may target minor CD19-negative clones.

γδCAR-T Cells Exhibit *in vivo* Activity Against Tumor Cell Lines

To investigate the *in vivo* efficacy of γδCAR-T, NSG mice were tail-vein injected with 1×10^6 Nalm6 cells, and treated on day 2 with either 4×10^6 γδCAR-T cells, sCAR-T, or γδT cells per mouse. CAR transduction efficacy was 75–85% in all experiments. Non-treated leukemia-bearing mice served as controls. Two weeks after the injection of effector cells, mice were sacrificed for evaluation of leukemic involvement of the bone marrow. The leukemic burden in the bone marrow of non-treated mice and of γδT cell treated mice was substantial (a median of 62 and 55% of bone marrow cells, respectively). The presence of human un-transduced γδT cells did not reduce significantly leukemia in this model ($p = 0.89$, Mann-Whitney). Treatment with either γδCAR-T or sCAR-T cells lead both to a drastic reduction in the leukemic burden in the bone marrow of recipient mice (to 5 and 0.1%, respectively, $p < 0.001$ compared to untreated or γδT cell treated mice), demonstrating *in vivo* activity of γδCAR-T cells (**Figure 4A**). Nevertheless, traces of leukemia were noted to be higher in recipients of γδCAR-T cells in comparison with the sCAR-T treated mice. In an intent to further improve the *in vivo* anti-tumor reactivity of γδCAR T cells, mice were conditioned with zoledronate, known to prime targets of γδT cells, and a second dose of γδCAR-T cells was administrated, both previously shown to improve anti-tumor effect of un-transduced γδT cells (21). Intraperitoneal injection of zoledronate (1.0 ug/gr) to leukemia-bearing mice on days −1, 2, 6, 8, and 10, still resulted in a median of 3% remaining leukemic cells in the bone marrow (**Figure 4B**). However, adding a second

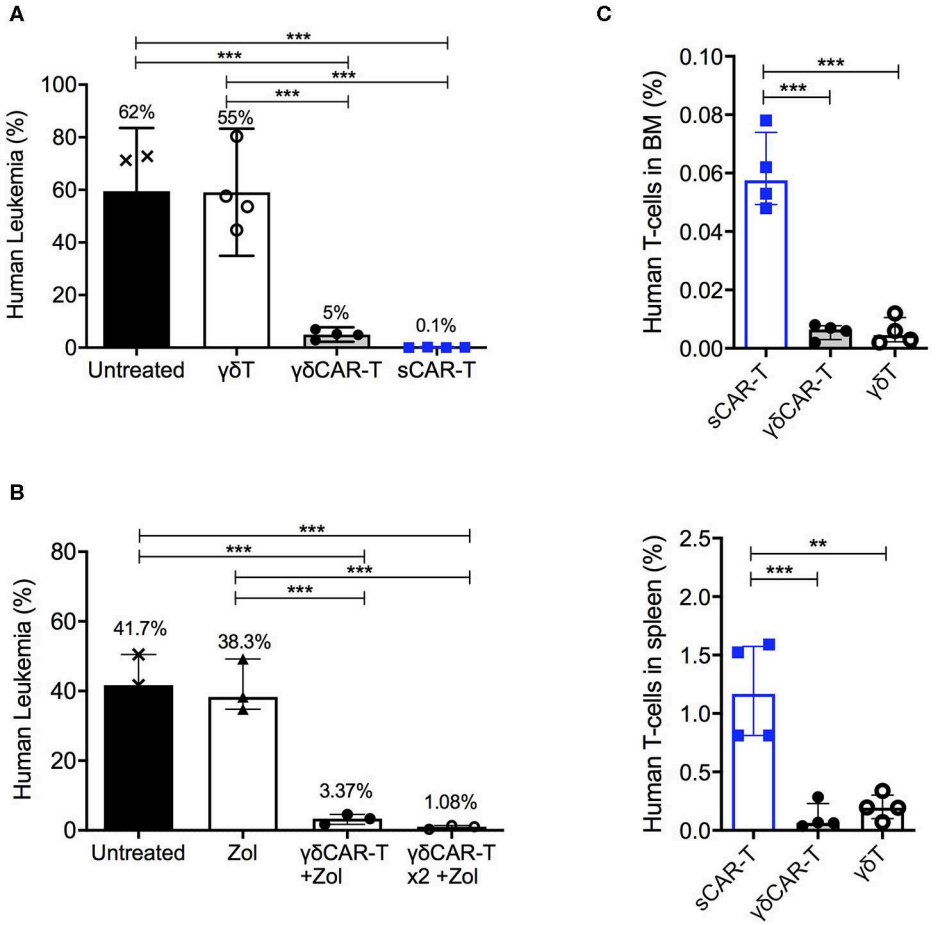

FIGURE 4 | *In vivo* activity of γδCAR-T cells. **(A)** Human leukemia (Nalm6) gated on CD45+ CD10+ in the bone marrow of NSG-mice either untreated or treated with un-transduced γδT cells, γδCAR-T, or sCAR-T cells after 14 days. **(B)** Human leukemia (Nalm6) gated on CD45+ CD10+ in the bone marrow of NSG-mice either untreated or treated with zoledronate (Zol) alone, Zol with γδCART cells, or repeated dose of Zol and γδCAR-T. **(C)** Human effector cell persistence of.i.v. injected sCAR-T, γδCAR-T, and un-transduced γδ-T cells in mice bone marrow (upper panel) and spleen (lower panel), 3 days post injection. $^{**}P \leq 0.01$, $^{***}P \leq 0.001$, Two tailed paired *T*-test. Bars are at the median value, and error bars represent interquartile range.

dose of γδCAR-T cells on day 7, 3×10^6 T cells per mouse, in addition to zoledronate administration regimen lead to further reduction in Nalm6 burden in the marrow to almost 1% ($p = 0.06$, **Figure 4B**).

Since early loss of effector T cells may be associated with target-positive relapse, we next tested the persistence of the infused effector cells within the mice. Cell-trace violet stained γδT, γδCAR-T, and sCAR-T cells (5×10^6 per mouse) were injected to leukemic mice. After 3 days, bone marrow and spleen were harvested and tested for presence of dye positive cells (**Figure 4C**). Lower number of human effector T cells were found in both the spleen and the bone marrow of murine recipients of γδCAR-T and γδT cells compared to recipients of sCAR-T cells ($p < 0.001$ for both comparisons in the bone marrow and $p < 0.01$ for both comparisons in the spleen). Thus, in the NSG model, we noted good anti-leukemic activity but limited persistence of γδCAR-T cells.

DISCUSSION

In this work we demonstrated the ability to effectively transduce and expand γδT cells with a CAR targeting CD19. γδCAR-T were effective against CD19+ tumor cell lines, both *in vivo* and *in vitro*. Moreover, we could see an effect against CD19- clones, which was CAR-independent.

Lack of allogenicity and potential of 3rd party-use make γδ cells excellent candidates as a CAR-T cell backbone. Attempts of γδT cell transduction with CARs have been previously reported, via zoledronate-based expansion of 1st-generation CARs (15) or proliferation of polyclonal γδT cells transduced with CD19 on an antigen-presenting cells (22). Both methods include a selection process, to ensure purity of the γδT cells, similar to our protocol. Of note, both methods showed *in vitro* efficacy against CAR target, but this was not compared to standard CAR-T cells, which in current days of commercially available CAR-T

cells is essential. We preformed head-to-head comparison of the γδCAR-T to sCAR-T, showing comparable transduction efficacy and *in vitro* cytotoxicity against CD19 positive targets, and an *in vivo* effect that was profound, but inferior to that of sCAR-T. We also demonstrated the presence of γδCAR-T cells in clinical products, though at low percentages. The Sadelain group has previously showed comparable activity of γδCAR-T and sCAR-T *in vitro* and *in vivo*, against an intraperitoneal Raji tumor model (23). Raji, a Burkitt-NHL cell line, is known to express co-stimulatory molecules (24), which may have assisted *in vivo* killing by the γδCAR-T cells. Similar to others (22), we too could not show complete clearance of the aggressive Nalm6 ALL cell line in murine models treated with γδCAR-T cells, which might be explained by the limited persistence of γδCAR-T cells in comparison to sCAR-T cells. Indeed repeated infusion of the γδCAR-T improved anti-leukemic results. Loss of γδCAR-T may be a result of several factors, including lack of a supporting microenvironment for these cells in an immune-suppressed mouse, which may be improved with cytokine supplementation such as IL-2 (25). Another possible contribution may be due to increased activation-induced cell death (AICD) known to occur with activated γδT cells. These challenges should be addressed in further work.

The loss of CD19 is a major problem in relapsed patients with persisting CAR-T cells, or patients with prior CD19-directed therapy (26). Current models of using two (or more) CARs transduced on a single cell (by various methods) (27) show some success in preclinical models, but clinical results have not yet matured. Also, sequential antigen loss has been shown in patients with NHL or ALL. Utilizing the natural non-MHC restricted targeting optional by γδT cells has shown anti-leukemic activity, which can be enhanced after priming with zoledronate (13). We showed that this effect is retained after CAR transduction of γδT cells, and is independent of CAR activation by its ligand, as demonstrated by targeting antigen-negative cells. Thus, exploiting this non-specific MHC-independent targeting mechanism on top of the CAR specificity may prevent antigen loss and subsequent relapse and requires further investigation.

In conclusion, we established a rapid and robust protocol for γδCAR-T cell production. These cells demonstrated anti-tumor activity *in vitro* and *in vivo*. γδCAR-T cell may provide a promising platform in the allogeneic setting, and may target antigen-negative clones. Further challenges, including improving *in vivo* persistence, are to be addressed prior to clinical application. The equations should be inserted in editable format from the equation editor.

DATA AVAILABILITY STATEMENT

The raw data supporting the conclusions of this article will be made available by the authors, without undue reservation.

ETHICS STATEMENT

The animal study was reviewed and approved by institutional ethical review process committee.

AUTHOR CONTRIBUTIONS

MR, EJ, IB, and MB contributed conception and design of the study. MR, AM, YA, and OI performed experiments and acquired the data. MR wrote the first draft of the manuscript. EJ, IB, JS, and MB revised it critically for important intellectual content. All authors contributed to manuscript revision, read, and approved the submitted version.

FUNDING

This work was funded by the Dotan Research Center for Hematologic Malignancies, Tel Aviv University, Israel.

ACKNOWLEDGMENTS

We would like to thank Prof. Shai Izraeli and members of his lab, Dr. Nira Bloom and Dr. Victoria Marcu-Malina for technical assistance and fruitful discussions, and Ms. Diana Bar for assistance with patient and volunteer samples.

REFERENCES

1. June CH, Sadelain M. Chimeric antigen receptor therapy. *N Engl J Med*. (2018) 379:64–73. doi: 10.1056/NEJMra1706169
2. Jacoby E, Shahani SA, Shah NN. Updates on CAR T-cell therapy in B-cell malignancies. *Immunol Rev*. (2019) 290:39–59. doi: 10.1111/imr.12774
3. Salter AI, Pont MJ, Riddell SR. Chimeric antigen receptor modified T cells: CD19 and the road beyond. *Blood*. (2018) 131:2621–9. doi: 10.1182/blood-2018-01-785840
4. Hamieh M, Dobrin A, Cabriolu A, van der Stegen SJC, Giavridis T, Mansilla-Soto J, et al. CAR T cell trogocytosis and cooperative killing regulate tumour antigen escape. *Nature*. (2019) 568:112–6. doi: 10.1038/s41586-019-1054-1
5. Shah NN, Fry TJ. Mechanisms of resistance to CAR T cell therapy. *Nat Rev Clin Oncol*. (2019) 16:372–85. doi: 10.1038/s41571-019-0184-6
6. Perna F, Berman SH, Soni RK, Hendrickson RC, Brennan CW, Sadelain M. Integrating proteomics and transcriptomics for systematic combinatorial chimeric antigen receptor therapy of AML article integrating proteomics and transcriptomics for systematic combinatorial chimeric antigen receptor therapy of AML. *Cancer Cell*. (2017) 32:506–19.e5. doi: 10.1016/j.ccell.2017.09.004
7. Hegde M, Mukherjee M, Grada Z, Pignata A, Landi D, Navai SA, et al. Tandem CAR T cells targeting HER2 and IL13R α 2 mitigate tumor antigen escape. *J Clin Invest*. (2016) 126:3036–52. doi: 10.1172/JCI83416
8. Shalabi H, Kraft IL, Wang HW, Yuan CM, Yates B, Delbrook C, et al. Sequential loss of tumor surface antigens following chimeric antigen receptor T-cell therapies in diffuse large B-cell lymphoma. *Haematologica*. (2018) 103:e215–8. doi: 10.3324/haematol.2017.183459
9. Legut M, Cole DK, Sewell AK. The promise of γδ T cells and the γδ T cell receptor for cancer immunotherapy. *Cell Mol Immunol*. (2015) 12:656–68. doi: 10.1038/cmi.2015.28
10. Silva-Santos B, Serre K, Norell H. γδ T cells in cancer. *Nat Rev Immunol*. (2015) 15:683–91. doi: 10.1038/nri3904
11. Fournié JJ, Sicard H, Poupot M, Bezombes C, Blanc A, Romagné F, et al. What lessons can be learned from γδ T cell-based cancer immunotherapy trials? *Cell Mol Immunol*. (2013) 10:35–41. doi: 10.1038/cmi.2012.39

12. Marcu-Malina V, Garelick D, Peshes-Yeloz N, Wohl A, Zach L, Nagar M, et al. Peripheral blood-derived, γ9δ2 t cell-enriched cell lines from glioblastoma multiforme patients exert anti-tumoral effects *in vitro*. *J Biol Regul Homeost Agents*. (2016) 30:17–30.
13. Airoldi I, Bertaina A, Prigione I, Zorzoli A, Pagliara D, Cocco C, et al. γδ T-cell reconstitution after HLA-haploidentical hematopoietic transplantation depleted of TCR-αβ+/CD19+ lymphocytes. *Blood*. (2015) 125:2349–58. doi: 10.1182/blood-2014-09-599423
14. Deniger DC, Moyes JS, Cooper LJN. Clinical applications of gamma deltaT cells with multivalent immunity. *Front Immunol*. (2014) 5:636. doi: 10.3389/fimmu.2014.00636
15. Rischer M, Pscherer S, Duwe S, Vormoor J, Rossig C. Human γδ T cells as mediators of chimaeric-receptor redirected anti-tumour immunity. *Br J Haematol*. (2004) 126:583–92. doi: 10.1111/j.1365-2141.2004.05077.x
16. Wilhelm M, Kunzmann V, Eckstein S, Reimer P, Weissinger F, Ruediger T, et al. γδ T cells for immune therapy of patients with lymphoid malignancies. *Blood*. (2003) 102:200–6. doi: 10.1182/blood-2002-12-3665
17. Itzhaki O, Jacoby E, Nissani A, Levi M, Nagler A, Kubi A, et al. Head-to-head comparison of in-house produced CD19 CAR-T cell in ALL and NHL patients. *J Immunother Cancer*. (2020) 8:e000148. doi: 10.1136/jitc-2019-000148
18. Jacoby E, Bielorai B, Avigdor A, Itzhaki O, Hutt D, Nussboim V, et al. Locally produced CD19 CAR T cells leading to clinical remissions in medullary and extramedullary relapsed acute lymphoblastic leukemia. *Am J Hematol*. (2018) 93:1485–92. doi: 10.1002/ajh.25274
19. Walker AJ, Majzner RG, Zhang L, Wanhainen KM, Long AH, Nguyen SM, et al. Tumor antigen and receptor densities regulate efficacy of a chimeric antigen receptor targeting anaplastic lymphoma kinase. *Mol Ther*. (2017) 25:2189–201. doi: 10.1016/j.ymthe.2017.06.008
20. Zhao D, Wu J, Zhao Y, Shao W, Cheng Q, Shao X, et al. Zoledronic acid inhibits TSC2-null cell tumor growth via RhoA/YAP signaling pathway in mouse models of lymphangioleiomyomatosis. *Cancer Cell Int*. (2020) 20:1–11. doi: 10.1186/s12935-020-1131-4
21. Santolaria T, Robard M, Leger A, Catros V, Bonneville M, Scotet E. Repeated systemic administrations of both aminobisphosphonates and human V 9V 2 T cells efficiently control tumor development *in vivo*. *J Immunol*. (2013) 191:1993–2000. doi: 10.4049/jimmunol.1300255
22. Deniger DC, Switzer K, Mi T, Maiti S, Hurton L, Singh H, et al. Bispecific T-cells expressing polyclonal repertoire of endogenous γδ T-cell receptors and introduced CD19-specific chimeric antigen receptor. *Mol Ther*. (2013) 21:638–47. doi: 10.1038/mt.2012.267
23. Themeli M, Kloss CC, Ciriello G, Fedorov VD, Perna F, Gonen M, et al. Generation of tumor-targeted human T lymphocytes from induced pluripotent stem cells for cancer therapy. *Nat Biotechnol*. (2013) 31:928–33. doi: 10.1038/nbt.2678
24. Brentjens RJ, Santos E, Nikhamin Y, Yeh R, Matsushita M, La Perle K, et al. Genetically targeted T cells eradicate systemic acute lymphoblastic leukemia xenografts. *Clin Cancer Res*. (2007) 13:5426–35. doi: 10.1158/1078-0432.CCR-07-0674
25. Casetti R, Perretta G, Taglioni A, Mattei M, Colizzi V, Dieli F, et al. Drug-induced expansion and differentiation of Vd9Vg2T cells *in vivo*: the role of exogenous IL-2. *J Immunol*. (2005) 175:1593–8. doi: 10.4049/jimmunol.175.3.1593
26. Pillai V, Muralidharan K, Meng W, Bagashev A, Oldridge DA, Rosenthal J, et al. CAR T-cell therapy is effective for CD19-dim B-lymphoblastic leukemia but is impacted by prior blinatumomab therapy. *Blood Adv*. (2019) 3:3539–49. doi: 10.1182/bloodadvances.2019000692
27. Hartmann J, Schüßler-Lenz M, Bondanza A, Buchholz CJ. Clinical development of CAR T cells—challenges and opportunities in translating innovative treatment concepts. *EMBO Mol Med*. (2017) 9:e201607485. doi: 10.15252/emmm.201607485

Conflict of Interest: The authors declare that the research was conducted in the absence of any commercial or financial relationships that could be construed as a potential conflict of interest.

frontiers in Immunology

ORIGINAL RESEARCH
published: 07 July 2020
doi: 10.3389/fimmu.2020.01396

Vγ9Vδ2 T Cells Activation Through Phosphoantigens Can Be Impaired by a RHOB Rerouting in Lung Cancer

*Chloé Laplagne [1,2,3], Sarah Meddour [1,2,3], Sarah Figarol [1,2,3], Marie Michelas [1,2,3], Olivier Calvayrac [1,2,3], Gilles Favre [1,2,3,4], Camille Laurent [1,2,3,4], Jean-Jacques Fournié [1,2,3], Stéphanie Cabantous [1,2,3] and Mary Poupot [1,2,3]**

[1] Centre de Recherches en Cancérologie de Toulouse, Inserm UMR1037, Toulouse, France, [2] Université Toulouse III Paul-Sabatier, Toulouse, France, [3] ERL 5294 CNRS, Toulouse, France, [4] IUCT-O, Toulouse, France

Vγ9Vδ2 T cells are known to be efficient anti-tumor effectors activated through phosphoantigens (PAg) that are naturally expressed by tumor cells or induced by amino bisphosphonates treatment. This PAg-activation which is TCR and butyrophilin BTN3A dependent can be modulated by NKG2D ligands, immune checkpoint ligands, adhesion molecules, and costimulatory molecules. This could explain the immune-resistance observed in certain clinical trials based on Vγ9Vδ2 T cells therapies. In NSCLC, encouraging responses were obtained with zoledronate administrations for 50% of patients. According to the *in vivo* results, we showed that the *in vitro* Vγ9Vδ2 T cell reactivity depends on the NSCLC cell line considered. If the PAg-pretreated KRAS mutated A549 is highly recognized and killed by Vγ9Vδ2 T cells, the EGFR mutated PC9 remains resistant to these killers despite a pre-treatment either with zoledronate or with exogenous BrHPP. The immune resistance of PC9 was shown not to be due to immune checkpoint ligands able to counterbalance NKG2D ligands or adhesion molecules such as ICAM-1 highly expressed by PC9. RHOB has been shown to be involved in the Vγ9Vδ2 TCR signaling against these NSCLC cell lines, in this study we therefore focused on its intracellular behavior. In comparison to a uniform distribution of RHOB in endosomes and at the plasma membrane in A549, the presence of large endosomal clusters of RHOB was visualized by a split-GFP system, suggesting that RHOB rerouting in the PC9 tumor cell could impair the reactivity of the immune response.

Keywords: RHOB, Vγ9Vδ2 T cells, phosphoantigen, endosomes, split-GFP, TCR activation

OPEN ACCESS

Edited by:
Ilan Bank,
Sheba Medical Center, Israel

Reviewed by:
Emmanuel Scotet,
Institut National de la Santé et de la Recherche Médicale (INSERM), France
Zsolt Sebestyen,
University Medical Center Utrecht, Netherlands

***Correspondence:**
Mary Poupot
mary.poupot@inserm.fr

Specialty section:
This article was submitted to T Cell Biology, a section of the journal Frontiers in Immunology

Received: *01 April 2020*
Accepted: *01 June 2020*
Published: *07 July 2020*

Citation:
Laplagne C, Meddour S, Figarol S, Michelas M, Calvayrac O, Favre G, Laurent C, Fournié J-J, Cabantous S and Poupot M (2020) Vγ9Vδ2 T Cells Activation Through Phosphoantigens Can Be Impaired by a RHOB Rerouting in Lung Cancer. Front. Immunol. 11:1396. doi: 10.3389/fimmu.2020.01396

INTRODUCTION

Gamma delta (γδ) T lymphocytes expressing the T cell receptor (TCR) Vγ9Vδ2 are a prominent γδ T cell subset in human peripheral blood representing 1–3% of blood mononuclear cells. Upon activation with non-peptide phosphoantigens (PAgs), these Vγ9Vδ2 T cells proliferate, produce chemokines and cytokines, and mediate cell cytotoxicity against a large spectrum of tumor cells (1). These molecules are metabolites from the methyl erythritol phosphate pathway in microbial pathogens (2) and from the eukaryotic mevalonate pathway in tumor cells which are thus spontaneously recognized and killed by Vγ9Vδ2 T cells (3, 4). In humans, treatment with aminobisphosphonates such as zoledronate can exacerbate Vγ9Vδ2 T cell reactivity through

the upregulation of the endogenous biosynthesis of PAgs in mammalian cells (5). This PAgs activation was clearly shown to be TCR-dependent. However, as Vγ9Vδ2 T cells express different activator and inhibitor receptors such as immune checkpoint inhibitors and natural killer (NK) receptors, their reactivity can also be exacerbated or curbed by ligands expressed by target cells (6, 7). Thus, even overproduction of endogenous PAgs might reflect the metabolic biases of cancer cells, and presumably occurs in most if not all types of tumors, some of which are resistant to Vγ9Vδ2 T killing. Accordingly, tumor-infiltrating γδ T cells have been detected in several solid and hematopoietic malignancies but are not always correlated with a good prognosis (8, 9). However, these cells remain very attractive candidates for cancer immunotherapies regarding a tumor regression associated with their significant amplification in the blood for some clinical trials based on PAg treatment or adoptive transfers of Vγ9Vδ2 T cells (10–12). In patients with non-small cell lung cancer (NSCLC), administration of zoledronate was correlated with an increase of Vγ9Vδ2 T cells in blood and a higher overall survival (13). A phase I clinical study showed the safety and potential anti-tumor effect of reinfused *ex-vivo* expanded Vγ9Vδ2 T cells in patients with advanced NSCLC refractory to or intolerant to current conventional treatment (14). These partial responses and the inevitable relapse with classical treatments make NSCLC incurable pathologies for which many mechanisms of acquired resistance have been elucidated, but the recurrent immune-resistance remains obscure. RHOB is a known tumor suppressor in lung cancer, and its downregulation, frequently observed in aggressive tumors (15), is associated with decreased overall survival (16). More recently, RHOB has also been shown to confers resistance to EGFR-tyrosine kinase inhibitors in NSCLC (17), suggesting different roles of this GTPase depending on the oncogenic and/or therapeutic context. Interestingly, RHOB was recently shown to mediate endogenous PAg recognition by the Vγ9Vδ2 TCR (18). RHOB interaction with endogenous PAg in the target cell could induce a modification of the conformation of the membrane butyrophilin BTN3A1 which then activates the Vγ9Vδ2 TCR (19). Here, we investigated the role of RHOB in the response to PAg-mediated γδ T cell activation in two NSCLC cell lines with the most represented oncogenic mutations KRAS and EGFR. After showing that A549 was well-recognized and killed by Vγ9Vδ2 T cells compared to PC9, we found different patterns of surface molecule expression for these two NSCLC cell lines. However, the resistance of PC9 to Vγ9Vδ2 T cell killing could be due to a rerouting of RHOB in late/degradation compartments that may prevent its function with BTN3A1 at the plasma membrane in PC9 cells.

MATERIALS AND METHODS

Reagents and Antibodies

Antibodies for flow cytometry analysis: BV310 anti-CD3, FITC anti-TCRVγ9Vδ2, PE or PeCy5 anti-CD107a, PeCy7 anti-IFNγ, PE anti-TIM3, PE anti-Galectin9, PeCy7 anti-PD1, APC anti-PDL1, PeCy5 anti-CD80, PE anti-CD80, PeCy5 anti-HLAABC, AF647 anti-CD31, PeCy7 anti-CD38, FITC anti-CD226, FITC anti-CD112, FITC anti-CD155, PE anti-LFA1, and isotype controls (BD Biosciences, Pont de Claix, France); BV421 anti-CD69 and isotype control (Miltenyi Biotech, Paris, France); PE anti-HLAE (eBiosciences); PE anti-ULPB2,5,6 (R&D Systems, Minneapolis, USA); APC anti-MICA/B (Biolegend, St-Quentin-en-Yvelines, France); PE anti-ICAM1 and PE anti-ICAM3 (Immunotech, Marseille, France); PE anti-LFA3 (Beckman Coulter, Fullerton, CA, USA).

Blocking antibodies: anti-BTN3A1 1 h at 10 μg/mL (103.2 clone, kindly gifted by ImCheck Therapeutics, Marseille, France), anti-γδTCR 1 h at 0.5 mg/mL (B1 clone, Biolegend), anti-ICAM1 (W-CAM-1 clone, Thermo fisher, Villebon sur Yvette, France) and anti-CD31 1 h at 10 μg/mL (HEC7 clone, Thermo fisher, Villebon sur Yvette, France). The exoenzyme C3 transferase was used as RHO inhibitor I overnight at 2 μg/mL (Cytoskeleton, Inc. Denver, USA).

Flow Cytometry Analysis

Cells were labeled with 5 μg/ml antibodies or isotype controls for 20 min at 4°C and analyzed on an LSRII cytometer (BD Biosciences, Pont de Claix, France). Data were analyzed using BD FACSDiva software, FlowJo software or FlowLogic software.

Vγ9Vδ2 T Cell Cultures

Primary Vγ9Vδ2 T cell cultures were generated from peripheral blood mononuclear cells (PBMCs) isolated from blood of healthy donors (Etablissement Français du Sang, Toulouse, France). Briefly, PBMC were stimulated with BrHPP (3 μM) and rhIL-2 (300 IU/ml) in complete RPMI 1640 culture medium (Invitrogen, Cergy Pontoise, France) supplemented with 10% fetal calf serum (Hy1, Thermo Scientific, USA), 100 g/ml streptomycin, 100 IU/ml penicillin and 1 mM sodium-pyruvate (Cambrex Biosciences, Rockland, ME, USA) for 14 days. Purity of the Vγ9Vδ2 T cells was >95% as determined by flow cytometry using an anti-TCRVγ9Vδ2 mAb.

Lung Cancer Cell Lines

The human NSCLC cell lines A549, H1299, H827, and PC9 were previously obtained from the American Type Culture Collection (Manassas, VA, USA) and cultured in RPMI 1640 medium containing 10% fetal bovine serum (FBS) and were maintained at 37°C in a humidified chamber containing 5% CO_2.

For the RHOB KO A549 and PC9, the TALEN sequences targeting RHOB were designed by CELLECTIS (Paris, France), and inserted into two plasmids comprising CMV and T7 promoters. Triple transfection of the two TALEN-encoding plasmids with a Puromycin selection cassette upstream RHOB gene was performed using the JetPrime® transfection agent (Polyplus transfection) according to the manufacturer's recommendations. Puromycin selection was performed for 48 h after transfection and the pool of surviving clones was subcloned by limit dilution in 96-well plates. For each subclone, RHOB DNA levels and RHOB protein expression were analyzed by PCR and Western Blot.

Cytotoxicity Assay

Lung cancer cell lines were treated at 70% of confluence with BrHPP (1 μM, 4 h, Innate Pharma, Marseille, France) or

Zoledronic acid monohydrate (Zometa, 5 μM, overnight, Sigma Aldrich, Saint Louis, USA). After washing, treated cancer cells were co-cultured in 96-wells plates with overnight IL-2-deprived Vγ9Vδ2 T cells (E:T ratio 1:1) in complete medium with anti-CD107a mAb or IgG1 control (5 μg/ml). Brefeldin A (10 μg/ml, Sigma Aldrich, St Quentin Fallavier, France) was added at 2 h of co-culture. After 4 h of co-culture cells were washed, stained and analyzed by flow cytometry. When mentioned, contact between γδ T cells and target cells was prevented thanks to a Transwell® system (Corning). For intracellular IFNγ expression, cells were fixed with PBS 2% paraformaldehyde and permeabilized with PBS containing 5% FCS and 1% saponin (Sigma-Aldrich) prior to staining for 30 min with the specified mAb for flow cytometry analysis.

Trogocytosis Analysis

Lung cancer cells were stained with the lipophilic green-emitting dye PKH67 (Sigma-Aldrich, Saint Louis, USA) according to the manufacturer's instructions. Then, PKH67-positive cells were co-cultured for 4 h in complete culture medium with PKH67-negative Vγ9Vδ2 T cells in 96-well U-bottom culture plates at a cell ratio of 1:1. After gentle centrifugation (110 g for 1 min) and co-cultures for 3 min or 4 h at 37°C, cells were washed with 0.5 mM PBS/EDTA. Trogocytosis was measured as the acquisition of PKH67 fluorescence, which was characterized via the increase of the mean fluorescence intensity (mfi) of PKH67 by a flow cytometry.

Monitoring RHOB Activity With a Split-GFP Reporter System

To evaluate the effect of PAg, A549, and PC9 cell lines were engineered to express the tripartite split-GFP biosensor system previously developed to monitor RHOB activity in single cells (20). To generate the split-GFP reporter cell line, sequential transductions were performed with lentiviruses encoding for GFP1-9, the detector fragment of the split-GFP system and the chimeric construct that coexpress both RHOB fused to the strand 10 of trisfGFP (GFP10-RHOB) and the RHO-binding domain of Rhotekin (RBD) fused to strand 11 of trisfGFP (RBD-GFP11) in A549-rtTA or PC9-rtTA cells. After recovery, cells were induced with 0.25 μg/mL doxycycline for 24 h and sorted by FACS based on GFP fluorescence. To improve the GFP fluorescence signal upon split-GFP complementation, a GFP nanobody (21) was expressed from a lentiviral expression vector on optimized cell lines.

For both fluorescence quantifications of RHOB activity and analysis of RHOB localization, reporter cells were grown on μ-Slide 8-well ibiTreat chambered coverslips (Ibidi, Biovalley). Cells were seeded at a density of 15,000 cells/well for PC9 and 35,000 cells/well for A549 for 24 h. Split-GFP reporter expression was induced for 24 h with 0.25 μg/ml Doxycycline in RPMI culture medium supplemented with 2% serum (PC9) and 10% serum (A549), and subsequently treated with PAg for 16 h with Zoledronic acid monohydrate or 4 h of BrHPP. To stop the experiment, cells were fixed with 4% PFA, PBS then stained with a cytoplasmic cell mask, HCS CellMaskTM Blue Stain (Thermo Fisher Scientific) according to the supplier's instructions. Quantitative image acquisition was performed using an Operetta high-content imaging system (Perkin Elmer) with a 20× objective lens in the 488/525 nm (GFP) and 360/405 nm (cell mask) channels. Analysis was performed with Harmony® software on an average of 1500 cells/well. The number of objects and the sum of cell area was determined from the cell mask staining. The percentage of GFP cells was calculated as: percentage GFP cells = (number of GFP-positive cells/number of all objects) × 100, where GFP-positive cells are defined by cells following this criteria: mean of fluorescence intensity (MFI) of the object>mean of MFI in the control wells without doxycycline. GFP intensity sum/cell area was defined as the (GFP intensity sum of GFP+ cells)/(HCS intensity sum of GFP+ cells).

For confocal analysis, cells were fixed with 3.7% PFA and permeabilized with 0.1% Triton X-100 in PBS buffer. Blocking was performed with 8% BSA, PBS for 30 min before adding primary antibodies. Anti-GFP10 polyclonal antibody (20) was used at 1:1,000 dilution for 1 h, followed by secondary antibody Alexa fluor 594 conjugate anti rabbit IgG (Life technologies) for 40 min. For labeling endosomes, the following primary antibodies were used: Rab7 [(D95F2) XP 9367, Cell signaling] 1:50, LAMP1 (H5G11) sc-18821, Santa Cruz Biotechnology 1:50. After overnight incubation, secondary antibodies were added Alexa fluor 594 conjugate anti rabbit IgG (Life technologies) and Alexa fluor 647 conjugate anti mouse IgG (Life technologies). Microscopy images were acquired using LSM 780 or LSM 880 (Zeiss, Oberkochen, Germany) confocal laser scanning microscopes using a 488 Argon laser with a 490–553 nm emission filter (GFP) Alexa 594 and DAPI labeling were acquired with Argon laser (543 nm) and 405 UV diode lasers, respectively, using 20x and 63×/1.4 oil immersion objectives. Image analysis was performed with ImageJ® software.

Statistical Analysis

Data are expressed as means ± SEM. For comparison of two series of normally distributed variables, we used paired and one-tailed Student's *t*-tests with $\alpha = 0.05$ for statistical significance. Statistical analysis were performed with Prism software.

RESULTS

Differential Activation of Vγ9Vδ2 T Cells by Different PAg-Treated NSCLC Cell Lines

To analyze the role of RHOB in Vγ9Vδ2 T cell reactivity against NSCLC, we first screened the basal reactivity of Vγ9Vδ2 T cells against four cell lines with different mutation statuses: A549 (KRAS mutant), H1299 (HRAS mutant), PC9 and H827 (EGFR mutant). The expression of CD107a and IFNγ by Vγ9Vδ2 T cells after co-cultures with the different tumor cell lines was measured by flow cytometry. Compared to the Daudi control target cells, which induced CD107a and IFNγ expression by Vγ9Vδ2 T cells, no basal reactivity was detected with the four NSCLC cell lines (**Figures 1A,B** black dots). However, incubation of these cell lines with zoledronate (red dots) or with an exogenous synthetic PAg, BrHPP (blue dots), induced a high increase of the percentage of IFNγ and CD107a positive Vγ9Vδ2 T cells in co-culture with A549, H827, and H1299 but

not with PC9 (**Figure 1B**). We then checked that this reactivity was due to an immunological synapse following a contact between Vγ9Vδ2 T cells and NSCLC target cells and not to PAg excreted in the co-culture medium. Vγ9Vδ2 T cells were thus incubated for 4 h with A549 or PC9, previously treated with PAg, and separated by a Transwell (TW) membrane or with their conditioned medium. As shown in **Figure 1C**, no CD107a expression was detected in Vγ9Vδ2 T cells in the TW condition or in the conditioned medium condition (CM) (**Figure 1C** for a representative experiment and **Supplementary Figure 1** for pooled experiments). Trogocytosis was also evaluated to confirm the contact dependent reactivity of Vγ9Vδ2 T cells against A549. Trogocytosis is the transfer of membrane patches following the establishment of an immunological synapse between a T lymphocyte and a target cell. The membrane transfer was measured by the increase of green (PKH67) fluorescence expressed by the Vγ9Vδ2 T following contact with the A549 cell line previously stained with the PKH67 fluorescent probe stably inserted into the plasma membrane. Vγ9Vδ2 T cells expressed PKH67 fluorescence after 4 h of contact with PAg-treated PKH67$^+$A549 compared to 5 min of contact (**Figure 1D** for a representative experiment and **Supplementary Figure 2** for pooled experiments). CD107a and IFNγ expression by Vγ9Vδ2 T cells, and their trogocytosis in reaction to A549 were correlated with the death of A549 (**Figure 1E** and **Supplementary Figure 3A**). On the contrary, PC9, even treated by phosphoantigens was relatively resistant to Vγ9Vδ2 T cell killing (**Figure 1F** and **Supplementary Figure 3B**).

Vγ9Vδ2 T cells can thus be highly activated to kill A549 but not PC9, when previously treated with phosphoantigens.

Expression of Different Patterns of Surface Ligands and Adhesion Molecules on A549 and PC9

The immunological synapse between Vγ9Vδ2 T cells and tumor cells involves different surface molecules such as activator and inhibitor ligands/receptors, and adhesion molecules. Expression of these molecules at the surface of A549, PC9, and the Vγ9Vδ2 T cells was performed by flow cytometry analysis. With regard to the adhesion molecule pattern, LFA-1, LFA-3, and CD155 were expressed at the same level by A549 and PC9 whilst ICAM-3, CD112, CD31, and the costimulatory ligands CD80/CD86 were not expressed (**Figure 2A** and **Supplementary Figure 4A**). However, PC9 expressed high levels of the adhesion molecule ICAM-1 compared to A549, and A549 expressed high level of CD38 compared to PC9. The corresponding receptors were checked at the surface of Vγ9Vδ2 T cells which thus expressed LFA-1, ICAM-1, ICAM-3, CD2, LFA-3, CD226, CD38, and CD31 (**Figure 2B**). Considering the activator and inhibitor ligands, A549 expressed less ULBPs and PDL1 than PC9 but more HLA-A,B,C whereas MICA/B and galectin-9 were not expressed neither by A549 nor by PC9 (**Figure 2A**), Vγ9Vδ2 T cells expressed the corresponding receptors NKG2A, NKG2D, PD1, and Tim-3 (**Figure 2B**). The level of expression of all these ligands/receptors on A549 and PC9 were not statistically affected by PAg treatment (**Supplementary Figure 4B**). We then investigated which surface molecules were involved in Vγ9Vδ2 T cell activation using blocking antibodies. We showed that blocking the LFA-3/CD2 axis decreased IFNγ expression by Vγ9Vδ2 T cells in contact with A549 pretreated either with zoledronate or with BrHPP whilst blocking ICAM-1/LFA-1 or CD31/CD38 had no effect (**Figure 2C**). On the contrary, the weak Vγ9Vδ2 T cell activation by PC9 was decreased at the level of the ICAM-1/LFA-1 axis, whilst blocking of LFA-3/CD2 and of CD31/CD38 had no effect (**Figure 2D**). Moreover, neither the blocking of NKG2D nor PD1 had an impact on Vγ9Vδ2 T cell activation by A549 or PC9.

Finally, A549 and PC9 displayed different patterns of surface ligands and adhesion molecules and involved different surface molecules in PAg-dependent activation of Vγ9Vδ2 T cells. However, these differences cannot be sufficient to explain the different activation of Vγ9Vδ2 T cells by PC9 compared to A549. Indeed, PC9 expresses a high proportion of the inhibitory PDL1 and a high amount of ICAM-1 and ULBPs which are supposed to favor a productive immunological synapse. Conversely, A549 expresses CD38 but also expresses the inhibitory ligand HLA-A,B,C and a weak amount of ULBPs.

As the difference in surface markers of the two NSCLC cell lines did not explain the difference in Vγ9Vδ2 T cells activation, we decided to explore inside the cells.

RHOB Deletion in PAg-Treated A549 Cell Lines Decreases Vγ9Vδ2 T Cell Activation

BTN3A1 was previously shown to be involved in Vγ9Vδ2 T cell TCR-dependent activation. BTN3A1 may interact with the Vγ9Vδ2 TCR upon association with RHOB activated by its interaction with endogenous phosphoantigens (18). Thus, we investigated the role of RHOB in Vγ9Vδ2 T cell activation by these NSCLC cell lines. Firstly, A549 and PC9 cell lines were shown to express BTN3A1 at the transcriptomic and protein level (**Figures 3A,B**). Interestingly, PAg treatment of these cell lines had no impact on their BTN3A1 expression. We then determined whether Vγ9Vδ2 T cell activation by zoledronate- or BrHPP-treated NSCLC cell lines was BTN3A1-dependent using a blocking antibody (103.2 clone). The percentage of Vγ9Vδ2 T cells expressing IFNγ, CD107a and CD69 following contact with BrHPP- or zoledronate-treated A549 was highly decreased by the presence of anti-BTN3A1 during the co-culture (**Figure 3C** for a representative experiment and **Figure 3D** for pooled experiments). BTN3A1 blocking also abrogated the weak activation of Vγ9Vδ2 T cells by the PC9 cell line (**Figure 3E** for a representative experiment and **Figure 3F** for pooled experiments). Thus, the high activation of Vγ9Vδ2 T cells by PAg-treated A549 and the weak activation by PAg-treated PC9 are totally dependent on BTN3A1. As RHOB has been implicated in the regulation of the immune response through BTN3A1 modulation (18), we studied the implication of this GTPase in Vγ9Vδ2 T cell activation by NSCLC cell lines. RHOB was knocked out in the A549 and PC9 cell lines by the TALEN gene silencing method (**Supplementary Figure 5**). We then assessed the effect of this knockdown (KO) on Vγ9Vδ2 T cell activation by measuring IFNγ and CD107a expression, and trogocytosis

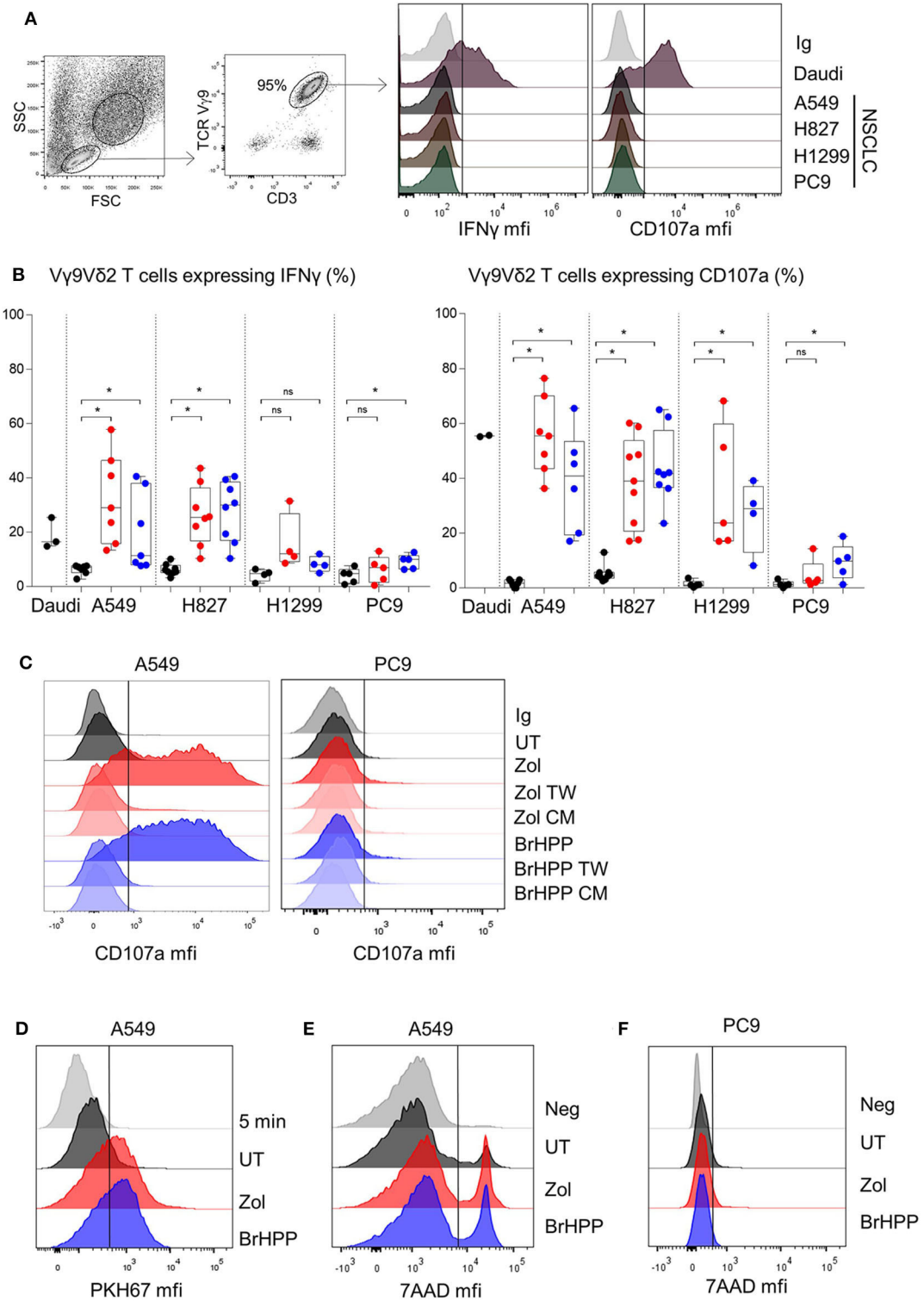

FIGURE 1 | PAg-treated NSCLC cell lines activate Vγ9Vδ2 T cells in a contact dependent manner. Flow cytometry analysis of the IFNγ and CD107a expression by Vγ9Vδ2 T cells in co-culture for 4 h with four different NSCLC cell lines without pretreatment **(A)** or with zoledronate (red dots) or BrHPP (blue dots) pretreatment [**(B)**, $n > 4$ independent experiments], with Transwell system or tumor cell lines conditioned medium in case of A549 and PC9 as target **(C)**. Flow cytometry analysis of the trogocytosis of the PKH67^{+} PAg-treated A549 cell line by the Vγ9Vδ2 T cells after 5 min or 4 h of co-culture, i.e., PKH67 expression by the Vγ9Vδ2 T cells **(D)**. Measure by flow cytometry of the 7-AAD positive PAg-treated-A549 **(E)** or -PC9 **(F)** after co-culture with Vγ9Vδ2 T cells for 4 h. *indicates $p < 0.05$, Student's paired *t*-test; ns: no significant.

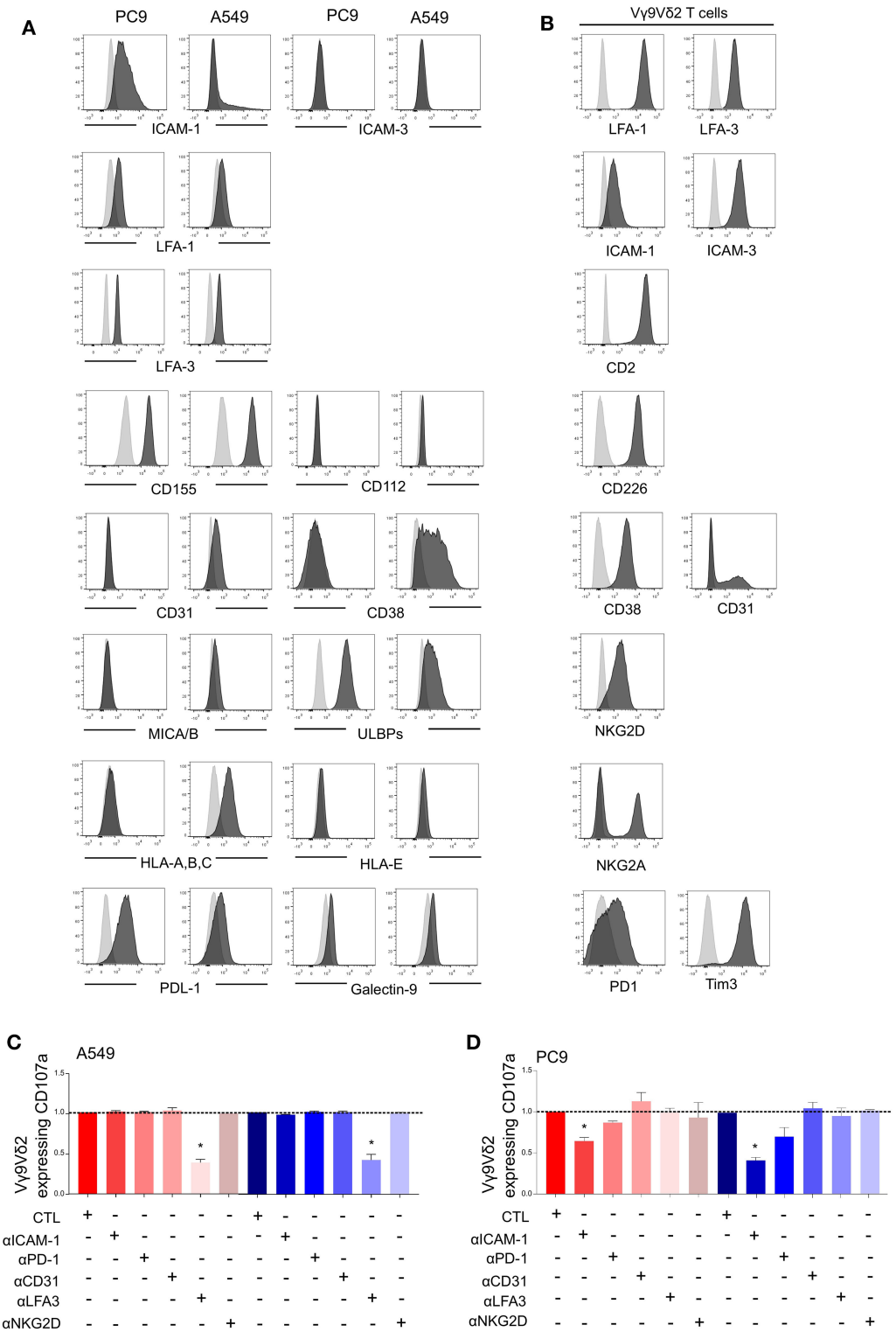

FIGURE 2 | Vγ9Vδ2 T cells activation by PAg-treated-A549 or -PC9 is dependent on different adhesion molecules. Flow cytometry analysis of the expression of surface markers (black) by PC9 and A549 cell lines **(A)** or by the Vγ9Vδ2 T cells **(B)** compared to the respective isotypic control (gray). CD107a expression by the Vγ9Vδ2 T cells after 4 h of co-culture with zoledronate-treated A549 [**(C)**, red] or BrHPP-treated A549 [**(C)**, blue] or with zoledronate-treated PC9 [**(D)**, red] or BrHPP-treated PC9 [**(D)**, blue] in the presence of different blocking antibodies normalized to the control condition (CTL) without blocking antibody. *indicates $p < 0.05$.

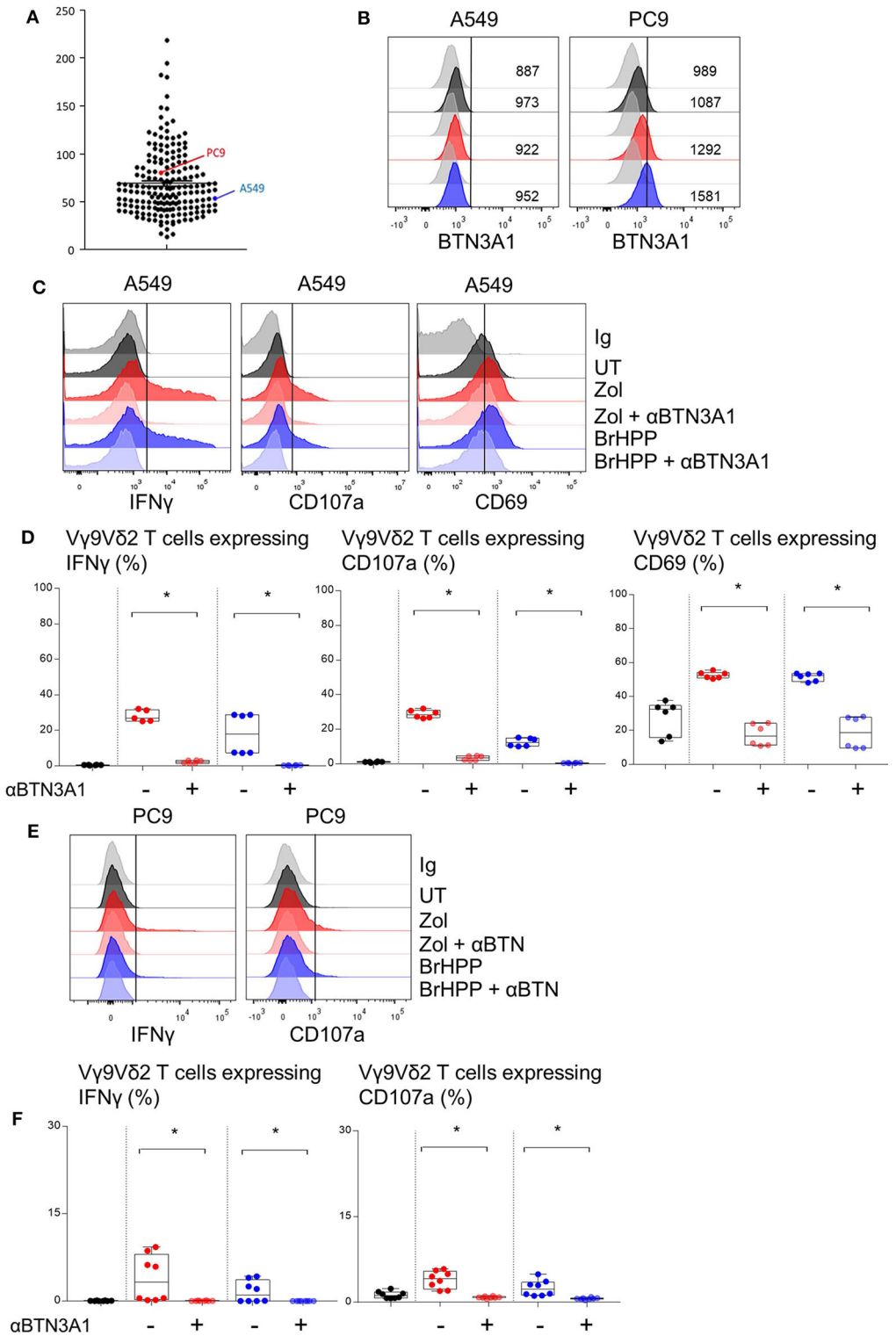

FIGURE 3 | PAg-treated A549/PC9 cell lines activating Vγ9Vδ2 T cells is BTN3A1 dependent. **(A)** mRNA expression of the BTN3A1 by A549 and PC9 cell lines among cancer cell lines in the Cancer Cell Line Encyclopedia (CCLE). **(B)** Flow cytometry analysis of the BTN3A1 expression by A549 and PC9 pre-treated or not (black) by zoledronate (red) or BrHPP (blue) and compared to the isotypic control (gray). **(C–F)** Flow cytometry analysis of the IFNγ, CD107a, and CD69 expression by Vγ9Vδ2 T cells in co-culture for 4 h with A549 [**(C,D)**: six independent experiments] or PC9 [**(E,F)**: six independent experiments] without pretreatment (black) or with zoledronate (red) or BrHPP (blue) pretreatment. *indicates $p < 0.05$.

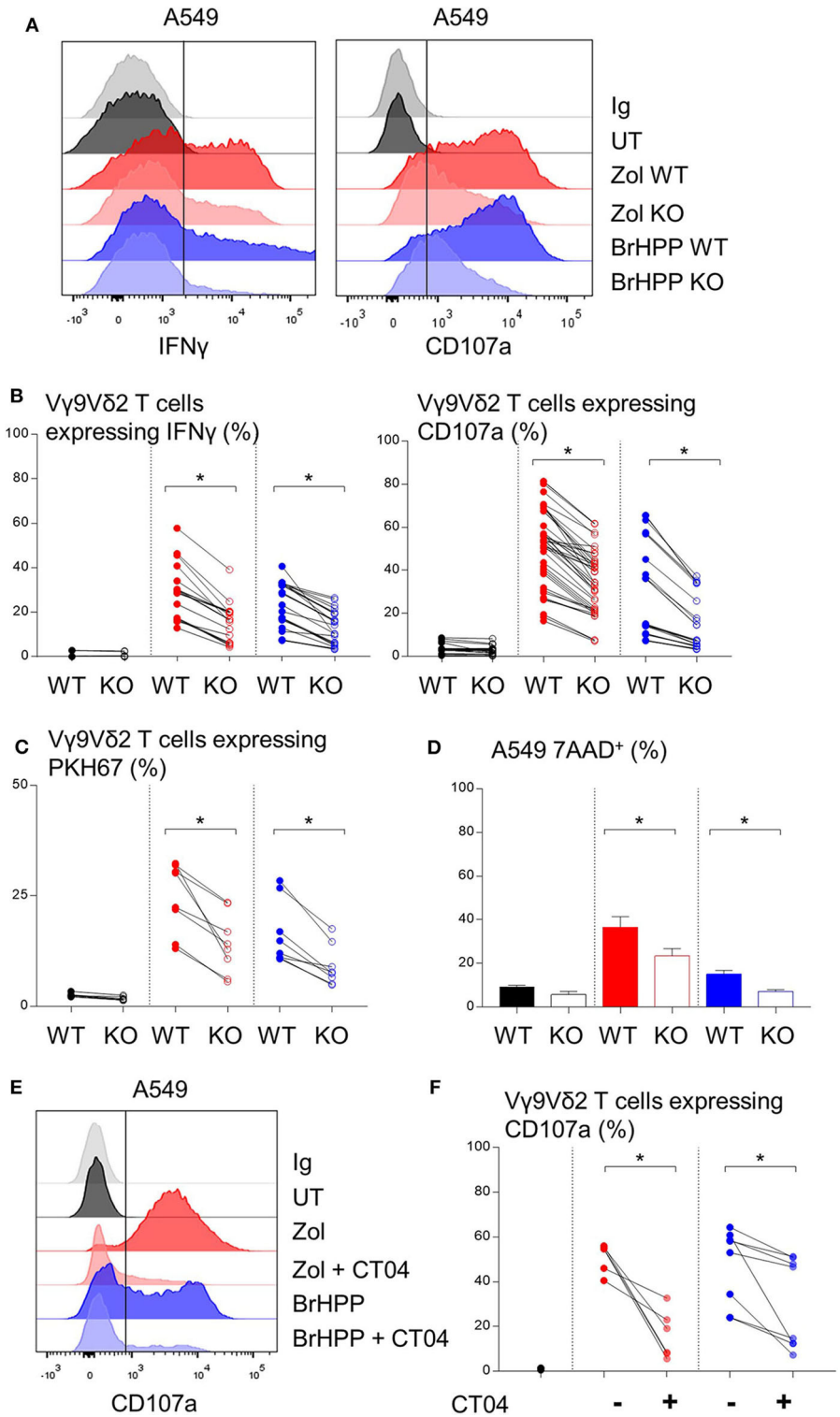

FIGURE 4 | Decrease of the Vγ9Vδ2 T cells activation by A549 with RHOB knock down. Flow cytometry analysis of the IFNγ and CD107a expression by Vγ9Vδ2 T cells in co-culture for 4 h with A549 wild type (WT) or knock down for RHOB (KO) with zoledronate (red) or BrHPP (blue) pretreatment [**(A)**: one representative experiment, **(B)**: $n > 10$ independent experiments]. **(C)** Flow cytometry analysis of the trogocytosis of the PKH67$^+$ PAg-pretreated-A549 cell line WT or KO by the Vγ9Vδ2 T cells (ratio of the Vγ9Vδ2 T cells expressing PKH67 4 h/5 min). **(D)** Flow cytometry analysis of the 7AAD expression by the WT or KO A549 cell line PAg-treated (zoledronate: red, BrHPP: blue) or not (black) in co-culture for 4 h with the Vγ9Vδ2 T cells. **(E,F)** CD107a expression by the Vγ9Vδ2 T cells analyzed by flow cytometry after 4 h of contact with PAg-pretreated A549 in the presence or not of the CT04 inhibitor [**(E)**: one representative experiment, **(F)**: $n > 4$ independent experiments]. *indicates $p < 0.05$.

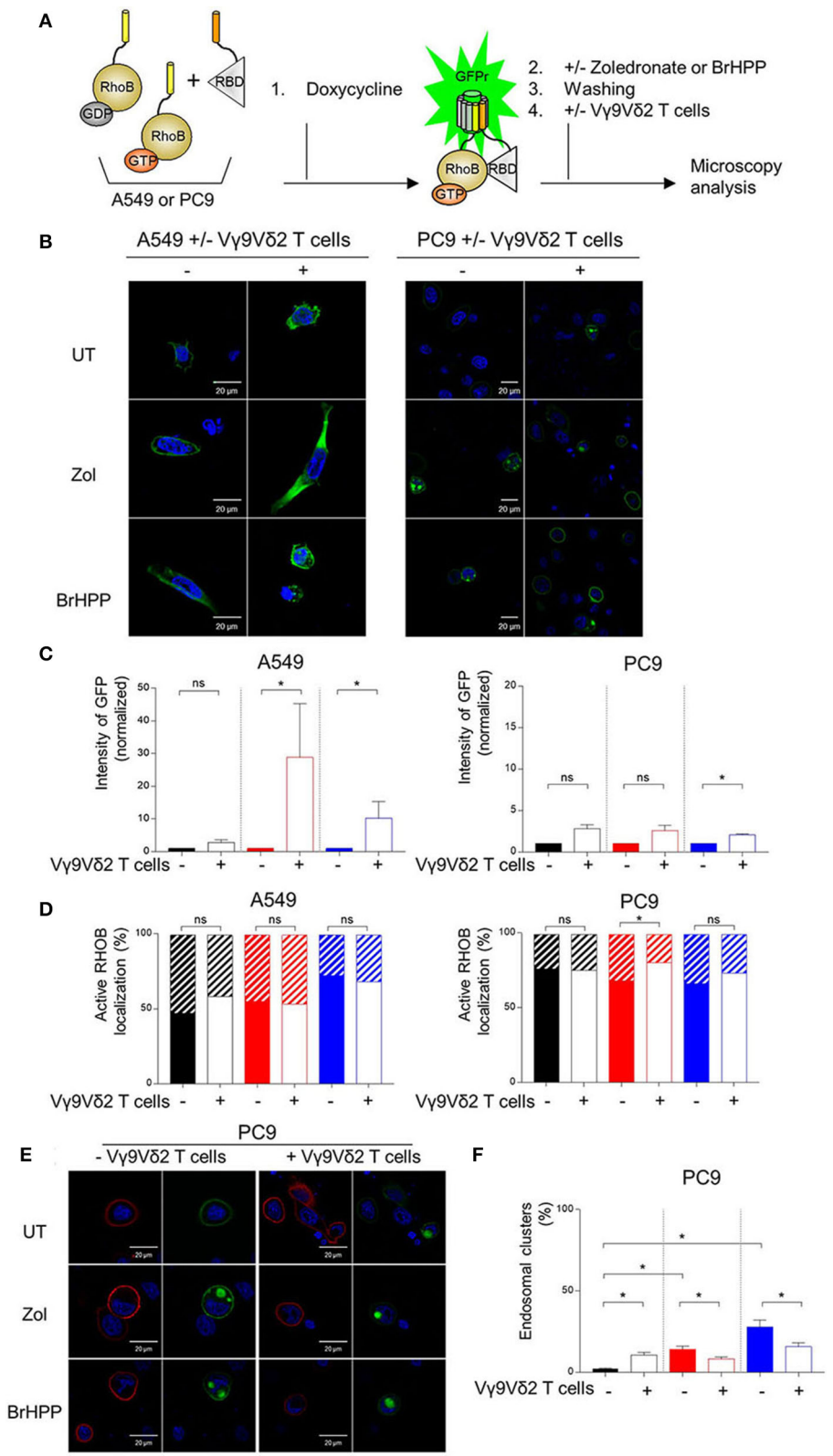

FIGURE 5 | Membrane localization of RHOB favored in A549 cells in contact with Vγ9Vδ2 T cells. **(A)** A549 and PC9 cells were engineered to stably express RHOB GTPase and monitor active RHOB using a split GFP system. Induction by Doxycycline of the tripartite split-GFP system in A549 and PC9, with or without (UT) pretreatment with zoledronate (zol) or BrHPP, and co-cultured or not with Vγ9Vδ2 T cells. Active RHOB (green fluorescence) was visualized by confocal microscopy

(Continued)

FIGURE 5 | (B) and quantified by Operetta [**(C)**: zoledronate: red, BrHPP: blue]. **(D)** Percentage of endosomal (hatched bars) or membrane (full bars) active RHOB quantified by confocal microscopy in A549 and PC9 cell lines PAg-treated (zoledronate: red, BrHPP: blue) or not (black) co-cultured with Vγ9Vδ2 T cells. **(E,F)** Confocal microscopy of total (red) and active (green) RHOB in PC9 cell line after PAg-treatment (zoledronate: red, BrHPP: blue) or not (black) and co-cultured or not with Vγ9Vδ2 T cells [**(E)**: representative images; **(F)**: % of PC9 presenting endosomal clusters based on 3 independent experiments among 30 cells]. *indicates $p < 0.05$, Student's paired *t*-test; ns: no significant.

after co-culture with the PAg-treated RHOB KO A549 or the PAg-treated RHOB KO PC9. IFNγ and CD107a expression by Vγ9Vδ2 T cells was lower in the co-culture with A549 RHOB KO treated either by zoledronate or BrHPP compared to the co-culture with PAg-treated A549 wild type (WT) (**Figure 4A** for a representative experiment and **Figure 4B** for pooled experiments). Trogocytosis of A549 by Vγ9Vδ2 T cells was also reduced when RHOB was knocked down which was correlated with reduced death of A549 RHOB KO compared to A549 WT (**Figures 4C,D**).

Furthermore, we used a RHO GTPase inhibitor, the exoenzyme C3 transferase (CT04) that specifically inhibits RHOA, B, C. We showed that inhibition of RHO GTPases abrogated CD107a expression by Vγ9Vδ2 T cells in co-culture with A549 previously treated with zoledronate or BrHPP (**Figure 4E** for a representative experiment and **Figure 4F** for pooled experiments).

Moreover, the weak activation of Vγ9Vδ2 T cells by PAg-treated PC9 was also dependent on RHOB (**Supplementary Figure 6**).

Rerouting of RHOB in Endosomal Clusters Could Impair the PAg-Dependent Vγ9Vδ2 T Activation in PC9 Cells

We then postulated that the PAg-treatment of tumor cell lines and/or their co-culture with Vγ9Vδ2 T cells could have an impact on RHOB activity using a fluorescent reporter based on the tripartite split-GFP system (22) which monitors the binding of activated RHOB to RBD, one of its effector domains (20). A549 and PC9 cells were engineered to stably express RHOB GTPase fused to strand 10 of trisfGFP (GFP10-RhoB) and the Rho-binding domain of Rhotekin (RBD) fused to strand 11 (RBD-11). The GFP1-9 detector fragment allows detection of the RHOB-GTP and RBD interaction (**Figure 5A**). Reporter cell lines were pre-treated with zoledronate (5 μM, overnight) or BrHPP (1 μM, 4 h) and co-cultured or not with Vγ9Vδ2 T cells. Treatment of A549 with these PAg induced and increased the number of fluorescent cells and their fluorescence intensity only in the presence of Vγ9Vδ2 T cells indicating a significant increase of RHOB activity in this tumor cell line (**Figure 5B**, representative images and **Figure 5C** quantification). Conversely, in PC9 cells, RHOB activity was not modulated by PAg treatment and slightly modulated in co-culture with Vγ9Vδ2 T cells, suggesting a different RHOB regulation mechanism in this cell line (**Figures 5B,C**). To take a closer look at RHOB function, we performed confocal imaging in untreated and PAg-treated conditions, in the presence or not of Vγ9Vδ2 T cells and we analyzed the distribution of active RHOB (**Figure 5D**, membrane localization full bars and endosomal localization hatched bars). Surprisingly, active RHOB was significantly twice as abundant in the endosomal compartment of A549 cells compared to PC9 cells (**Figure 5D**, quantification). High resolution microscopy allowed us to analyze endosomal organization in PC9. Untreated reporter PC9 showed faint plasma membrane localization of RHOB/RBD complexes. Interestingly, treatment with zoledronate or BrHPP induced an accumulation of large endosomal clusters (**Figure 5E**, representative images). Quantification of the number of these structures indicated an increase of activated RHOB located in endosomal clusters in PAg-treated PC9 co-cultured or not with Vγ9Vδ2 T cells (**Figure 5F**). These endosomal clusters were reported randomly in PC9 cells co-cultured with Vγ9Vδ2 T cells independently of the treatment. Interestingly, these endosomal structures did not appear in the PAg-treated A549 co-cultured or not with Vγ9Vδ2 T cells (**Supplementary Figure 7**), suggesting that this endosomal reorganization was not due to the treatment with P-Ag mevalonate inhibitors. To identify the nature of these structures, we analyzed the localization of activated RHOB with different endosomal markers. Representative images and plot profile analysis on confocal stacks indicated a co-localization partly with late endosomal marker Rab7 and to a lesser extend with the LAMP1 lysosomal marker only after PAg-treated PC9 were co-cultured with Vγ9Vδ2 T cells independently of the treatment (**Figure 6**). These results indicate that in PC9 cells, endosomal RHOB is located in the late endosomal and on route to the lysosomal compartment.

DISCUSSION

The anti-tumor effect of Vγ9Vδ2 T cells depends on the phosphoantigens expressed by tumor cells but also on certain activator ligands (MICA/B and ULBPs) and adhesion molecules, essential to stabilize the immunological synapse. As PAg is not expressed by all tumor cells, treatment with exogenous PAg such as BrHPP or with aminobisphosphonates which induce endogenous PAg production such as isopentenyl pyrophosphate (IPP), is required to activate the anti-tumor functions of Vγ9Vδ2 T cells. However, Vγ9Vδ2 T cell activation can also be lowered by inhibitory signals that can be expressed by the tumor microenvironment and in particular by tumor cells. In this study, none of the NSCLC cell lines were able to spontaneously activate Vγ9Vδ2 T cells. However, pre-treatment with BrHPP or zoledronate sensitized some of them to Vγ9Vδ2 T cell killing. Indeed, amongst them, A549 was able to strongly activate IFNγ and CD107a expression by Vγ9Vδ2 T cells whereas PC9 induced a weak activation of these lymphocytes. Interestingly, these two cell lines express RHOB but wear different mutation, KRAS for A549 and EGFR for PC9. However, nothing was described

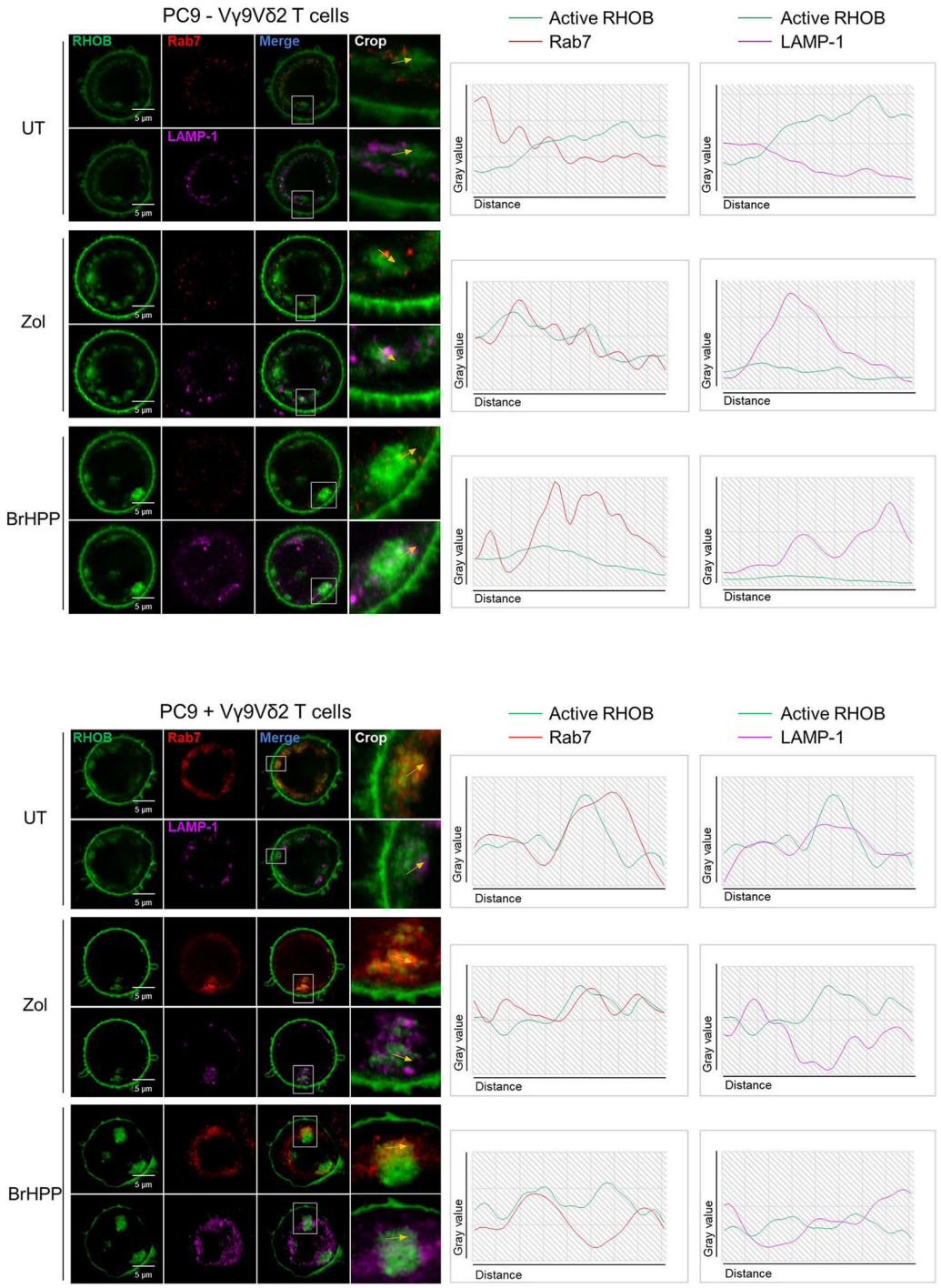

FIGURE 6 | Rerouting of RHOB in endosomal clusters in PAg-treated PC9 cells in contact with Vγ9Vδ2 T cells. Co-localization analysis by confocal microscopy of active RHOB (green), Rab7 (red) for late endosome/MVB marker and LAMP-1 (pink) as lysosomal marker, in PC9 cells pre-treated or not (UT) with zoledronate (zol) or BrHPP, and co-cultured (lower) or not (upper) with Vγ9Vδ2 T cells (representative image, crop on the key zone, and plot profile analysis beside showed by yellow arrows).

concerning some phenotypic specificities which could explain the different sensitivity of these cells toward Vγ9Vδ2 T killers.

Surprisingly, exploring their surface molecule pattern, we showed that these two NSCLC cell lines could differentially express NKG2D ligands, immune checkpoint ligands, and adhesion molecules. PC9 highly expressed ICAM-1, ULBPs, and PDL1 whereas A549 highly expressed CD38 and HLA-A,B,C, the two cell lines expressed LFA-1, LFA-3, and CD155

but not ICAM-3, CD112, MICA/B, HLA-E, or galectin-9. The presence of ULBPs ligands could partially explain the reactivity of Vγ9Vδ2 T cells against NSCLC cell lines. However, blocking NKG2D expressed at the surface of Vγ9Vδ2 T did not decrease their activation which is thus only induced here by PAg and not by other activator ligands. Furthermore, we showed that blocking of ICAM-3/LFA-3 decreased the cytolytic activity of Vγ9Vδ2 T against A549 and blocking of ICAM-1/LFA-1 decreased this activity against PC9. For these two cell lines, stabilization of the immunological synapse around TCR/BTN3A1 is thus coordinated by two different adhesion systems. If LFA-1 engagement by ICAM-1 is sufficient to activate iNKT cells (23) in this model of lung cancer/Vγ9Vδ2 T, interactions of adhesion molecules are not sufficient to induce an activating signaling in Vγ9Vδ2 T cells. However, according to the literature, these interactions are necessary when their inhibition highly decreases Vγ9Vδ2 T activation (9, 24). But this does not explain the difference between A549 and PC9. First, we thought that the high expression of PDL1 by PC9 could explain the inhibition of Vγ9Vδ2 T activation. However, PD1 blocking did not induce an increase in CD107a or IFNγ expression by Vγ9Vδ2 T cells. As surface inhibitor markers were not at the origin of the weak activation of Vγ9Vδ2 T cells, we focused on RHOB inside the cells. According to the literature (18) and thanks to NSCLC cell lines with a RHOB KO, we showed that RHOB was involved in the Vγ9Vδ2 T activation through endogenous PAg induced by a zoledronate treatment but also through exogenous PAg such as BrHPP. The non-reactivity of Vγ9Vδ2 T cells with the conditioned medium of BrHPP pre-treated tumor cells or in co-culture with these cells separated by a porous membrane (Transwell), demonstrated that BrHPP was able to penetrate inside the tumor cell and to activate membrane BTN3A1 shown to be essential for this activation (19). RHOB is thus also involved in the activation of Vγ9Vδ2 T cells through the exogenous PAg, BrHPP. Interestingly, the ICAM-1 signaling cascade is also highly dependent on RHO proteins, as ICAM-1 crosslinking induces actin reorganization which involves RHOB proteins (25). PC9 expresses a high amount of ICAM-1 which is involved in the immunological synapse with Vγ9Vδ2 T but does not efficiently activate the latter. To explain the weak reactivity of Vγ9Vδ2 T cells against PAg-pretreated PC9, we examined RHOB activity and its localization. The similar reactivity of Vγ9Vδ2 T cells against A549 and PC9 pulsed with the 20.1 BTN3A1 agonist (**Supplementary Figure 8**) supports the important role of RHOB in the PAg-induced response in this model. Our results show that active RHOB is localized in endosomes and at the plasma membrane of both A549 and PC9 cell lines. This is in agreement with previous reports of GFP-RHOB fusions in human epithelial cells (26). Our results indicate that active RHOB is increased in PAg-treated A549 cells co-cultured with Vγ9Vδ2 T cells, whereas only a slight increase of active RHOB is observed in PC9 cells co-cultured with Vγ9Vδ2 T cells independently of PAg treatment. It is important to note that the activation of RhoB in co-culture of A549 and Vγ9Vδ2 T is mainly dependent on the treatment by the PAg (**Figure 5C**). It has been previously established that treatment with PAg induces an increase of active RHOB that will modify the conformation of the BTN3A1 at the plasma membrane, which allows the activation of Vγ9Vδ2 T cells (18). The fact that the presence of Vγ9Vδ2 T cells further increases RHOB activity suggests that RHOB may be activated by exogenous stress signals and cytokines that would come from activated Vγ9Vδ2 T cells. Indeed, in other contexts involving immune cells, RHOB has been shown to be upregulated by environmental stress, cytokines, and LPS, and regulating this latter signaling (27–29). Our hypothesis would be that signals secreted by activated Vγ9Vδ2 T cells would contribute to RHOB activation in a cooperative manner with PAg. These results corroborate with the Vγ9Vδ2 T cell activation observed with A549 or -PC9 treated with PAg (**Figure 1** and **Supplementary Figure 1**). Altogether this indicates that the reactivity of these cell lines is strongly linked to RHOB function. In terms of subcellular localization, both cell lines contain active RHOB at the plasma membrane, with a stronger distribution in PC9 cells. A higher proportion of active RHOB is present in the endosomal compartment in A549 compared to PC9, however they differ strongly in terms of endosomal distribution. Whereas in A549, endosomal RHOB is diffusely distributed, in PC9 endosomal active RHOB was found in large clusters that co-localized with late Rab7 endosomal and LAMP-1 lysosomal markers. It is known that Vγ9Vδ2 T cell activation occurs at the plasma membrane through the involvement of BTN3A1 that is addressed by RHOB vesicles from the endosomes to the plasma membrane (18). In our model, PAg treatment of PC9 cells is not sufficient to trigger an increase in RHOB activation but requires the contact with Vγ9Vδ2 T cells, as untreated conditions in the presence of Vγ9Vδ2 T cells did not induce a significant increase in RHOB activity. One hypothesis of the weaker activation of RHOB in PC9 cells is that beyond the mode of recognition with T cells, the organization of endosomal RHOB-mediated signaling is not efficient for addressing important signaling molecules such as BTN3A1 at the plasma membrane. It was reported that RHOB interacts with the intracellular domain of BTN3A1 at the plasma membrane (18). BTN3A1 was shown as essential to Vγ9Vδ2 T cell recognition but not sufficient for this process as its homologous BTN2A1, the phosphoantigens being also essential. Actually, it was recently described that BTN2A1 synergized with BTN3A1 in sensitizing PAg-exposed cells for Vγ9Vδ2 TCR-mediated responses, these two butyrophilins beings key ligands that bind possibly two different domains of this TCR (30, 31). As for BTN3A1, the level of expression of BTN2A1 mRNA in PC9 is very close to that in A549 (**Supplementary Figure 9**). Thus, we can expect that these two cell lines express a similar level of BTN2A1 at their membrane, the BNT3A1 expression being equivalent (**Figure 3B**). Therefore, the weak activation of the Vγ9Vδ2 T cell by the PC9 cell line should not be due to the lack of BTN2A1. RHOB has not yet been shown to be associated to the intracellular B30.2 domain of the BTN2A1. Actually, it could be interesting to know if RHOB, as for BNT3A1, can be involved in the modification of the conformation of the BTN2A1. The organization of endosomal RHOB could then have an impact also on the BTN2A1. Further investigations should be pursued to evaluate whether such a mechanism is preserved in PC9. This endosomal signaling could be favored due to the genetic background of these cells, i.e., as they express an activated

EGFR mutant whose expression may modify intracellular RHOB mediated trafficking. Indeed, RHOB is known to prolong endosomal signaling of EGFR following its internalization (32). RHOB is a short-lived protein that is rapidly degraded through the endo-lysosomal pathway (33) and its degradation is delayed by inhibition of its isoprenylation. Treatment with PAg, while necessary for the activation of Vγ9Vδ2 T cells, contributes to a rerouting of RHOB in late/degradation compartments that may accelerate its degradation and prevent its function in endocytic trafficking to the plasma membrane in PC9 cells.

This study demonstrates for the first time that Vγ9Vδ2 T cell activation by PAg-treated tumor cells can be variable depending on several factors such as oncogenic mutation, RHOB activity, and surface markers. Our results indicate that this response is strongly influenced by RHOB function. Therefore, the regulation of endocytic traffic by RHOB in the tumor cell could be decisive for the immune response and may explain the resistance of some tumor cells that nevertheless highly express RHOB.

DATA AVAILABILITY STATEMENT

The datasets presented in this study can be found in online repositories. The names of the repository/repositories and accession number(s) can be found below: https://portals.broadinstitute.org/ccle/data, CCLE.

AUTHOR'S NOTE

The precise mechanism of Vγ9 T cells phosphoantigen (PAg)-activation remains elusive even the butyrophilin BTN3A and the RHOB GTPase are known as essential in this activation. RHOB which can have a dualistic role in cancer, was shown as conferring resistance to EGFR-tyrosine kinase inhibitors in lung cancer and frequently downregulated in aggressive lung cancer. Besides, Vγ9 T cells based therapies could be an issue for advanced lung cancers refractory to or intolerant of current conventional treatment. The role of RHOB in the PAg-activation of Vγ9 T cells in lung cancer has to be depicted when Vγ9 T cells reactivity depends on the lung tumor cell lines status.

AUTHOR CONTRIBUTIONS

CLap, SM, MM, and SF performed the experiments. SF and OC performed the KO cell lines. SC, OC, J-JF, GF, and CLau participated to the discussion of the results. MP and SC designed experiments and wrote the manuscript. MP supervised the study. All authors contributed to the article and approved the submitted version.

FUNDING

This work was funded by INSERM, CNRS, the University Hospital of Bordeaux and Toulouse III University.

ACKNOWLEDGMENTS

We are grateful to our healthcare professionals for their boundless investment during the COVID-19 crisis. We acknowledge ImCheck Therapeutics for giving us the 103.2 antibody. We acknowledge the Technologic Platform of the CRCT.

SUPPLEMENTARY MATERIAL

The Supplementary Material for this article can be found online at: https://www.frontiersin.org/articles/10.3389/fimmu.2020.01396/full#supplementary-material

REFERENCES

1. Kabelitz D, Wesch D, Pitters E, Zöller M. Characterization of tumor reactivity of human V gamma 9V delta 2 gamma delta T cells *in vitro* and in SCID mice *in vivo*. *J Immunol.* (2004) 173:6767–76. doi: 10.4049/jimmunol.173.11.6767
2. Poupot M, Fournié J-J. Non-peptide antigens activating human Vgamma9/Vdelta2 T lymphocytes. *Immunol Lett.* (2004) 95:129–38. doi: 10.1016/j.imlet.2004.06.013
3. Gober H-J, Kistowska M, Angman L, Jenö P, Mori L, de Libero G. Human T cell receptor gammadelta cells recognize endogenous mevalonate metabolites in tumor cells. *J Exp Med.* (2003) 197:163–8. doi: 10.1084/jem.20021500
4. Hebbeler AM, Cairo C, Cummings JS, Pauza CD. Individual Vgamma2-Jgamma1.2+ T cells respond to both isopentenyl pyrophosphate and Daudi cell stimulation: generating tumor effectors with low molecular weight phosphoantigens. *Cancer Immunol Immunother CII.* (2007) 56:819–29. doi: 10.1007/s00262-006-0235-6
5. Roelofs AJ, Jauhiainen M, Mönkkönen H, Rogers MJ, Mönkkönen J, Thompson K. Peripheral blood monocytes are responsible for gammadelta T cell activation induced by zoledronic acid through accumulation of IPP/DMAPP. *Br J Haematol.* (2009) 144:245–50. doi: 10.1111/j.1365-2141.2008.07435.x
6. Rossi C, Gravelle P, Decaup E, Bordenave J, Poupot M, Tosolini M, et al. Boosting γδ T cell-mediated antibody-dependent cellular cytotoxicity by PD-1 blockade in follicular lymphoma. *Oncoimmunology.* (2019) 8:1554175. doi: 10.1080/2162402X.2018.1554175
7. Girard P, Charles J, Cluzel C, Degeorges E, Manches O, Plumas J, et al. The features of circulating and tumor-infiltrating γδ T cells in melanoma patients display critical perturbations with prognostic impact on clinical outcome. *Oncoimmunology.* (2019) 8:1601483. doi: 10.1080/2162402X.2019.1601483
8. Groh V, Rhinehart R, Secrist H, Bauer S, Grabstein KH, Spies T. Broad tumor-associated expression and recognition by tumor-derived gamma delta T cells of MICA and MICB. *Proc Natl Acad Sci USA.* (1999) 96:6879–84. doi: 10.1073/pnas.96.12.6879
9. Corvaisier M, Moreau-Aubry A, Diez E, Bennouna J, Mosnier J-F, Scotet E, et al. Vγ9Vδ2 T cell response to colon carcinoma cells. *J Immunol.* (2005) 175:5481–8. doi: 10.4049/jimmunol.175.8.5481
10. Fournié J-J, Sicard H, Poupot M, Bezombes C, Blanc A, Romagné F, et al. What lessons can be learned from γδ T cell-based cancer immunotherapy trials? *Cell Mol Immunol.* (2013) 10:35–41. doi: 10.1038/cmi.2012.39
11. Casetti R, Perretta G, Taglioni A, Mattei M, Colizzi V, Dieli F, et al. Drug-induced expansion and differentiation of Vγ9Vδ2 T cells *in vivo*: the role of exogenous IL-2. *J Immunol.* (2005) 175:1593–8. doi: 10.4049/jimmunol.175.3.1593
12. Sicard H, Ingoure S, Luciani B, Serraz C, Fournié J-J, Bonneville M, et al. *In vivo* immunomanipulation of Vγ9Vδ2 T cells with a synthetic phosphoantigen in a preclinical nonhuman primate model. *J Immunol.* (2005) 175:5471–80. doi: 10.4049/jimmunol.175.8.5471

13. Izumi H, Yamasaki A, Takeda K, Kodani M, Touge H, Tanaka N, et al. Acute-phase reaction induced by zoledronate and its effect on prognosis of patients with advanced non-small cell lung cancer. *Lung Cancer Amst Neth.* (2018) 122:200–5. doi: 10.1016/j.lungcan.2018.06.022
14. Kakimi K, Matsushita H, Murakawa T, Nakajima J. γδ T cell therapy for the treatment of non-small cell lung cancer. *Transl Lung Cancer Res.* (2014) 3:23–33. doi: 10.3978/j.issn.2218-6751.2013.11.01
15. Mazieres J, Antonia T, Daste G, Muro-Cacho C, Berchery D, Tillement V, et al. Loss of RhoB expression in human lung cancer progression. *Clin Cancer Res Off J Am Assoc Cancer Res.* (2004) 10:2742–50. doi: 10.1158/1078-0432.CCR-03-0149
16. Calvayrac O, Pradines A, Raymond-Letron I, Rouquette I, Bousquet E, Lauwers-Cances V, et al. RhoB determines tumor aggressiveness in a murine EGFRL858R-induced adenocarcinoma model and is a potential prognostic biomarker for Lepidic lung cancer. *Clin Cancer Res.* (2014) 20:6541–50. doi: 10.1158/1078-0432.CCR-14-0506
17. Calvayrac O, Mazières J, Figarol S, Marty-Detraves C, Raymond-Letron I, Bousquet E, et al. The RAS-related GTPase RHOB confers resistance to EGFR-tyrosine kinase inhibitors in non-small-cell lung cancer via an AKT-dependent mechanism. *EMBO Mol Med.* (2017) 9:238–50. doi: 10.15252/emmm.201606646
18. Sebestyen Z, Scheper W, Vyborova A, Gu S, Rychnavska Z, Schiffler M, et al. RhoB mediates phosphoantigen recognition by Vγ9Vδ2 T cell receptor. *Cell Rep.* (2016) 15:1973–85. doi: 10.1016/j.celrep.2016.04.081
19. Harly C, Guillaume Y, Nedellec S, Peigné C-M, Mönkkönen H, Mönkkönen J, et al. Key implication of CD277/butyrophilin-3 (BTN3A) in cellular stress sensing by a major human γδ T-cell subset. *Blood.* (2012) 120:2269–79. doi: 10.1182/blood-2012-05-430470
20. Koraïchi F, Gence R, Bouchenot C, Grosjean S, Lajoie-Mazenc I, Favre G, et al. High-content tripartite split-GFP cell-based assays to screen for modulators of small GTPase activation. *J Cell Sci.* (2018) 131:jcs210419. doi: 10.1242/jcs.210419
21. Rothbauer U, Zolghadr K, Muyldermans S, Schepers A, Cardoso MC, Leonhardt H. A versatile nanotrap for biochemical and functional studies with fluorescent fusion proteins. *Mol Cell Proteomics MCP.* (2008) 7:282–9. doi: 10.1074/mcp.M700342-MCP200
22. Cabantous S, Nguyen HB, Pedelacq J-D, Koraïchi F, Chaudhary A, Ganguly K, et al. A new protein-protein interaction sensor based on tripartite split-GFP association. *Sci Rep.* (2013) 3:2854. doi: 10.1038/srep02854
23. Sharma A, Lawry SM, Klein BS, Wang X, Sherer NM, Zumwalde NA, et al. LFA-1 ligation by high-density ICAM-1 is sufficient to activate IFN-γ release by innate T lymphocytes. *J Immunol.* (2018) 201:2452–61. doi: 10.4049/jimmunol.1800537
24. Liu Z, Guo B, Lopez RD. Expression of intercellular adhesion molecule (ICAM)-1 or ICAM-2 is critical in determining sensitivity of pancreatic cancer cells to cytolysis by human gammadelta-T cells: implications in the design of gammadelta-T-cell-based immunotherapies for pancreatic cancer. *J Gastroenterol Hepatol.* (2009) 24:900–11. doi: 10.1111/j.1440-1746.2008.05668.x
25. Etienne-Manneville S, Manneville JB, Adamson P, Wilbourn B, Greenwood J, Couraud PO. ICAM-1-coupled cytoskeletal rearrangements and transendothelial lymphocyte migration involve intracellular calcium signaling in brain endothelial cell lines. *J Immunol.* (2000) 165:3375–83. doi: 10.4049/jimmunol.165.6.3375
26. Wherlock M, Gampel A, Futter C, Mellor H. Farnesyltransferase inhibitors disrupt EGF receptor traffic through modulation of the RhoB GTPase. *J Cell Sci.* (2004) 117:3221–31. doi: 10.1242/jcs.01193
27. Kamon H, Kawabe T, Kitamura H, Lee J, Kamimura D, Kaisho T, et al. TRIF-GEFH1-RhoB pathway is involved in MHCII expression on dendritic cells that is critical for CD4 T-cell activation. *EMBO J.* (2006) 25:4108–19. doi: 10.1038/sj.emboj.7601286
28. Ocana-Morgner C, Wahren C, Jessberger R. SWAP-70 regulates RhoA/RhoB-dependent MHCII surface localization in dendritic cells. *Blood.* (2009) 113:1474–82. doi: 10.1182/blood-2008-04-152587
29. Liu S, Huang L, Lin Z, Hu Y, Chen R, Wang L, et al. RhoB induces the production of proinflammatory cytokines in TLR-triggered macrophages. *Mol Immunol.* (2017) 87:200–6. doi: 10.1016/j.molimm.2017.04.015
30. Rigau M, Ostrouska S, Fulford TS, Johnson DN, Woods K, Ruan Z, et al. Butyrophilin 2A1 is essential for phosphoantigen reactivity by γδ T cells. *Science.* (2020) 367:eaay5516. doi: 10.1126/science.aay5516
31. Karunakaran MM, Willcox CR, Salim M, Paletta D, Fichtner AS, Noll A, et al. Butyrophilin-2A1 directly binds germline-encoded regions of the Vγ9Vδ2 TCR and is essential for phosphoantigen sensing. *Immunity.* (2020) 52:487–98.e6. doi: 10.1016/j.immuni.2020.02.014
32. Gampel A, Parker PJ, Mellor H. Regulation of epidermal growth factor receptor traffic by the small GTPase rhoB. *Curr Biol CB.* (1999) 9:955–8. doi: 10.1016/S0960-9822(99)80422-9
33. Pérez-Sala D, Boya P, Ramos I, Herrera M, Stamatakis K. The C-terminal sequence of RhoB directs protein degradation through an endo-lysosomal pathway. *PLoS ONE.* (2009) 4:e8117. doi: 10.1371/journal.pone.0008117

Conflict of Interest: The authors declare that the research was conducted in the absence of any commercial or financial relationships that could be construed as a potential conflict of interest.

frontiers in Immunology

ORIGINAL RESEARCH
published: 21 July 2020
doi: 10.3389/fimmu.2020.01405

Comparison of a Novel Bisphosphonate Prodrug and Zoledronic Acid in the Induction of Cytotoxicity in Human Vγ2Vδ2 T Cells

Daisuke Okuno[1], Yuki Sugiura[2], Noriho Sakamoto[1], Mohammed S. O. Tagod[3], Masashi Iwasaki[4], Shuto Noda[3], Akihiro Tamura[3], Hiroaki Senju[1], Yasuhiro Umeyama[1], Hiroyuki Yamaguchi[1], Makoto Suematsu[2], Craig T. Morita[5], Yoshimasa Tanaka[3,4] and Hiroshi Mukae[1]*

[1] Department of Respiratory Medicine, Graduate School of Biomedical Sciences, Nagasaki University, Nagasaki, Japan, [2] Department of Biochemistry, Keio University School of Medicine, Tokyo, Japan, [3] Center for Medical Innovation, Nagasaki University, Nagasaki, Japan, [4] Center for Innovation in Immunoregulative Technology and Therapeutics, Graduate School of Medicine, Kyoto University, Kyoto, Japan, [5] Department of Internal Medicine and the Interdisciplinary Graduate Program in Immunology, University of Iowa Carver College of Medicine, Veterans Affairs Health Care System, Iowa City, IA, United States

OPEN ACCESS

Edited by:
Dieter Kabelitz,
University of Kiel, Germany

Reviewed by:
Martin Thurnher,
Innsbruck Medical University, Austria
Shirin Kalyan,
University of British Columbia, Canada

***Correspondence:**
Yoshimasa Tanaka
ystanaka@nagasaki-u.ac.jp

Specialty section:
This article was submitted to T Cell Biology, a section of the journal Frontiers in Immunology

Received: 19 February 2020
Accepted: 01 June 2020
Published: 21 July 2020

Citation:
Okuno D, Sugiura Y, Sakamoto N, Tagod MSO, Iwasaki M, Noda S, Tamura A, Senju H, Umeyama Y, Yamaguchi H, Suematsu M, Morita CT, Tanaka Y and Mukae H (2020) Comparison of a Novel Bisphosphonate Prodrug and Zoledronic Acid in the Induction of Cytotoxicity in Human Vγ2Vδ2 T Cells. Front. Immunol. 11:1405. doi: 10.3389/fimmu.2020.01405

Increasing attention has been paid to human γδ T cells expressing Vγ2Vδ2 T cell receptor (also termed Vγ9Vδ2) in the field of cancer immunotherapy. We have previously demonstrated that a novel bisphosphonate prodrug, tetrakis-pivaloyloxymethyl 2-(thiazole-2-ylamino)ethylidene-1,1-bisphosphonate (PTA), efficiently expands peripheral blood Vγ2Vδ2 T cells to purities up to 95–99% in 10–11 days. In the present study, we first examined the effect of PTA on farnesyl diphosphate synthase (FDPS) using liquid chromatography mass spectrometry (LC-MS) to analyze the mechanism underlying the PTA-mediated expansion of Vγ2Vδ2 T cells. We find that the prodrug induced the accumulation of both isopentenyl diphosphate (IPP) and dimethylallyl diphosphate (DMAPP), direct upstream metabolites of FDPS. This indicates that not only IPP but also DMAPP plays an important role in PTA-mediated stimulation of Vγ2Vδ2 T cells. We next analyzed TCR-independent cytotoxicity of Vγ2Vδ2 T cells. When human lung cancer cell lines were challenged by Vγ2Vδ2 T cells, no detectable cytotoxicity was observed in 40 min. The lung cancer cell lines were, however, significantly killed by Vγ2Vδ2 T cells after 4–16 h in an effector-to-target ratio-dependent manner, demonstrating that Vγ2Vδ2 T cell-based cell therapy required a large number of cells and longer time when tumor cells were not sensitized. By contrast, pulsing tumor cell lines with 10–30 nM of PTA induced significant lysis of tumor cells by Vγ2Vδ2 T cells even in 40 min. Similar levels of cytotoxicity were elicited by ZOL at concentrations of 100–300 μM, which were much higher than blood levels of ZOL after infusion (1–2 μM), suggesting that standard 4 mg infusion of ZOL was not enough to sensitize lung cancer cells in clinical settings. In addition, Vγ2Vδ2 T cells secreted interferon-γ (IFN-γ) when challenged by lung cancer cell lines pulsed with PTA

in a dose-dependent manner. Taken together, PTA could be utilized for both expansion of Vγ2Vδ2 T cells *ex vivo* and sensitization of tumor cells *in vivo* in Vγ2Vδ2 T cell-based cancer immunotherapy. For use in patients, further studies on drug delivery are essential because of the hydrophobic nature of the prodrug.

Keywords: bisphosphonate, cytotoxicity, mass spectroscopy, prodrug, Vγ2Vδ2 T cells

INTRODUCTION

Cancer is the leading cause of deaths in developed countries. Despite recent successes in cancer immunotherapy harnessing programmed death-1 (PD-1) (1–5) and cytotoxic T lymphocyte-associated protein-4 (CTLA-4) immune checkpoint inhibitors (6), significant limitations exist for the antibody-based immunotherapies. It is thus imperative to develop additional approaches to increase the efficacy of cancer treatments. Adoptive transfer of T cells expressing T cell receptors (TCRs) that recognize tumor cells is one such strategy that shows promise (7, 8).

TCR is a membrane-anchored heterodimeric protein consisting of either α and β or γ and δ chains expressed as part of a complex with cluster of differentiation 3 (CD3). Most αβ T cells expressing α and β TCR chains recognize antigenic peptides in the context of the major histocompatibility complex (MHC) class I or class II molecules with the help of CD4 or CD8 co-receptors, whereas other αβ T cell subsets respond to lipid antigens and vitamin B precursors bound to monomorphic MHC class I-related proteins, such as CD1 family members and MR1 (9). By contrast, the mechanism underlying the antigen recognition by γδ T cells expressing γ and δ chains remains unclear. In humans, most circulating γδ T cells express Vγ2Vδ2 (also termed Vγ9Vδ2) and recognize foreign phosphoantigens (pAgs) like (*E*)-4-hydroxy-3-methylbut-2-enyl diphosphate (HMBPP) derived from pathogenic microbes (10–12) and self pAgs like isopentenyl diphosphate (IPP) (13–15). Recently, it has been demonstrated that pAgs bind to the intracellular B30.2 domain of butyrophilin (BTN) 3A1 (16–24) and the interaction between pAgs and B30.2 is sensed by Vγ2Vδ2 TCR in a BTN2A1-dependent manner (25). However, the precise mode of recognition by Vγ2Vδ2 T cells of the BTN complex has not been fully elucidated (26, 27).

Because HMBPP and IPP are pyrophosphomonoesters that can be readily hydrolyzed by esterases, nitrogen-containing bisphosphonates (N-BPs) are often utilized as stimulators for Vγ2Vδ2 T cells (28–30). N-BPs such as pamidronate (PAM) and zoledronic acid (ZOL) inhibit farnesyl diphosphate synthase (FDPS) in the mevalonate pathway (31–33), resulting in the accumulation of upstream metabolites that are recognized by Vγ2Vδ2 T cells in the context of BTN2A1 and BTN3A1. Although, ZOL is one of the most potent inhibitors of FDPS, its membrane permeability is limited because it is negatively charged. We thus previously designed and synthesized a series of N-BP prodrugs and demonstrated that treatment of antigen-presenting cells with tetrakis-pivaloyloxymethyl 2-(thiazole-2-ylamino)ethylidene-1,1-bisphosphonate (PTA) inhibited intracellular FDPS, leading to the deprivation of geranylgeranylated Rap1A, and efficiently expanded peripheral blood Vγ2Vδ2 T cells (34–37).

In the present study, we examined the mechanism by which PTA induced the stimulation of Vγ2Vδ2 T cells using mass spectrometry and determined the TCR-independent, natural (NK)-like cellular cytotoxicity, and TCR-dependent cellular cytotoxicity of PTA-expanded Vγ2Vδ2 T cells against lung cancer cells.

MATERIALS AND METHODS

Mass Spectrometry

Tetrakis-pivaloyloxymethyl 2-(thiazole-2-ylamino)ethylidene-1,1-bisphosphonate (PTA, Techno Suzuta Co., Ltd., Heiwa-machi, Nagasaki, Japan) was dissolved in deoxymethyl sulfoxide (Nacalai Tesque, Inc., Nakagyo-ku, Kyoto, Japan) at a concentration of 1 mM and the stock solution was stored at −80°C until used. Raji Burkitt's lymphoma cells were obtained from the Japanese Collection of Research Bioresources Cell Bank (JCRB) of the National Institutes of Biomedical Innovation, Health, and Nutrition, Sennan, Osaka, Japan. Raji cells were grown in RPMI1640 medium (Merck & Co., Inc., Kenilworth, NJ), containing 10% fetal calf serum (FCS, Merck & Co., Inc.), 10^{-5} M 2-mercaptoethanol (Wako Pure Chemical Industries, Ltd., Chuo-ku, Osaka, Japan), 100 μg/ml streptomycin (Meiji Seika Pharma Co., Ltd., Chuo-ku, Tokyo, Japan), 100 U/ml of penicillin (Meiji Seika Pharma Co., Ltd.) (complete RPMI1640 medium) in 75 cm^2 flasks (Corning Inc., Corning, NY). The cells (1×10^6 cells) were treated with 0, 50, 100, 200, or 500 nM PTA in 1 ml of the complete RPMI1640 medium in 15 ml conical tubes (AGC Techno Glass Co., Ltd., Haibara, Shizuoka, Japan) at 37°C with 5% CO_2 for 2 h. The cell suspensions were centrifuged at 600 × g at 4°C for 5 min. After the supernatants were removed, the cell pellets were dispersed by tapping and resuspended in 5 ml of cold Dulbecco's phosphate buffered saline (-) (PBS, Nissui Pharmaceutical Co., Ltd., Taito-ku, Tokyo, Japan). The cell pellets were washed two more times with cold PBS and placed in liquid nitrogen and stored at −80°C.

For the analysis of IPP and DMAPP in cell lysates, anionic metabolites were measured using an Orbitrap-type MS (Q-Exactive Focus; Thermo Fisher Scientific) connected to a high-performance ion-chromatography (IC) system (ICS-5000+; Thermo Fisher Scientific) that enables highly selective and sensitive metabolite quantification due to IC-separation and the Fourier-transform MS principle (38). The IC was equipped with an anion electrolytic suppressor (Thermo Scientific Dionex

AERS 500; Thermo Fisher Scientific) to convert the potassium hydroxide gradient into pure water before the sample entered the mass spectrometer. Separation was performed using a Thermo Scientific Dionex IonPac AS11-HC, with a 4-μm particle-size column. The IC flow rate of 0.25 ml/min was supplemented post-column with 0.18 ml/min makeup flow of MeOH. The potassium hydroxide gradient conditions for IC separation were as follows: from 1 to 100 mM (0–40 min), 100 mM (40–50 min), and 1 mM (50.1–60 min), at a column temperature of 30°C. The Q-Exactive Focus mass spectrometer was operated under an ESI negative mode for all detections. Full mass scan (*m/z* 70–900) was used at a resolution of 70,000. The automatic gain control target was set at 3×10^6 ions, and the maximum ion injection time was 100 ms. Source ionization parameters were optimized with a spray voltage of 3 kV, and other parameters were as follows: transfer temperature of 320°C, S-Lens level of 50, heater temperature of 300°C, Sheath gas at 36, and Aux gas at 10.

Preparation of PBMC

Peripheral blood samples were obtained from healthy adult volunteers and lung cancer patients after approval of the Institutional Review Board of Nagasaki University Hospital and with written informed consent. All protocols were performed in accordance with the Guidelines and Regulations of Nagasaki University Hospital. The blood samples were treated with 1/100 volume of heparin sodium (Mochida Pharmaceutical., Co., Ltd., Shinjuku-ku, Tokyo, Japan) and diluted with an equal volume of PBS. The diluted blood (20 ml) was loaded on 20 ml of Ficoll-Paque™ PLUS (GE Healthcare BioSciences AB, Uppsala, Sweden) in a 50 ml conical tube (Corning Inc.), which was centrifuged at 600 × g at room temperature for 30 min. The fluffy layer was collected into a 50 ml conical tube and diluted with 2.5 volumes of PBS. The diluted peripheral blood mononuclear cells (PBMC) were centrifuged at 900 × g at 4°C for 10 min and the supernatant was removed. The cell pellets were dispersed by tapping and resuspended in PBS in a 15 ml conical tube, which was centrifuged at 600 × g at 4°C for 5 min. After the supernatant was removed, the cell pellets were dispersed by tapping and resuspended in 7 ml of Yssel's medium (39), consisting of Iscove's modified Dulbecco's medium (Thermo Fisher Scientific, Waltham, MA), supplemented with 10% human AB serum (Cosmo Bio Co., Ltd., Koto-ku, Tokyo, Japan), 3.6×10^{-2} M $NaHCO_3$ (Nacalai Tesque Inc.), 3.3×10^{-5} M 2-aminoethanol (Nacalai Tesque Inc.), 40 mg/l transferrin apo form (Nacalai Tesque Inc.), 5 mg/l human recombinant insulin (Merck & Co., Inc.), 2 mg/l linoleic acid (Merck & Co., Inc.), 2 mg/l oleic acid (Merck & Co., Inc.), 2 mg/ml palmitic acid (Merck & Co., Inc.), 100 μg/ml streptomycin, 100 U/ml of penicillin or RPMI1640 medium.

Expansion of Vγ2Vδ2 T Cells

To 1.5 ml of PBMC ($1–2.5 \times 10^6$ cells/ml of Yssel's medium) in a well of a 24-well plate (Corning Inc.) was added 1.5 μl of 1 mM PTA stock solution to give a final concentration of 1 μM. The cells were incubated at 37°C with 5% CO_2 for 24 h, to which was added interleukin-2 (IL-2, Shionogi Pharmaceutical Co., Ltd., Chuo-ku, Osaka, Japan) to give a concentration of 100 U/ml. After incubation at 37°C with 5% CO_2 for one more day, the medium was replaced with Yssel's medium containing 100 U/ml IL-2. On day 2 through day 5, 100 U/ml of IL-2 was added to the medium and Vγ2Vδ2 cells were expanded. On day 6, 1.5 ml of Yssel's medium was added to the well. After being mixed well with a pipet, 1.5 ml of the cell suspension was transferred to another well. On day 7, the medium was replaced with the complete RPMI1640 medium plus 100 U/ml IL-2 and Vγ2Vδ2 T cells were expanded by day 11 and stored in liquid nitrogen until used. Cells were observed under a microscope (Nikon Corp., Minato-ku, Tokyo, Japan) on day 5 and the proportion of Vδ2 cells was determined by flow cytometry on days 0, 8, and 11 as described below. IFN-γ production was determined on day 2 as described below.

Flow Cytometric Analysis

PBMC and PTA-expanded cells (2×10^5 cells) were dispensed into a 96-well round bottom plate (Corning Inc.) and incubated with 50 μl of PBS containing 2% FCS and monoclonal antibodies (mAbs), including fluorescein isothiocyanate (FITC)-conjugated anti-TCR Vδ2 mAb (BD Biosciences, San Diego, CA) or anti-CD27 mAb (BioLegend, San Diego, CA) and phycoerythrin (PE)-conjugated anti-CD3, CD86, CD94, or CD161 mAbs (BD Biosciences), or anti-CD25 mAb (Tombo Biosciences, Co., Ltd., Kobe, Hyogo, Japan), or anti-CD45RO, CD69, NKG2D, DNAM-1, TRAIL, Fas-L, CD56, HLA-DR, HLA-DQ, or CD45RA mAbs (BioLegend), on ice for 15 min. To the wells were added 200 μl of PBS containing 2% FCS and the plate was centrifuged at 600 × g at 4°C for 2 min. After the supernatants were removed, the cell pellets were dispersed by vortexing and resuspended in 200 μl of PBS/2% FCS. The cells were washed two more times with 200 μl of PBS/2% FCS and resuspended in 400 μl of PBS/2% FCS. The cells were analyzed using a FACSCalibur flow cytometer (Becton Dickenson, Franklin Lakes, NJ) and the cell population was visualized using FlowJo ver. 10 (FlowJo LLC, Ashland, OR).

Enzyme-Linked Immunosorbent Assay for IFN-γ

For determination of IFN-γ production from peripheral blood Vγ2Vδ2 T cells in response to PTA or ZOL, PBMC suspensions (4.35×10^5 cells in 100 μl of Yssel's medium) were placed in a 96-well flat-bottom plate (Corning Inc.), to which was added 100 μl each of PTA at concentrations of 1, 3, 10, 30, 100, 300, or 1,000 nM, or zoledronic acid (ZOL, Novartis International AG, Basel, Switzerland) at concentrations of 10, 30, 100, 300, 1 μM, 3 μM, or 10 μM. The plate was incubated at 37°C with 5% CO_2 for 24 h. To each well was added IL-2 at a final concentration of 100 U/ml. After additional 24 h incubation, the cell suspensions were mixed and the plate was centrifuged at 600 × g at 4°C for 2 min. The supernatants were transferred into a 96-well round bottom plate and placed at −80°C for 16 h. The samples were thawed and interferon-γ (IFN-γ) levels were determined by enzyme-linked immunosorbent assay (ELISA, Peprotech, Rocky Hill, NJ) according to the manufacturer's instruction.

For determination of IFN-γ production from PTA-expanded Vγ2Vδ2 T cells in response to PTA or ZOL, PBMC derived from a healthy adult volunteer was stimulated with 1 μM

PTA for 11 days and the PTA-expanded Vγ2Vδ2 T cells were frozen as described above. PC-9 human lung adenocarcinoma was obtained from RIKEN BioResource Research Center (Tsukuba, Ibaraki, Japan), PC-6 human lung small cell carcinoma from Immuno-Biological Laboratories, Fujioka, Gunma, Japan), and H1975 human lung adenocarcinoma and H520 human lung squamous cell carcinoma from American Type Culture Collection (Manassas, VA). The human lung cancer cell lines were grown in 30 ml of the complete RPMI1640 medium at 37°C with 5% CO_2 in 75 cm^2 flasks. After the culture supernatants were removed and the cells were washed with 10 ml PBS, 2 ml each of 0.25 w/v% trypsin/1 mM ethylenediaminetetraacetic acid (EDTA) (Thermo Fisher Scientific) was added to the flasks, which were placed at 37°C with 5% CO_2 for 2 min. To the flasks was added 10 ml each of the complete RPMI1640 medium and the cell suspensions were transferred into 15 ml conical tubes. After being centrifuged at 600 × g at 4°C for 5 min, the supernatants were removed and the cell pellets were dispersed by tapping. The cells were resuspended in 5 ml of the complete RPMI1640 medium, washed twice, and resuspended in the complete RPMI1640 medium. The cell suspensions (1.4×10^6 cells/ml) were treated with PTA at final concentrations of 15.625, 31.25, 62.5, 125, 250, 500, or 1,000 nM, or with ZOL at final concentrations of 15.625, 31.25, 62.5, 125, 250, 500, or 1,000 μM at 37°C with 5% CO_2 for 2 h. The cells were washed three times with 5 ml of the complete RPMI1640 medium and resuspended in 350 μl of the complete RPMI1640 medium. The tumor cell suspensions (4×10^5 cells/100 μl) were dispensed into a 96-well round bottom plate, containing PTA-expanded Vγ2Vδ2 T cells (4×10^5 cells/100 μl). The plate was incubated at 37°C with 5% CO_2 for 16 h. Then, the cell suspensions were mixed and the plate was centrifuged at 600 × g at 4°C for 2 min. The supernatants were transferred into a 96-well round bottom plate and placed at −80°C for 16 h. The samples were thawed and interferon-γ (IFN-γ) levels were determined by ELISA according to the manufacturer's instruction.

Luminescence-Based Cytotoxicity Assay

For determination of NK-like activity of PTA-expanded Vγ2Vδ2 T cells, PC-9, PC-6, H1975, and H520 human lung cancer cell suspensions (2×10^4 cells/200 μl) were dispensed into a 96-well flat bottom plate, which was incubated at 37°C with 5% CO_2 for 16 h. After the culture supernatants were aspirated, PTA-expanded Vγ2Vδ2 T cells were added to each well at effector-to-target (E/T) ratios of 0.3125:1, 0.625:1, 1.25:1, 2.5:1, 5:1, 10:1, 20:1, 40:1, or 80:1, and incubated at 37°C with 5% CO_2 for 4 or 16 h. Then, the culture supernatants were aspirated and the wells were gently washed three times with 200 μl of the complete RPMI1640 medium. To the wells was added 100 μl each of CellTiterGlo® Reagent (PerkinElmer Inc., Waltham, MA), and the cell lysates were transferred into a 96-well optiplate (PerkinElmer Inc.). Luminescence was measured through an ARVO multi-plate reader (PerkinElmer Inc.). All measurements were performed in triplicate.

For determination of cellular cytotoxicity of PTA-expanded Vγ2Vδ2 T cells against PTA- or ZOL-treated PC-9, PC-6, H1975, and H520, the human lung cancer cell suspensions (2×10^4 cells/200 μl) were dispensed into a 96-well flat bottom plate, which was incubated at 37°C with 5% CO_2 for 16 h. After the culture supernatants were aspirated, 200 μl of a serially-diluted PTA was added to each well in triplicate at concentrations of 0, 0.78125, 1.5625, 3.125, 6.25, 12.5, 25, 50, or 100 nM, or a serially-diluted ZOL at final concentrations of 0, 7.8125, 15.625, 31.25, 62.5, 125, 250, 500, or 1,000 μM. The plate was incubated at 37°C with 5% CO_2 for 2 h. After the supernatants were aspirated, 200 μl of PTA-expanded Vγ2Vδ2 T cells (3×10^5 cells) were added to each well. The plate was incubated at 37°C with 5% CO_2 for 4 or 16 h. Then, the culture supernatants were aspirated and the wells were gently washed three times with 200 μl of the complete RPMI1640 medium. To the wells was added 100 μl each of CellTiterGlo Reagent® (PerkinElmer Inc.), and the cell lysates were transferred into a 96-well optiplate (PerkinElmer Inc.). Luminescence was measured through an ARVO multi-plate reader (PerkinElmer Inc.).

Time-Resolved Fluorescence-Based Cytotoxicity Assay

Vγ2Vδ2 T cell-mediated cellular cytotoxicity was determined using a non-radioactive cellular cytotoxicity assay kit (Techno Suzuta Co., Ltd.). PC-9, PC-6, H1975, and H520 human cancer cell lines (1×10^6 cells/ml) in 15 ml conical tubes were treated with 0, 3, 10, 30, 100, 300, or 1,000 nM of PTA, or 0, 3, 10, 30, 100, 300, or 1,000 μM of ZOL at 37°C with 5% CO_2 for 2 h and then pulsed with 2.5 μl of 10 mM bis(butyryloxymethyl) 4′-(hydroxymethyl)-2,2′:6′,2″-terpyridine-6,6″-dicarboxylate (BM-HT, Techno Suzuta Co., Ltd.) at 37°C with 5% CO_2 for 15 min. During the incubation, BM-HT was hydrolyzed by intracellular esterases to give 4′-(hydroxymethyl)-2,2′:6′,2″-terpyridine-6,6″-dicarboxylate (HT) (40). To the conical tubes was added 5 ml of the complete RPMI140 medium and the tubes were centrifuged at 600 × g at 4°C for 5 min. After the supernatants were removed, the cell pellets were dispersed by tapping and resuspended in 5 ml of the complete RPMI1640 medium. The cells were washed two more times and resuspended in 20 ml of the complete RPMI1640 medium. The tumor cell suspensions (5×10^3 cells/100 μl) were dispensed into a 96-well round bottom plate, to which were added 4×10^5 Vγ2Vδ2 T cells/100 μl at an E/T ratio of 80:1. The plate was centrifuged at 200 × g at ambient temperature for 2 min and then incubated at 37°C with 5% CO_2 for 40 min. Detergent (Techno Suzuta Co., Ltd.) at a final concentration of 5×10^{-5} M was added to wells for the determination of the maximum release. After the cell suspensions were mixed, the plate was centrifuged at 600 × g for 2 min and the supernatants (25 μl each) were removed to a new 96-well round bottom plate containing 250 μl of europium (Eu) solution (Techno Suzuta Co., Ltd.). After the Eu/HT complex solution was mixed, 200 μl samples were transferred to a 96-well optical plate (Thermo Fisher Scientific Inc.). Time-resolved fluorescence was measured through an ARVO multi-plate reader (PerkinElmer Inc.). All measurements were performed in triplicate. Specific lysis (%) was calculated as 100 × [experimental release (counts) – spontaneous release (counts)]/[maximum release (counts) – spontaneous release (counts)].

Intracellular Staining for IFN-γ

PC-9 human lung cancer cells (1×10^6 cells/ml) were treated with 1 ml of the complete RPMI1640 medium or the medium containing 1 μM PTA or with 1 mM ZOL at 37°C with 5% CO_2 for 2 h. The cells were washed three times with 5 ml of the complete RPMI1640 medium and resuspended in 100 μl of the complete RPMI1640 medium. The tumor cell suspensions (5×10^5 cells/50 μl) were dispensed into a 96-well round bottom plate, containing PTA-expanded Vγ2Vδ2 T cells (5×10^5 cells/50 μl). The plate was incubated at 37°C with 5% CO_2. After 2 h, brefeldin A (Merck & Co., Inc.) was added to each well at a final concentration of 10 μg/ml and the plate was incubated at 37°C with 5% CO_2 for 2 more hours. Then, the cell suspensions were mixed and the plate was centrifuged at 600 × g at 4°C for 2 min. After the supernatants were removed, the plate was vortexed, to which was added 200 μl of PBS/2% FCS. The cells were washed two more times with 200 μl of PBS/2% FCS. Then, the cells were stained with FITC-conjugated anti-TCR Vδ2 mAb in 50 μl of PBS/2% FCS. After incubation on ice for 15 min, the cells were washed four times with PBS and fixed with 200 μl of 1% paraformaldehyde in PBS. After incubation at ambient temperature for 15 min, the plate was centrifuged at 600 × g at 4°C for 2 min. After the supernatants were removed, the plate was vortexed, to which was added 200 μl of PBS/2% FCS/0.5% saponin (Wako Pure Chemical Industries, Ltd.)/0.1% sodium azide (Merck & Co. Inc.) or Tween 20 (Nacalai Tesque). After incubation at ambient temperature for 30 min, the cells were stained with PE-conjugated anti-IFN-γ mAb (BD Biosciences) in 50 μl of PBS/2% FCS/0.5% saponin/0.1% sodium azide. After 15 min, the cells were washed three times with 200 μl of PBS/2% FCS/0.5% saponin/0.1% sodium azide and examined for intracellular IFN-γ using a FACSCalibur flow cytometer and the cell population was visualized using FlowJo ver. 10. For intracellular staining of IFN-γ in PBMC, freshly isolated PBMC were stimulated with 1 μM of PTA for 2 days and examined for the production of IFN-γ as described above.

RESULTS

Intracellular Accumulation of IPP and DMAPP in PTA-Treated Target Cells

Nitrogen-containing bisphosphonates (B-BPs) inhibit farnesyl diphosphate synthase (FDPS) as illustrated in **Figure 1A**. Whereas, two metabolites, isopentenyl diphosphate (IPP), and dimethylallyl diphosphate (DMAPP) exist in the direct upstream of FDPS, attention has been paid only to IPP, because IPP and DMAPP are structural isomers and it has been difficult to isolate and identify these two molecular species on mass spectrometry (MS). We introduced a novel liquid chromatography-mass spectrometry (LC-MS) system and attempted to separate these isomers on LC-MS. After Raji Burkitt's lymphoma cells were treated with tetrakis-pivaloyloxymethyl 2-(thiazole-2-ylamino) ethylidene-1,1-bisphosphonate (PTA), an N-BP prodrug, the cell lysates were examined for IPP and DMAPP. As shown in **Figure 1B**, both IPP and DMAPP were markedly increased after treatment of the cells with 50 or 100 nM of PTA for 2 h in the extracted ion chromatogram (XIC) for $m/z = 244.9985$. Standard IPP was eluted at the retention time of 29.9 min and DMAPP at 30.3 min (**Figure 1C**), confirming their structural identity, which was further corroborated by daughter ion analysis (**Figures 2A,B**).

In order to examine the dose-dependent effect of PTA on the intracellular accumulation of IPP and DMAPP, Raji cells (1×10^6 cells) were treated with a half-log serial dilution of PTA at 37°C for 2 h and the intracellular IPP and DMAPP concentrations were quantified through LC-MS with synthetic IPP and DMAPP being used as references and expressed as nmoles/10^6 cells. As illustrated in the left panel of **Figure 2C**, both IPP and DMAPP accumulated in the cells in a PTA dose-dependent manner: 0.010 ± 0.001 nmole at 0 nM, 0.084 ± 0.003 nmole at 10 nM, 0.152 ± 0.012 nmole at 30 nM, 0.222 ± 0.005 nmole at 100 nM for IPP and 0.000 ± 0.000 nmole at 0 nM, 0193 ± 0.011 nmole at 10 nM, 0.352 ± 0.020 nmole at 30 nM, 0.485 ± 0.022 nmole at 100 nM for DMAPP. The concentrations of DMAPP in Raji cells were consistently higher than those of IPP at any concentrations of PTA. When the P31/FUJ monocytic cell line was examined for IPP and DMAPP accumulation, essentially the same results were obtained: 0.009 ± 0.000 nmole at 0 nM, 0.072 ± 0.004 nmole at 10 nM, 0.158 ± 0.006 nmole at 30 nM, 0.222 ± 0.007 nmole at 100 nM for IPP, and 0.000 ± 0.000 nmole at 0 nM, 0.115 ± 0.006 nmole at 10 nM, 0.226 ± 0.002 nmole at 30 nM, 0.330 ± 0.014 nmole at 100 nM for DMAPP as depicted in the right panel of **Figure 2C**. In PTA-treated P31/FUJ cells, the concentrations of DMAPP were higher than those of IPP at any PTA concentrations, as observed in Raji cells. Interestingly, zoledronic acid (ZOL), one of the most potent commercially available N-BPs, induced a low level of IPP and DMAPP in both cell lines even at a concentration of as high as 1,000 μM within 2 h of pulsing (**Figure 2D**). Although only a low level of DMAPP was observed in Raji cells after ZOL treatment for 2 h, the accumulation was dependent on ZOL concentrations: 0.000 ± 0.000 nmole at 0 μM, 0.001 ± 0.000 nmole at 100 μM, 0.002 ± 0.000 nmole at 300 μM, 0.07 ± 0.000 nmole at 1,000 μM. These results clearly demonstrated that PTA induced intracellular accumulation of IPP and DMAPP more efficiently than ZOL.

Expansion by PTA of Vγ2Vδ2 T Cells Derived From Healthy Adults and Lung Cancer Patients

Because intracellular accumulation of IPP and DMAPP by PTA leads to the recognition by Vγ2Vδ2 T cells, we next attempted to expand Vγ2Vδ2 T cells. Before implementing the expansion using PTA, we first examined the effect of media on the expansion of Vγ2Vδ2 T cells by ZOL. We compared RPMI1640 medium, one of the most frequently-used media, with Yssel's medium (39) used for the expansion of human natural killer (NK) cells and killer αβ T cells. After PBMC were stimulated with ZOL and expanded in the presence of IL-2, significant cell clustering was observed under a microscope as shown in **Figure S1A**. Regarding the initial phase of stimulation, RPMI1640 medium induced more pronounced responses in PBMC than Yssel's medium. When it comes to the proportion of Vγ2δV2 T cells, the initial

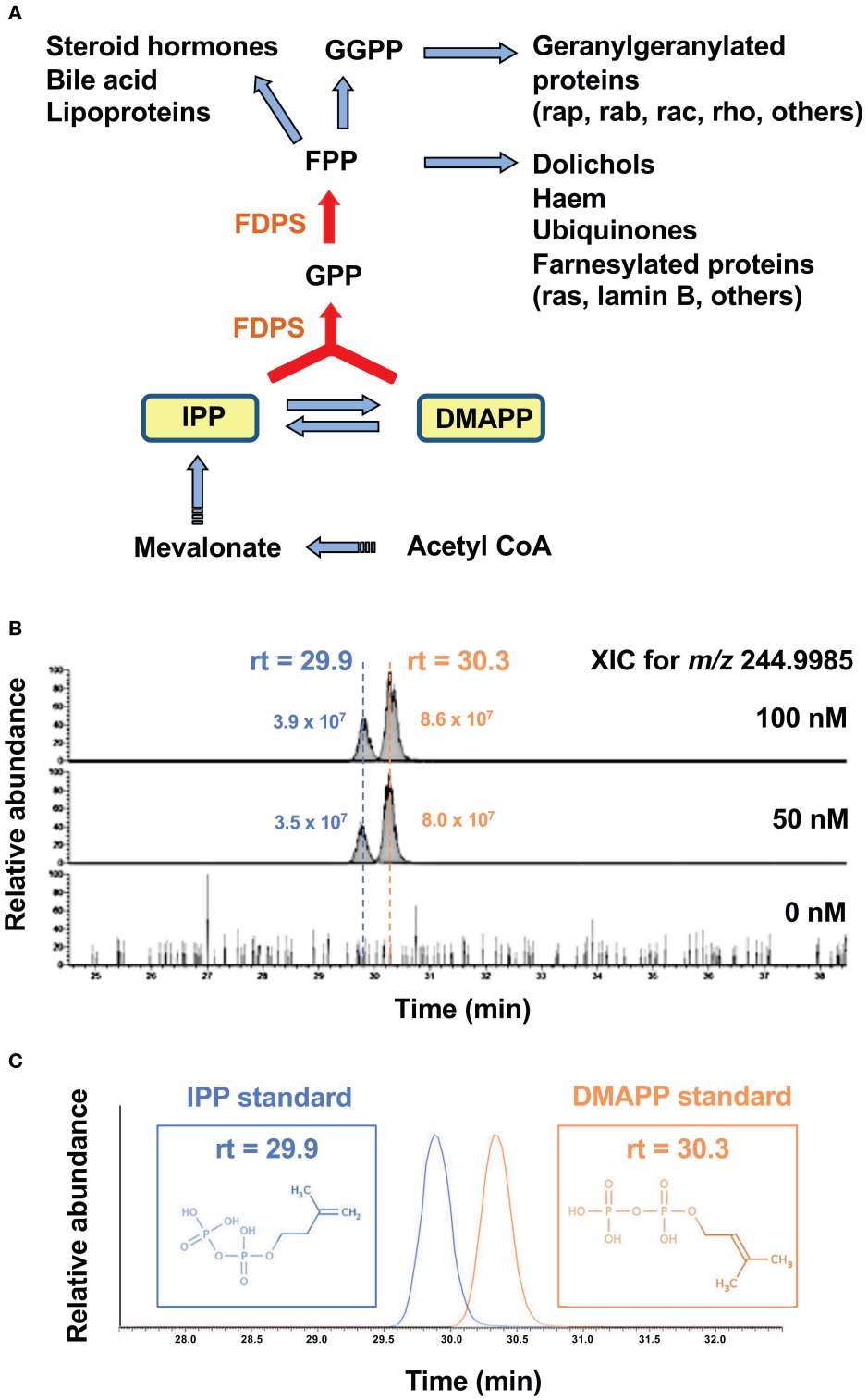

FIGURE 1 | Accumulation of IPP and DMAPP in target cells after treatment with PTA. **(A)** The mevalonate pathway and the metabolites in the upstream of FDPS. Isoprenoid metabolites are synthesized from acetyl- CoA via mevalonate through IPP and DMAPP. By the action of isomerase, IPP is converted into DMAPP. FDPS, a target of PTA, catalyzes the synthesis of GPP from IPP and DMAPP, and that of FPP from GPP and IPP. Metabolites in the direct upstream of FDPS are IPP and DMAPP. **(B)** Mass spectrometric analysis of IPP and DMAPP in target cells after treatment with PTA. After treatment of Raji Burkitt's lymphoma cells with PTA (0, 50, 100 nM) for 2 h, the samples were analyzed through LC-MS and the extracted ion chromatograms (XIC) for $m/z = 244.9985$ were depicted. **(C)** Identification of IPP and DMAPP using standard compounds. The retention time for the standard IPP was 29.9 min and that for standard DMAPP was 30.3 min.

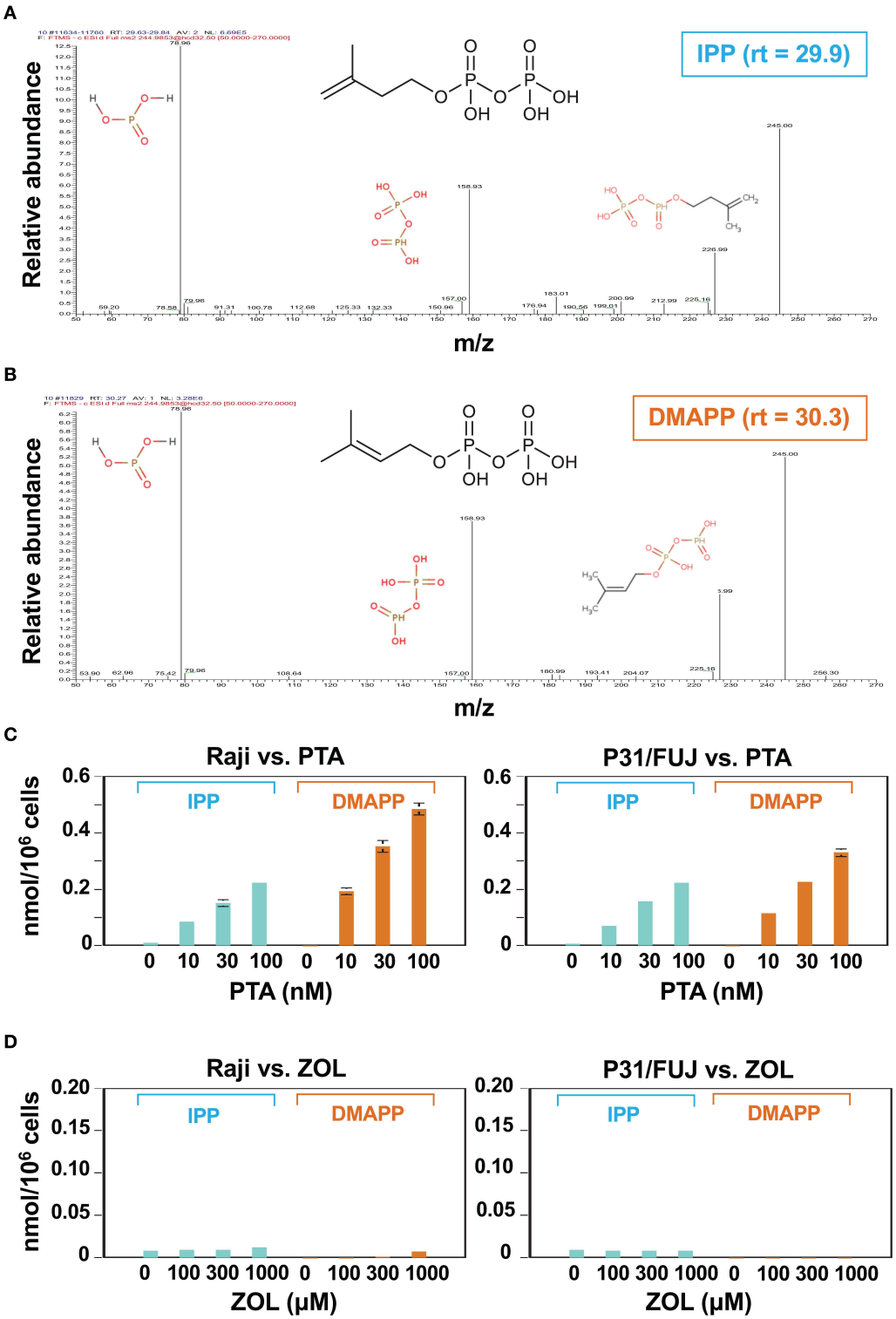

FIGURE 2 | Identification and quantitative analysis of IPP and DMAPP. Daughter ion analyses of IPP **(A)** and DMAPP **(B)**. The molecular species eluted at the retention time of 29.9 and 30.3 were analyzed using IC-ESI-MS (Q-Exactive Focus; Thermo Fisher Scientific, Bremen, Germany). Molecular identification by fragmentation patterns was conducted with referring METLIN database (https://metlin.scripps.edu). Quantitative analysis of IPP and DMAPP in Raji Burkitt's lymphoma cells and P31/FUJ monocytic cells treated with PTA **(C)** or ZOL **(D)**. Cell lines (10^6 cells each) were treated with 1 ml of a half-log serial dilution of PTA or ZOL at 37°C for 2 h and then IPP and DMAPP (nmol/10^6 cells) were quantified using the respective standard controls.

percentage of Vδ2 T cells was 0.94% among the lymphocyte gate of PBMC. After expansion by ZOL in RPMI1640 medium, the proportion of Vδ2 T cells was increased up to 39.3% on day 6 and 42.8% on day 7. In case of Yssel's medium, the proportion was 43.0% on day 6 and 65.8% on day 7, respectively (**Figure S1B**), indicating that YM medium supported the specific expansion of Vγ2Vδ2 T cells. After expansion for 11 days, the total number of Vδ2 T cells in Yssel's medium was greater than that in RPMI1640 medium (**Figure S1C**). Taken together, Yssel's medium was superior to RPMI1640 medium for the specific expansion of Vγ2Vδ2 T cells.

We next compared PTA and ZOL in the expansion of Vγ2Vδ2 T cells in Yssel's medium. When PBMC were stimulated with a serial dilution of PTA or ZOL in the presence of IL-2, cell clustering was observed on day 5 as shown in **Figure 3A**. Consistent with the dose-dependency in the intracellular accumulation of IPP and DMAPP (**Figure 2C**), 31.25 nM of PTA was sufficient to induce cell clustering in PBMC, whereas 5 μM of ZOL was required for cell clustering on day 5. The difference between PTA and ZOL in the induction of cell clustering in PBMC was 160-fold (31.25 nM vs. 5 μM). As shown in **Figure 3B**, the proportions of Vγ2Vδ2 T cells on day 8 were 3.87, 12.6, 54.5, and 70.1% when stimulated with 0, 156.25 nM, 1.25 μM, and 5 μM of ZOL, and 69.6, 86.7, and 94.8% with 31.25, 125 nM, and 1 μM of PTA, respectively, demonstrating that PTA induced the specific expansion of Vγ2Vδ2 T cells to a greater degree than ZOL.

We next examined the IFN-γ production from PBMC stimulated with PTA or ZOL for 2 days. As depicted in **Figure 3C**, the half maximal concentration of PTA for inducing IFN-γ in PBMC was about 5 nM and that of ZOL was 200 nM, demonstrating that the difference between PTA and ZOL in the induction of IFN-γ production from peripheral blood Vγ2Vδ2 T cells was 40-fold. When PTA-treated PBMC was examined for IFN-γ by intracellular staining on flow cytometry, $Vδ2^+$ T cells producing IFN-γ were detected (**Figure 3D**). Non-$Vδ2^+$ T cells also produced a low level of IFN-γ by inflammatory cytokines possibly derived from dendritic cells, consisting with previous reports (41, 42). We then examined the effect of PTA on the expansion of Vγ2Vδ2 T cells in lung cancer patients (**Figure 3E**). The initial proportions of $Vδ2^+CD3^+$ T cells in peripheral blood lymphocytes derived from lung cancer patients LC01 and LC02 were 1.43 and 2.91%, respectively. After stimulation with PTA and IL-2 for 11 days, the proportions of $Vδ2^+CD3^+$ T cells were increased to 98.39 and 99.74%, respectively. The demographic data of these lung cancer patients is shown in **Figure 3F**. The results demonstrated that Vγ2Vδ2 T cells of lung cancer patients could be efficiently expanded by PTA, which might be used for adoptive transfer therapy.

TCR-Independent Cellular Cytotoxicity Elicited by PTA-Expanded Vγ2Vδ2 T Cells

Human Vγ2Vδ2 T cells exhibit at least three types of cellular cytotoxicity, TCR-independent, TCR-dependent, and antibody-dependent cytotoxicity. We first analyzed cell surface markers expressed on PTA-expanded Vγ2Vδ2 T cells through flow cytometry. As shown in **Figure S2**, the purity of Vγ2Vδ2 T cells after expansion with PTA and IL-2 for 11 days was 99.2 and 98.5% in healthy adult volunteers HD01 and HD02, respectively. Most of the PTA-expanded Vγ2Vδ2 T cells exhibited a $CD45RA^-CD27+$ phenotype and were categorized into effector memory cells. The expression of NKG2D (CD314) C-type lectin receptor was detected on almost all the cells, while another C-type lectin receptor, CD94, was expressed in a subset of Vγ2Vδ2 T cells. DNAM-1 (CD226), an immunoglobulin superfamily receptor was expressed on almost all the cells, demonstrating that NK cell-like effector functions are expected in the PTA-expanded Vγ2Vδ2 T cells, in addition to Vγ2Vδ2 TCR-dependent killer activity. It is noteworthy that the PTA-expanded Vγ2Vδ2 T cells expressed antigen-presenting cell-related molecules like CD86, HLA-DR, and HLA-DQ, suggesting that tumor antigen-presentation by Vγ2Vδ2 T cells are expected after killing of tumor cells. In the present study, therefore, we further analyzed TCR-independent and -dependent cytotoxicity of the PTA-expanded Vγ2Vδ2 T cells.

We then examined TCR-independent, NK-like activity exhibited by PTA-expanded Vγ2Vδ2 T cells against lung cancer cells. When PC-9 human lung adenocarcinoma, PC-6 human lung small cell carcinoma, H1975 human lung adenocarcinoma, and H520 human lung squamous cell carcinoma cells were challenged by Vγ2Vδ2 T cells, no explicit cytotoxicity was observed in 40 min as shown in **Figure S3**, indicating that Vγ2Vδ2 T cells could not kill lung cancer cells in an early phase (within 40 min) even at an effector-to-target (E/T) ratio of 80:1.

When the incubation was extended to 4 h, 20–30% of specific lysis was observed in all the four lung cancer cell lines at an E/T ratio of 80:1. Further extension of the culture to 16 h gave more extensive cellular cytotoxicity even at an E/T ratio of 10:1 as shown in the left panels of **Figure 4**. It is thus likely that Vγ2Vδ2 T cells require relatively long time to kill lung cancer cells when TCR is not involved in the recognition.

TCR-Dependent Killing of Lung Cancer Cells by Vγ2Vδ2 T Cells

We next compared PTA and ZOL in the TCR-dependent killing of lung cancer cells by Vγ2Vδ2 T cells. When PTA- or ZOL-pulsed lung cancer cell lines were challenged by Vγ2Vδ2 T cells for 40 min at an E/T ratio of 80:1, the specific lysis rate attained to around 30% in all the lung cancer cell lines as shown in the middle panels of **Figure 4**. The concentrations required for the half maximal specific lysis rates were 10–30 nM for PTA and 100–300 μM for ZOL, with the difference between the two compounds in the sensitization of tumor cells being ∼10,000-fold.

When the incubation was extended to 4 h, more than 50% of PTA- or ZOL-pulsed lung cancer cells were killed by Vγ2Vδ2 T cells at an E/T ratio of 15:1, with the drug concentrations required for the half-maximal specific lysis rates being essentially the same as those for 40 min as shown in the right panels of **Figure 4**. Further prolongation of the incubation time to 16 h resulted in

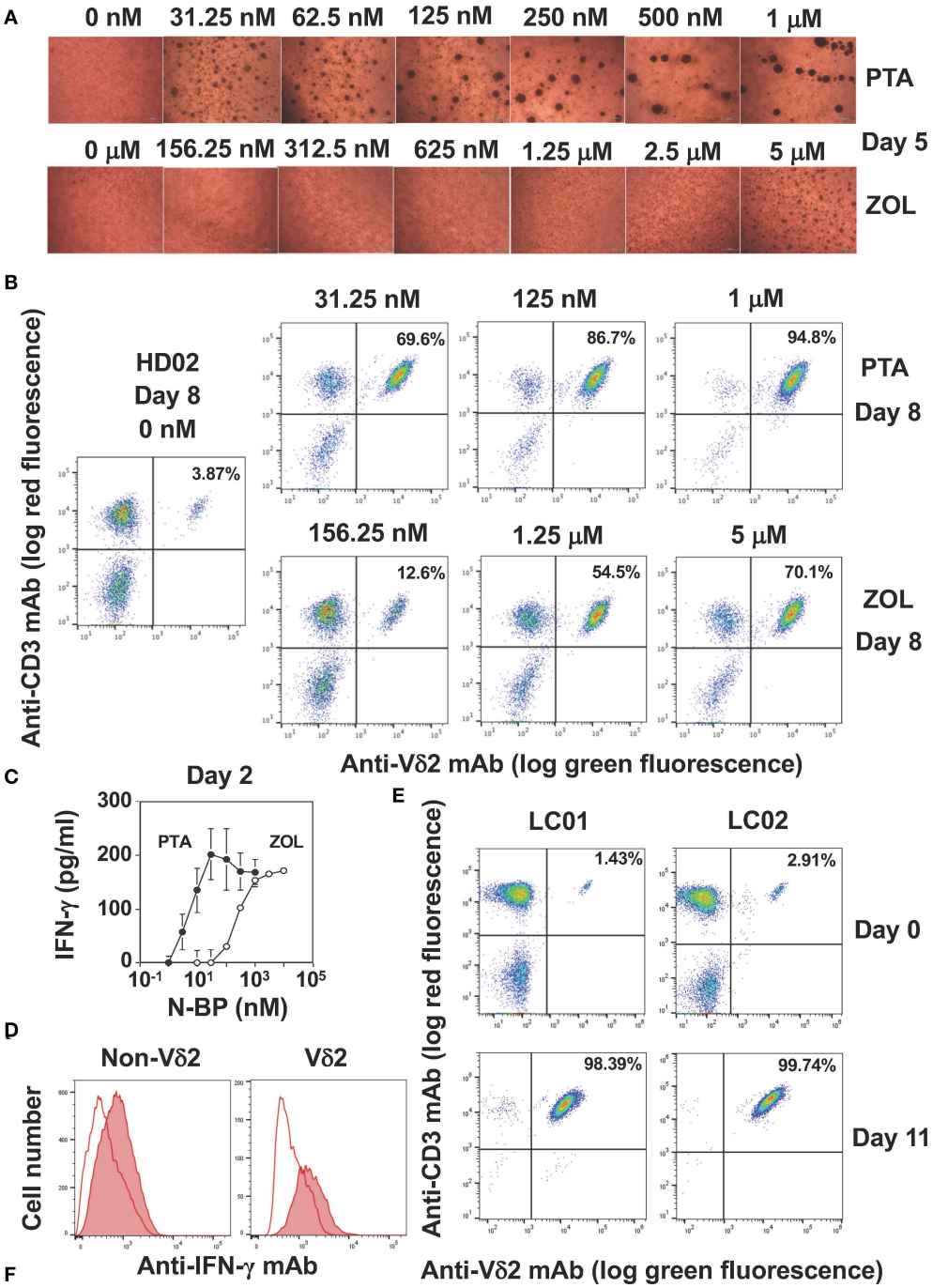

Patient	Age	Sex	Type	TNM classification	Stage	Previous treatment
LC01	70	M	Sq	cT2aN2M0	IIIA	None
LC02	54	M	Sq	cT1bN3M0	IIIB	None

FIGURE 3 | Comparison of PTA and ZOL in the expansion of peripheral blood Vγ2Vδ2 T cells. **(A)** Microscopic observation of PBMC from a healthy adult stimulated with PTA or ZOL. PBMC derived from a healthy donor (HD02) were stimulated with a serial dilution of PTA or ZOL and the cell clustering was observed under a microscope on day 5. **(B)** Flow cytometric analysis of PBMC stimulated with PTA or ZOL. PBMC derived from HD02 was stimulated as in **(A)** were examined for the expression of CD3 and Vδ2 on day 8. **(C)** IFN-γ production by Vγ2Vδ2 T cells in response to PTA or ZOL. After stimulation of PBMC with PTA or ZOL for 2 days, IFN-γ was measured through ELISA. **(D)** Intracellular staining of IFN-γ in PBMC stimulated with PTA. PBMC stimulated with PTA in **(C)** was examined for intracellular IFN-γ through flow cytometry. **(E)** Expansion of Vγ2Vδ2 T cells by PTA **(D)**. Flow cytometric analysis was performed on days 0 and 11 after stimulation of PBMC with 1 μM of PTA derived from lung cancer patients (LC01 and LC02). **(F)** Clinical characteristics of the LC01 and LC02 lung cancer patients.

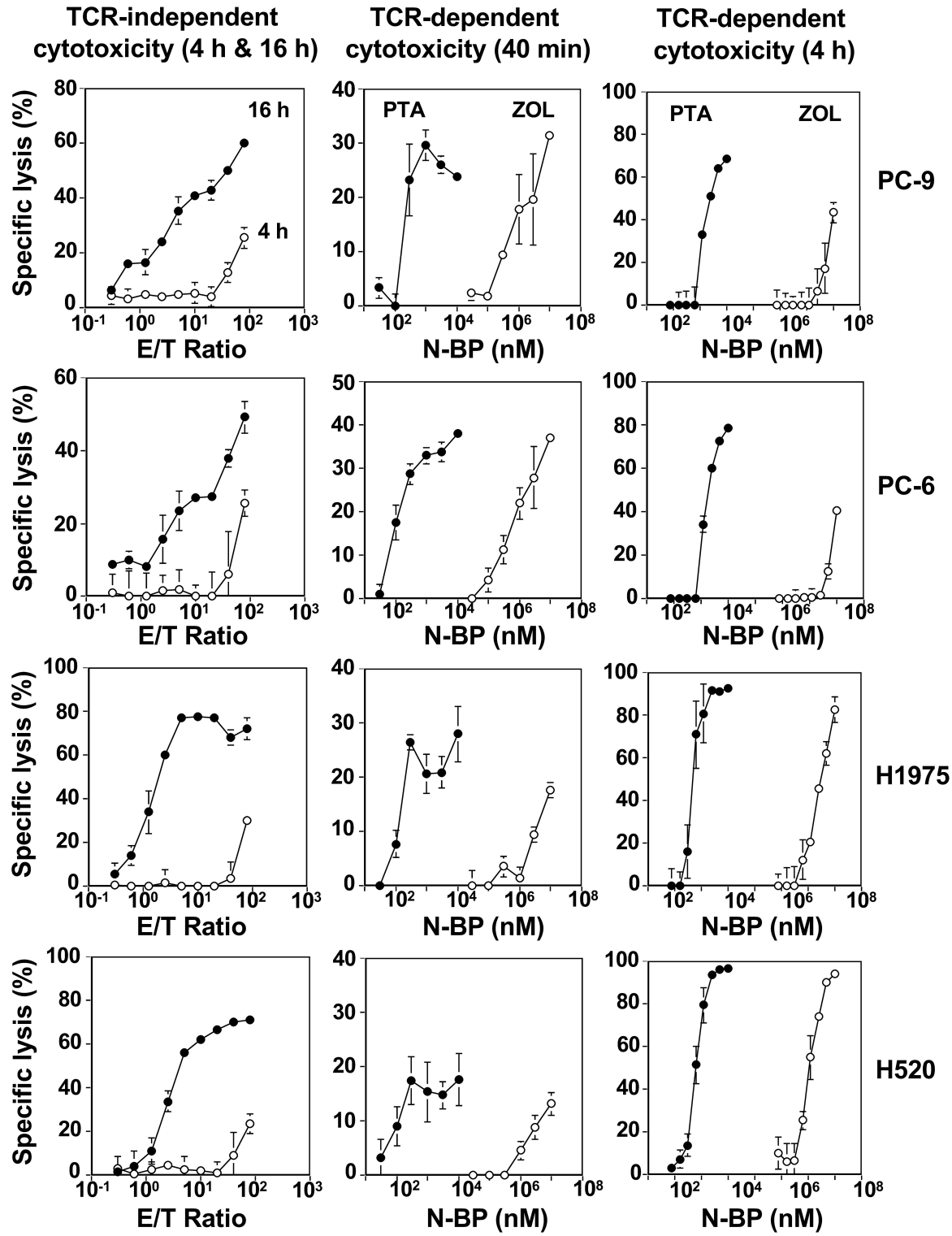

FIGURE 4 | Vγ2Vδ2 T cell-mediated cytotoxicity against human lung cancer cells. (Left panels) TCR-independent cytotoxicity mediated by Vγ2Vδ2 T cells against lung cancer cell lines. PC-9 human lung adenocarcinoma, PC-6 human lung small cell carcinoma, H1975 human lung adenocarcinoma, and H520 human lung squamous

(Continued)

FIGURE 4 | cell carcinoma cells lines were challenged by PTA-expanded Vγ2Vδ2 T cells at E/T ratios of 0.3125:1, 0.625:1, 1.25:1, 2.5;1, 5;1, 10:1, 20:1, 40:1, and 80:1. After incubation for 4 h (○) or 16 h (•), the amount of adenosine triphosphate in viable, adherent cells were quantified by using a luciferase assay system and the specific lysis (%) was determined. (Middle panels) Early phase of TCR-dependent cellular cytotoxicity by Vγ2Vδ2 T cells against human lung cancer cells. Human lung cancer cell lines PC-9, PC-6, H1975, and H520 were pretreated with PTA (•) at concentrations of 3, 10, 30, 100, 300, and 1,000 nM, or ZOL (○) at concentrations of 3, 10, 30, 100, 300, and 1,000 μM and challenged by PTA-expanded Vγ2Vδ2 T cells at an E/T ratio of 80:1. After incubation for 40 min, the amount of 4′-(hydroxymethyl)-2,2′:6′,2″-terpyridine-6,6″-dicarboxylate (HT), a hydrolyzate derived from PTA by the action of intracellular esterases, released from dead target cells was quantified by harnessing Eu-based time-resolved fluorescence and the specific lysis (%) was determined. (Right panels) Later phase of TCR-dependent cellular cytotoxicity by Vγ2Vδ2 T cells against human lung cancer cells. PC-9, PC-6, H1975, and H520 human lung cancer cells (2×10^4 cells) were pretreated with PTA (•) at concentrations of 0.78125, 1.5625, 3.125, 6.25, 12.5, 25, 50, or 100 nM, or ZOL (○) at concentrations of 7.8125, 15.625, 31.25, 62.5, 125, 250, 500, or 1,000 μM and challenged by PTA-expanded Vγ2Vδ2 T cells (3×10^5 cells). After incubation for 4 h, the amount of adenosine triphosphate in viable, adherent cells were quantified by using a luciferase assay system and the specific lysis (%) was determined.

the maximal specific lysis rate of 80% or greater, and the drug concentrations required for the half-maximal specific rates were essentially the same as those for 40 min and 4 h (**Figure S4**).

IFN-γ Production From Vγ2Vδ2 T Cells in Response to PTA-Pulsed Lung Cancer Cells

Finally, we compared PTA and ZOL in the induction of IFN-γ in Vγ2Vδ2 T cells. When PTA- or ZOL-pulsed lung cancer cells were incubated with Vγ2Vδ2 T cells, IFN-γ was secreted from Vγ2Vδ2 T cells in a compound dose-dependent manner, in which the drug concentrations required for the half-maximal IFN-γ production were 10–30 nM for PTA and 100–300 μM for ZOL (**Figure 5A**), consistent with the results observed in cellular cytotoxicity assay. The secretion of IFN-γ from Vγ2Vδ2 T cells was confirmed by intracellular staining of IFN-γ as shown in **Figure 5B**, in which the amount of IFN-γ secreted from Vγ2Vδ2 T cells in response to PTA-pulsed lung cancer cells was more than that to ZOL-pulsed target cells.

DISCUSSION

Since the success of CTLA-4 and PD-1 immune checkpoint inhibitors, increasing attention has been paid to cancer immunotherapy (1, 5). Adoptive transfer of immune effector cells is one of the most promising strategies, because the critical phase of cancer immunotherapy is the killing of tumor cells by immune effector cells. Whereas, a variety of immune effector cells are involved in the eradication of tumor cells, it is generally difficult to prepare a large number of functionally robust immune effector cells for adoptive immunotherapy. For instance, NK cells occupy 10–20% of peripheral blood mononuclear cells. When NK cells are stimulated, nearly 100-fold expansion is observed in 10 days (43). Prolonged culture, however, leads to the accumulation of functionally altered or exhausted phenotype of NK cells, resulting in the limitation of NK cell-based immunotherapy (44). Regarding $CD8^+$ αβ T cells, the proportion of tumor antigen-specific $CD8^+$ αβ T cells in tumor-infiltrating T lymphocytes (TILs) is only 10% and it is difficult to expand a large number of functional tumor antigen-specific $CD8^+$ T cells for adoptive immunotherapy (45). By contrast, it is relatively easy to expand Vγ2Vδ2 T cells using pyrophosphomonoester pAgs or N-BPs for adoptive immunotherapy. Previously, we synthesized PTA, a novel N-BP prodrug, and demonstrated that PTA induced an efficient expansion of Vγ2Vδ2 T cells. Because the mechanism underlying the responses of Vγ2Vδ2 T cells to PTA was, however, not fully elucidated, we first examined the effect of PTA on the activity of FDPS in tumor cells as a model system, a possible target of PTA, at a molecular level.

Since the discovery that metabolites in the mevalonate pathway in human and other animal cells and the 2-*C*-methyl-D-erythritol 4-phosphate/1-deoxy-D-xylulose 5-phosphate (MEP/DOXP) non-mevalonate pathway in microbial pathogens, attention has been paid to IPP as an endogenous ligand and HMBPP as a foreign PAg (46). After it was found that PAM and ZOL inhibited FDPS in the mevalonate and non-mevalonate pathways, N-BPs, especially ZOL, have been used for the expansion of Vγ2Vδ2 T cells in the laboratory and for clinical trials, because the inhibition of FDPS by N-BPs leads to the intracellular accumulation of IPP, which is the metabolite upstream of FDPS and has activity in stimulating Vγ2Vδ2 T cells in a BTN2A1/3A1-dependent manner (31–33, 47, 48).

Whereas, both IPP and DMAPP are the direct upstream metabolites of FDPS, DMAPP has not been studied extensively, because it is difficult to distinguish DMAPP from IPP in N-BP-pulsed target cells on MS analyses. We recently developed a methodology to isolate and identify the two metabolites. In this study, we applied this strategy to detect IPP and DMAPP in tumor cells pulsed with PTA, an N-BP prodrug, which by itself has no inhibitory activity for FDPS. PTA is a hydrophobic prodrug compound and readily permeates target cell membranes. Once PTA is incorporated into target cells, intracellular esterases hydrolyze the prodrug to give (thiazole-2-ylamino)ethylidene-1,1-bisphosphonate (TA), a hydrophilic compound that directly inhibits FDPS. It is difficult for TA to permeate the membrane, resulting in the accumulation of the compound within the target cells (36).

Based on the present LC-MS study, it is clear that both IPP and DMAPP accumulate in tumor cells pulsed with PTA and that the amount of DMAPP in the PTA-pulsed cells is ∼2-fold greater than that of IPP in Raji Burkitt's lymphoma cells and ∼1.5-fold in P31/FUJ monocytic cells. Since the Vγ2Vδ2 T cell-stimulating activity of IPP is 2 to 3-fold higher than that of DMAPP (15), the physiological significance of the intracellularly accumulated DMAPP in the tumor sensitization for Vγ2Vδ2 T

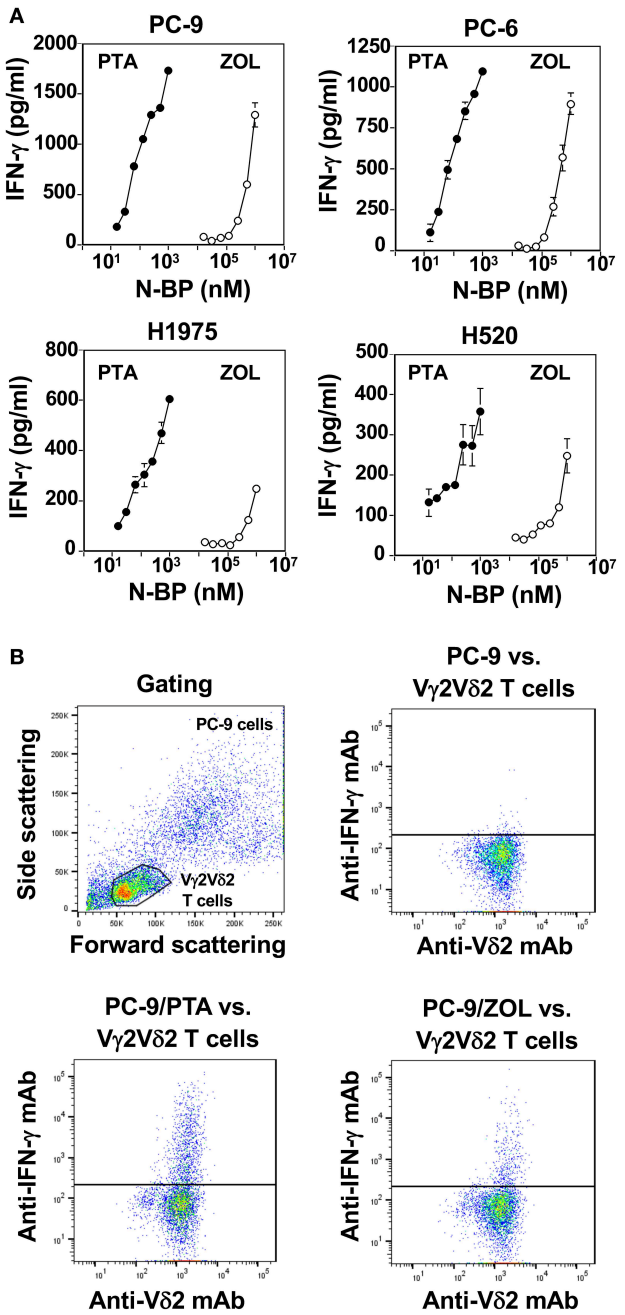

FIGURE 5 | Comparison of PTA and ZOL in the induction of IFN-γ from Vγ2Vδ2 T cells. **(A)** Determination of IFN-γ produced by Vγ2Vδ2 T cells in response to lung cancer cell lines pulsed with PTA or ZOL. Human lung cancer cells, PC-9, PC-6, H1975, and H520 (4×10^5 cells), pretreated with PTA (•) at concentrations of 15.625, 31.25, 62.5, 125, 250, 500, or 1,000 nM, or ZOL (○) at concentrations of 7.8125, 15.625, 31.25, 62.5, 125, 250, 500, or 1,000 μM were challenged by PTA-expanded Vγ2Vδ2 T cells (4×10^5 cells). After incubation for 16 h, the culture supernatants were examined for IFN-γ levels through ELISA. **(B)** Intracellular staining of IFN-γ in Vγ2Vδ2 T cells in response to human lung cancer cells pretreated with PTA or ZOL. PC-9 human lung cancer cells (1×10^6 cells/ml) were treated with 1 ml of the complete RPMI1640 medium or the medium containing 1 μM PTA or with 1 mM ZOL at 37°C with 5% CO_2 for 2 h. Then, the cells were examined for intracellular IFN-γ using a FACSCalibur flow cytometer and the cell population was visualized using FlowJo ver. 10.

cells is equivalent to that of IPP. Taken together, it is most likely that both IPP and DMAPP are equally functional and important in stimulating Vγ2Vδ2 T cells when antigen-presenting cells are pulsed with PTA.

For developing adoptive transfer of Vγ2Vδ2 T cells, it is imperative to establish an efficient protocol for preparing Vγ2Vδ2 T cells, in which the number and purity are the two major issues. We examined the effect of medium on the expansion of Vγ2Vδ2 T cells. Since ZOL is commonly used to expand Vγ2Vδ2 T cells in the laboratory, we used ZOL as a stimulant. In order to establish or maintain human NK cells and CD8 killer T cells, Yssel's medium is often used (39). We thus compared Yssel's medium with one of the most commonly used RPMI1640 medium in the expansion of Vγ2Vδ2 T cells. Based on the present study, stimulation of PBMC with ZOL/IL-2 in RPMI1640 medium resulted in non-specific, stimulatory effects on lymphocytes including NK cells and αβ T cells at the initial phase of expansion until day 4–5, but the non-specific stimulation failed to sustain longer expansion of Vγ2Vδ2 T cells. In contrast, non-specific stimulation of lymphocytes was limited in Yssel's medium at the initial phase and specific expansion of Vγ2Vδ2 T cells was observed until day 11, resulting in the high number and purity of Vγ2Vδ2 T cells.

It was previously shown that negatively-charged N-BPs taken up by monocytes or dendritic cells through fluid-phase endocytosis inhibited FDPS, resulting in the depletion of the downstream metabolites including geranylgeranyl diphosphate (49). One of the metabolites derived from geranylgeranyl diphosphate is geranylgeraniol that might stabilize proaspase-1 (50). Procaspase-1 is a precursor of caspase-1 that converts pro-interleukin-1 (IL-1β) into mature IL-1β and pro-IL-18 into mature IL-18. Since IL-1β induces inflammation and IL-18 enhances the inflammation, the depletion of geranylgeraniol might induce inflammation. Furthermore, it was demonstrated that soluble factors such as IL-18 derived from dendritic cells pulsed with ZOL enhanced the production of IFN-γ in non-Vδ2 cells like NK cells when PBMC were treated with ZOL/IL-2 (41, 42). In addition, the inhibition of FDPS by PTA results in the accumulation of IPP and DMAPP, followed by the condensation of IPP and adenosine monophosphate (AMP) to yield triphosphoric acid 1-adenosin-5′-yl ester 3-(3-methylbut-3-enyl) ester (APPPI) (51). It was demonstrated that mitochondrial and lysosomal membrane permeabilization was inhibited by APPPI, resulting in cell death and subsequent inflammation. The present study indicates that Yssel's medium somehow prevents the inflammation caused by IL-1β/IL-18/IFN-γ and APPPI and sustains the specific expansion of Vγ2Vδ2 T cells triggered by accumulation of IPP and DMAPP in a BTN2A1/3A1-dependent manner.

We then compared PTA and ZOL in the stimulation and expansion of peripheral blood Vγ2Vδ2 T cells. The half-maximal concentration of PTA required for stimulating circulating Vγ2Vδ2 T cells was ∼30 nM, whereas that of ZOL was ∼5 μM, demonstrating that PTA was about 100-fold more effective in stimulating peripheral blood Vγ2Vδ2 T cells

than ZOL. In stimulating peripheral blood Vγ2Vδ2 T cells with ZOL, the major subsets of antigen-presenting cells are adherent cells, such as monocytes and dendritic cells (52). These cells can take up many small molecules including positively- or negatively-charged compounds through fluid-phase endocytosis (49, 53). Although ZOL is negatively-charged under a physiological condition, the drug can be taken up by monocytes and dendritic cells at a clinical concentration of 2 μM (54). Based on the findings in the present study, it is reasonable to use ZOL for the expansion of Vγ2Vδ2 T cells, whereas PTA is more convenient and efficient to obtain a large number of highly purified Vγ2Vδ2 T cells for adoptive transfer therapy for cancer and possibly for infectious diseases, because the number and purity of PTA-expanded Vγ2Vδ2 T cells are higher than those of ZOL-stimulated Vγ2Vδ2 T cells. Phenotypic analysis of the PTA-expanded Vγ2Vδ2 T cells revealed that most of them exhibited effector memory phenotype (55) and expressed NK cell receptors like NKG2D and DNAM-1. As previously reported, antigen-presenting cell-related molecules such as CD86, HLA-DQ, and HLA-DR were also expressed, suggesting that Vγ2Vδ2 T cells might serve as antigen-presenting cells as well as immune effector cells.

When N-BP-expanded Vγ2Vδ2 T cells are used for adoptive cell therapy for cancer, TCR-dependent recognition of tumor cells is not anticipated, except for particular malignant cells, such as Dauid Burkitt's lymphoma and RPMI8226 multiple myeloma cells, based on previous studies (56). In this study, we examined the TCR-independent, NK-like cellular cytotoxicity of Vγ2Vδ2 T cells against lung cancer cell lines. Since human NK cells kill malignant cells including K562 erythrocytoma cells in 40 min (43), we employed the same 40 min protocol for the killing by Vγ2Vδ2 T cells of lung cancer cell lines, including PC-9 human lung adenocarcinoma, PC-6 human lung small cell carcinoma, H1975 human lung adenocarcinoma, and H520 human lung squamous cell carcinoma cells. Based on the time-resolved fluorescence assay, the lung cancer cell lines were resistant to NK-like activity of Vγ2Vδ2 T cells in a relatively short period of incubation.

Vγ2Vδ2 T cells-mediated NK-like cytotoxicity against lung cancer cells became apparent after 4 h of incubation at an E/T ratio of 80:1, based on luminescence-based assay. Further extension of the incubation increased the specific lysis rates even at an E/T ratio of 2.5:1. These results demonstrate that Vγ2Vδ2 T cells can kill lung cancer cells in an NK-like manner, whereas a higher E/T ratio and a longer incubation time are required for the manifestation of the Vγ2Vδ2 TCR-independent, NK-like cellular cytotoxicity, compared to those for conventional human NK cells against K562 cells.

It was previously demonstrated that commercially available N-BPs such as PAM and ZOL could sensitize not only monocytes and dendritic cells, but also tumor cells (52, 57). In this assay system, N-BP-sensitized tumor cells were killed by Vγ2Vδ2 T cells in a TCR-dependent manner (56). We then compared PTA and ZOL in the sensitization of lung cancer cells, PC-9, PC-6, H1975, and H520, for Vγ2Vδ2 T cells. In the 40-min assay, the concentrations required for the half-maximal specific lysis rates were 10–30 nM for PTA in all the lung cancer cell lines. By contrast, 100–300 μM of ZOL was required for the same level of cellular cytotoxicity, with the difference between PTA and ZOL being ∼10,000-fold. Further extension of incubation time to 4 or 16 h also resulted in essentially the same difference between the two compounds.

It is worthy of note that 100–300 μM of ZOL is required for the sensitization of lung cancer cells for Vγ2Vδ2 T cells, which is much higher than the plasma concentration (1–2 μM) after infusion of 4 mg of ZOL (54). This finding confirms that ZOL can be used for the expansion of Vγ2Vδ2 T cells, because antigen-presenting cells like monocytes and dendritic cells can take up ZOL efficiently through fluid-phase endocytosis (49, 53). It is, however, unlikely that ZOL can sensitize lung cancer cells for Vγ2Vδ2 T cells, since the plasma ZOL concentration (1–2 μM) is not enough to fully inhibit FDPS in lung cancer cells.

By contrast, PTA readily permeates tumor cell membranes, where esterases hydrolyze the prodrug to yield an active TA that can efficiently inhibit FDPS (36). It is thus prerequisite to develop N-BP prodrugs for successful Vγ2Vδ2 T cell-based immunotherapy for lung cancer. Although pivaloyloxymethyl group-protected prodrugs of N-BPs exhibit a high level of activity for sensitizing Vγ2Vδ2 T cells, they are generally too hydrophobic and suitable drug delivery system has to be developed in the future.

DATA AVAILABILITY STATEMENT

The datasets generated for this study are available on request to the corresponding author.

ETHICS STATEMENT

The studies involving human participants were reviewed and approved by Institutional Review Board of Nagasaki University Hospital. The patients/participants provided their written informed consent to participate in this study.

AUTHOR CONTRIBUTIONS

YS and YT designed the research. DO, YS, MT, MI, SN, AT, HS, YU, and YT performed the experiments. DO, YS, NS, HY, MS, CM, YT, and HM prepared the manuscript. YT and HM supervised the overall project. All authors discussed the results and commented on the manuscript.

FUNDING

This work was supported by Grants-in-Aid for Scientific Research from the Ministry of Education, Science, Culture, Sports, and Technology of Japan (MEXT) (16K08844 to YT) by Grants-in-Aid for Scientific Research from Japan

Agency for Medical Research and Development (A48 and A90 to YT) and by Grants from the Department of Veterans Affairs (Veterans Health Administration, Office of Research and Development, Biomedical Laboratory Research and Development) (1 I01 BX000972-01A1) to CM and from the National Cancer Institute P30CA086862 (Core Support). CM is the Kelting Family Scholar in Rheumatology. The content of this manuscript are solely the responsibility of the authors and do not necessarily represent the official views of the granting agencies.

ACKNOWLEDGMENTS

The authors are grateful to Ms. Yoshiko Akiyama for technical assistance.

SUPPLEMENTARY MATERIAL

The Supplementary Material for this article can be found online at: https://www.frontiersin.org/articles/10.3389/fimmu.2020.01405/full#supplementary-material

REFERENCES

1. Brahmer JR, Tykodi SS, Chow LQ, Hwu WJ, Topalian SL, Hwu P, et al. Wigginton: Safety and activity of anti-PD-L1 antibody in patients with advanced cancer. *N Engl J Med.* (2012) 366:2455–65. doi: 10.1056/NEJMoa1200694
2. Iwai Y, Ishida M, Tanaka Y, Okazaki T, Honjo T, Minato N. Involvement of PD-L1 on tumor cells in the escape from host immune system and tumor immunotherapy by PD-L1 blockade. *Proc Natl Acad Sci USA.* (2002) 99:12293–7. doi: 10.1073/pnas.192461099
3. Nishimura H, Okazaki T, Tanaka Y, Nakatani K, Hara M, Matsumori A, et al. Autoimmune dilated cardiomyopathy in PD-1 receptor-deficient mice. *Science.* (2001) 291:319–22. doi: 10.1126/science.291.5502.319
4. Okazaki T, Tanaka Y, Nishio R, Mitsuiye T, Mizoguchi A, Wang J, et al. Autoantibodies against cardiac troponin I are responsible for dilated cardiomyopathy in PD-1-deficient mice. *Nat Med.* (2003) 9:1477–83. doi: 10.1038/nm955
5. Topalian SL, Hodi FS, Brahmer JR, Gettinger SN, Smith DC, McDermott DF, et al. Safety, activity, and immune correlates of anti-PD-1 antibody in cancer. *N Engl J Med.* (2012) 366:2443–54. doi: 10.1056/NEJMoa1200690
6. Hodi FS, Mihm MC, Soiffer RJ, Haluska FG, Butler M, Seiden MV, et al. Biologic activity of cytotoxic T lymphocyte-associated antigen 4 antibody blockade in previously vaccinated metastatic melanoma and ovarian carcinoma patients. *Proc Natl Acad Sci USA.* (2003) 100:4712–7. doi: 10.1073/pnas.0830997100
7. Dieli F, Vermijlen D, Fulfaro F, Caccamo N, Meraviglia S, Cicero G, et al. Targeting human γδ T cells with zoledronate and interleukin-2 for immunotherapy of hormone-refractory prostate cancer. *Cancer Res.* (2007) 67:7450–7. doi: 10.1158/0008-5472.CAN-07-0199
8. Kobayashi H, Tanaka Y, Yagi J, Minato N, Tanabe K. Phase I/II study of adoptive transfer of γδ T cells in combination with zoledronic acid and IL-2 to patients with advanced renal cell carcinoma. *Cancer Immunol Immunother.* (2011) 60:1075–84. doi: 10.1007/s00262-011-1021-7
9. Rossjohn J, Gras S, Miles JJ, Turner SJ, Godfrey DI, McCluskey J. T cell antigen receptor recognition of antigen-presenting molecules. *Annu Rev Immunol.* (2015) 33:169–200. doi: 10.1146/annurev-immunol-032414-112334
10. Adam P, Hecht S, Eisenreich W, Kaiser J, Grawert T, Arigoni D, et al. Biosynthesis of terpenes: studies on 1-hydroxy-2-methyl-2-*(E)*-butenyl 4-diphosphate reductase. *Proc Natl Acad Sci USA.* (2002) 99:12108–13. doi: 10.1073/pnas.182412599
11. Constant P, Davodeau F, Peyrat MA, Poquet Y, Puzo G, Bonneville M, et al. Stimulation of human γδ T cells by nonpeptidic mycobacterial ligands. *Science.* (1994) 264:267–70. doi: 10.1126/science.8146660
12. Hintz M, Reichenberg A, Altincicek B, Bahr U, Gschwind RM, Kollas AK, et al. Identification of *(E)*-4-hydroxy-3-methyl-but-2-enyl pyrophosphate as a major activator for human γδ T cells in *Escherichia coli*. *FEBS Lett.* (2001) 509:317–22. doi: 10.1016/s0014-5793(01)03191-x
13. Kabelitz D, Wesch D, Pitters E, Zöller M. Potential of human γδ T lymphocytes for immunotherapy of cancer. *Int J Cancer.* (2004) 112:727–32. doi: 10.1002/ijc.20445
14. Kabelitz D, Wesch D, He W. Perspectives of γδ T cells in tumor immunology. *Cancer Res.* (2007) 67:5–8. doi: 10.1158/0008-5472.CAN-06-3069
15. Tanaka Y, Morita CT, Nieves E, Brenner MB, Bloom RB. Natural and synthetic non-peptide antigens recognized by human γδ T cells. *Nature.* (1995) 375:155–8. doi: 10.1038/375155a0
16. Gu S, Sachleben JR, Boughter CT, Nawrocka WI, Borowska MT, Tarrasch JT, et al. Phosphoantigen-induced conformational change of butyrophilin 3A1 (BTN3A1) and its implication on Vγ9Vδ2 T cell activation. *Proc Natl Acad Sci USA.* (2017) 114:E7311–20. doi: 10.1073/pnas.1707547114
17. Gu S, Borowska MT, Boughter CT, Adams JE. Butyrophilin3A proteins and Vγ9Vδ2 T cell activation. *Semin Cell Dev Biol.* (2018) 84:65–74. doi: 10.1016/j.semcdb.2018.02.007
18. Harly C, Guillaume Y, Nedellec S, Peigné CM, Mönkkönen H, Mönkkönen J, et al. Key implication of CD277/butyrophilin-3 (BTN3A) in cellular stress sensing by a major human γδ T-cell subset. *Blood.* (2012) 120:2269–79. doi: 10.1182/blood-2012-05-430470
19. Salim M, Knowles TJ, Baker AT, Davey MS, Jeeves M, Sridhar P, et al. BTN3A1 discriminates γδ T cell phosphoantigens from nonantigenic small molecules via a conformational sensor in its B30.2 domain. *ACS Chem Biol.* (2017) 12:2631–43. doi: 10.1021/acschembio.7b00694
20. Sandstrom A, Peigné CM, Léger A, Crooks JE, Konczak F, Gesnel MC, et al. The intracellular B30.2 domain of butyrophilin 3A1 binds phosphoantigens to mediate activation of human Vγ9Vδ2 T cells. *Immunity.* (2014) 40:490–500. doi: 10.1016/j.immuni.2014.03.003
21. Sebestyen Z, Scheper W, Vyborova A, Gu S, Rychnavska Z, Schiffler M, et al. RhoB mediates phosphoantigen recognition by Vγ9Vδ2 T cell receptor. *Cell Rep.* (2016) 15:1973–85. doi: 10.1016/j.celrep.2016.04.081
22. Vantourout P, Laing A, Woodward MJ, Zlatareva I, Apolonia L, Jones AW, et al. Heteromeric interactions regulate butyrophilin (BTN) and BTN-like molecules governing γδ T cell biology. *Proc Natl Acad Sci USA.* (2018) 115:1039–44. doi: 10.1073/pnas.1701237115
23. Wang H, Henry O, Distefano MD, Wang YC, Räikkönen J, Mönkkönen J, et al. Butyrophilin 3A1 plays an essential role in prenyl pyrophosphate stimulation of human Vγ2Vδ2 T cells. *J Immunol.* (2013) 191:1029–42. doi: 10.4049/jimmunol.1300658
24. Wang H, Nada MH, Tanaka Y, Sakuraba S, Morita CT. Critical roles for coiled-coil dimers of butyrophilin 3A1 in the sensing of prenyl pyrophosphates by human Vγ2Vδ2 T cells. *J Immunol.* (2019) 203:607–26. doi: 10.4049/jimmunol.1801252
25. Rigau M, Ostrouska S, Fulford TS, Johnson DN, Woods K, Ruan Z, et al. Butyrophilin 2A1 is essential for phosphoantigen reactivity by γδ T cells. *Science.* (2020) 367:eaay5516. doi: 10.1126/science.aay5516
26. Willcox BE, Willcox RC. γδ TCR ligands: the quest to solve a 500-million-year-old mystery. *Nat Immunol.* (2019) 20:121–28. doi: 10.1038/s41590-018-0304-y
27. Yang Y, Li L, Yuan L, Zhou X, Duan J, Xiao H, et al. A structural change in butyrophilin upon phosphoantigen binding underlies phosphoantigen-mediated Vγ9Vδ2 T cell activation. *Immunity.* (2019) 50:1043–53.e5. doi: 10.1016/j.immuni.2019.02.016
28. Nada MH, Wang H, Workalemahu G, Tanaka Y, Morita CT. Enhancing adoptive cancer immunotherapy with Vγ2Vδ2 T cells through pulse zoledronate stimulation. *J Immunother Cancer.* (2017) 5:9. doi: 10.1186/s40425-017-0209-6
29. Wilhelm M, Kunzmann V, Eckstein S, Reimer P, Weissinger F, Ruediger T, et al. γδ T cells for immune therapy of patients with lymphoid malignancies. *Blood.* (2003) 102:200–6. doi: 10.1182/blood-2002-12-3665

30. Wilhelm M, Smetak M, Schaefer-Eckart K, Kimmel B, Birkmann J, Einsele H, et al. Successful adoptive transfer and *in vivo* expansion of haploidentical γδ T cells. *J Transl Med.* (2014) 12:45. doi: 10.1186/1479-5876-12-45
31. Dunford JE. Molecular targets of the nitrogen containing bisphosphonates: the molecular pharmacology of prenyl synthase inhibition. *Curr Pharm Des.* (2010) 16:2961–9. doi: 10.2174/138161210793563617
32. Gober HJ, Kistowska M, Angman L, Jenö P, Mori L, De Libero G. Human T cell receptor γδ cells recognize endogenous mevalonate metabolites in tumor cells. *J Exp Med.* (2003) 197:163–8. doi: 10.1084/jem.20021500
33. Thompson K, Rojas-Navea J, Rogers MJ. Alkylamines cause Vγ9Vδ2 T-cell activation and proliferation by inhibiting the mevalonate pathway. *Blood.* (2006) 107:651–4. doi: 10.1182/blood-2005-03-1025
34. Matsumoto K, Hayashi K, Murata-Hirai K, Iwasaki M, Okamura H, Minato N, et al. Targeting cancer cells with a bisphosphonate prodrug. *ChemMedChem.* (2016) 11:2656–63. doi: 10.1002/cmdc.201600465
35. Tanaka Y, Iwasaki M, Murata-Hirai K, Matsumoto K, Hayashi K, Okamura H, et al. Anti-tumor activity and immunotherapeutic potential of a bisphosphonate prodrug. *Sci Rep.* (2017) 7:5987. doi: 10.1038/s41598-017-05553-0
36. Tanaka Y, Murata-Hirai K, Iwasaki M, Matsumoto K, Hayashi K, Kumagai A, et al. Expansion of human γδ T cells for adoptive immunotherapy using a bisphosphonate prodrug. *Cancer Sci.* (2018) 109:587–99. doi: 10.1111/cas.13491
37. Zhang Y, Leon A, Song Y, Studer D, Haase C, Koscielski LA, et al. Activity of nitrogen-containing and non-nitrogen-containing bisphosphonates on tumor cell lines. *J Med Chem.* (2006) 49:5804–14. doi: 10.1021/jm060280e
38. Hu S, Wang J, Ji EH, Christison T, Lopez L, Huang Y. Targeted metabolomic analysis of head and neck cancer cells using high performance ion chromatography coupled with a Q exactive HF mass spectrometer. *Anal Chem.* (2015) 87:6371–9. doi: 10.1021/acs.analchem.5b01350
39. Yssel H, De Vries JE, Koken M, Van Blitterswijk W, Spits H. Serum-free medium for generation and propagation of functional human cytotoxic and helper T cell clones. *J Immunol Methods.* (1984) 72:219–27. doi: 10.1016/0022-1759(84)90450-2
40. Sakai Y, Mizuta S, Kumagai A, Tagod MSO, Senju H, Nakamura T, et al. Live cell labeling with terpyridine derivative proligands to measure cytotoxicity mediated by immune cells. *ChemMedChem.* (2017) 12:2006–13. doi: 10.1002/cmdc.201700626
41. Nussbaumer O, Gruenbacher G, Gander H, Thurnher M. DC-like cell-dependent activation of human natural killer cells by the bisphosphonate zoledronic acid is regulated by γδ T lymphocytes. *Blood.* (2011) 118:2743–51. doi: 10.1182/blood-2011-01-328526
42. Maniar A, Zhang X, Lin W, Gastman BR, Pauza CD, Strome SE, et al. Human γδ T lymphocytes induce robust NK cell-mediated antitumor cytotoxicity through CD137 engagement. *Blood.* (2010) 116:1726–33. doi: 10.1182/blood-2009-07-234211
43. Senju H, Kumagai A, Nakamura Y, Yamaguchi H, Nakatomi K, Fukami S, et al. Effect of IL-18 on the expansion and phenotype of human natural killer cells: application to cancer immunotherapy. *Int J Biol Sci.* (2018) 14:331–40. doi: 10.7150/ijbs.22809
44. Oka N, Markova T, Tsuzuki K, Li W, El-Darawish Y, Pencheva-Demireva M, et al. IL-12 regulates the expansion, phenotype, and function of murine NK cells activated by IL-15 and IL-18. *Cancer Immunol Immunother.* (2020). doi: 10.1007/s00262-020-02553-4. [Epub ahead of print].
45. Scheper W, Kelderman S, Fanchi LF, Linnemann C, Bendle G, de Rooij MAJ, et al. Low and variable tumor reactivity of the intratumoral TCR repertoire in human cancers. *Nat Med.* (2019) 25:89–94. doi: 10.1038/s41591-018-0266-5
46. Kabelitz D. Human γδ T cells: from a neglected lymphocyte population to cellular immunotherapy: a personal reflection of 30 years of γδ T cell research. *Clin Immunol.* (2016) 172:90–7. doi: 10.1016/j.clim.2016.07.012
47. Bergstrom JD, Bostedor RG, Masarachia PJ, Reszka AA, Rodan G. Alendronate is a specific, nanomolar inhibitor of farnesyl diphosphate synthase. *Arch Biochem Biophys.* (2000) 373:231–41. doi: 10.1006/abbi.1999.1502
48. van Beek E, Pieterman E, Cohen L, Löwik C, Papapoulos S. Nitrogen-containing bisphosphonates inhibit isopentenyl pyrophosphate isomerase/farnesyl pyrophosphate synthase activity with relative potencies corresponding to their antiresorptive potencies *in vitro* and *in vivo*. *Biochem Biophys Res Commun.* (1999) 255:491–4. doi: 10.1006/bbrc.1999.0224
49. Thompson K, Rogers MJ, Coxon FP, Crockett CJ. Cytosolic entry of bisphosphonate drugs requires acidification of vesicles after fluid-phase endocytosis. *Mol Pharmacol.* (2006) 69:1624–32. doi: 10.1124/mol.105.020776
50. Montero MT, Matilla J, Gómez-Mampaso E, Lasunción AM. Geranylgeraniol regulates negatively caspase-1 autoprocessing: implication in the Th1 response against *Mycobacterium tuberculosis*. *J Immunol.* (2004) 173:4936–44. doi: 10.4049/jimmunol.173.8.4936
51. Mitrofan LM, Castells FB, Pelkonen J, Mönkkönen J. Lysosomal-mitochondrial axis in zoledronic acid-induced apoptosis in human follicular lymphoma cells. *J Biol Chem.* (2010) 285:1967–79. doi: 10.1074/jbc.M109.038935
52. Miyagawa F, Tanaka Y, Yamashita S, Minato N. Essential requirement of antigen presentation by monocyte lineage cells for the activation of primary human γδ T cells by aminobisphosphonate antigen. *J Immunol.* (2001) 166:5508–14. doi: 10.4049/jimmunol.166.9.5508
53. Roelofs AJ, Jauhiainen M, Mönkkönen H, Rogers MJ, Mönkkönen J, Thompson K. Peripheral blood monocytes are responsible for γδ T cell activation induced by zoledronic acid through accumulation of IPP/DMAPP. *Br J Haematol.* (2009) 144:245–50. doi: 10.1111/j.1365-2141.2008.07435.x
54. Skerjanec A, Berenson J, Hsu C, Major P, Miller WH, Ravera C, et al. The pharmacokinetics and pharmacodynamics of zoledronic acid in cancer patients with varying degrees of renal function. *J Clin Pharmacol.* (2003) 43:154–62. doi: 10.1177/0091270002239824
55. Odaira K, Kimura SN, Fujieda N, Kobayashi Y, Kambara K, Takahashi T, et al. $CD27^{-}CD45^{+}$ γδ T cells can be divided into two populations, $CD27^{-}$CD45(int) and CD27(-)CD45(hi) with little proliferation potential. *Biochem Biophys Res Commun.* (2016) 478:1298–303. doi: 10.1016/j.bbrc.2016.08.115
56. Bukowski JF, Morita CT, Tanaka Y, Bloom BR, Brenner MB, Band H. Vγ2Vδ2 TCR-dependent recognition of non-peptide antigens and Daudi cells analyzed by TCR gene transfer. *J Immunol.* (1995) 154:998–1006.
57. Kato Y, Tanaka Y, Miyagawa F, Yamashita S, Minato N. Targeting of tumor cells for human γδ T cells by nonpeptide antigens. *J Immunol.* (2001) 167:5092–8. doi: 10.4049/jimmunol.167.9.5092

Conflict of Interest: YT is a co-inventor of Japanese Patent 2014-257451 on the development of the method to expand γδ T cells using PTA, a novel bisphosphonate prodrug and of Japanese Patent 2014-73475 on the development of a non-radioactive cellular cytotoxicity assay using BM-HT, a precursor of a novel Eu^{3+} chelate-forming compound.

The remaining authors declare that the research was conducted in the absence of any commercial or financial relationships that could be construed as a potential conflict of interest.

frontiers in Immunology

REVIEW
published: 29 September 2020
doi: 10.3389/fimmu.2020.564499

Aiming for the Sweet Spot: Glyco-Immune Checkpoints and γδ T Cells in Targeted Immunotherapy

Margarita Bartish[1]*, *Sonia V. del Rincón*[1,2], *Christopher E. Rudd*[3,4] and *H. Uri Saragovi*[1,2,5]*

[1] Lady Davis Institute, Jewish General Hospital, Translational Center for Research in Cancer, McGill University, Montreal, QC, Canada, [2] Oncology and Experimental Medicine, McGill University, Montreal, QC, Canada, [3] Division of Immuno-Oncology, Research Center Maisonneuve-Rosemont Hospital, Montreal, QC, Canada, [4] Département de Médecine, Université de Montréal, Montreal, QC, Canada, [5] Pharmacology and Therapeutics, and Ophthalmology and Vision Sciences, McGill University, Montreal, QC, Canada

Though a healthy immune system is capable of recognizing and eliminating emergent cancerous cells, an established tumor is adept at escaping immune surveillance. Altered and tumor-specific expression of immunosuppressive cell surface carbohydrates, also termed the "tumor glycocode," is a prominent mechanism by which tumors can escape anti-tumor immunity. Given their persistent and homogeneous expression, tumor-associated glycans are promising targets to be exploited as biomarkers and therapeutic targets. However, the exploitation of these glycans has been a challenge due to their low immunogenicity, immunosuppressive properties, and the inefficient presentation of glycolipids in a conventional major histocompatibility complex (MHC)-restricted manner. Despite this, a subset of T-cells expressing the gamma and delta chains of the T-cell receptor (γδ T cells) exist with a capacity for MHC-unrestricted antigen recognition and potent inherent anti-tumor properties. In this review, we discuss the role of tumor-associated glycans in anti-tumor immunity, with an emphasis on the potential of γδ T cells to target the tumor glycocode. Understanding the many facets of this interaction holds the potential to unlock new ways to use both tumor-associated glycans and γδ T cells in novel therapeutic interventions.

Keywords: gangliosides, sialic acid, tumor marker ganglioside, γδ T cells, immunotherapy, cancer

OPEN ACCESS

Edited by:
Jurgen Kuball,
Utrecht University, Netherlands

Reviewed by:
Dennis Beringer,
University Medical Center Utrecht, Netherlands
Christelle Harly,
INSERM U1232 Centre de Recherche en Cancérologie et Immunologie Nantes Angers (CRCINA), France

***Correspondence:**
H. Uri Saragovi
uri.saragovi@mcgill.ca
Margarita Bartish
margarita.bartish@mail.mcgill.ca

Specialty section:
This article was submitted to T Cell Biology, a section of the journal Frontiers in Immunology

Received: *21 May 2020*
Accepted: *31 August 2020*
Published: *29 September 2020*

Citation:
Bartish M, del Rincón SV, Rudd CE and Saragovi HU (2020) Aiming for the Sweet Spot: Glyco-Immune Checkpoints and γδ T Cells in Targeted Immunotherapy. Front. Immunol. 11:564499. doi: 10.3389/fimmu.2020.564499

INTRODUCTION

The cornerstone of a healthy immune system is the ability to distinguish "self" from "nonself," to mount a response to "nonself" while minimizing the reactivity to "self" (1). A tumor originates from cells that remain mostly "self." Thus, identifying meaningful differences between pathological and healthy cells has been difficult in the dynamic tumor microenvironment (TME). Nonetheless, the erratic pattern of gene expression, altered metabolism, deregulated signaling pathways, and often high mutational burden results in the presentation of neoantigens on the surface of tumor cells. These novel antigens can be recognized by both the innate and adaptive arms of the immune system, although this response can be counteracted by the TME via immunoediting, immunoevasion, and immunosuppression.

For example, tumors can exploit inhibitory receptors on T-cells by inducing an unresponsive or exhausted state (2).

Research in the area of novel immunotherapies has been focused on deploying, re-educating or enhancing immune defenses to overcome the suppressive, detrimental TME. The past decade has witnessed a revolution in the application of immunotherapy for the treatment of cancer, resulting in the approval of immune checkpoint blockade (ICB). ICB uses monoclonal antibodies (mAbs) directed against the inhibitory receptors (IRs) present on the surface of T cells, or the natural ligands of IRs, often expressed by cancer cells. The blockade of IR-ligand interactions reduces the inhibitory regulation of T cells. ICB against cytotoxic T-lymphocyte–associated antigen 4 (CTLA-4) and programmed death 1 (PD-1) or the PD-1 ligand (PD-L1) have produced survival benefits for an ever-expanding list of malignancies (3). However, only a limited subset of patients benefit from ICB, and there are, at times, toxic side effects due to inflammation and autoimmunity (4). Thus, there is a need to understand the mechanisms used by cancer cells to suppress and shape immune responses and to involve novel immune cell subsets in the design of anti-tumor targeted therapies. Here, we discuss the role of glycans in the context of immunity.

The changes in gene expression that accompany malignant transformation have a significant impact on the glycome, glycoproteome and glycolipidome—the glycocode of cancer cells—leading to the overexpression and *de novo* expression of novel glycan epitopes (5). These have been studied extensively in the context of promoting tumor cell-intrinsic aspects of proliferation, signaling and metastasis. Relatively recently, the glycocode of tumor cells has been implicated in suppressing anti-tumor immunity, emerging as a novel immune checkpoint, and, thus, a target for immunotherapy. While now recognized as an axis of immune modulation with druggable and therapeutic potential (6), its potential has remained underdeveloped clinically. Moreover, the subset of immune cells that attack carbohydrate targets remains poorly understood. In this review, we discuss the way in which γδ T cells have the potential to become effectors against carbohydrate moieties on cancer cells.

GLYCOSYLATION IN THE TUMOR-IMMUNE CELL INTERPLAY

All cells are covered with a dense coat of glycans, chains of carbohydrates that are covalently attached to proteins or lipids (7). Glycan diversity is immense, stemming from the numerous monosaccharide building blocks that can be assembled into linear or branched chains of various lengths by multiple types of chemical bonds, and diversified further by coupling to proteins, nucleic acids or lipids (8). This diversity creates a unique glycan "landscape" of expression for each cell and constitutes a major aspect of the molecular interface between cells and their environment. Glycans are also important for the transport of nascent proteins to the surface of cells as well as, in a larger context, the maintenance of tissue structure and extracellular matrix organization, cell membrane integrity, cell-cell adhesion, and cellular signaling. To immune cells, surface glycans serve as an identifying feature of a cell, a calling card of sorts (9, 10).

Aberrant glycosylation is a hallmark feature of cancer cells (11–13). Key among the distinguishing features of a tumor's "glycan topography" is the anomalous expression of sialic acid–carrying glycans (sialoglycans) (14). Sialic acids are a family of negatively charged, nine-carbon sugar molecules linked to mucins, extracellular matrix, cell surface glycoproteins (N- and O-linked oligosaccharide chains), or glycolipids by α-2,3; α-2,6 and α-2,8 linkages (15).

Tumor cells are covered with a dense layer of sialoglycans, some of which are uniquely associated with malignancy (16). This coating protects tumor cells from being recognized and eradicated by the immune system, as it can both mask their "non-self" immunogenicity and interfere with immune cell function (17, 18). For instance, elevated sialylation of cancer cells disrupts the interaction of the NK-activating receptor natural killer group 2D (NKG2D) with ligands on the tumor cells, reducing NK-activating signals derived from tumor cells (19). This strategy by tumor cells is reminiscent of sialic acid coatings used by parasites and other pathogens to evade immunity (20). Despite these examples linking protein sialylation to pathology, we note that this post-translational modification is not always deleterious. Sialylation of some proteins is associated with neuroprotective signals (15).

The Sialic Acid-Siglec Axis of Tumor Immunomodulation

As "self-associated molecular patterns" (SAMPs), sialic acids are recognized by sialic acid-binding Ig-type lectins (Siglecs). Twenty years of study document the importance of sialic acids in discriminating "self" and "non-self," showing the existence of natural antibodies to a variety of sialidase-treated immune cells in human serum [reviewed in (21)]. In humans, the Siglec family comprises 14 members. These are subdivided into the conserved Siglecs:−1 (Sialoadhesin/CD169),−2 (CD22),−4 (Myelin-associated glycoprotein/MAG),−15, and the CD33-related Siglecs−3,−5 to−11,−14 and−16 (22). The Siglecs are composed of modular immunoglobulin-like (Ig-like) domains, usually with the V-like domain at the N-terminus mediating binding to sialic acids. This domain shows a high degree of sequence similarity to other Ig-like domains in the receptor family with the exception of the C-2 set Ig domains near the plasma membrane. The cytoplasmic domains have immunoreceptor tyrosine-based inhibition motifs (ITIMs) that bind to the protein tyrosine phosphatases src homology region 2 domain-containing phosphatases 1 and 2 (SHP-1 and SHP-2). SHP-1 has a clear negative signaling role, while SHP-2 has been shown to play both positive and negative roles in immune cells.

Functionally, Siglec binding to sialic acid facilitates tolerance to cell membrane antigens expressed by the same cell. In B cells, for example, Siglec-sialic acid binding suppresses B cell activation and stimulates B cell apoptosis (23–25). While a key physiological mechanism to prevent autoimmunity, inhibitory Siglec-sialic acid interaction illustrates how an immunological fail-safe can be hijacked by tumors to escape host immunity. The engagement of

Siglec-7 and Siglec-9 on NK cells by tumor-associated sialic acids inhibits NK cell activation (26–28). Conversely, the loss of Siglec-7 expression on an NK cell line promotes sustained cytotoxic activity against leukemia cells *in vitro* (29). Furthermore, the binding of the cancer-associated sialylated glycoform of MUC1 to Siglec-9 on macrophages resulted in their differentiation to immunosuppressive so-called M2 macrophages with upregulated PD-L1 expression (30). Tumor-associated macrophages were also shown to express Siglec-15, and the interaction between Siglec-15 on M2 macrophages and tumor-associated sialyl-Tn (sTn) antigen elevated macrophage-produced TGF-β, a known pleiotropic mediator of pro-tumor responses (31). Recently, tumor-expressed CD24 (a highly sialylated glycoprotein) was shown to hinder the ability of tumor-associated macrophages to phagocytize tumors via binding to Siglec-10 (32). The expression of multiple members of the Siglec family was shown on myeloid-derived suppressor cells (MDSCs) of glioma patients, although the functional consequences of this expression on this already immune suppressive cell type are unclear (33).

The innate and adaptive arms of the immune system can influence each other, thus the effects of sialoglycan-Siglec interactions may indirectly affect the activation status and function of the cells of adaptive immunity. For example, the interaction between sialylated antigens and Siglec-E (murine ortholog of human Siglec-9) on dendritic cells can influence the T cell population, favoring differentiation of antigen-specific regulatory T cells and reducing the numbers of effector T cells (34). Although the expression of Siglecs on normal T cells is low, these can become elevated in tumor-infiltrating lymphocytes (TILs), resulting in suppressed anti-tumor T cell function (35, 36). In melanoma, Haas et al. identified Siglec-9 expression on tumor-infiltrating, but not peripheral, $CD8^+$ cells (36). By disrupting the sialoglycan-Siglec pathway between tumor cells and T cells, Stanczak et al. demonstrated a delay of tumor growth and an increased infiltration of $CD8^+$ T cells in a mouse model of colorectal cancer (35).

Given the role of tumor sialylation in the establishment of an immunosuppressive TME, both sides of the sialoglycan-Siglec axis have been targeted therapeutically. To reduce the sensitivity of immune cells to tumor sialoglycans, Siglec function can be blocked with monoclonal antibodies (mAbs). MAbs have been tested pre-clinically against Siglec-7 (26), Siglec-9 (35), and Siglec-15 (37). A challenge of this approach is to confine the response to the tumor setting, as deregulated immune activation might have detrimental consequences outside of TME. The expression of Siglec-9, for example, is restricted to TILs, thus its systemic inhibition by a mAb is unlikely to impact peripheral cytotoxic $CD8^+$ T cell function. However, Siglec-9 is also abundantly expressed by neutrophils and a blocking antibody could result in their uncontrolled and potentially damaging activation. An alternative direction is to target the causative agents of immunosuppression, namely sialoglycans on the tumor cells, rather than on receptors of immune cells. Stalling *de novo* sialic acid synthesis, via the use of glycomimetic sialic acid analogs that cannot be attached to the glycan chain, has been shown to reduce the density of sialoglycans on the tumor surface and delay of tumor growth and metastasis (38, 39).

Finally, the sialoglycan coverage on tumor cells might be "shaved" using sialidases, sialic acid trimming enzymes. In the 1960s and 1970s, it was found that injecting a tumor-bearing animal with growth-arrested tumor digests treated with sialidases—a very early form of cancer vaccination—impeded the growth of the pre-existing tumor in mouse (40) and dog (17) cancer models (41). Despite promising results in early trials on advanced patients using sialidase-treated cancer cells to boost the immune response, this form of immunotherapy did not become a standard of care (42, 43). In recent years, in an approach the authors termed precision glycocalyx editing, a pre-clinical study coupled a recombinant sialidase to a therapeutic mAb against the human epidermal growth factor receptor 2 (HER2) (44). The antibody directed the effects of the sialidase to the HER2-expressing tumor cells, simultaneously reducing Siglec-mediated NK cell suppression and exposing the tumor cells to NK cell-mediated antibody-dependent cytotoxicity.

GANGLIOSIDES AS PART OF THE TUMOR "GLYCOCODE"

Among the key sialic acid-containing glycocompounds found on the surface of tumors are the gangliosides—a family of glycosphingolipids with one or several sialic acid molecules attached to the extracellular carbohydrate chain. Though named after the cell type from which they were first isolated—"Ganglienzellen," neurons—gangliosides are ubiquitously expressed on the membranes of all eukaryotic cells, typically clustering in cholesterol-rich lipid microdomains or rafts (45). Indeed, evidence suggests that gangliosides co-localize with signaling molecules and adhesion molecules in glyco-signaling domains on the cell surface (46).

It is the unique glycan tree-structure that defines each different ganglioside. In ganglioside nomenclature, the prefix G stands for "ganglio" while the letters M (mono-), D (di-), T (tri-) and Q (quad-) denote the number of sialic acid molecules. Further classification is made on the basis of thin layer chromatography migration and is represented by Arabic numerals and lower case letters reflecting the order of migration of each corresponding type (47). GM1 is expressed on most eukaryotic cells and has a prominent role in the activation of intracellular signals in neuronal and lymphoid cells. In particular, GM1 represents the major ganglioside component of the brain (48), with several key neuronal functions becoming compromised as a consequence of decreasing GM1 levels during, for example, aging (49, 50). In contrast, GD2 and GD3 are almost exclusively expressed in tumor cells (51). As such, GD2 and GD3, are examples of a subset of gangliosides referred to as tumor marker gangliosides (TMGs), a family comprising about 20 different gangliosides present preferentially or almost exclusively and at high density on the cell surface of certain cancers (**Table 1**).

Ganglioside biosynthesis begins in the endoplasmic reticulum, with the synthesis of the ceramide precursor, common to all glycosphingolipids, and continues in the Golgi apparatus where the ceramide is converted to glucosylceramide. Sugar residues—galactose, glucose and sialic acids—are added, one by one,

TABLE 1 | Tumor marker ganglioside targets.

Malignancy	GD2	GD3	Fucosyl-GM1	GM2	GM3	PolySia (52)	Sialyl Lewis X
Neuroblastoma	(53–55)	(55)	(56)	(57, 58)	(59)	(60, 61)	
Melanoma	(55)	(55, 62)	(63)	(64)	(65)		
Glioma	(66)	(67–69)		(52, 70)	(71–73)	(74)	
Non-small cell lung cancer (NSCLC)			(75)	(76)	(77, 78)	(79, 80)	(81, 82)
Small cell lung cancer (SCLC)	(83)	(83)	(75, 83, 84)	(83)			
Breast carcinoma	(85)	(85–87)		(85)	(85)	(88)	(81, 82)
Renal cell cancer			(89)	(90)	(91)		(92)
Ovarian cancer	(93)	(94)	(93)	(93)	(95)		
Soft tissue sarcomas	(96)	(96)					
Osteosarcoma	(97)	(98, 99)					
Ewing's sarcoma	(100, 101)	(99)			(102)		
Desmoplastic Round Cell	(103)	(99)					
Rhabdomyosarc.	(99)	(99)					
Retinoblastoma	(104)				(105)		
Wilms tumor					(91, 106)	(107)	
Medullary thyroid cancer						(108)	
Prostate Cancer				(109)			
Gastric cancer				(109)		(109)	(81)
Endometrial				(109)		(52, 109)	
Pancreatic				(109)		(109)	(81)
Colon Cancer				(109)			(81, 82)
Esophageal							(81)
Head and neck							(81, 82)

Select cancers where there is evidence for TMG expression in >50% of all patients in the indicated malignancy. This table is shown to exemplify the prevalence of TMGs. The cells with no entry reflect ≤50% prevalence, or that we omitted literature that we deem unreliable for this review because very few biopsies were phenotyped. The list ranges from ~95% (Neuroblastoma), to ~80% (Melanoma), to ~50% (Head and Neck) of patients. When expressed in a patient the TMGs are present homogeneously in tumor nodules and cells. Gold color denotes literature from many laboratories, or evidence confirmed by the authors of this review.

catalyzed by specific glycosyltransferases. Some gangliosides can also result from the removal of a sugar or sugar branch by glycosidases. As several enzymes or pathways can generate a ganglioside, their biosynthesis is hard to target. Nonetheless, this strategy has been explored in pre-clinical studies. The inhibition of glucosylceramide synthase, the enzyme which catalyzes the first step in glycosphingolipid synthesis, by N-butyldeoxynojirimycin (NB-DNJ) has been shown to temporarily delay tumor onset in a mouse melanoma model (110). However, prolonged treatment with NB-DNJ is toxic, and in the absence of the inhibitor, ganglioside levels rapidly recovered. Targeting GD3 synthase, the enzyme responsible for the biosynthesis of GD2 and GD3, reduced tumor stem cell functionality, abrogated *in vivo* tumor formation (111), and interfered with the epithelial-to-mesenchymal transition and metastasis in murine models (112).

Upon export to the plasma membrane, the sphingolipid (ceramide) part of the molecule—two lipid tails consisting of the long-chain amino alcohol sphingosine coupled to a fatty acid—anchors the ganglioside to the cell surface, while the glycan moiety is exposed to the external environment. Apart from the plasma membrane, their main cellular location, gangliosides are also detected in other cellular organelles, including the nuclear envelope (113) and mitochondria (114). Importantly, they can also be actively "shed" and taken up by other cells (115). The excretion of gangliosides from a cell into the extracellular environment is poorly studied, and may be the result of release in the form of exosomes, microparticles, or as micelles given the physical properties of the gangliosides (hydrophobic tail and hydrophilic head). Extracellular gangliosides improve tumorigenicity of poorly tumorigenic cells in mouse models (116) and have been implicated as a mechanism by which tumors suppress immune cell function (117, 118).

Biology and Function of Tumor Marker Gangliosides

As the term "tumor marker" suggests, TMG expression is tightly associated with malignant cells. **Table 1** summarizes the cancer types with a high TMG prevalence across patients. However, in addition to their status as biomarkers of malignancy, GD2 and GD3 play active roles during cancer development, with proven links to tumor growth, metastasis, and immune evasion.

Because of their accumulation on the outer leaflet of the plasma membrane (with the sugars being extracellular), gangliosides participate in cellular communication. The carbohydrate "head" of gangliosides can interact with proteins, lipids, and glycans present in the extracellular matrix and on other cells. It can also interact laterally within the membrane to regulate lipid rafts or microdomain formation (119). As components of rafts, gangliosides affect signaling processes during cancer progression. For example, GD2 and GD3 promote

ligand-independent activation of wild type receptor tyrosine kinases (RTKs), including EGF-R, TrkA, TrkB, PDGF-R, IGF1-R, MET, as well as cytoplasmic *src*-related kinases (e.g., Src, Lck) (98, 120, 121). The expression of GD2 and GD3 can therefore be viewed as pro-oncogenic and may be etiological in tumors where oncogenic mutations are not clearly identified.

The pro-tumor roles of tumor gangliosides have been implicated at all stages of tumor development. GD2 expression was linked to breast cancer stem cell phenotypes, while suppression of its biosynthesis in breast cancer cell lines decreased mammosphere formation and tumor initiation (111). *In vitro* experiments have connected ganglioside production to an increase in cancer cell migration and invasion (98). Conversely, a mAb against GD2 was shown to induce apoptosis in small cell lung cancer cells (83, 122) and an anti-GD3 antibody inhibited the growth of human melanoma cells *in vitro* (123). Cancer cells devoid of GM2 and GM3 synthases formed avascular tumors, suggesting the involvement of TMGs in angiogenesis during tumor growth (124). Additionally, the exogenous addition of GD3 to glioma cells stimulated VEGF production, suggesting a role for tumor-shed gangliosides in *de novo* blood vessel formation (125). In patient-derived melanoma cells, ganglioside expression is tightly linked to melanoma aggressiveness and patient survival, with patients expressing GD3 having the shortest survival (126).

Building on the discussion of glycan-containing sialic acids as a segment of the tumor glycocode used by the tumor to evade anti-tumor immunity, GD2 and GD3 can be regarded as immunosuppressive, even in cases where other immune escape proteins such as PD-1 or PD-L1 are absent. Indeed, the observations that TMGs can inhibit antibody production and lymphocyte proliferation were first made decades ago (127, 128). This is increasingly relevant in modern immunotherapy as it is possible that the high failure rate of conventional ICB therapy in melanoma (targeting PD-1 or PD-L1) is associated with high GD2/GD3 expression, a hypothesis that we are evaluating experimentally. As sialic acid-containing compounds, GD2 and GD3 can interact with Siglecs (129–131). Siglec-7, in particular, displays a strong affinity for the α2,8-linked disialic acids found on GD2 and GD3 (132). Additionally, TMGs influence the recruitment and function of immune cells in Siglec-independent ways. TMGs interfere with IL-2/IL-2R binding, key to T cell proliferation (133). They have also been shown to induce apoptosis in T cells (90) and dendritic cells (134), and impair antigen presentation in human monocytes (135). In a tumor model engineered to lack GM3, GM2, GM1, and GD1a, the observed impairment of tumor growth was attributed to a reduction, and decreased activity, of MDSCs (136). Intriguingly, the presence of MDSCs could be restored by exogenous supplementation of gangliosides which suggests a direct connection between tumor-produced gangliosides and the recruitment of immunosuppressive MDSCs to the TME.

TMGs as Therapeutic Targets

In 2009, GD2 was "ranked" by the NCI as 12th in priority of all clinical cancer antigens, with additional three gangliosides (GD3, fucosyl-GM1, and N-acetyl GM3) included in the list of 75 prioritized antigens (137). The high expression of GD2 and GD3 in cancer makes these promising targets for therapeutic intervention. Moreover, when GD2 or GD3 are present in a cancer, tumor cells express them stably and homogeneously, and tumor microheterogeneity with regards to TMG expression has not been reported. GD2 or GD3 persist throughout tumor progression, and expression does not appear to downregulate after chemotherapy, in at least the reported studies of neuroblastoma (138), osteosarcoma (139), and in the *ex vivo* examination of several cell lines (140).

The etiological role of GD2/GD3 in oncogenesis and immune suppression are additional features that would make these glycolipids ideal therapeutic targets for clinical translation. However, exploiting GD2 or GD3 has been challenging. Monoclonal antibodies against GD2 [Dinutuximab/Ch14.18 mAb (141–143) and 3F8 mAb (144)] and GD3 [BEC2 (145), R24 (146)] achieved partial success in cancer therapy as passive immunity (i.e., the administration of purified antibodies against a target). However, they cause serious adverse effects, such as high-grade visceral pain, that is not blocked by morphine (147). While Ch14.18 mAb, in combination with GM-CSF and IL-2, stimulates antibody-dependent cell-mediated cytotoxicity and improves overall survival in neuroblastoma (141), in clinical trials it had low efficacy or exhibited a low therapeutic index [reviewed in (148)]. More recently, engineered chimeric antigen receptors (CAR) expressing an anti-GD2 mAb sequence in T or NK cells, were used in combination with ICB inhibitors and cytokines (149), but the cells did not persist in circulation and the treatment showed no efficacy (150). The failure is not surprising given that the CAR was engineered from mAbs that also exhibit a low therapeutic index in passive immunity. In addition to the clinical CAR T cell studies performed in neuroblastoma and melanoma, pre-clinically, CAR anti-GD2 T cells have recently been tested against breast cancer (151) and diffuse midline glioma (152).

Historically, the development of anti-GD2 or anti-GD3 vaccines has been tried without success. Glycolipids are poorly immunogenic and are not thought to be processed by antigen presenting cells or presented by MHC antigens. While lipids can be recognized by specialized CD1 (MHC class I-like molecules)–restricted T cells, each ganglioside does not have a unique type of lipid. In fact, the lipid tails can be heterogeneous within a single ganglioside (ranging in carbon chain length, oxidation and saturation state). Hence, only subtle differences exist between normal GM1 and tumor GD2 and GD3 carbohydrate heads, and their lipid tails can be shared or can exhibit heterogeneity across all gangliosides whether they are normal or TMGs. Thus, when using whole TMGs as immunogens, there are concerns with regards to tolerance, cross-reactivity or transient and ineffective immune reactions.

Notwithstanding the aforementioned concerns, initial attempts at developing GD2/GD3 vaccines used native GD2 or GD3 glycolipids chemically conjugated to carriers (153, 154). These were somewhat immunogenic and induced humoral responses that delayed tumor growth in mice via a complement-dependent cytotoxicity (CDC) mechanism. However, anti-ganglioside antibody titers were not long-lasting even after multiple immunizations, and there was no

correlation between humoral titer and tumor therapeutic efficacy (147).

THE POTENTIAL OF γδ T CELLS IN TARGETING THE "GLYCOCODE"

γδ T cells, expressing the gamma and delta chains of the T-cell receptor (TCR) coupled to the CD3 invariant signaling chains, are a subclass of T lymphocytes whose defining characteristic is their ability to display traits of both the innate and adaptive immune systems (155). They express a TCR whose engagement with its target mediates T cell activation. Human γδ T cell subsets—the subsets in other species will differ—are classified according to the Vδ chain in the TCR. Vδ(1-8) together with one of 6 different Vγ chains (2–5, 8, and 9) forms the mature TCR via V(D)J recombination. In this manner, they generate TCR diversity similarly to conventional αβ T cells.

On the other hand, the TCRs of the γδ type recognize qualitatively distinct antigens, with kinetics, antigen recognition mechanisms and tissue localization fundamentally distinct from αβ T cells. While some γδ T cells can found in circulation, with the Vγ9Vδ2 being the major subset corresponding to about 5% of total $CD3^+$ cells in the periphery (156), the two other main γδ T cell subsets, Vδ1 and Vδ3, are predominantly tissue-resident. Like innate immune cells, γδ T cells recognize targets with broad patterns of pathogen-encoded or dysregulated-self signatures, as opposed to the specificity displayed by the αβ T cells.

Antigen Recognition by γδ T Cells

Unlike αβ T cells, γδ T cells do not rely on peptide presentation by the MHC complex of antigen-presenting cell to become activated. The precise mechanisms behind γδ T cell antigen recognition remains a field of intense research, complicated by the vast array of structurally diverse classes of self and non-self-ligands recognized by the γδ TCR (157). This includes soluble and membrane-bound proteins and peptides of a wide range of sizes, as well as non-protein targets such as phospholipids, non-peptidic antigens and carbohydrates.

Although often referred to as MHC-unrestricted, some of the most well-characterized targets of γδ-TCR include the non-classical class I MHC molecules. The MHC-I related molecules T10 and T22, found specifically in mice, were the first ligands whose binding to the γδ-TCR was confirmed biochemically (158, 159). Recognition of lipids presented by the CD1 family of MHC class I-like proteins was established a few years later (160–162) and is a key aspect of TME-related γδ T cell biology. Vδ1 and Vδ3 T cells can recognize the sphingolipid α-galactosylceramide (α-GalCer) presented by CD1d and, as a consequence, upregulate cytokine production characteristic of Th0 (i.e. IFNγ and IL-4), Th1 (i.e., IFNγ) and Th2 (i.e., IL-4) cells (163, 164). Recently, a third type of non-classical class I MHC molecule, the MHC-related protein 1 (MR1), was shown to be a target of γδ-TCR (165). This protein is involved in the presentation of microbial metabolites related to vitamin B2 biosynthesis and is known to stimulate a special subset of αβ T cells known as mucosal-associated invariant T cells (MAIT cells). Intriguingly, the resolved crystal structure of a γδTCR–MR1–antigen complex revealed a key difference to the previously proposed modes of TCR-ligand recognition. The γδ TCR was found to bind underneath the MR1 antigen-binding cleft, suggesting a new "antigen-agnostic" mode of TCR-target interaction, the biological implications of which are not yet understood.

In addition to targets presented as a part of non-classical MHC molecules, several types of non-peptidic antigens have been described to activate T cells with γδ TCRs. Tumor cell recognition, in particular, is enhanced by the ability of γδ T cells to recognize such antigens, which often are by-products of dysregulated tumor processes (and which do not bind MHC molecules). Phosphoantigens, or phosphorylated non-peptide antigens, are the classical example of this principle. The phosphoantigen isopentenyl pyrophosphate (IPP) accumulates in tumor cells due to the deregulated mevalonate pathway (166), and specifically and potently activates Vγ9Vδ2 T cells (167). Although phosphoantigens were originally thought to activate the γδ TCR directly, new evidence shows that this recognition requires the participation of Ig superfamily family members known as the butyrophilins. In addition to the previously implicated butyrophilin 3A1 (168–170), two recent studies identified butyrophilin 2A1 as key for the recognition of phosphoantigens by γδ T cells (171, 172). Rigau et al. propose a model in which the phosphoantigen production by a target cell modifies a complex composed of butyrophilin 3A1 and butyrophilin 2A1 causing it to co-bind and activate the Vγ9Vδ2 TCR.

In addition to TCR receptor-mediated activation, it should be emphasized that γδ T cells also express other activating receptors, such as the NK cell receptors (173, 174). Building on an early study showing susceptibility to carcinogenesis in the absence of γδ T cells (175), Strid et al. showed that activation of NKG2D receptor by ligand Rae-1 (known as MICA in humans) on tissue-resident Vγ5Vδ1 γδ T cells inhibits skin cancer in a mouse model (176). In addition to skin, the role of NKG2D for γδ T cell activation was further shown in peripheral Vγ9Vδ2 cells (177). In NK cells, the NKG2D receptor has previously been mentioned in this text as being disrupted by elevated levels of sialylation on tumor cells. Given its now known functional roles in γδ T cells, it is thus possible that the immunosuppressive effects of elevated cancer cell sialylation can extend to impaired γδ T cell function.

γδ T Cell Targeting of Carbohydrates in Tumor Gangliosides

The broad repertoire of targets recognizable by the γδ TCR as well as other receptors on the γδ T cells is suggestive of their potential use against specific carbohydrate targets on tumor cells, such as TMGs. However, this is an emergent field and concrete examples of such carbohydrate reactivity remain scarce.

The role of CD1d in γδ T cell activation provides an indirect example in which the spheres of γδ T cells and TMGs intersect. In one study, ovarian tumor-shed GD3 inhibited NKT-cell activation, with GD3 binding with high affinity to both human and murine CD1d. *In vivo* administration of GD3 suppressed α-GalCer-induced NKT cell activation in a dose-dependent

manner, leading to the establishment of an immunosuppressive TME (94). While experimentally proven only in the context of NKT cells, it is possible that anti-GD3 blockade of the GD3-CD1d interaction would free up its recognition by, and subsequent activation of, γδ T cells, providing an additional therapeutic benefit. It should be noted that GD3-CD1d interaction can conversely have an immune activating effect. In melanoma, GD3 has been shown to activate NKT cells in a CD1d-dependent manner (178, 179).

Key to the potential of γδ T cells in targeting tumor-associated glycans is the fact that they do not require MHC presentation of antigens. This is relevant to tumor glycobiology because pure carbohydrates are typically not presented by MHC (180). While αβ T cells can recognize MHC-processed glycopeptides (peptides attached to a glycan), an early study determined the MHC-unrestricted carbohydrate specificity of γδ T cells (181). In addition, some MHC-restricted T-cell epitopes can be unaffected by glycosylation. An H-2Kb-restricted peptide retains an ability to be presented in its glycosylated form (hence, presentation is unaffected by peptide glycosylation) as the tethered carbohydrate fits in the central region of the TCR binding site. Hence, manipulation of γδ or αβ TCRs may yield previously unexploited strategies to target non-protein antigens in an MHC-unrestricted manner.

We recently reported the generation of synthetic GD2 and GD3 carbohydrate head-groups displayed on a multivalent polyamidoamine scaffold (PAMAM-GD2 and PAMAM-GD3). The PAMAM-GDs are lipid-free, water-soluble, inexpensive to produce, well-characterized chemically and structurally (including a crucial β-configuration at the first sugar), and identical to native carbohydrate head-groups on the surface of tumors (182, 183). These products (hereafter,

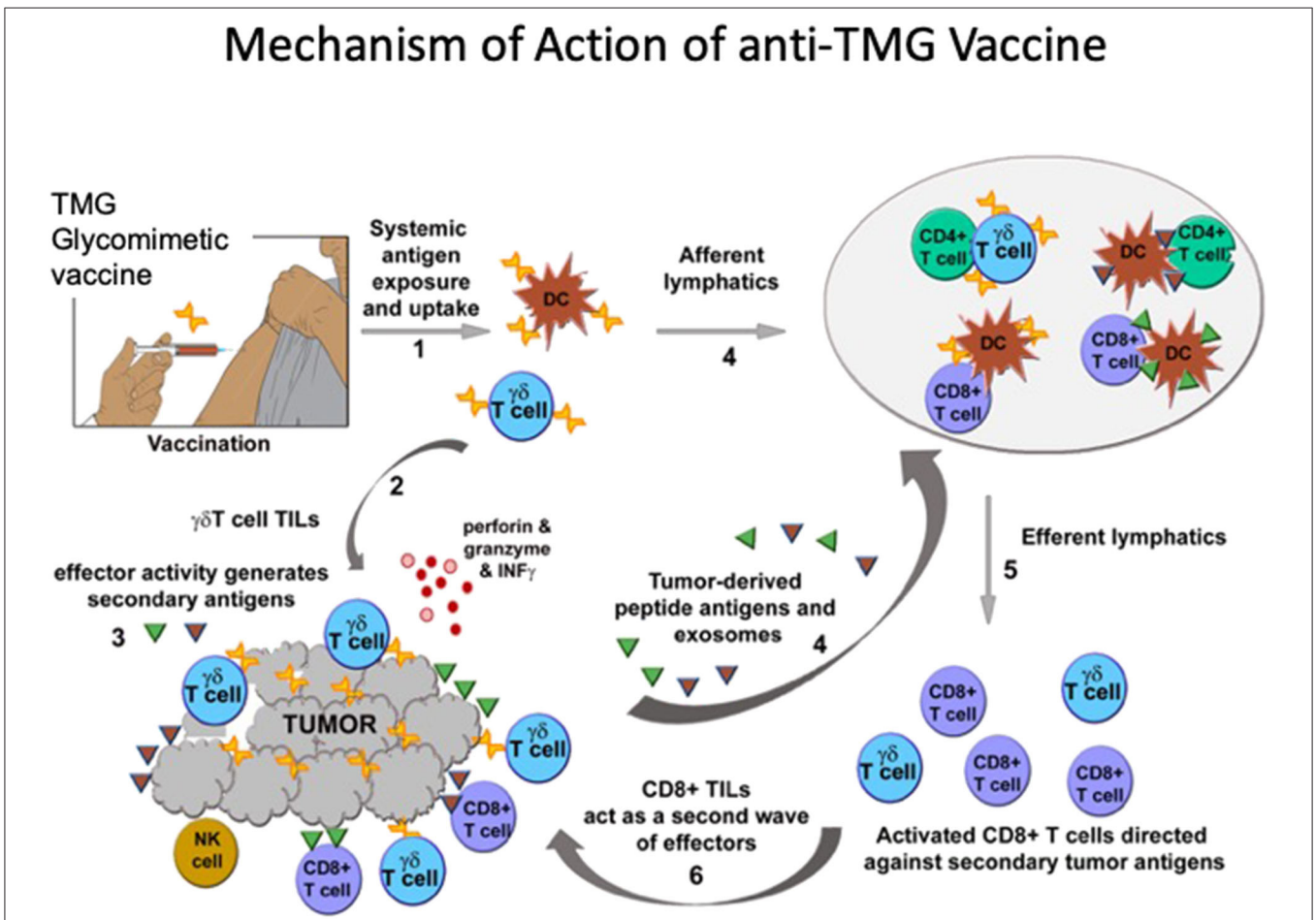

FIGURE 1 | TMG glycomimetic vaccine mechanisms of immune activation. After systemic delivery of the vaccine antigens, (1) there is a rapid expansion of γδ T cells. It is unknown whether γδ TCRs expand by binding directly to the vaccine glycomimetic product, or whether the antigen is presented by DCs. Expansion of γδ T cells is independent of whether mice bear tumors expressing TMGs, so while the vaccine may also block the immune-suppressive action of TMGs upon T cells this mechanism is unlikely to account for the initial expansion. (2) In mice bearing TMG-expressing tumors, vaccination affords a significant increase in γδ T cells TILs. (3) The effector activity generates secondary antigens or neoantigens. (4) Putative neoantigens (not yet identified) circulate and are presented to CD8+ αβ T cells which (5, 6) expand as a second wave mainly comprising CD8+ T cells that also become TILs. The generation of *in vivo* T-cell memory in glycomimetic vaccines was not evaluated. However, anti-TMG humoral immunity (evaluated as a surrogate marker) matures and class-switches from IgM to IgG.

called vaccines) are potent immunogens—when inoculated in mice, they stimulate B- and T cell immunity. The vaccines, as monotherapy, are therapeutic against four aggressive and metastatic syngeneic cancer models, significantly reducing primary tumors, metastatic burden, and importantly extending overall survival. Unexpectedly, this study revealed the expansion of γδ T cells mediated by a pure carbohydrate dendrimer. This occurs rapidly after vaccination in mice (independent of tumor presence) and in tumor-bearing mice (or upon tumor challenge) was followed by the expansion of the $CD8^+$ T cells *in vivo*. Adoptive transfer of a relatively low number of the T cells isolated after vaccination is also therapeutic in tumor models (182).

The data support the notion that vaccination can expand and activate γδ T cells directly (and perhaps through APCs), which then bypass the immunosuppressive TME and become TILs (**Figure 1**). Expansion of γδ T cells is detected in tumor-bearing as well as in non-tumor-bearing mice. Hence while the vaccine may also block the immune-suppressive action of TMGs upon T cells this mechanism is unlikely to account for the initial expansion, but may be relevant to anti-tumor efficacy. The initial expansion of γδ T cells is followed by a second wave of expansion and recruitment of $CD8^+$ effector TILs. The ability of γδ T cells to activate other T cell subsets has been shown previously (184, 185). It is possible that the second wave of $CD8^+$ effector TILs recognize neoantigens presented, or shed, by injured or stressed tumor cells. We note that while *in vivo* T-cell memory generated by glycomimetic vaccines was not evaluated, the anti-TMG humoral immunity matures and class-switches from IgM to IgG, and is a surrogate marker of memory.

The mechanism of action of the PAMAM-GD2 and GD3 vaccines and the role of γδ T cells in mediating immunity against TMGs is paradigm-shifting, because virtually all previous experimental and clinical data using vaccines directed against TMGs have focused on humoral immunity rather than on cellular immunity. Such bias was perhaps motivated by the early promising results of using anti-TMG mAbs as therapeutic agents.

The γδ T cells are susceptible to PD-1–mediated inhibition (186, 187), and the tumor models where the vaccines were evaluated express high levels of PD-L1. The high therapeutic efficacy suggests that the vaccines partially overcome the inhibitory effects of PD-L1 upon γδ T cells. Ongoing studies are evaluating whether combination therapy with ICB might augment the anti-cancer effects of vaccines.

Adoptive transfer of T cells isolated from vaccinated mice resulted in the appearance of γδ T cells as TILs, and in a high therapeutic index. However, the study did not evaluate the sequence of γδ TCRs that were expanded, and did not address whether the glycomimetic vaccine products bind directly to the γδ TCRs or are presented via CD1, for example. Moreover, the antigens and the mechanism causing a second wave of $CD8^+$ T cell expansion, whether it is γδ T cell dependent, and whether it is relevant therapeutically, are key for the proper development of a future cancer vaccine. The TMG glycomimetic cancer vaccine is an exciting approach that requires further evaluation of immune-mechanisms and connections between TMG and γδ T cells. Also, it is noteworthy that the concept of harnessing γδ T cells and targeting sugars for cancer therapy has been under examination for non-cancer pathologies ranging from anti-viral, anti-bacteria, and anti-parasitic therapy (188–191) to autoimmune diseases (192).

THERAPEUTIC TARGETING OF γδ T CELLS

The scientific literature regarding the clinical efficacy of γδ T cell therapy is overall positive, supporting the further exploration of their use in a clinical setting (156, 193). Studies performed thus far included patients with hematological malignancies (follicular lymphoma, multiple myeloma and acute myeloid leukemia), and non-hematological tumors, such as renal cell, breast and prostate cancer (194). Vδ1+ cells have shown promising results pre-clinically (195), and the infiltration of these cells correlated with necrotizing tumors and patient survival in melanoma (196). However, the bulk of clinical studies have used Vγ9Vδ2 T-cells due to their relatively high availability in the peripheral blood and their potential to be cultured, expanded and activated *ex vivo*. To activate the Vγ9Vδ2 T-cells, the butyrophilin-mediated reactivity of the Vγ9Vδ2 TCR to phosphoantigens can be exploited, using chemical compounds to elevate or mimic the expression of phosphoantigens either on tumor cells or on antigen-presenting cells in the TME. Such compounds include aminobisphosphonates (for example pamidronate and zoledronate) or synthetic phosphoantigen analogs (197, 198). The approach offers a useful tool for expansion, but is not necessarily a useful therapeutic approach, because the expanded Vγ9Vδ2 T cells are nearly monoclonal and are not specific for a desired antigen. Indeed, the clinical response in the trials conducted thus far has been minimal [reviewed in (199) and (200)]. Therefore, these experiments are an interrogation of γδ T cell biology, with some examination of safety parameters. Furthermore, the clinical data strongly point to the need for a combinatorial approach with other immune-based therapies for maximum efficacy (193, 201). Even with these limitations, the early results reported are encouraging (193).

CAR γδT cell Therapy

T cells engineered to express chimeric antigen receptors (CARs) comprise a branch of immunotherapy that combines the antigen specificity of monoclonal antibodies with the signaling motifs of receptors to promote the proliferation of cytotoxic effector T cells. CAR therapy has been successfully applied in several types of hematologic malignancies (202–204), and while translation to solid tumors has been somewhat limited there is some success reported with CARs in breast cancer (151) and diffuse midline glioma (152).

It is possible that engineered CAR T cells, just as naturally occurring T cells, are restricted by the immunosuppressive TME. This could impair T cell recruitment, function, and survival. In this context, γδ CAR T cells are an intriguing alternative target. Transduction of γδ T cells with CARs might direct their cytotoxic activity specifically against a tumor antigen, while retaining their

TABLE 2 | Immunotherapeutic approaches involving γδ T cells or γδ TCRs.

Features and mechanisms	Cancer immunotherapy approaches		
	Ganglioside Vaccines	**mAbs, CAR-T, TILs, protein vaccines, antigen-pulsed dendritic cells, neoantigens**	**Therapeutic γδ T cells**
HLA-independent	Yes	No	Yes
Can present antigens	Yes	No/Poor	Yes/No
Can expand endogenous cytotoxic cells	Yes	No/Poor	Yes
Polyclonal responses	Yes	Yes in some, No in others	No/unknown
Genetic engineering required	No	Yes in some, No in others	Yes in some No in others
Target translates from animal models to humans	Yes	Often variable and model-or target-dependent	In progress
Validated targets	Yes	Yes in some, No in others	Yes/unknown
Target has known etiology in cancer	Yes	Yes in some, No in others	Yes/unknown
Invariant expression of tumor target	Yes	No	Unknown
Target expression may be quantified (personalized medicine)	Yes	Yes in some, No in others	No/unknown
Adjuvant or multiple dosing required	No	Yes	Unknown
Platform addressing multiple molecular targets	Yes	Yes in some, no in others	No
May be applied to multiple indications	Yes	Mostly no	No
Time to manufacture	Short	Long	Long
Manufacturing costs	Lower/low	High	High
Lymphodepletion or chemotherapy or cytokine treatment required	No	Yes	Yes/unknown
FDA regulatory hurdles	Lower	Higher	Higher
Examples of late preclinical or clinical development	Academic programs	Gritstone, Targovax, Gradalis, Agenus, Jounce, BioNTech, Neon, Precision Biologics, Vaccibody, Juno, Aurora, Triumvira, Adicet, Kite, etc	GammaDelta, Incysus, Gadeta, Lymphact, Immatics, etc

The relative advantages and disadvantages of each are listed. The experience is evolving rapidly, and this list is only presented as an example, not meant to be comprehensive.

other advantageous features such as the ability to cross-present antigen to αβ T cells. Moreover, a key advantage of the non-MHC restricted nature of γδ T cells is that CAR γδ T-cell preparations can be generated and expanded from pooled healthy donors.

To maximize the efficacy of the CAR therapy, an ideal antigen for CAR generation would need to be tumor-specific, highly and stably expressed by all malignant cells, and etiological to tumor development. Highlighting the therapeutic potential of TMGs, one of the first studies to engineer γδ CAR T cells used the GD2-antigen (205). The authors reported that GD2-CARs of both Vδ1 and Vδ2 subsets were expanded in sufficient numbers for clinical studies. The expression of the GD2-CAR by γδ T cells enhanced their innate cytotoxicity by directing its effects against GD2-expressing tumor cells. Further amplifying the anti-tumor immune response, expanded CAR-transduced Vδ2 cells retained the ability to internalize and cross-present tumor antigens to αβ T lymphocytes.

γδ T cells were originally thought to lack memory, and this was a concern in the design of CAR γδ T cell therapies. A lack of memory potentially translates into short-lived anti-tumor responses, but this may be overcome by using the CAR γδ T cell therapy in multiple treatment cycles. Encouragingly, recent data from mouse and human studies suggest that γδ T cells indeed have characteristics reminiscent of memory αβ T lymphocytes, promoting antigen-specific adaptive immunity (206–209). For example, in mice infected with B. pertussis, lung resident memory γδ T cells were shown to expand upon secondary infection with increased production of the cytokine, IL-17 (207). In humans, Vδ1+ and Vδ2+ γδ T cells are evidenced to promote microbial-specific adaptive immunity (208, 209).

CONCLUDING REMARKS

The concept of the "glycocode" (6, 210) poses that protein glycosylation—with sialic acids appearing to be key—regulates biological events that are crucial to immunity and cancer progression, comparable to, but beyond, the PD-1–type of checkpoint inhibition. This concept extends to the glycosylation of membrane and matrix proteins, mucins, and gangliosides, where TMGs represent a glyco-immune-checkpoint. Vaccines, antibodies, small molecules, soluble glycoproteins, enzymatic cleavage of sialic acids, or soluble competitors targeting the glyco-immune-checkpoint would be a promising approach to therapy (211).

It will be important to consider γδ T cell biology in the context of strategies targeting the glycocode and sialic acid-containing protein and ganglioside targets. **Table 2** shows a comparison of the features of different cancer immunotherapies, including many that have a γδ T cell mechanism of action. **Table 2** lists our view of their relative advantages and disadvantages. We present

an overview of their current stage of development, which we view as a benchmark of the time that each approach has been in development (factoring time and investment of resources) and the degree of expectation of success. However, based on history, most approaches are expected to perhaps find a narrow niche or indication where they may be of utility. Unfortunately, most will either fail clinically, or will face difficult regulatory hurdles, or become untenable in the marketplace.

Our work in developing glycomimetic vaccines surprisingly resulted in early activation of γδ T cells *in vivo*, and in high therapeutic efficacy in cancer. In addition to cancer, conceptually, this advance is applicable to therapies for other pathologies (e.g., antivirals) that could benefit from the activation of the innate and the adaptive immune systems by targeting sialic acids and other glycans.

AUTHOR CONTRIBUTIONS

All authors listed have made a substantial, direct and intellectual contribution to the work, and approved it for publication.

FUNDING

For this work HS received funding from the Canadian Institutes for Health Research (CIHR) (PJT-162291), the CIHR Proof-of-Principle Tier 1 (POP-1), and the GlycoNet Network of Centers of Excellence. SR was funded by the CIHR (PJT-162260), the McGill Interdisciplinary Initiative in Infection and Immunity (Mi4), and the Cole Foundation. CR was supported by a Canadian Institutes for Health Research Foundation Award (159912).

REFERENCES

1. Medzhitov R, Janeway CA Jr. Decoding the patterns of self and nonself by the innate immune system. *Science.* (2002) 296:298–300. doi: 10.1126/science.1068883
2. Wherry EJ, Kurachi M. Molecular and cellular insights into T cell exhaustion. *Nat Rev Immunol.* (2015) 15:486–99. doi: 10.1038/nri3862
3. Hargadon KM, Johnson CE, Williams CJ. Immune checkpoint blockade therapy for cancer: an overview of FDA-approved immune checkpoint inhibitors. *Int Immunopharmacol.* (2018) 62:29–39. doi: 10.1016/j.intimp.2018.06.001
4. Haslam A, Prasad V. Estimation of the percentage of US patients with cancer who are eligible for and respond to checkpoint inhibitor immunotherapy drugs. *JAMA Netw Open.* (2019) 2:e192535. doi: 10.1001/jamanetworkopen.2019.2535
5. Peixoto A, Relvas-Santos M, Azevedo R, Santos LL, Ferreira JA. Protein glycosylation and tumor microenvironment alterations driving cancer hallmarks. *Front Oncol.* (2019) 9:380. doi: 10.3389/fonc.2019.00380
6. RodrIguez E, Schetters STT, van Kooyk Y. The tumour glyco-code as a novel immune checkpoint for immunotherapy. *Nat Rev Immunol.* (2018) 18:204–11. doi: 10.1038/nri.2018.3
7. Varki A. Biological roles of glycans. *Glycobiology.* (2017) 27:3–49. doi: 10.1093/glycob/cww086
8. Ghazarian H, Idoni B, Oppenheimer SB. A glycobiology review: carbohydrates, lectins and implications in cancer therapeutics. *Acta Histochem.* (2011) 113:236–47. doi: 10.1016/j.acthis.2010.02.004
9. Rabinovich GA, van Kooyk Y, Cobb BA. Glycobiology of immune responses. *Ann N Y Acad Sci.* (2012) 1253:1–15. doi: 10.1111/j.1749-6632.2012.06492.x
10. Kiessling LL. Chemistry-driven glycoscience. *Bioorg Med Chem.* (2018) 26:5229–38. doi: 10.1016/j.bmc.2018.09.024
11. Pinho SS, Reis CA. Glycosylation in cancer: mechanisms and clinical implications. *Nat Rev Cancer.* (2015) 15:540–55. doi: 10.1038/nrc3982
12. Fuster MM, Esko JD. The sweet and sour of cancer: glycans as novel therapeutic targets. *Nat Rev Cancer.* (2005) 5:526–42. doi: 10.1038/nrc1649
13. Hakomori S. Tumor malignancy defined by aberrant glycosylation and sphingo(glyco)lipid metabolism. *Cancer Res.* (1996) 56:5309–18.
14. Bull C, Stoel MA, den Brok MH, Adema GJ. Sialic acids sweeten a tumor's life. *Cancer Res.* (2014) 74:3199–204. doi: 10.1158/0008-5472.CAN-14-0728
15. Gagnon M, Saragovi HU. Gangliosides: therapeutic agents or therapeutic targets? *Expert Opin Ther Patents.* (2002) 12:1215–23. doi: 10.1517/13543776.12.8.1215
16. Heimburg-Molinaro J, Lum M, Vijay G, Jain M, Almogren A, Rittenhouse-Olson K. Cancer vaccines and carbohydrate epitopes. *Vaccine.* (2011) 29:8802–26. doi: 10.1016/j.vaccine.2011.09.009
17. Sedlacek HH, Meesmann H, Seiler FR. Regression of spontaneous mammary tumors in dogs after injection of neuraminidase-treated tumor cells. *Int J Cancer.* (1975) 15:409–16. doi: 10.1002/ijc.2910150307
18. Currie GA, Bagshawe KD. The masking of antigens on trophoblast and cancer cells. *Lancet.* (1967) 1:708–10. doi: 10.1016/S0140-6736(67)92183-6
19. Cohen M, Elkabets M, Perlmutter M, Porgador A, Voronov E, Apte RN, et al. Sialylation of 3-methylcholanthrene-induced fibrosarcoma determines antitumor immune responses during immunoediting. *J Immunol.* (2010) 185:5869–78. doi: 10.4049/jimmunol.1001635
20. Wesener DA, Dugan A, Kiessling LL. Recognition of microbial glycans by soluble human lectins. *Curr Opin Struct Biol.* (2017) 44:168–78. doi: 10.1016/j.sbi.2017.04.002
21. Chen GY, Brown NK, Zheng P, Liu Y. Siglec-G/10 in self-nonself discrimination of innate and adaptive immunity. *Glycobiology.* (2014) 24:800–6. doi: 10.1093/glycob/cwu068
22. Pearce OM, Laubli H. Sialic acids in cancer biology and immunity. *Glycobiology.* (2016) 26:111–28. doi: 10.1093/glycob/cwv097
23. Macauley MS, Pfrengle F, Rademacher C, Nycholat CM, Gale AJ, von Drygalski A, et al. Antigenic liposomes displaying CD22 ligands induce antigen-specific B cell apoptosis. *J Clin Invest.* (2013) 123:3074–83. doi: 10.1172/JCI69187
24. Lanoue A, Batista FD, Stewart M, Neuberger MS. Interaction of CD22 with alpha2,6-linked sialoglycoconjugates: innate recognition of self to dampen B cell autoreactivity? *Eur J Immunol.* (2002) 32:348–55. doi: 10.1002/1521-4141(200202)32:2<348::AID-IMMU348>3.0.CO;2-5
25. Macauley MS, Paulson JC. Siglecs induce tolerance to cell surface antigens by BIM-dependent deletion of the antigen-reactive B cells. *J Immunol.* (2014) 193:4312–21. doi: 10.4049/jimmunol.1401723
26. Hudak JE, Canham SM, Bertozzi CR. Glycocalyx engineering reveals a Siglec-based mechanism for NK cell immunoevasion. *Nat Chem Biol.* (2014) 10:69–75. doi: 10.1038/nchembio.1388
27. Jandus C, Boligan KF, Chijioke O, Liu H, Dahlhaus M, Demoulins T, et al. Interactions between Siglec-7/9 receptors and ligands influence NK cell-dependent tumor immunosurveillance. *J Clin Invest.* (2014) 124:1810–20. doi: 10.1172/JCI65899
28. Falco M, Biassoni R, Bottino C, Vitale M, Sivori S, Augugliaro R, etal. Identification and molecular cloning of p75/AIRM1, a novel member of the sialoadhesin family that functions as an inhibitory receptor in human natural killer cells. *J Exp Med.* (1999) 190:793–802. doi: 10.1084/jem.190.6.793
29. Huang CH, Liao YJ, Fan TH, Chiou TJ, Lin YH, Twu YC. A developed NK-92MI cell line with Siglec-7(neg) phenotype exhibits high and sustainable cytotoxicity against leukemia cells. *Int J Mol Sci.* (2018) 19:1073. doi: 10.3390/ijms19041073
30. Beatson R, Tajadura-Ortega V, Achkova D, Picco G, Tsourouktsoglou TD, Klausing S, et al. The mucin MUC1 modulates the tumor immunological microenvironment through engagement of the lectin Siglec-9. *Nat Immunol.* (2016) 17:1273–81. doi: 10.1038/ni.3552
31. Takamiya R, Ohtsubo K, Takamatsu S, Taniguchi N, Angata T. The interaction between Siglec-15 and tumor-associated sialyl-Tn antigen enhances TGF-beta secretion from monocytes/macrophages

through the DAP12-Syk pathway. *Glycobiology.* (2013) 23:178–87. doi: 10.1093/glycob/cws139
32. Barkal AA, Brewer RE, Markovic M, Kowarsky M, Barkal SA, Zaro BW, et al. CD24 signalling through macrophage Siglec-10 is a target for cancer immunotherapy. *Nature.* (2019) 572:392–6. doi: 10.1038/s41586-019-1456-0
33. Santegoets KCM, Gielen PR, Bull C, Schulte BM, Kers-Rebel ED, Kusters B, et al. Expression profiling of immune inhibitory Siglecs and their ligands in patients with glioma. *Cancer Immunol Immunother.* (2019) 68:937–49. doi: 10.1007/s00262-019-02332-w
34. Perdicchio M, Ilarregui JM, Verstege MI, Cornelissen LA, Schetters ST, Engels S, et al. Sialic acid-modified antigens impose tolerance via inhibition of T-cell proliferation and *de novo* induction of regulatory T cells. *Proc Natl Acad Sci USA.* (2016) 113:3329–34. doi: 10.1073/pnas.1507706113
35. Stanczak MA, Siddiqui SS, Trefny MP, Thommen DS, Boligan KF, von Gunten S, et al. Self-associated molecular patterns mediate cancer immune evasion by engaging Siglecs on T cells. *J Clin Invest.* (2018) 128:4912–23. doi: 10.1172/JCI120612
36. Haas Q, Boligan KF, Jandus C, Schneider C, Simillion C, Stanczak MA, et al. Siglec-9 regulates an effector memory CD8(+) T-cell subset that congregates in the melanoma tumor microenvironment. *Cancer Immunol Res.* (2019) 7:707–18. doi: 10.1158/2326-6066.CIR-18-0505
37. Wang J, Sun J, Liu LN, Flies DB, Nie X, Toki M, et al. Siglec-15 as an immune suppressor and potential target for normalization cancer immunotherapy. *Nat Med.* (2019) 25:656–66. doi: 10.1038/s41591-019-0374-x
38. Bull C, Boltje TJ, M. Wassink, de Graaf AM, van Delft FL, den Brok MH, Adema GJ. Targeting aberrant sialylation in cancer cells using a fluorinated sialic acid analog impairs adhesion, migration, and *in vivo* tumor growth. *Mol Cancer Ther.* (2013) 12:1935–46. doi: 10.1158/1535-7163.MCT-13-0279
39. Bull C, Boltje TJ, van Dinther EA, Peters T, de Graaf AM, Leusen JH, et al. Targeted delivery of a sialic acid-blocking glycomimetic to cancer cells inhibits metastatic spread. *ACS Nano.* (2015) 9:733–45. doi: 10.1021/nn5061964
40. Rios A, Simmons RL. Immunospecific regression of various syngeneic mouse tumors in response to neuraminidase-treated tumor cells. *J Natl Cancer Inst.* (1973) 51:637–44.
41. Sedlacek HH, Seiler FR. Immunotherapy of neoplastic diseases with neuraminidase: contradictions, new aspects, revised concepts. *Cancer Immunol Immunother.* (1978) 5:153–63. doi: 10.1007/BF00199623
42. Sedlacek HH, Seiler FR, Schwick HG. Neuraminidase and tumor immunotherapy. *Klinische Wochenschrift.* (1977) 55:199–214. doi: 10.1007/BF01487712
43. Benjamini E, Rennick DM. Cancer immunotherapy: facts and fancy. *CA Cancer J Clin.* (1979) 29:362–70. doi: 10.3322/canjclin.29.6.362
44. Xiao H, Woods EC, Vukojicic P, Bertozzi CR. Precision glycocalyx editing as a strategy for cancer immunotherapy. *Proc Natl Acad Sci USA.* (2016) 113:10304–9. doi: 10.1073/pnas.1608069113
45. Pike LJ. Lipid rafts: bringing order to chaos. *J Lipid Res.* (2003) 44:655–67. doi: 10.1194/jlr.R200021-JLR200
46. Iwabuchi K, Zhang Y, Handa K, Withers DA, Sinay P, Hakomori S. Reconstitution of membranes simulating "glycosignaling domain" and their susceptibility to lyso-GM3. *J Biol Chem.* (2000) 275:15174–81. doi: 10.1074/jbc.275.20.15174
47. Svennerholm L. Chromatographlc separation of human brain gangliosides*. *J Neurochem.* (1963) 10:613–23. doi: 10.1111/j.1471-4159.1963.tb08933.x
48. Wiegandt H. The structure and the function of gangliosides. *Angew Chem Int Ed Engl.* (1968) 7:87–96. doi: 10.1002/anie.196800871
49. Xie X, Wu G, Lu ZH, Ledeen RW. Potentiation of a sodium-calcium exchanger in the nuclear envelope by nuclear GM1 ganglioside. *J Neurochem.* (2002) 81:1185–95. doi: 10.1046/j.1471-4159.2002.00917.x
50. Mutoh T, Tokuda A, Miyadai T, Hamaguchi M, Fujiki N. Ganglioside GM1 binds to the Trk protein and regulates receptor function. *Proc Natl Acad Sci USA.* (1995) 92:5087–91. doi: 10.1073/pnas.92.11.5087
51. Cavdarli S, Delannoy P, Groux-Degroote S. O-acetylated gangliosides as targets for cancer immunotherapy. *Cells.* (2020) 9:741. doi: 10.3390/cells9030741
52. Elkashef SM, Allison SJ, Sadiq M, Basheer HA, Ribeiro Morais G, Loadman PM, et al. Polysialic acid sustains cancer cell survival and migratory capacity in a hypoxic environment. *Sci Rep.* (2016) 6:33026. doi: 10.1038/srep33026
53. Hettmer S, Ladisch S, Kaucic K. Low complex ganglioside expression characterizes human neuroblastoma cell lines. *Cancer Lett.* (2005) 225:141–9. doi: 10.1016/j.canlet.2004.11.036
54. Mujoo K, Cheresh DA, Yang HM, Reisfeld RA. Disialoganglioside GD2 on human neuroblastoma cells: target antigen for monoclonal antibody-mediated cytolysis and suppression of tumor growth. *Cancer Res.* (1987) 47:1098–104.
55. Cheresh DA, Pierschbacher MD, Herzig MA, Mujoo K. Disialogangliosides GD2 and GD3 are involved in the attachment of human melanoma and neuroblastoma cells to extracellular matrix proteins. *J Cell Biol.* (1986) 102:688–96. doi: 10.1083/jcb.102.3.688
56. Kozireski-Chuback D, Wu G, Ledeen RW. Developmental appearance of nuclear GM1 in neurons of the central and peripheral nervous systems. *Brain Res Dev Brain Res.* (1999) 115:201–8. doi: 10.1016/S0165-3806(99)00062-0
57. Cavanna B, Carpo M, Pedotti R, Scarpini E, Meucci N, Allaria S, et al. Anti-GM2 IgM antibodies: clinical correlates and reactivity with a human neuroblastoma cell line. *J Neuroimmunol.* (1999) 94:157–64. doi: 10.1016/S0165-5728(98)00245-8
58. Vrionis FD, Wikstrand CJ, Fredman P, Mansson JE, Svennerholm L, Bigner DD. Five new epitope-defined monoclonal antibodies reactive with GM2 and human glioma and medulloblastoma cell lines. *Cancer Res.* (1989) 49:6645–51.
59. Mirkin BL, Clark SH, Zhang C. Inhibition of human neuroblastoma cell proliferation and EGF receptor phosphorylation by gangliosides GM1, GM3, GD1A and GT1B. *Cell Prolif.* (2002) 35:105–15. doi: 10.1046/j.1365-2184.2002.00228.x
60. Hildebrandt H, Becker C, Gluer S, Rosner H, Gerardy-Schahn R, Rahmann H. Polysialic acid on the neural cell adhesion molecule correlates with expression of polysialyltransferases and promotes neuroblastoma cell growth. *Cancer Res.* (1998) 58:779–84.
61. Valentiner U, Muhlenhoff M, Lehmann U, Hildebrandt H, Schumacher U. Expression of the neural cell adhesion molecule and polysialic acid in human neuroblastoma cell lines. *Int J Oncol.* (2011) 39:417–24. doi: 10.3892/ijo.2011.1038
62. Pukel CS, Lloyd KO, Travassos LR, Dippold WG, Oettgen HF, Old LJ. GD3, a prominent ganglioside of human melanoma. Detection and characterisation by mouse monoclonal antibody. *J Exp Med.* (1982) 155:1133–47. doi: 10.1084/jem.155.4.1133
63. Nicolae CD, Nicolae I. Antibodies against GM1 gangliosides associated with metastatic melanoma. *Acta Dermatovenerol Croat.* (2013) 21:86–92. Available online at: https://www.google.com/url?sa=t&rct=j&q=&esrc=s&source=web&cd=&cad=rja&uact=8&ved=2ahUKEwi89qDt_u7rAhWCVt8KHfdDCy0QFjAEegQIAxAB&url=https%3A%2F%2Fhrcak.srce.hr%2Ffile%2F157175&usg=AOvVaw2Dh0g9sCEJOlzGbsnZPvU7
64. Hoon DS, Ando I, Sviland G, Tsuchida T, Okun E, Morton DL, et al. Ganglioside GM2 expression on human melanoma cells correlates with sensitivity to lymphokine-activated killer cells. *Int J Cancer.* (1989) 43:857–62. doi: 10.1002/ijc.2910430520
65. Tsuchida T, Saxton RE, Morton DL, Irie RF. Gangliosides of human melanoma. *Cancer.* (1989) 63:1166–74. doi: 10.1002/1097-0142(19890315)63:6<1166::AID-CNCR2820630621>3.0.CO;2-5
66. Mennel HD, Bosslet K, Wiegandt H, Sedlacek HH, Bauer BL, Rodden AF. Expression of GD2-epitopes in human intracranial tumors and normal brain. *Exp Toxicol Pathol.* (1992) 44:317–24. doi: 10.1016/S0940-2993(11)80218-6
67. Lama G, Mangiola A, Proietti G, Colabianchi A, Angelucci C, A DA, et al. Progenitor/stem cell markers in brain adjacent to glioblastoma: GD3 ganglioside and NG2 proteoglycan expression. *J Neuropathol Exp Neurol.* (2016) 75:134–47. doi: 10.1093/jnen/nlv012
68. Ohkawa Y, Momota H, Kato A, Hashimoto N, Tsuda Y, Kotani N, et al. Ganglioside GD3 enhances invasiveness of gliomas by forming a complex with platelet-derived growth factor receptor alpha and yes kinase. *J Biol Chem.* (2015) 290:16043–58. doi: 10.1074/jbc.M114.635755
69. Birks SM, Danquah JO, King L, Vlasak R, Gorecki DC, Pilkington GJ. Targeting the GD3 acetylation pathway selectively induces apoptosis in glioblastoma. *Neuro Oncol.* (2011) 13:950–60. doi: 10.1093/neuonc/nor108
70. Hedberg KM, Mahesparan R, Read TA, Tysnes BB, Thorsen F, Visted T, et al. The glioma-associated gangliosides 3'-isoLM1, GD3 and GM2 show selective area expression in human glioblastoma

xenografts in nude rat brains. *Neuropathol Appl Neurobiol.* (2001) 27:451–64. doi: 10.1046/j.1365-2990.2001.00353.x
71. Fujimoto Y, Izumoto S, Suzuki T, Kinoshita M, Kagawa N, Wada K, et al. Ganglioside GM3 inhibits proliferation and invasion of glioma. *J Neurooncol.* (2005) 71:99–106. doi: 10.1007/s11060-004-9602-3
72. Noll EN, Lin J, Nakatsuji Y, Miller RH, Black PM. GM3 as a novel growth regulator for human gliomas. *Exp Neurol.* (2001) 168:300–9. doi: 10.1006/exnr.2000.7603
73. Bassi R, Viani P, Giussani P, Riboni L, Tettamanti G. GM3 ganglioside inhibits endothelin-1-mediated signal transduction in C6 glioma cells. *FEBS Lett.* (2001) 507:101–4. doi: 10.1016/S0014-5793(01)02966-0
74. Trouillas J, Daniel L, Guigard MP, Tong S, Gouvernet J, Jouanneau E, et al. Polysialylated neural cell adhesion molecules expressed in human pituitary tumors and related to extrasellar invasion. *J Neurosurg.* (2003) 98:1084–93. doi: 10.3171/jns.2003.98.5.1084
75. Brezicka FT, Olling S, Nilsson O, Bergh J, Holmgren J, Sorenson S, et al. Immunohistological detection of fucosyl-GM1 ganglioside in human lung cancer and normal tissues with monoclonal antibodies. *Cancer Res.* (1989) 49:1300–5.
76. Yamada T, Bando H, Takeuchi S, Kita K, Li Q, Wang W, et al. Genetically engineered humanized anti-ganglioside GM2 antibody against multiple organ metastasis produced by GM2-expressing small-cell lung cancer cells. *Cancer Sci.* (2011) 102:2157–63. doi: 10.1111/j.1349-7006.2011.02093.x
77. Blanco R, Dominguez E, Morales O, Blanco D, Martinez D, Rengifo CE, et al. Prognostic significance of N-Glycolyl GM3 ganglioside expression in non-small cell lung carcinoma patients: new evidences. *Patholog Res Int.* (2015) 2015:132326. doi: 10.1155/2015/132326
78. Hayashi N, Chiba H, Kuronuma K, Go S, Hasegawa Y, Takahashi M, et al. Detection of N-glycolyated gangliosides in non-small-cell lung cancer using GMR8 monoclonal antibody. *Cancer Sci.* (2013) 104:43–7. doi: 10.1111/cas.12027
79. Tanaka F, Otake Y, Nakagawa T, Kawano Y, Miyahara R, Li M, et al. Prognostic significance of polysialic acid expression in resected non-small cell lung cancer. *Cancer Res.* (2001) 61:1666–70. Available online at: https://cancerres.aacrjournals.org/content/canres/61/4/1666.full.pdf
80. Tanaka F, Otake Y, Nakagawa T, Kawano Y, Miyahara R, Li M, et al. Expression of polysialic acid and *STX*, a human polysialyltransferase, is correlated with tumor progression in non-small cell lung cancer. *Cancer Res.* (2000) 60:3072–80. Available online at: https://cancerres.aacrjournals.org/content/60/11/3072.full-text.pdf
81. Liang JX, Liang Y, Gao W. Clinicopathological and prognostic significance of sialyl Lewis X overexpression in patients with cancer: a meta-analysis. *Onco Targets Ther.* (2016) 9:3113–25. doi: 10.2147/OTT.S102389
82. Natoni A, Macauley MS, O'Dwyer ME. Targeting selectins and their ligands in cancer. *Front Oncol.* (2016) 6:93. doi: 10.3389/fonc.2016.00093
83. Yoshida S, Fukumoto S, Kawaguchi H, Sato S, Ueda R, Furukawa K. Ganglioside G_{D2} in small cell lung cancer cell lines: enhancement of cell proliferation and mediation of apoptosis. *Cancer Res.* (2001) 61:4244–52. Available online at: https://cancerres.aacrjournals.org/content/61/10/4244.full-text.pdf
84. Watarai S, Kiura K, Shigeto R, Shibayama T, Kimura I, Yasuda T. Establishment of monoclonal antibodies specific for ganglioside GM1: detection of ganglioside GM1 in small cell lung carcinoma cell lines and tissues. *J Biochem.* (1994) 116:948–54. doi: 10.1093/oxfordjournals.jbchem.a124651
85. Liang YJ, Ding Y, Levery SB, Lobaton M, Handa K, Hakomori SI. Differential expression profiles of glycosphingolipids in human breast cancer stem cells vs. cancer non-stem cells. *Proc Natl Acad Sci USA.* (2013) 110:4968–73. doi: 10.1073/pnas.1302825110
86. Steenackers A, Vanbeselaere J, Cazet A, Bobowski M, Rombouts Y, Colomb F, et al. Accumulation of unusual gangliosides G(Q3) and G(P3) in breast cancer cells expressing the G(D3) synthase. *Molecules.* (2012) 17:9559–72. doi: 10.3390/molecules17089559
87. Bobowski M, Vincent A, Steenackers A, Colomb F, Van Seuningen I, Julien S, et al. Estradiol represses the G(D3) synthase gene ST8SIA1 expression in human breast cancer cells by preventing NFkappaB binding to ST8SIA1 promoter. *PLoS ONE.* (2013) 8:e62559. doi: 10.1371/journal.pone.0062559
88. Wang X, Li X, Zeng YN, He F, Yang XM, Guan F. Enhanced expression of polysialic acid correlates with malignant phenotype in breast cancer cell lines and clinical tissue samples. *Int J Mol Med.* (2016) 37:197–206. doi: 10.3892/ijmm.2015.2395
89. Das T, Sa G, Hilston C, Kudo D, Rayman P, Biswas K, et al. GM1 and tumor necrosis factor-alpha, overexpressed in renal cell carcinoma, synergize to induce T-cell apoptosis. *Cancer Res.* (2008) 68:2014–23. doi: 10.1158/0008-5472.CAN-07-6037
90. Biswas K, Richmond A, Rayman P, Biswas S, Thornton M, Sa G, et al. GM2 expression in renal cell carcinoma: potential role in tumor-induced T-cell dysfunction. *Cancer Res.* (2006) 66:6816–25. doi: 10.1158/0008-5472.CAN-06-0250
91. Sakakibara N, Gasa S, Kamio K, Makita A, Nonomura K, Togashi M, et al. Distinctive glycolipid patterns in Wilms' tumor and renal cell carcinoma. *Cancer Lett.* (1991) 57:187–92. doi: 10.1016/0304-3835(91)90155-B
92. Borzym-Kluczyk M, Radziejewska I, Cechowska-Pasko M. Increased expression of MUC1 and sialyl Lewis antigens in different areas of clear renal cell carcinoma. *Clin Exp Nephrol.* (2015) 19:732–7. doi: 10.1007/s10157-014-1013-y
93. Ravindranath MH, Muthugounder S, Presser N, Selvan SR, Santin AD, Bellone S, et al. Immunogenic gangliosides in human ovarian carcinoma. *Biochem Biophys Res Commun.* (2007) 353:251–8. doi: 10.1016/j.bbrc.2006.12.001
94. Webb TJ, Li X, Giuntoli RL, 2nd, Lopez PH, Heuser C, Schnaar RL, et al. Molecular identification of GD3 as a suppressor of the innate immune response in ovarian cancer. *Cancer Res.* (2012) 72:3744–52. doi: 10.1158/0008-5472.CAN-11-2695
95. Prinetti A, Aureli M, Illuzzi G, Prioni S, Nocco V, Scandroglio F, et al. GM3 synthase overexpression results in reduced cell motility and in caveolin-1 upregulation in human ovarian carcinoma cells. *Glycobiology.* (2010) 20:62–77. doi: 10.1093/glycob/cwp143
96. Chang HR, Cordon-Cardo C, Houghton AN, Cheung NK, Brennan MF. Expression of disialogangliosides GD2 and GD3 on human soft tissue sarcomas. *Cancer.* (1992) 70:633–8.
97. Heiner JP, Miraldi F, Kallick S, Makley J, Neely J, Smith-Mensah WH, et al. Localization of GD2-specific monoclonal antibody 3F8 in human osteosarcoma. *Cancer Res.* (1987) 47:5377–81.
98. Shibuya H, Hamamura K, Hotta H, Matsumoto Y, Nishida Y, Hattori H, et al. Enhancement of malignant properties of human osteosarcoma cells with disialyl gangliosides GD2/GD3. *Cancer Sci.* (2012) 103:1656–64. doi: 10.1111/j.1349-7006.2012.02344.x
99. Dobrenkov K, Ostrovnaya I, Gu J, Cheung IY, Cheung NK. Oncotargets GD2 and GD3 are highly expressed in sarcomas of children, adolescents, young adults. *Pediatr Blood Cancer.* (2016) 63:1780–5. doi: 10.1002/pbc.26097
100. Lipinski M, Braham K, Philip I, Wiels J, Philip T, Goridis C, et al. Neuroectoderm-associated antigens on Ewing's sarcoma cell lines. *Cancer Res.* (1987) 47:183–7.
101. Kailayangiri S, Altvater B, Meltzer J, Pscherer S, Luecke A, Dierkes C, et al. The ganglioside antigen G(D2) is surface-expressed in Ewing sarcoma and allows for MHC-independent immune targeting. *Br J Cancer.* (2012) 106:1123–33. doi: 10.1038/bjc.2012.57
102. Scursoni AM, Galluzzo L, Camarero S, Lopez J, Lubieniecki F, Sampor C, et al. Detection of N-glycolyl GM3 ganglioside in neuroectodermal tumors by immunohistochemistry: an attractive vaccine target for aggressive pediatric cancer. *Clin Dev Immunol.* (2011) 2011:245181. doi: 10.1155/2011/245181
103. Modak S, Gerald W, Cheung NK. Disialoganglioside GD2 and a novel tumor antigen: potential targets for immunotherapy of desmoplastic small round cell tumor. *Med Pediatr Oncol.* (2002) 39:547–51. doi: 10.1002/mpo.10151
104. Portoukalian J, David MJ, Gain P, Richard M. Shedding of GD2 ganglioside in patients with retinoblastoma. *Int J Cancer.* (1993) 53:948–51. doi: 10.1002/ijc.2910530614
105. Torbidoni AV, Scursoni A, Camarero S, Segatori V, Gabri M, Alonso D, et al. Immunoreactivity of the 14F7 Mab raised against N-Glycolyl GM3 Ganglioside in retinoblastoma tumours. *Acta Ophthalmol.* (2015) 93:e294–300. doi: 10.1111/aos.12578
106. Scursoni AM, Galluzzo L, Camarero S, Pozzo N, Gabri MR, de Acosta CM, et al. Detection and characterization of N-glycolyated gangliosides in

Wilms tumor by immunohistochemistry. *Pediatr Dev Pathol.* (2010) 13:18–23. doi: 10.2350/08-10-0544.1
107. Roth J, Zuber C, Wagner P, Blaha I, Bitter-Suermann D, Heitz PU. Presence of the long chain form of polysialic acid of the neural cell adhesion molecule in Wilms' tumor. Identification of a cell adhesion molecule as an oncodevelopmental antigen and implications for tumor histogenesis. A*m J Pathol.* (1988) 133:227–40.
108. Komminoth P, Roth J, Saremaslani P, Matias-Guiu X, Wolfe HJ, Heitz PU. Polysialic acid of the neural cell adhesion molecule in the human thyroid: a marker for medullary thyroid carcinoma and primary C-cell hyperplasia. An immunohistochemical study on 79 thyroid lesions. *Am J Surg Pathol.* (1994) 18:399–411. doi: 10.1097/00000478-199404000-00008
109. Zhang S, Cordon-Cardo C, Zhang HS, Reuter VE, Adluri S, Hamilton WB, et al. Selection of tumor antigens as targets for immune attack using immunohistochemistry: I. Focus on gangliosides. *Int J Cancer.* (1997) 73:42–9.
110. Guerrera M, Ladisch S. N-butyldeoxynojirimycin inhibits murine melanoma cell ganglioside metabolism and delays tumor onset. *Cancer Lett.* (2003) 201:31–40. doi: 10.1016/S0304-3835(03)00459-2
111. Battula VL, Shi Y, Evans KW, Wang RY, Spaeth EL, Jacamo RO, et al. Ganglioside GD2 identifies breast cancer stem cells and promotes tumorigenesis. *J Clin Invest.* (2012) 122:2066–78. doi: 10.1172/JCI59735
112. Sarkar TR, Battula VL, Werden SJ, Vijay GV, Ramirez-Pena EQ, Taube JH, et al. GD3 synthase regulates epithelial-mesenchymal transition and metastasis in breast cancer. *Oncogene.* (2015) 34:2958–67. doi: 10.1038/onc.2014.245
113. Ledeen R, Wu G. GM1 in the nuclear envelope regulates nuclear calcium through association with a nuclear sodium-calcium exchanger. *J Neurochem.* (2007) 103(Suppl. 1):126–34. doi: 10.1111/j.1471-4159.2007.04722.x
114. Sano R, Annunziata I, Patterson A, Moshiach S, Gomero E, Opferman J, et al. GM1-ganglioside accumulation at the mitochondria-associated ER membranes links ER stress to Ca(2+)-dependent mitochondrial apoptosis. *Mol Cell.* (2009) 36:500–11. doi: 10.1016/j.molcel.2009.10.021
115. Lauc G, Heffer-Lauc M. Shedding and uptake of gangliosides and glycosylphosphatidylinositol-anchored proteins. *Biochim Biophys Acta.* (2006) 1760:584–602. doi: 10.1016/j.bbagen.2005.11.014
116. Ladisch S, Kitada S, Hays EF. Gangliosides shed by tumor cells enhance tumor formation in mice. *J Clin Invest.* (1987) 79:1879–82. doi: 10.1172/JCI113031
117. McKallip R, Li R, Ladisch S. Tumor gangliosides inhibit the tumor-specific immune response. *J Immunol.* (1999) 163:3718–26.
118. Lu P, Sharom FJ. Immunosuppression by YAC-1 lymphoma: role of shed gangliosides. *Cell Immunol.* (1996) 173:22–32. doi: 10.1006/cimm.1996.0248
119. Krengel U, Bousquet PA. Molecular recognition of gangliosides and their potential for cancer immunotherapies. *Front Immunol.* (2014) 5:325. doi: 10.3389/fimmu.2014.00325
120. Tong W, Maira M, Gagnon M, Saragovi HU. Ligands binding to cell surface ganglioside GD2 cause Src-dependent activation of N-Methyl-D-aspartate receptor signaling and changes in cellular morphology. *PLoS ONE.* (2015) 10:e0134255. doi: 10.1371/journal.pone.0134255
121. Cazet A, Bobowski M, Rombouts Y, Lefebvre J, Steenackers A, Popa I, et al. The ganglioside G(D2) induces the constitutive activation of c-Met in MDA-MB-231 breast cancer cells expressing the G(D3) synthase. *Glycobiology.* (2012) 22:806–16. doi: 10.1093/glycob/cws049
122. Aixinjueluo W, Furukawa K, Zhang Q, Hamamura K, Tokuda N, Yoshida S, et al. Mechanisms for the apoptosis of small cell lung cancer cells induced by anti-GD2 monoclonal antibodies: roles of anoikis. *J Biol Chem.* (2005) 280:29828–36. doi: 10.1074/jbc.M414041200
123. Dippold WG, Knuth A, Meyer zum Buschenfelde KH. Inhibition of human melanoma cell growth *in vitro* by monoclonal anti-GD3-ganglioside antibody. *Cancer Res.* (1984) 44:806–10.
124. Liu Y, Wondimu A, Yan S, Bobb D, Ladisch S. Tumor gangliosides accelerate murine tumor angiogenesis. *Angiogenesis.* (2014) 17:563–71. doi: 10.1007/s10456-013-9403-4
125. Koochekpour S, Merzak A, Pilkington GJ. Vascular endothelial growth factor production is stimulated by gangliosides and TGF-β isoforms in human glioma cells *in vitro*. *Cancer Lett.* (1996) 102:209–15. doi: 10.1016/0304-3835(96)04161-4
126. Tringali C, Silvestri I, Testa F, Baldassari P, Anastasia L, Mortarini R, et al. Molecular subtyping of metastatic melanoma based on cell ganglioside metabolism profiles. *BMC Cancer.* (2014) 14:560. doi: 10.1186/1471-2407-14-560
127. Agarwal MK, Neter E. Effect of selected lipids and surfactants on immunogenicity of several bacterial antigens. *J Immunol.* (1971) 107:1448–56.
128. Ladisch S, Gillard B, Wong C, Ulsh L. Shedding and immunoregulatory activity of YAC-1 lymphoma cell gangliosides. *Cancer Res.* (1983) 43:3808–13.
129. Rapoport E, Mikhalyov I, Zhang J, Crocker P, Bovin N. Ganglioside binding pattern of CD33-related siglecs. *Bioorg Med Chem Lett.* (2003) 13:675–8. doi: 10.1016/S0960-894X(02)00998-8
130. Nicoll G, Avril T, Lock K, Furukawa K, Bovin N, Crocker PR. Ganglioside GD3 expression on target cells can modulate NK cell cytotoxicity via siglec-7-dependent and -independent mechanisms. *Eur J Immunol.* (2003) 33:1642–8. doi: 10.1002/eji.200323693
131. Ito A, Handa K, Withers DA, Satoh M, Hakomori S. Binding specificity of siglec7 to disialogangliosides of renal cell carcinoma: possible role of disialogangliosides in tumor progression. *FEBS Lett.* (2001) 504:82–6. doi: 10.1016/S0014-5793(01)02734-X
132. Yamaji T, Teranishi T, Alphey MS, Crocker PR, Hashimoto Y. A small region of the natural killer cell receptor, Siglec-7, is responsible for its preferred binding to alpha 2,8-disialyl and branched alpha 2,6-sialyl residues. A comparison with Siglec-9. *J Biol Chem.* (2002) 277:6324–32. doi: 10.1074/jbc.M110146200
133. Lu P, Sharom FJ. Gangliosides are potent immunosuppressors of IL-2-mediated T-cell proliferation in a low protein environment. *Immunology.* (1995) 86:356–63.
134. Peguet-Navarro J, Sportouch M, Popa I, Berthier O, Schmitt D, Portoukalian J. Gangliosides from human melanoma tumors impair dendritic cell differentiation from monocytes and induce their apoptosis. *J Immunol.* (2003) 170:3488–94. doi: 10.4049/jimmunol.170.7.3488
135. Heitger A, Ladisch S. Gangliosides block antigen presentation by human monocytes. *Biochim Biophys Acta.* (1996) 1303:161–8. doi: 10.1016/0005-2760(96)00091-4
136. Wondimu A, Liu Y, Su Y, Bobb D, Ma JS, Chakrabarti L, et al. Gangliosides drive the tumor infiltration and function of myeloid-derived suppressor cells. *Cancer Res.* (2014) 74:5449–57. doi: 10.1158/0008-5472.CAN-14-0927
137. Cheever MA, Allison JP, Ferris AS, Finn OJ, Hastings BM, Hecht TT, et al. The prioritization of cancer antigens: a national cancer institute pilot project for the acceleration of translational research. *Clin Cancer Res.* (2009) 15:5323–37. doi: 10.1158/1078-0432.CCR-09-0737
138. Kramer K, Gerald WL, Kushner BH, Larson SM, Hameed M, Cheung NK. Disaloganglioside GD2 loss following monoclonal antibody therapy is rare in neuroblastoma. *Med Pediatr Oncol.* (2001) 36:194–6. doi: 10.1002/1096-911X(20010101)36:1<194::AID-MPO1046>3.0.CO;2-B
139. Poon VI, Roth M, Piperdi S, Geller D, Gill J, Rudzinski ER, et al. Ganglioside GD2 expression is maintained upon recurrence in patients with osteosarcoma. *Clin Sarcoma Res.* (2015) 5:4. doi: 10.1186/s13569-014-0020-9
140. Doronin, II, Vishnyakova PA, Kholodenko IV, Ponomarev ED, Ryazantsev DY, et al. Ganglioside GD2 in reception and transduction of cell death signal in tumor cells. *BMC Cancer.* (2014) 14:295. doi: 10.1186/1471-2407-14-295
141. Yu AL, Gilman AL, Ozkaynak MF, London WB, Kreissman SG, Chen HX, et al. Children's Oncology, Anti-GD2 antibody with GM-CSF, interleukin-2, and isotretinoin for neuroblastoma. *N Engl J Med.* (2010) 363:1324–34. doi: 10.1056/NEJMoa0911123
142. Saleh MN, Khazaeli MB, Wheeler RH, Allen L, Tilden AB, Grizzle W, et al. Phase I trial of the chimeric anti-GD2 monoclonal antibody ch14.18 in patients with malignant melanoma. *Hum Antibodies Hybridomas.* (1992) 3:19–24. doi: 10.3233/HAB-1992-3104
143. Handgretinger R, Anderson K, Lang P, Dopfer R, Klingebiel T, Schrappe M, et al. A phase I study of human/mouse chimeric antiganglioside GD2 antibody ch14.18 in patients with neuroblastoma. *Eur J Cancer.* (1995) 31A:261–7. doi: 10.1016/0959-8049(94)00413-Y
144. Cheung NK, Neely JE, Landmeier B, Nelson D, Miraldi F. Targeting of ganglioside GD2 monoclonal antibody to neuroblastoma. *J Nucl Med.* (1987) 28:1577–83.

145. McCaffery M, Yao TJ, Williams L, Livingston PO, Houghton AN, Chapman PB. Immunization of melanoma patients with BEC2 anti-idiotypic monoclonal antibody that mimics GD3 ganglioside: enhanced immunogenicity when combined with adjuvant. *Clin Cancer Res.* (1996) 2:679–86.
146. Bajorin DF, Chapman PB, Wong G, Coit DG, Kunicka J, Dimaggio J, et al. Phase I evaluation of a combination of monoclonal antibody R24 and interleukin 2 in patients with metastatic melanoma. *Cancer Res.* (1990) 50:7490–5.
147. Navid F, Santana VM, Barfield RC. Anti-GD2 antibody therapy for GD2-expressing tumors. *Curr Cancer Drug Targets.* (2010) 10:200–9. doi: 10.2174/156800910791054167
148. Keyel ME, Reynolds CP. Spotlight on dinutuximab in the treatment of high-risk neuroblastoma: development and place in therapy. *Biologics.* (2019) 13:1–12. doi: 10.2147/BTT.S114530
149. Esser R, Muller T, Stefes D, Kloess S, Seidel D, Gillies SD, et al. NK cells engineered to express a GD2 -specific antigen receptor display built-in ADCC-like activity against tumour cells of neuroectodermal origin. *J Cell Mol Med.* (2012) 16:569–81. doi: 10.1111/j.1582-4934.2011.01343.x
150. Gargett T, Yu W, Dotti G, Yvon ES, Christo SN, Hayball JD, et al. GD2-specific CAR T cells undergo potent activation and deletion following antigen encounter but can be protected from activation-induced cell death by PD-1 blockade. *Mol Ther.* (2016) 24:1135–49. doi: 10.1038/mt.2016.63
151. Seitz CM, Schroeder S, Knopf P, Krahl AC, Hau J, Schleicher S, et al. GD2-targeted chimeric antigen receptor T cells prevent metastasis formation by elimination of breast cancer stem-like cells. *Oncoimmunology.* (2020) 9:1683345. doi: 10.1080/2162402X.2019.1683345
152. Mount CW, Majzner RG, Sundaresh S, Arnold EP, Kadapakkam M, Haile S, et al. Potent antitumor efficacy of anti-GD2 CAR T cells in H3-K27M(+) diffuse midline gliomas. *Nat Med.* (2018) 24:572–9. doi: 10.1038/s41591-018-0006-x
153. Chapman PB, Morrisey D, Panageas KS, Williams L, Lewis JJ, Israel RJ, et al. Vaccination with a bivalent G_{M2} and G_{D2} ganglioside conjugate vaccine: a trial comparing doses of G_{D2}-keyhole limpet hemocyanin. *Clin Cancer Res.* (2000) 6:4658–62. Available online at: https://clincancerres.aacrjournals.org/content/6/12/4658.full-text.pdf
154. Ragupathi G, Livingston PO, Hood C, Gathuru J, Krown SE, Chapman PB, et al. Consistent antibody response against ganglioside GD2 induced in patients with melanoma by a GD2 lactone-keyhole limpet hemocyanin conjugate vaccine plus immunological adjuvant QS-21. *Clin Cancer Res.* (2003) 9:5214–20. Available online at: https://clincancerres.aacrjournals.org/content/9/14/5214.full-text.pdf
155. Vantourout P, Hayday A. Six-of-the-best: unique contributions of γδ T cells to immunology. *Nat Rev Immunol.* (2013) 13:88–100. doi: 10.1038/nri3384
156. Hoeres T, Smetak M, Pretscher D, Wilhelm M. Improving the efficiency of Vγ9Vδ2 T-cell immunotherapy in cancer. *Front Immunol.* (2018) 9:800. doi: 10.3389/fimmu.2018.00800
157. Born WK, Kemal Aydintug M, O'Brien RL. Diversity of γδ T-cell antigens. *Cell Mol Immunol.* (2013) 10:13–20. doi: 10.1038/cmi.2012.45
158. Crowley MP, Fahrer AM, Baumgarth N, Hampl J, Gutgemann I, Teyton L, et al. A population of murine γδ T cells that recognize an inducible MHC class Ib molecule. *Science.* (2000) 287:314–6. doi: 10.1126/science.287.5451.314
159. Wingren C, Crowley MP, Degano M, Chien Y, Wilson IA. Crystal structure of a γδ T cell receptor ligand T22: a truncated MHC-like fold. *Science.* (2000) 287:310–4. doi: 10.1126/science.287.5451.310
160. Bai L, Picard D, Anderson B, Chaudhary V, Luoma A, Jabri B, et al. The majority of CD1d-sulfatide-specific T cells in human blood use a semiinvariant Vδ1 TCR. *Eur J Immunol.* (2012) 42:2505–10. doi: 10.1002/eji.201242531
161. Luoma AM, Castro CD, Mayassi T, Bembinster LA, Bai L, Picard D, et al. Crystal structure of Vδ1 T cell receptor in complex with CD1d-sulfatide shows MHC-like recognition of a self-lipid by human γδ T cells. *Immunity.* (2013) 39:1032–42. doi: 10.1016/j.immuni.2013.11.001
162. Agea E, Russano A, Bistoni O, Mannucci R, Nicoletti I, Corazzi L, et al. Human CD1-restricted T cell recognition of lipids from pollens. *J Exp Med.* (2005) 202:295–308. doi: 10.1084/jem.20050773
163. Uldrich AP, Le Nours J, Pellicci DG, Gherardin NA, McPherson KG, Lim RT, et al. CD1d-lipid antigen recognition by the γδ TCR. *Nat Immunol.* (2013) 14:1137–45. doi: 10.1038/ni.2713
164. Mangan BA, Dunne MR, O'Reilly VP, Dunne PJ, Exley MA, O'Shea D, et al. Cutting edge: CD1d restriction and Th1/Th2/Th17 cytokine secretion by human Vδ3 T cells. *J Immunol.* (2013) 191:30–4. doi: 10.4049/jimmunol.1300121
165. Le Nours J, Gherardin NA, Ramarathinam SH, Awad W, Wiede F, Gully BS, et al. A class of γδ T cell receptors recognize the underside of the antigen-presenting molecule MR1. *Science.* (2019) 366:1522–7. doi: 10.1126/science.aav3900
166. Tanaka Y, Morita CT, Tanaka Y, Nieves E, Brenner MB, Bloom BR. Natural and synthetic non-peptide antigens recognized by human γδ T cells. *Nature.* (1995) 375:155–8. doi: 10.1038/375155a0
167. Gober HJ, Kistowska M, Angman L, Jeno P, Mori L, de Libero G. Human T cell receptor γδ cells recognize endogenous mevalonate metabolites in tumor cells. *J Exp Med.* (2003) 197:163–8. doi: 10.1084/jem.20021500
168. Harly C, Guillaume Y, Nedellec S, Peigne CM, Monkkonen H, Monkkonen J, et al. Key implication of CD277/butyrophilin-3 (BTN3A) in cellular stress sensing by a major human γδ T-cell subset. *Blood.* (2012) 120:2269–79. doi: 10.1182/blood-2012-05-430470
169. Sandstrom A, Peigne CM, Leger A, Crooks JE, Konczak F, Gesnel MC, et al. The intracellular B30.2 domain of butyrophilin 3A1 binds phosphoantigens to mediate activation of human Vγ9Vδ2 T cells. *Immunity.* (2014) 40:490–500. doi: 10.1016/j.immuni.2014.03.003
170. Willcox CR, Vantourout P, Salim M, Zlatareva I, Melandri D, Zanardo L, et al. Butyrophilin-like 3 directly binds a human Vγ4+ T cell receptor using a modality distinct from clonally-restricted antigen. *Immunity.* (2019) 51:813–25.e4. doi: 10.1016/j.immuni.2019.09.006
171. Karunakaran MM, Willcox CR, Salim M, Paletta D, Fichtner AS, Noll A, et al. Butyrophilin-2A1 directly binds germline-encoded regions of the Vγ9Vδ2 TCR and is essential for phosphoantigen sensing. *Immunity.* (2020) 52:487–98.e6. doi: 10.1016/j.immuni.2020.02.014
172. Rigau M, Ostrouska S, Fulford TS, Johnson DN, Woods K, Ruan Z, et al. Butyrophilin 2A1 is essential for phosphoantigen reactivity by γδ T cells. *Science.* (2020) 367:aay516. doi: 10.1126/science.aay5516
173. Correia DV, Lopes A, Silva-Santos B. Tumor cell recognition by γδ T lymphocytes: T-cell receptor vs. NK-cell receptors. *Oncoimmunology.* (2013) 2:e22892. doi: 10.4161/onci.22892
174. Silva-Santos B, Strid J. Working in "NK Mode": natural killer group 2 member d and natural cytotoxicity receptors in stress-surveillance by γδ T cells. *Front Immunol.* (2018) 9:851. doi: 10.3389/fimmu.2018.00851
175. Girardi M, Oppenheim DE, Steele CR, Lewis JM, Glusac E, Filler R, et al. Regulation of cutaneous malignancy by γδ T cells. *Science.* (2001) 294:605–9. doi: 10.1126/science.1063916
176. Strid J, Roberts SJ, Filler RB, Lewis JM, Kwong BY, Schpero W, et al. Acute upregulation of an NKG2D ligand promotes rapid reorganization of a local immune compartment with pleiotropic effects on carcinogenesis. *Nat Immunol.* (2008) 9:146–54. doi: 10.1038/ni1556
177. Lanca T, Correia DV, Moita CF, Raquel H, Neves-Costa A, Ferreira C, et al. The MHC class Ib protein ULBP1 is a nonredundant determinant of leukemia/lymphoma susceptibility to γδ T-cell cytotoxicity. *Blood.* (2010) 115:2407–11. doi: 10.1182/blood-2009-08-237123
178. Park JE, Wu DY, Prendes M, Lu SX, Ragupathi G, Schrantz N, et al. Fine specificity of natural killer T cells against GD3 ganglioside and identification of GM3 as an inhibitory natural killer T-cell ligand. *Immunology.* (2008) 123:145–55. doi: 10.1111/j.1365-2567.2007.02760.x
179. Wu DY, Segal NH, Sidobre S, Kronenberg M, Chapman PB. Cross-presentation of disialoganglioside GD3 to natural killer T cells. *J Exp Med.* (2003) 198:173–81. doi: 10.1084/jem.20030446
180. Weintraub A. Immunology of bacterial polysaccharide antigens. *Carbohydr Res.* (2003) 338:2539–47. doi: 10.1016/j.carres.2003.07.008
181. Speir JA, Abdel-Motal UM, Jondal M, Wilson IA. Crystal structure of an MHC class I presented glycopeptide that generates carbohydrate-specific CTL. *Immunity.* (1999) 10:51–61. doi: 10.1016/S1074-7613(00)80006-0
182. Tong W, Maira M, Roychoudhury R, Galan A, Brahimi F, Gilbert M, et al. Vaccination with tumor-ganglioside glycomimetics activates a selective

immunity that affords cancer therapy. *Cell Chem Biol.* (2019) 26:1013–26.e4. doi: 10.1016/j.chembiol.2019.03.018
183. Tong W, Sprules T, Gehring K, Saragovi HU. Rational design of peptide ligands against a glycolipid by NMR studies. *Methods Mol Biol.* (2012) 928:39–52. doi: 10.1007/978-1-62703-008-3_4
184. Brandes M, Willimann K, Moser B. Professional antigen-presentation function by human γδ T Cells. *Science.* (2005) 309:264–8. doi: 10.1126/science.1110267
185. Brandes M, Willimann K, Bioley G, Levy N, Eberl M, Luo M, et al. Cross-presenting human γδ T cells induce robust CD8+ alphabeta T cell responses. *Proc Natl Acad Sci USA.* (2009) 106:2307–12. doi: 10.1073/pnas.0810059106
186. Castella B, Foglietta M, Sciancalepore P, Rigoni M, Coscia M, Griggio V, et al. Anergic bone marrow Vγ9Vδ2 T cells as early and long-lasting markers of PD-1-targetable microenvironment-induced immune suppression in human myeloma. *Oncoimmunology.* (2015) 4:e1047580. doi: 10.1080/2162402X.2015.1047580
187. Hoeres T, Holzmann E, Smetak M, Birkmann J, Wilhelm M. PD-1 signaling modulates interferon-gamma production by Gamma Delta (γδ) T-Cells in response to leukemia. *Oncoimmunology.* (2019) 8:1550618. doi: 10.1080/2162402X.2018.1550618
188. Neves PC, Rudersdorf RA, Galler R, Bonaldo MC, de Santana MG, Mudd PA, et al. CD8+ gamma-delta TCR+ and CD4+ T cells produce IFN-gamma at 5-7 days after yellow fever vaccination in Indian rhesus macaques, before the induction of classical antigen-specific T cell responses. *Vaccine.* (2010) 28:8183–8. doi: 10.1016/j.vaccine.2010.09.090
189. Neves PC, Santos JR, Tubarao LN, Bonaldo MC, Galler R. Early IFN-gamma production after YF 17D vaccine virus immunization in mice and its association with adaptive immune responses. *PLoS ONE.* (2013) 8:e81953. doi: 10.1371/journal.pone.0081953
190. Muia RP, Yu H, Prescher JA, Hellman U, Chen X, Bertozzi CR, et al. Identification of glycoproteins targeted by *Trypanosoma cruzi* trans-sialidase, a virulence factor that disturbs lymphocyte glycosylation. *Glycobiology.* (2010) 20:833–42. doi: 10.1093/glycob/cwq037
191. Poole J, Day CJ, von Itzstein M, Paton JC, Jennings MP. Glycointeractions in bacterial pathogenesis. *Nat Rev Microbiol.* (2018) 16:440–52. doi: 10.1038/s41579-018-0007-2
192. Yuki N. Carbohydrate mimicry: a new paradigm of autoimmune diseases. *Curr Opin Immunol.* (2005) 17:577–82. doi: 10.1016/j.coi.2005.09.004
193. Fisher JP, Heuijerjans J, Yan M, Gustafsson K, Anderson J. γδ T cells for cancer immunotherapy: a systematic review of clinical trials. *Oncoimmunology.* (2014) 3:e27572. doi: 10.4161/onci.27572
194. Fournie JJ, Sicard H, Poupot M, Bezombes C, Blanc A, Romagne F, et al. What lessons can be learned from γδ T cell-based cancer immunotherapy trials? *Cell Mol Immunol.* (2013) 10:35–41. doi: 10.1038/cmi.2012.39
195. Maeurer MJ, Martin D, Walter W, Liu K, Zitvogel L, Halusczcak K, et al. Human intestinal Vδ1+ lymphocytes recognize tumor cells of epithelial origin. *J Exp Med.* (1996) 183:1681–96. doi: 10.1084/jem.183.4.1681
196. Bialasiewicz AA, Ma JX, Richard G. Alpha/beta- and gamma/delta TCR(+) lymphocyte infiltration in necrotising choroidal melanomas. *Br J Ophthalmol.* (1999) 83:1069–73. doi: 10.1136/bjo.83.9.1069
197. Moulin M, Alguacil J, Gu S, Mehtougui A, Adams EJ, Peyrottes S, et al. Vγ9Vδ2 T cell activation by strongly agonistic nucleotidic phosphoantigens. *Cell Mol Life Sci.* (2017) 74:4353–67. doi: 10.1007/s00018-017-2583-0
198. Kunzmann V, Bauer E, Feurle J, Weissinger F, Tony HP, Wilhelm M. Stimulation of γδ T cells by aminobisphosphonates and induction of antiplasma cell activity in multiple myeloma. *Blood.* (2000) 96:384–92. doi: 10.1182/blood.V96.2.384
199. Sebestyen Z, Prinz I, Dechanet-Merville J, Silva-Santos B, Kuball J. Translating γδ (γδ) T cells and their receptors into cancer cell therapies. *Nat Rev Drug Discov.* (2020) 19:169–84. doi: 10.1038/s41573-019-0038-z
200. Deniger DC, Moyes JS, Cooper LJ. Clinical applications of gamma delta T cells with multivalent immunity. *Front Immunol.* (2014) 5:636. doi: 10.3389/fimmu.2014.00636
201. Nicol AJ, Tokuyama H, Mattarollo SR, Hagi T, Suzuki K, Yokokawa K, et al. Clinical evaluation of autologous gamma delta T cell-based immunotherapy for metastatic solid tumours. *Br J Cancer.* (2011) 105:778–86. doi: 10.1038/bjc.2011.293
202. Garfall AL, Maus MV, Hwang WT, Lacey SF, Mahnke YD, Melenhorst JJ, et al. Chimeric antigen receptor T cells against CD19 for multiple myeloma. *N Engl J Med.* (2015) 373:1040–7. doi: 10.1056/NEJMoa1504542
203. Maude SL, Frey N, Shaw PA, Aplenc R, Barrett DM, Bunin NJ, et al. Chimeric antigen receptor T cells for sustained remissions in leukemia. *N Engl J Med.* (2014) 371:1507–17. doi: 10.1056/NEJMoa1407222
204. Porter DL, Hwang WT, Frey NV, Lacey SF, Shaw PA, Loren AW, et al. Chimeric antigen receptor T cells persist and induce sustained remissions in relapsed refractory chronic lymphocytic leukemia. *Sci Transl Med.* (2015) 7:303ra139. doi: 10.1126/scitranslmed.aac5415
205. Capsomidis A, Benthall G, Van Acker HH, Fisher J, Kramer AM, Abeln Z, et al. Chimeric antigen receptor-engineered human gamma delta T cells: enhanced cytotoxicity with retention of cross presentation. *Mol Ther.* (2018) 26:354–65. doi: 10.1016/j.ymthe.2017.12.001
206. Ribot JC, deBarros A, Pang DJ, Neves JF, Peperzak V, Roberts SJ, et al. CD27 is a thymic determinant of the balance between interferon-gamma- and interleukin 17-producing γδ T cell subsets. *Nat Immunol.* (2009) 10:427–36. doi: 10.1038/ni.1717
207. Misiak A, Wilk MM, Raverdeau M, Mills KH. IL-17-Producing innate and pathogen-specific tissue resident memory γδ T cells expand in the lungs of bordetella pertussis-infected mice. *J Immunol.* (2017) 198:363–74. doi: 10.4049/jimmunol.1601024
208. Davey MS, Willcox CR, Joyce SP, Ladell K, Kasatskaya SA, McLaren JE, et al. Clonal selection in the human Vδ1 T cell repertoire indicates γδ TCR-dependent adaptive immune surveillance. *Nat Commun.* (2017) 8:14760. doi: 10.1038/ncomms14760
209. Dimova T, Brouwer M, Gosselin F, Tassignon J, Leo O, Donner C, et al. Effector Vgamma9Vδ2 T cells dominate the human fetal γδ T-cell repertoire. *Proc Natl Acad Sci USA.* (2015) 112:E556–65. doi: 10.1073/pnas.1412058112
210. Dube DH, Bertozzi CR. Glycans in cancer and inflammation–potential for therapeutics and diagnostics. *Nat Rev.* (2005) 4:477–88. doi: 10.1038/nrd1751
211. Astronomo RD, Burton DR. Carbohydrate vaccines: developing sweet solutions to sticky situations? *Nat rev.* (2010) 9:308–24. doi: 10.1038/nrd3012

Conflict of Interest: HS is inventor in patents for anti-TMG vaccines.

The remaining authors declare that the research was conducted in the absence of any commercial or financial relationships that could be construed as a potential conflict of interest.

Advantages of publishing in Frontiers

OPEN ACCESS
Articles are free to read for greatest visibility and readership

FAST PUBLICATION
Around 90 days from submission to decision

HIGH QUALITY PEER-REVIEW
Rigorous, collaborative, and constructive peer-review

TRANSPARENT PEER-REVIEW
Editors and reviewers acknowledged by name on published articles

Frontiers
Avenue du Tribunal-Fédéral 34
1005 Lausanne | Switzerland

Visit us: www.frontiersin.org
Contact us: frontiersin.org/about/contact

REPRODUCIBILITY OF RESEARCH
Support open data and methods to enhance research reproducibility

DIGITAL PUBLISHING
Articles designed for optimal readership across devices

FOLLOW US
@frontiersin

IMPACT METRICS
Advanced article metrics track visibility across digital media

EXTENSIVE PROMOTION
Marketing and promotion of impactful research

LOOP RESEARCH NETWORK
Our network increases your article's readership